Synthesis and Functionalization of *N*-Heterocycles *via* Bismuth catalyzed S$_E$Ar reaction and Nickel Catalyzed C-H/C-N bond activation

by

Namrata Prusty

CHEM11201704003

National Institute of Science Education and Research,

Bhubaneswar, Odisha

A thesis submitted to the

Board of Studies in Chemical Sciences

In partial fulfillment of requirements

for the Degree of

DOCTOR OF PHILOSOPHY

of

HOMI BHABHA NATIONAL INSTITUTE

May, 2023

Homi Bhabha National Institute[1]

Recommendations of the Viva Voce Committee

As members of the Viva Voce Committee, we certify that we have read the dissertation prepared by **Namrata Prusty** entitled "**Synthesis and Functionalization of *N*-Heterocycles *via* Bismuth catalyzed S$_E$Ar reaction and Nickel Catalyzed C-H/C-N bond activation**" and recommend that it may be accepted as fulfilling the thesis requirement for the award of Degree of Doctor of Philosophy.

Chairman - Prof. A. Srinivasan   Date: 28.08.'23

Guide / Convener - Dr. Ponneri C. Ravikumar   Date: 28/08/2023

Examiner – Prof. Krishna P. Kaliappan   Date: 28/08/2023

Member 1- Dr. C. S. Purohit   Date: 28/08/2023.

Member 2- Dr. S. Nembenna   Date: 28/08/2023

Member 3- Dr. Tabrez Khan   Date: 28/08/23

        Final approval and acceptance of this thesis is contingent upon the candidate's submission of the final copies of the thesis to HBNI.

        I/We hereby certify that I/we have read this thesis prepared under my/our direction and recommend that it may be accepted as fulfilling the thesis requirement.

Date: 28/08/2023

Signature

Place: NISER, Bhubaneswar

Guide: Dr. Ponneri C. Ravikumar

---

[1] This page is to be included only for final submission after successful completion of viva voce.

STATEMENT BY AUTHOR

This dissertation has been submitted in partial fulfillment of requirements for an advanced degree at Homi Bhabha National Institute (HBNI) and is deposited in the library to be made available to borrowers under rules of the HBNI.

Brief quotations from this dissertation are allowable without special permission, provided that accurate acknowledgement of source is made. Requests for permission for extended quotation from or reproduction of this manuscript in whole or in part may be granted by the Competent Authority of HBNI when in his or her judgment the proposed use of the material is in the interests of scholarship. In all other instances, however, permission must be obtained from the author.

Namrata Prusty

DECLARATION

I, hereby declare that the investigation presented in the thesis has been carried out by me. The work is original and has not been submitted earlier as a whole or in part for a degree / diploma at this or any other Institution / University.

Namrata Prusty

List of Publications

(A) <u>**Published Research Paper**</u> (# pertaining to thesis)**:**

[#]**1)** <u>**Namrata Prusty,**</u> Lakshmana K. Kinthada, Rohit Meena, Rajesh Chebolu, and Ponneri C. Ravikumar. Bismuth(iii)-catalyzed regioselective alkylation of tetrahydroquinolines and indolines towards the synthesis of bioactive core-biaryl oxindoles and CYP19 inhibitors. ***Org. Biomol. Chem.*** **2021**, *19*, 891-905.

[#]**2)** <u>**Namrata Prusty**</u>[†], Shyam Kumar Banjare[†], Smruti Ranjan Mohanty, Tanmayee Nanda, Komal Yadav, and Ponneri C. Ravikumar. Synthesis and Photophysical Study of Heteropolycyclic and Carbazole Motif: Nickel-Catalyzed Chelate-Assisted Cascade C–H Activations/Annulations. ***Org. Lett.*** **2021,** *23*, 9041–9046. (†-*authors contributed equally*)

[#]**3)** <u>**Namrata Prusty,**</u> Smruti Ranjan Mohanty, Shyam Kumar Banjare, Tanmayee Nanda, and Ponneri C. Ravikumar. Switching the Reactivity of the Nickel-Catalyzed Reaction of 2-Pyridones with Alkynes: Easy Access to Polyaryl/Polyalkyl Quinolinones. ***Org. Lett.*** **2022,** *24*, 6122–6127.

[#]**4)** <u>**Namrata Prusty**</u>, Lipsa Gamango, Pragati Biswal, Arijit Sahoo, Soumya Ranjan Bag, and Ponneri C. Ravikumar. Nickel Catalyzed Aromatic C-N Bond activation of 2-Pyridones with Boronic acid: A Easy Access to Phenyl pyridine molecules. (***Manuscript communicated***)

(B) <u>**Book Chapter**</u>**:**

5) Pragati Biswal, <u>**Namrata Prusty**</u>, and Ponneri C. Ravikumar. Synthesis of Heteropolycyclic Aromatic Hydrocarbons Through Directed C-H Functionalization. ***In Handbook of CH-Functionalization, D. Maiti (Ed.) Wiley-VCH Publishers***, **2022**.

(C) Other Research Publications:

6) **<u>Namrata Prusty</u>**, Arijit Sahoo, Lipsa Gamango, Gopal Krusna Das Adhikari and Ponneri C. Ravikumar. Nickel Catalyzed C-H Bond activation for the synthesis of fluorinated compounds. (***Manuscript under preparation***).

7) Smruti Ranjan Mohanty, **<u>Namrata Prusty</u>**, Lokesh Gupta, Pragati Biswal, and Ponneri C. Ravikumar. Cobalt(III)-Catalyzed C-6 Alkenylation of 2-Pyridones by Using Terminal Alkyne with High Regioselectivity. ***J. Org. Chem.*** **2021,** *86*, 9444–9454.

8) Smruti Ranjan Mohanty, **<u>Namrata Prusty</u>**, Shyam Kumar Banjare, Tanmayee Nanda, and Ponneri C. Ravikumar. Overcoming the challenges towards selective C(6)-H functionalisation of 2-pyridone with maleimide through Mn(I)-catalyst: Easy access to all carbon quaternary center. ***Org. Lett***. **2022**, *24*, 848-852.

9) Smruti Ranjan Mohanty, **<u>Namrata Prusty</u>**, Tanmayee Nanda, Shyam Kumar Banjare, and Ponneri C. Ravikumar. Pyridone directed selective Ru catalyzed olefination of sp^2(C-H) bond by using acrylate as reacting partner: Creation of drug analogues. ***J. Org. Chem.*** **2022**, *87*, 6189-6201.

10) Smruti Ranjan Mohanty, **<u>Namrata Prusty</u>**, Tanmayee Nanda, Pranav Shridhar Mahulkar and Ponneri C. Ravikumar. Directing Group Assisted Selective C-H Activation of Six-Membered *N*-heterocycle. *(**Manuscript communicated**)*

11) Pragati Biswal, Tanmayee Nanda, **<u>Namrata Prusty</u>**, Smruti Ranjan Mohanty, and Ponneri C. Ravikumar. Rhodium-Catalyzed Oxidative Annulation of Aniline with N-allylbenzimidazole: Synthesis of 2-Methylindoles via C-N bond Cleavage. ***J. Org. Chem.*** **2023**, *88*, 7988–7997.

12) Gopal Krushna Das Adhikari, Smruti Ranjan Mohanty, Shyam Kumar Banjare, **<u>Namrata Prusty</u>**, Gajiram Murmu, and Ponneri C. Ravikumar. Annulation of Indole-2-Carboxamides

with Bicycloalkenes catalyzed by Ru(II) at room temperature: An easy access to β-carboline-1-one derivatives under mild conditions. ***J. Org. Chem.* 2023,** *88*, 952−959.

13) Gopal Krushna Das Adhikari, Bedadyuti Vedvyas Pati, Smruti Ranjan Mohanty, **<u>Namrata Prusty</u>**, and Ponneri C. Ravikumar. Co(II) Catalyzed C-H/N-H Annulation of Cyclic Alkenes with Benzamides at room temperature: An access to the core skeleton of hexahydrobenzo[c]phenanthridine-type alkaloids. ***Asian J. Org. Chem.* 2022,** *11*, e202200150.

14) Shyam Kumar Banjare, Annapurna Saxsena, Tanmayee Nanda, **<u>Namrata Prusty</u>**, and Ponneri. C. Ravikumar. Weak-chelation assisted regioselective ortho-(sp^2)-H ethynylation of *N*-aryl γ-lactam utilizing cobalt (III)-catalyst. ***Org. Lett.* 2023,** *25*, 251−255.

15) Tanmayee Nanda, Shubham Kumar Dhal, Gopal Krushna Das Adhikari, **<u>Namrata Prusty</u>**, and Ponneri C. Ravikumar. Olefination, and Carboamination: Revealing Two different Pathways in ortho C-H Functionalization of Phenol. ***Chem. Commun.* 2023**, *59*, 8818-8821.

Conferences:

1. "Regioselective C-6 Functionalization of Tetrahydroquinolines" **<u>Namrata Prusty</u>**, Lakshman K. Kinthada, Rohit Meena, Rajesh Chebolu, and Ponneri C. Ravikumar*; National Conference on Organic Synthesis (**N-COS-2020**), Organized by PG Department of Chemistry, Berhampur University, Odisha during 02-03 March, 2020. (**In-person poster presentation and, Short oral presentation**)

2. Facile Synthesis of Hetero-polycyclic and Carbazole Motif through Nickel-Catalyzed Chelate Assisted Cascade C-H Activations/Annulations" Namrata Prusty†, Shyam Kumar Banjare†, Smruti Ranjan Mohanty, Tanmayee Nanda, and Ponneri C. Ravikumar*; 27th CRSI-NSC Kolkata four-day symposium (hybrid mode **poster presentation**) held on 26th to 29th September, 2021.

3. 'Synthesis and Photophysical Study of Hetero-polycyclic and Carbazole Motif: Nickel-Catalyzed Chelate Assisted Cascade C-H Activations/Annulations" **<u>Namrata Prusty</u>**†, Shyam Kumar Banjare†, Smruti Ranjan Mohanty, Tanmayee Nanda, Komal Yadav, and Ponneri C. Ravikumar*; Presented in National Conference on Recent Advances in Heterocyclic Chemistry (**RAHC-2022**), Ravenshaw University, Cuttack, Odisha (online **oral presentation**).

Namrata Prusty

Dedicated to

My Father
Mr. Nimain Charan Prusty
&
My Mother
Mrs. Urmila Prusty

ACKNOWLEDGEMENTS

CONTENTS

Chapter 1: **Introduction to electrophilic aromatic substitution reaction for C-C bond formation** (**Scheme 1**).

Abstract: Electrophilic aromatic substitution (S_EAr) reactions are useful method to construct C-C bonds. Friedel Craft reaction is an important class of S_EAr for C-C bond formation. The major limitation of this reaction is the use of stoichiometric metal reagents and regioselectivity (*ortho/para*). Therefore, milder and catalytic version of Friedel Crafts reaction would be more advantageous in terms of limiting the use of reagent, and regioselectivity. In recent years there has been an increased activity to study this reaction under catalytic conditions.

N-heteroarenes are found to be the core structure of many biologically active compounds and pharmaceuticals. Hence, functionalization of N-heterocycles is an important aspect of medicinal chemistry wherein substituents could help increase the affinity of these compounds for a certain biological target. In this regard Catalytic Friedel Craft reaction would be a useful tool for direct functionalization of aromatic C-H bonds.
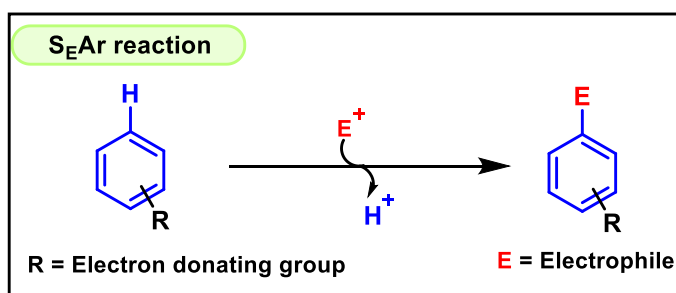
Scheme 1: S_EAr reaction for C-C bond formation

Chapter 2. **Bismuth(III)-catalyzed regioselective alkylation of tetrahydroquinolines and indolines towards the synthesis of bioactive core-biaryl oxindoles and CYP19 inhibitors.**

Abstract: We described bismuth (III)-catalyzed regioselective functionalization at C-6 position of tetrahydroquinolines and C-5 position of indolines (**Scheme 2**). For the first

time, one pot symmetrical and unsymmetrical arylation of isatins with tetrahydroquinolines was accomplished giving a completely new product skeleton in good to excellent yields. Most importantly, this protocol leads to the formation of a challenging highly strained quaternary carbon stereogenic center. Benzhydryl and 1-phenylethyl trichloroacetimidates have been used as the alkylating partners to functionalize the C-6 and C-5 positions of tetrahydroquinolines and indolines respectively. The scope of the developed methodology has been extended for the synthesis of bioactive CYP19-inhibitor analogue.
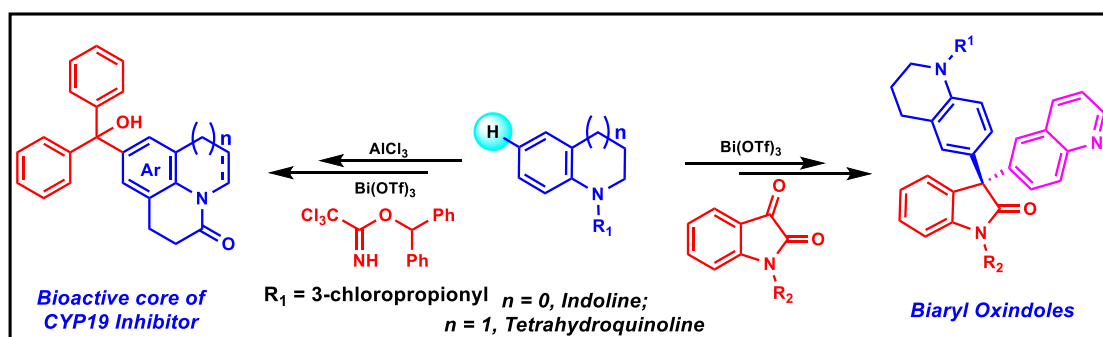
Scheme 2: Alkylation of tetrahydroquinoline and indoline using Bismuth catalyst

Chapter 3: Introduction to C-H bond activation for C-C bond formation.

Abstract: The transition metal catalyzed C-H bond activation has been used as an efficient method to construct C-C bonds on a heterocyclic moiety (**Scheme 3**). Directed C-H activation enables the synthesis and selective functionalization of more complex molecules of importance in medicinal chemistry and pharmaceuticals. In transition metal catalyzed C-H bond activation reaction, the use of 3d transition metal catalyst has received considerable attention in recent years as compared to 4d and 5d metal. It is because of their low cost, unique reactivity profiles, and high earth crust abundance. Among the first row-transition metals, nickel (Ni) catalysts have drawn considerable attention in recent years because of its ability to exhibit variable oxidation states which enables catalytic reactions that are mechanistically distinct from other metals. Moreover, it is isoelectronic to palladium.
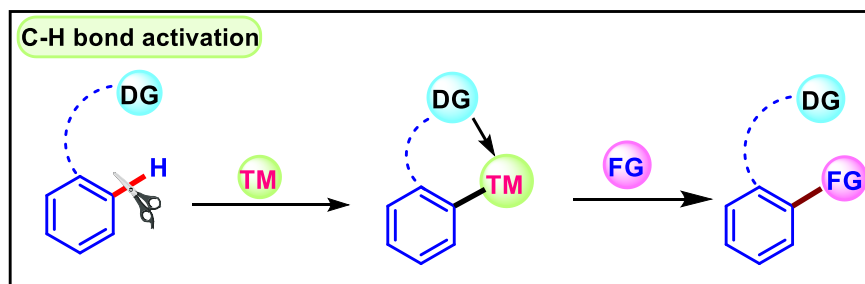
Scheme 3: Nickel catalyzed C-H bond activation for C-C bond formation.

Chapter 4. **Synthesis and Photophysical Study of Hetero-polycyclic and Carbazole Motif: Nickel-Catalyzed Chelate Assisted Cascade C-H Activations/Annulations.**

Abstract: Here, a nickel catalyzed synthesis of polyarylcarbazole through sequential C-H bond activations has been described (**Scheme 4**). Regioselective indole C2/C3 functionalization has been achieved in presence of indole C(7)-H which is quite challenging. Further, this approach also gives easy access to building hetero-polycyclic motif through C6/C7 C-H functionalization of indoline. This methodology is not only limited to aromatic internal alkynes as coupling partners, aliphatic alkynes have also shown good tolerance. Notably, during the optimization we have observed the catalytic enhancement with sodium iodide as an additive. We have also studied the photophysical properties of these highly conjugated molecules.
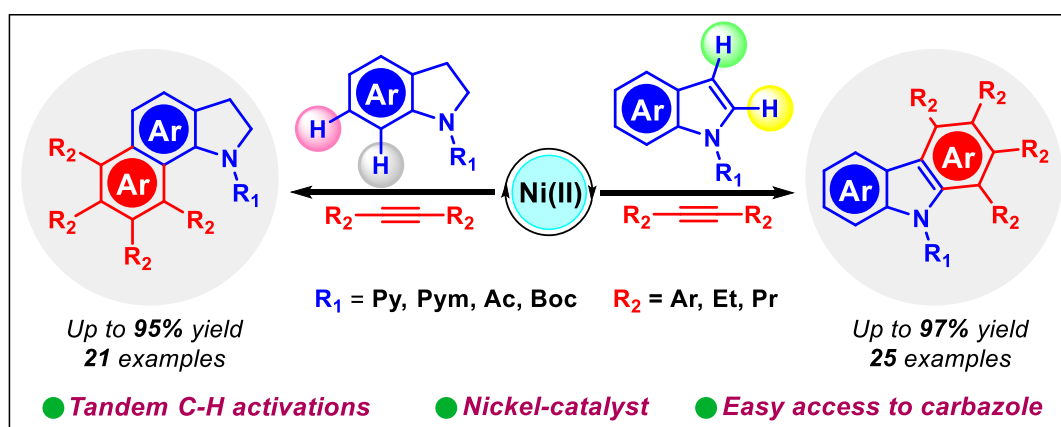
Scheme 4: Nickel catalyzed cascade C-H bond activation of indoline and indole.

Chapter 5. **Switching the Reactivity of Nickel Catalyzed reaction of 2-Pyridones with Alkynes: Easy Access to Poly-Aryl/Alkyl Quinolinones.**

Abstract: A Ni-catalyzed C6- followed by C5 cascade C-H activation/[2+2+2] annulation of 2-pyridone with alkynes has been achieved (**Scheme 5**). A change in the reaction pathway was achieved by tuning the reaction condition and incorporation of the directing group. A wide variety of substrates and alkynes are amenable to this transformation. The key to success for this transformation is the use of sodium iodide as an additive. More importantly, we detected the five-membered metallacyclic intermediate through HRMS wherein iodide is ligated to the metal.
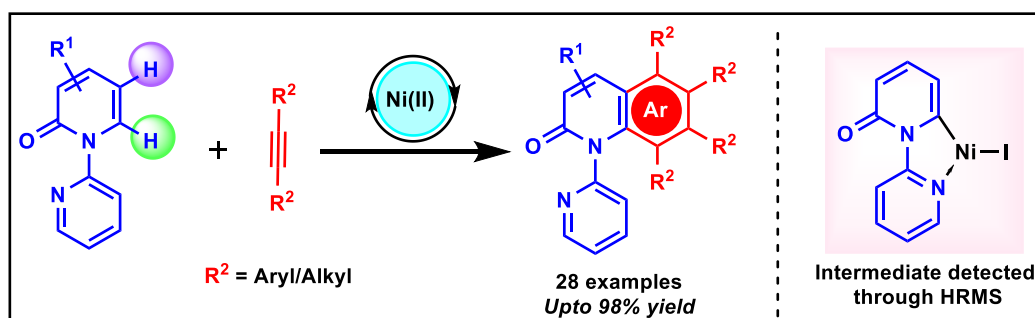
Scheme 5: Nickel catalyzed cascade C-H bond activation of 2-pyridylpyridone.

Chapter 6: **Introduction to Nickel catalyzed C-N activation for C-C bond formation.**

Abstract: The C−N bond is one of the most abundant chemical bonds found in many organic molecules. The activation and transformation of C−N bonds by using transition-metal catalysis has emerged as a powerful tool for the formation of C−C, C-N, C-X (X = O, S) bond. As compared to catalytic C−H bond activation reactions, transition-metal catalyzed C−N bond activation is considerably underexplored. It has been identified as an emerging area of organic transformations. Transition metal mediated C–N bond activation reactions have been found to be a key step in several catalytic coupling methods. The reactive M-C-N

intermediate formed from the inert C–N bond activation reacts with suitable coupling partners to form new C-C bonds (**Scheme 6**).
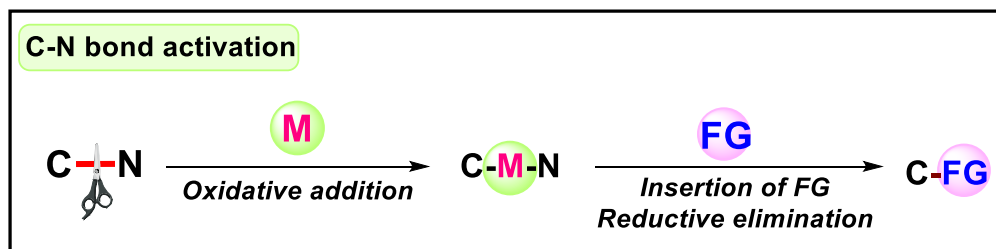
Scheme 6: Nickel catalyzed C-N bond activation for C-C bond formation.

Chapter 7. Nickel Catalyzed Aromatic C-N Bond activation of 2-Pyridylpyridones for the synthesis of substituted Phenylpyridines using Boronic acid as coupling partner

Abstract: We have demonstrated a nickel-catalyzed aromatic C-N bond activation of 2-pyridylpyridone to afford phenyl pyridine by using phenyl boronic acid as coupling partner (**Scheme 7**). Although amines have been extensively researched for a long time, their use in synthetic processes has remained restricted to methods that involve the breakage of the amine C-N bond. We have found that amines can be used for the synthesis of substituted 2-phenylpyridine using Ni catalysis. This approach offers new tools to synthesize C-C bonds that are used in multi-step synthesis. A wide variety of substrates and boronic acids are amenable to this transformation.

Scheme 7: Nickel catalyzed aromatic C-N bond activation of 2-pyridylpyridone.

List of figures

List of schemes

List of tables

List of Abbreviations

DG	Directing group
FG	Functional group
NMR	Nuclear magnetic resonance
^{1}H NMR	Proton nuclear magnetic resonance
^{13}C NMR	Carbon nuclear magnetic resonance
MHz	Megahertz
ppm	Parts per million
IR	Infrared
$CHCl_3$	Chloroform
$CDCl_3$	Chloroform-d
HRMS	High resolution mass spectrometry
calcd	Calculated
mg	milligram
mmol	millimole
mp	melting point
mL	milliliter
min.	minute
h	hour
Fig.	Figure
TLC	Thin-layer chromatography
UV	Ultraviolet

DMF	Dimethylformamide
MeCN	Acetonitrile
DCE	1,2-dichloroethane
PhMe	Toluene
THF	Tetrahydrofuran
TFE	Trifluoroethanol
EtOAc	Ethylacetate
DCM	Dichloromethane
MeOH	Methanol
EtOH	Ethanol
^{t}BuOH	*tert*-Butanol
Et$_2$O	Diethylether
AcOH	Acetic acid
Ac$_2$O	Acetic anhydride
Et$_3$N	Triethylamine
DIAD	Diisopropyl azodicarboxylate
DMAP	4-Dimethylaminopyridine
DBU	Diazabicycloundacane
CCl$_3$CN	Trichloroacetonitrile
NaH	Sodium hydride
Bi(OTf)$_3$	Bismuth triflate
In(OTf)$_3$	Indium triflate
ZnCl$_2$	Zinc chloride
AlCl$_3$	Aluminium chloride

NaHCO$_3$	Sodium bicarbonate
Na$_2$SO$_4$	Sodium sulfate
OTf	trifluoromethanesulfonate
Ts	Tosyl
Ms	Mesyl
Bn	Benzyl
NaBH$_4$	Sodium borohydride
NaBH$_3$CN	Sodium cyano borohydride
CuI	Copper iodide
K$_2$CO$_3$	Potassium carbonate
K$_3$PO$_4$	Tripotassium phosphate
Ni(OTf)$_2$	Nickel trifluoromethanesulfonate
Ni(acac)$_2$	Nickel bis(acetylacetonate
PPh$_3$	Triphenyl phosphine
NaI	Sodium iodide
Py	Pyridine
Pym	Pyrimidine
DDQ	2,3-Dichloro-5,6-dicyano-1,4-benzoquinone
DMEDA	Dimethylethylenediamine
MeOTf	Methyl trifluoromethanesulfonate
BHT	Butylated hydroxytoluene
TEMPO	(2,2,6,6-Tetramethylpiperidin-1-yl)oxyl
rt	Room temperature

Chapter 1

Introduction to Electrophilic Aromatic Substitution Reaction

Chapter 1

Introduction to Electrophilic Aromatic Substitution Reaction
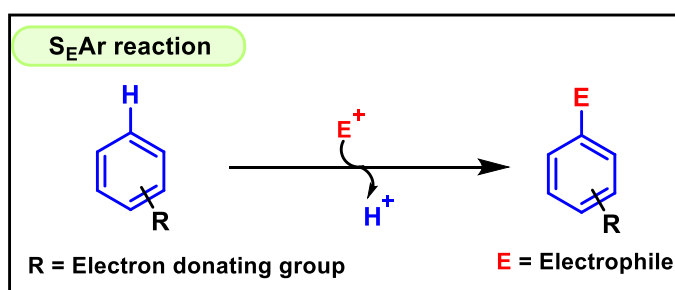
1.1 INTRODUCTION

Electrophilic aromatic substitution (S_EAr) reactions are one of the most researched and useful reactions in organic synthesis.[1] In an electrophilic aromatic substitution process, a hydrogen atom connected to an aromatic molecule is replaced by an electrophile to give a substituted product (Figure 1.1), but only when a catalyst is present. This approach is commonly employed to incorporate functional groups into aromatic rings. Because it involves breaking a C–H bond and forming a new C–E bond (where E is an electrophilic atom like Cl, Br, N, or S), the process is known as " C–H bond functionalization method."

Figure 1.1: Schematic Diagram of S_EAr reaction
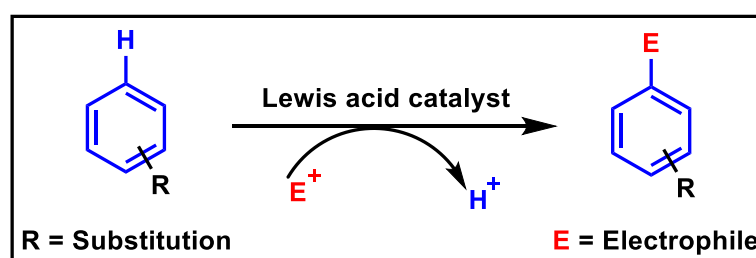
1.2 TYPES OF S_EAr REACTIONS:

In general, there are about six important electrophilic aromatic substitution reactions in organic chemistry, for example: Friedel-Crafts acylation, Friedel-Crafts alkylation

chlorination, bromination, nitration, and sulfonation (Figure 1.2).[2] For the relatively inert

aromatic ring to engage in assault, each of these reactions needs an acid catalyst to activate

the electrophile so that the relatively unreactive aromatic ring will attack it.

Friedel-Craft Acylation: In Friedel-Craft acylation, the aromatic ring reacts with the acyl

halide breaking the C–H bond to produce carbon-carbon bonds to aromatic molecules in

presence of Lewis acids.

Figure 1.2: Types of S_EAr reactions

SI no.	Electrophile	Lewis Acid	E	Name
1	Cl_2	$AlCl_3/FeCl_3$	Cl	Chlorination
2	Br_2	$AlBr_3/FeBr_3$	Br	Bromination
3	HNO_3	H_2SO_4	NO_2	Nitration
4	SO_3	H_2SO_4	SO_3H	Sulfonation
5	R-X	$AlCl_3/FeCl_3$	R	Friedel-Crafts Alkylation
6	R-C(=O)-X	$AlCl_3/FeCl_3$	R-C(=O)-	Friedel-Crafts Acylation

Friedel-Craft Alkylation:

In Friedel-Craft alkylation, the aromatic ring reacts with the alkyl halide to form alkylated

arene ring. The Lewis acid activate the alkyl halide thereby enabling the attack of arene

ring on the electrophilic carbon alkyl halide.

Halogenation (Cl/Br): At room temperature and in the presence of a Lewis acid catalyst,

benzene reacts with chlorine or bromine, replacing one of the hydrogen atoms on the ring

with chlorine or bromine atom.

Nitration: At a temperature of no more than 50 °C, benzene combines with concentrated nitric acid and concentrated sulfuric acid to produce nitrobenzene, in which the NO_2 group replaces the hydrogen atom from the aromatic ring.

Sulphonation: Sulphonation is the process where hydrogen atom of aromatic ring replaced with a sulfonic acid (-SO_3H) functional group. The reaction occurs at a higher-temperature.

1.3 MECHANISM OF ELECTROPHILIC AROMATIC SUBSTITUTION

In the initial stage of electrophilic aromatic substitution, the electrophile gets a pair of electrons from the aromatic ring (Figure 1.3). However, aromatic compounds are substantially less reactive since this electron pair forms part of a delocalized aromatic sextet. They show such a lack of reactivity that the generation of an electrophile should be strong enough to react with the aromatic ring which requires use of a Lewis acid as a catalyst. A carbocation intermediate formed as a result of addition of electrophile to the aromatic ring. Usually, the first step is the rate-determining step in electrophilic aromatic substitution. Because of the formation of new sigma bond in the first step, the intermediate is called a sigma complex (also called as Wheland intermediate).[3]

Figure 1.3: Representation of a typical electrophilic aromatic substitution (EAS) reaction mechanism
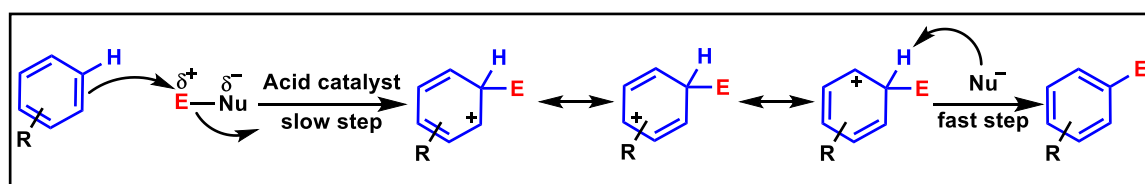
Despite being resonance stabilized, the carbocation has only four π-electrons, hence it is not an aromatic. Therefore, compared to the initial aromatic ring, the sigma complex is substantially more reactive. So, in presence of nucleophile, the second step is fast which leads to the electrophile substituted aromatic compound.

1.4 EFFECTS OF RING SUBSTITUENTS ON REACTION RATE

The aromatic ring bearing electron donating group (EDG) react faster than benzene, because they make the aromatic ring more reactive; hence they are activating groups.[1]

Figure 1.4: Effects of Ring Substituents on aromatic ring
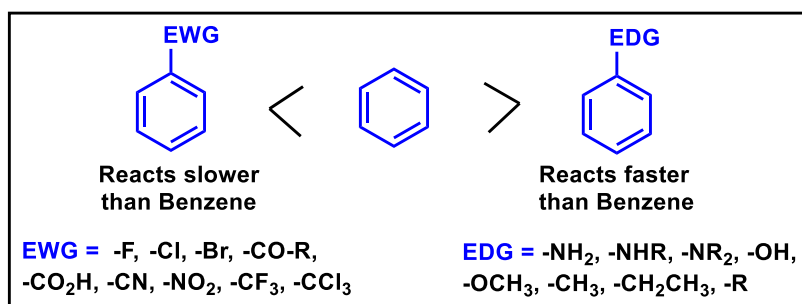
On the other hand, aromatic ring bearing electron withdrawing group (EWG) react slowly than benzene. As a result of making the aromatic ring less reactive, these groups are deactivating groups. (Figure 1.4).

1.5 SUBSTITUENT EFFECTS AND PRODUCT DISTRIBUTION IN ELECTROPHILIC AROMATIC SUBSTITUTION REACTIONS

If a substituent is already present in the aromatic ring, it shows ring attack by the incoming electrophile to attach the second substituent to the ring. Only one product is observed for a single substitution in the benzene ring. However, in case of second substitution, there is a possibility of formation of product from any of the three *ortho*, *meta*, *para* isomers. If the substituent is electron donating group (EDG), it directs the incoming substitution at *ortho* and *para* position whereas, if the substituent is electron withdrawing group (EWG), it directs the incoming substitution at *meta* position. Now consider the example of the product distribution from the nitration of toluene (Scheme 1.1). In this case, the nitro group can attack the ring from three different sites forming the possible *o*-, *m*-, *p*-nitrotoluene product.

From the product distribution, it was found that the *ortho* and *para* isomers predominate over the *meta* isomer which formed in very small amounts. Therefore, in this instance, the methyl group acts as an *ortho*, *para* director by directing or orienting the entering substituent into positions *ortho* and *para* to itself.

Scheme 1.1: Effects of EDG substituent of aromatic ring in the S_EAr reaction
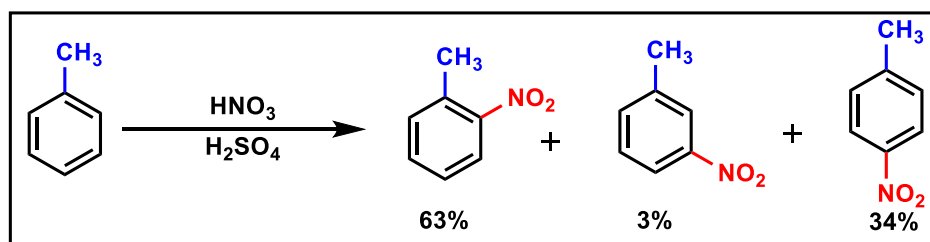
Considering another example of a nitration reaction of nitrobenzene (Scheme 1.2), incoming nitro group goes to *meta* position. Minor quantities of the *ortho* and *para* isomers are also formed.

Scheme 1.2: Effects of EWG substituent of aromatic ring in the S_EAr reaction
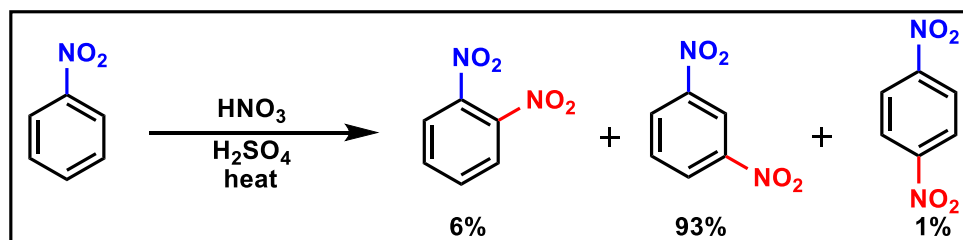
According to the literature reports and the above discussion, it is noted that a mixture of products is typically produced in the electrophilic substitution reaction, demonstrating the regioselectivity issue with the reaction. And later, in order to achieve good regio/site selectivity in S_EAr substitution processes, this issue was addressed by several researchers with the use of Lewis acid catalyst.

And using Lewis acid catalyst, Friedel-Craft alkylation reaction is one of the S_EAr reactions which plays an important role in functionalising of C–H bond of aromatic ring and forming C–C bond.[4]

1.6 FRIEDEL-CRAFT ALKYLATION

In 1887 Charles Friedel and James Mason Crafts proposed the first example of Friedel–Crafts alkylation (Friedel-Craft alkylation) by using Lewis acid catalyst ($AlCl_3$) for the first time, synthesized amylbenzene from the reaction of amyl chloride in benzene with $AlCl_3$ catalyst (Scheme 1.3).[5]

Scheme 1.3: AlCl₃ mediated first Friedel craft alkylation reaction between amyl chloride and benzene
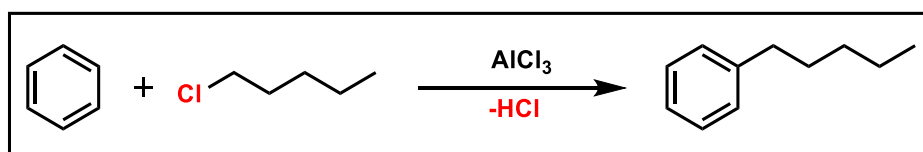
In the subsequent years, many additional Lewis acids, including BF_3, $BeCl_2$, $TiCl_4$, $SbCl_5$, or $SnCl_4$, have been considered as catalyst in Friedel-Craft alkylation reaction. Powerful Bronsted-acids like hydrofluoric acid, sulfuric acid, or super acids like $HSO_3F \cdot SbF_5$ and $HF \cdot SbF_5$ have also been observed to carry out this reaction.[6]

Despite its enormous utility, Friedel-Crafts alkylation has significant drawbacks because toxic alkyl halides and use of stoichiometric or super stoichiometric amounts of a Lewis acid or Bronsted acid results in significant amounts of salt side products.[6] Hence, the development of Friedel-Craft reactions employing just catalytic quantities of a metal or acid catalyst would be particularly desirable due to the requirement of more environmentally and economically sustainable processes.

Scheme 1.4: Scandium triflate mediated catalytic Friedel craft alkylation reaction
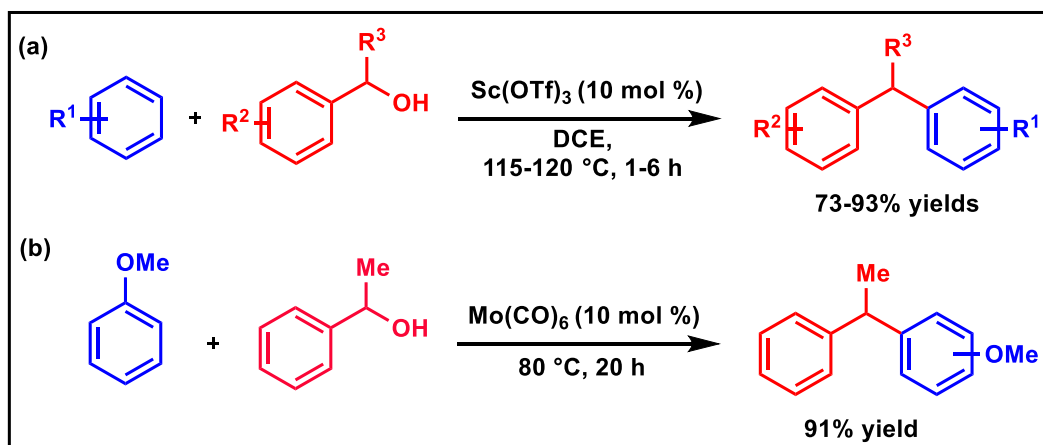
After several research, the first catalytic Friedel-Craft alkylation reaction has independently been performed by Fukuzawa[7] and Shimizu[8] et al. in 1996 and 1997 respectively where they have taken alcohol as the alkylating reagent. $Sc(OTf)_3$ has been used by the Fukuzawa group as a moisture and air stable catalyst (Scheme 1.4a), whereas the Shimizu group used the Lewis acid catalyst, $Mo(CO)_6$ (10 mol%) under the strict avoidance of air and atmospheric moisture (Scheme 1.4b). The desired 1,1-diarylalkanes were obtained in high yields by alkylating a variety of arenes, such as *p*-xylene, benzene, or mesitylenes, with benzyl alcohols.

After achieving this, new protocols using a range of Lewis and Bronsted acids were developed, leading to lower catalyst loadings, and consequently enhancing efficiency. Many catalytic Friedel-Craft alkylations using alcohols have been reported utilizing $Cl_2Si(OTf)_2$, $Hf(OTf)_4$,[9] $Yb(OTf)_3$, $La(OTf)_3$,[10] $InCl_3$,[11] $NbCl_5$,[12] strong Brønsted acids[13] as catalysts.

In this context, bismuth salts have proven to be effective catalysts because they are non-toxic, cost-effective, and easily accessible catalysts with Lewis acidic characteristics. Hence, the Rueping group chose to investigate the bismuth-catalyzed benzylation of arenes

and heteroarenes (Scheme 1.5a) in 2006 given that some bismuth salts are compatible with air and moisture.[14] This environmentally benign method is appealing for producing

Scheme 1.5: Catalytic Friedel-Crafts reaction
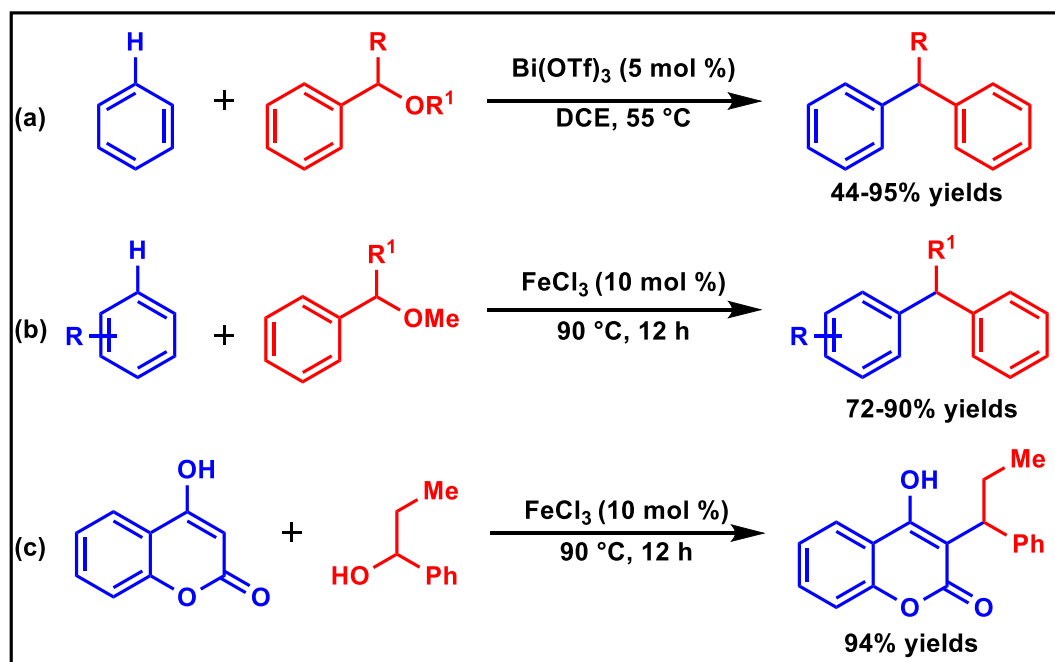
diarylmethane derivatives due to the mild reaction conditions, high yields, broad substrate scope, and astonishingly low catalyst loading. Shi et al. reported a Friedel-Crafts alkylation method in 2008 in which a variety of benzyl methyl ethers were efficiently transformed to benzyl arenes in mild reaction conditions (Scheme 1.5b).[15] Aryl heteroaryl methanes and di- or tri-aryl methanes were also easily and practically synthesized using this method. The efficient iron(III)-catalyzed one-step synthesis of phenprocoumon was proposed by Beller group in 2007,[16] which is a common warfarin-class anticoagulant used in thrombosis prophylaxis, serves as an example of this catalytic Friedel-Craft reaction. Phenprocoumon was effectively synthesized from 4- hydroxycoumarin and 1-phenylpropan-1-ol in a 94% yield (Scheme 1.5c).

1.7 FRIEDEL-CRAFT REACTIONS IN VARIOUS HETEROARENE

There are many reports of Friedel-Craft alkylation with heteroarene compounds. To synthesize novel C6-substituted tetrahydroquinolines, Meshram *et al.* (2017) proposed a straightforward and inventive technique for the C6-functionalization of unprotected tetrahydroquinoline with chromenes or *β*-nitrostyrenes in water (Scheme 1.6).[17]

Scheme 1.6: Reaction of tetrahydroquinoline with chromenes or *β*-nitrostyrenes
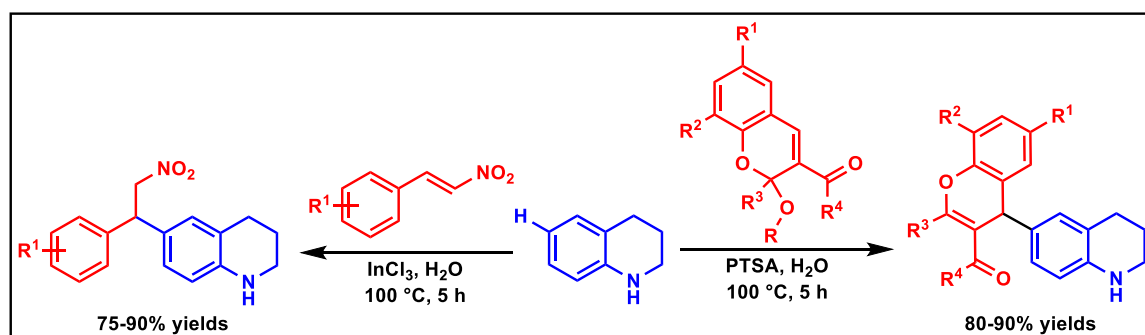
This process is simple and efficient, with minimal costs and mild reaction conditions. The C6-alkylated products of tetrahydroquinoline were produced with good regioselectivity, avoiding the production of compounds that are C5, C7, C8, or *N*-alkylated.

Scheme 1.7: Reaction of aniline with glyoxylates
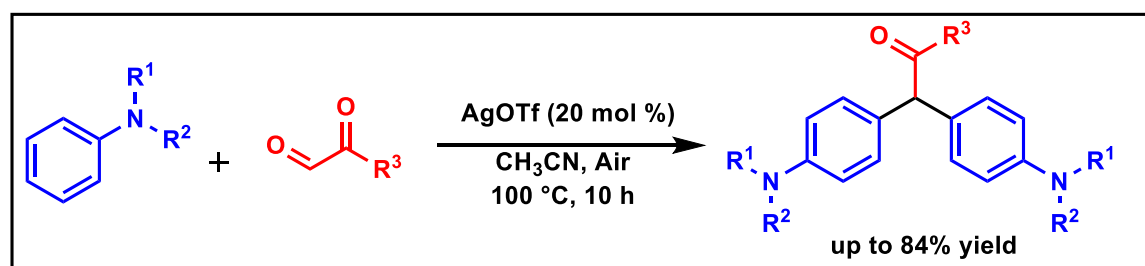
In 2022, Pan et al. developed a Lewis-acid-catalyzed reaction involving anilines and glyoxylates for the production of diarylmethanes (Scheme 1.7).[18] A number of anilines-based diarylmethanes, bearing 1°, 2°, and 3° anilines, were produced in good yields under the AgOTf catalysis.

1.8 FRIEDEL-CRAFT REACTIONS WITH VARIOUS COUPLING PARTNER

The Friedel-Crafts alkylation reaction has employed a wide range of alkylating partners, including alcohols, alkyl halides, ethers, alkenes, and aldehydes. Isatins (1*H*-indole-2,3-dione) are flexible synthetic substrates utilized as precursors for the synthesis of a wide range of heterocyclic compounds, including indoles and quinolines.[19] Over the past two decades, there has been a substantial advancement in the use of isatins for chemical synthesis. In this regard, Halperin et al. in 2004 reported the synthesis of a number of substituted 3,3-biaryl-1,3-dihydroindol-2-ones from the corresponding isatins.[20] Using a two-step process, the unsymmetric compounds were produced. Using properly substituted aryl magnesium halide, the initial step comprised a Grignard addition to isatin. The crucial second step involved in generating a quaternary center at the 3-position of the oxindole ring, which was achieved by condensation of monoarylated product with an appropriate aromatic ring to generate diaryloxindoles C using the Friedel-Crafts method (Scheme 1.8a).

Scheme 1.8: Reaction of isatin as electrophile with arene
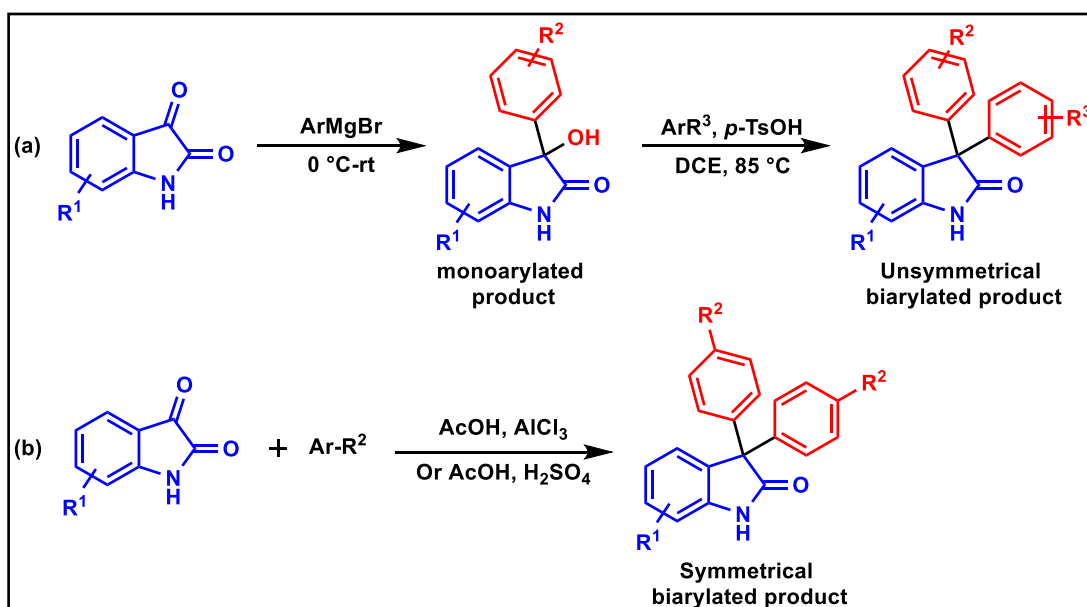
Later in 2005, Neel et al. and in 2007, Uddin et al. independently reported the synthesis of symmetrical 3,3-Bisaryloxindoles[21] employing isatin with substituted phenyl derivatives in a Friedel-Crafts reaction (Scheme 1.8b).

Scheme 1.9: Reaction of trichloroacetimidate as electrophile with arene
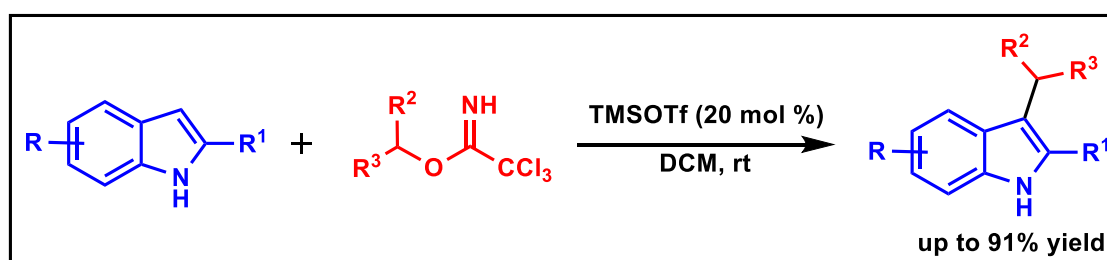
In the alkylation of various functional groups, such as anilines, sulfonamides, alcohols, carboxylic acids, thiols, electron-rich alkenes, and aromatic systems, another coupling partner, trichloroacetimidates, usually act as electrophiles.[22] The imidate has a basic nitrogen that, in mild circumstances, can be activated by a catalytic quantity of a Lewis acid. The conversion of the imidate leaving group to trichloroacetamide is the driving force for alkylation and facilitates imidate displacement. By facilitating Friedel-Crafts alkylations, this rearrangement only needs a catalytic quantity of a Lewis acid.

1.9 CONCLUSION

In this chapter, we have discussed the Electrophilic aromatic substitution reaction methods for the synthesis of *N*-heterocyclic molecules. The major limitations of S_EAr reactions are regeoselectivity, use of stoichiometric amount of acid catalyst and the production of large amounts of salt by-products. And this can be overcome by using appropriate metal salt as the Lewis acid catalyst. It is also observed that using of catalytic amount of Lewis acid catalyst affording the product with good regioselectivity employing Friedel-Craft alkylation method.

1.10 REFERENCES:

1. Klumpp, D.A. Electrophilic Aromatic Substitution. *In Arene Chemistry,* John Wiley & Sons, Inc, **2015***,* pp. 1.

2. Kapoor, Y.; Kumar, K. Aromatic Substitution Reactions: An Overview. *SF J Pharm Anal Chem.* **2020**, *3*, 1019.

3. Stuyver, T.; Danovich, D.; De Proft, F.; Shaik, S. Electrophilic Aromatic Substitution Reactions: Mechanistic Landscape, Electrostatic and Electric-Field Control of Reaction Rates, and Mechanistic Crossovers. *J. Am. Chem. Soc.* **2019**, *141*, 9719−9730.

4. (a) Roberts, R. M.: Khalaf, A. A. Friedel-Crafts Alkylation Chemistry. A Century of Discovery; Marcel Dekker: New York, **1984**. (b) Olah, G. A.; Krishnamurit, R.; Prakash, G. K. S. Friedel-Crafts Alkylation in Comprehensive Organic Synthesis; Trost, B. M.; Fleming, I., Eds.; Pergamon: Oxford, UK, **1991**, Vol. *3*, Chapter 1.8, p 293.

5. Friedel, C.; Crafts, J. M. Organic Chemistry. *J. Chem. Soc.* **1877**, *32*, 725–791.

6. Rueping, M.; Nachtsheim, B. J. A Review of New Developments in the Friedel-Crafts Alkylation - from Green Chemistry to Asymmetric Catalysis. *Beilstein J. Org. Chem.* **2010**, *6*, 1–24.

7. (a) Tsuchimoto, T.; Tobita, K.; Hiyama, T.; Fukuzawa, S.-i. Scandium(III) Triflate Catalyzed Friedel-Crafts Alkylation with Benzyl and Allyl Alcohols. *Synlett* **1996**, 557–559. (b) Tsuchimoto, T.; Tobita, K.; Hiyama, T.; Fukuzawa, S.-i. Scandium(III) Triflate-Catalyzed Friedel−Crafts Alkylation Reactions. *J. Org. Chem.* **1997**, *62*, 6997–7005.

8. Shimizu, I.; Khien, K. M.; Nagatomo, M.; Nakajima, T.; Yamamoto, A. Molybdenum-Catalyzed Aromatic Substitution with Olefins and Alcohols. *Chem. Lett.* **1997**, *26*, 851–852.

9. Shiina, I.; Suzuki, M. The catalytic Friedel–Crafts alkylation reaction of aromatic compounds with benzyl or allyl silyl ethers using $Cl_2Si(OTf)_2$ or $Hf(OTf)_4$. *Tetrahedron Lett.* **2002**, *43*, 6391–6394.

10. Noji, M.; Ohno, T.; Fuji, K.; Futaba, N.; Tajima, H.; Ishii, K. Secondary Benzylation Using Benzyl Alcohols Catalyzed by Lanthanoid, Scandium, and Hafnium Triflate. *J. Org. Chem.* **2003**, *68*, 9340–9347.

11. (a) Sun, H.-B.; Li, B.; Chen, S.; Li, J.; Hua, R. An efficient synthesis of unsymmetrical diarylmethanes from the dehydration of arenes with benzyl alcohols using InCl$_3$·4H$_2$O/acetylacetone catalyst system. *Tetrahedron* **2007**, *63*, 10185–10188. (b) Sun, G.; Sun, H.; Wang, Z.; Zhou, M.-M. A Novel InCl$_3$/SiO$_2$-Catalyzed Hydroarylation of Arenes with Styrenes under Solvent-Free Conditions. *Synlett* **2008**, *7*, 1096–1100.

12. Yadav, J. S.; Bhunia, D. C.; Krishna, K. V.; Srihari, P. Niobium(V) pentachloride: an efficient catalyst for C–, N–, O–, and S-nucleophilic substitution reactions of benzylic alcohols. *Tetrahedron Lett.* **2007**, *48*, 8306–8310.

13. (a) Le Bras, J.; Muzart, J. Brønsted-acid-catalyzed coupling of electron-rich arenes with substituted allylic and secondary benzylic alcohols. *Tetrahedron* **2007**, *63*, 7942–7948. (b) Sanz, R.; Martínez, A.; Miguel, D.; Álvarez-Gutiérrez, J. M.; Rodríguez, F. Brønsted Acid-Catalyzed Nucleophilic Substitution of Alcohols. *Adv. Synth. Catal.* **2006**, *348*, 1841–1845. (c) Sanz, R.; Miguel, D.; Álvarez-Gutiérrez, J. M.; Rodríguez, F. Brønsted Acid Catalyzed C3-Selective Propargylation and Benzylation of Indoles with Tertiary Alcohols. *Synlett* **2008**, *7*, 975–978.

14. Rueping, M.; Nachtsheim, B. J.; Ieawsuwan W. An Effective Bismuth-Catalyzed Benzylation of Arenes and Heteroarenes. *Adv. Synth. Catal.* **2006**, *348*, 1033–1037.

15. Wang, B.-Q.; Xiang, S.-K.; Sun, Z.-P.; Guan, B.-T.; Hu, P.; Zhao, K.-Q.; Shi, Z.-J. Benzylation of arenes through FeCl$_3$-catalyzed Friedel–Crafts reaction *via* C–O activation of benzyl ether. *Tetrahedron Lett.* **2008**, *49*, 4310–4312.

16. Kischel, J.; Mertins, K.; Michalik, D.; Zapf, A.; Beller, M. A General and Efficient Iron-Catalyzed Benzylation of 1,3-Dicarbonyl Compounds. *Adv. Synth. Catal.* **2007**, *349*, 865−870.

17. Kumar, N. S.; Kumar, R. N. N.; Rao, L. C.; Muthineni, N.; Ramesh, T.; Babu, N. J.; Meshram, H. M. Acid-catalyzed protocol for the synthesis of novel 6-substituted tetrahydroquinolines by highly regioselective C6-functionalization of tetrahydroquinolines with chromene hemiacetals or *β*-nitrostyrenes. *Synthesis* **2017**, *49*, 3171–3182.

18. Li, W.; Wang, D.; Liang, X.; Jin, Z.; Zhou, S.; Chen, G.; Pan, Y. Lewis-Acid-Catalyzed Selective Friedel–Crafts Reaction or Annulation between Anilines and Glyoxylates. *Org. Lett.* **2022**, *24*, 3086−3091.

19. Klumpp, D. A.; Yeung, K. Y.; Prakash, G. K. S.; Olah, G. A. Preparation of 3,3-diaryloxindoles by superacid-induced condensations of isatins and aromatics with a combinatorial approach. *J. Org. Chem.* **1998**, *63*, 4481−4484.

20. Natarajan, A.; Fan, Y.-H.; Chen, H.; Guo, Y.; Iyasere, J.; Harbinski, F.; Christ, W. J.; Aktas, H.; Halperin, J. A. 3,3-Diaryl-1,3-Dihydroindol-2-Ones as Antiproliferatives Mediated by Translation Initiation Inhibition. *J. Med. Chem.* **2004**, *47*, 1882–1885.

21. (a) Neel, D. A.; Brown, M. L.; Lander, P. A.; Grese, T. A.; Defauw, J. M.; Doti, R. A.; Fields, T.; Kelley, S. A.; Smith, S.; Zimmerman, K. M.; Steinberg, M. I.; Jadhav, P. K. 3,3-Bisaryloxindoles as mineralocorticoid receptor antagonists. *Bioorg. Med. Chem. Lett.* **2005**, *15*, 2553−2557. (b) Uddin, M. K.; Reignier, S. G.; Coulter, T.; Montalbetti, C.; Grånäs, C.; Butcher, S.; Krog-Jensen, C.; Felding, J. Syntheses and antiproliferative evaluation of oxyphenisatin derivatives. *Bioorg. Med. Chem. Lett.* **2007**, *17*, 2854−2857.

22. Suzuki, T.; Chisholm, J. D. Friedel-Crafts Alkylation of Indoles with Trichloroacetimidates. *Tetrahedron Lett.* **2019**, *60*, 1325−1329.

Chapter 2

Bismuth(III)-catalyzed regioselective alkylation of tetrahydroquinolines and indolines towards the synthesis of bioactive core-biaryl oxindoles and CYP19 inhibitors

Chapter 2

Bismuth(III)-catalyzed regioselective alkylation of tetrahydroquinolines and indolines towards the synthesis of bioactive core-biaryl oxindoles and CYP19 inhibitors

Bioactive core of CYP19 Inhibitor   R$_1$ = 3-chloropropionyl   *n = 0, Indoline; n = 1, Tetrahydroquinoline*   *Biaryl Oxindoles*
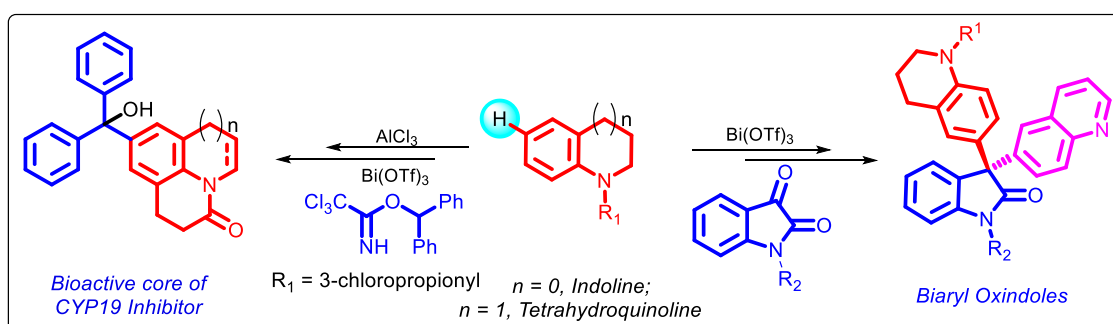
2.1 ABSTRACT: Bismuth(III)-catalyzed regioselective functionalization at the C-6 position of tetrahydroquinolines and the C-5 position of indolines has been demonstrated. For the first time, one pot symmetrical and unsymmetrical arylation of isatins with tetrahydroquinolines was accomplished giving a completely new product skeleton in good to excellent yields. Most importantly, this protocol leads to the formation of a highly strained quaternary carbon stereogenic center, which is a challenging task. Benzhydryl and 1-phenylethyl trichloroacetimidates have been used as the alkylating partners to functionalize the C-6 and C-5 positions of tetrahydroquinolines and indolines, respectively. The scope of the developed methodology has been extended for the synthesis of the bioactive CYP19-inhibitor and its analogue.

2.2 INTRODUCTION

Tetrahydroquinoline and indoline skeletons are the common structural motifs present in a wide range of pharmaceuticals and bioactive natural products.[1] As substituted

tetrahydroquinolines and indolines show significant effects on biological metabolism[2] and they show pharmaceutical activity towards Alzheimer's disease, obesity, asthma, epilepsy, antitumor, antibiotic, bradykinin antagonist, schistosomicidal, and anti-proliferative activities, the synthesis and functionalization of tetrahydroquinolines and indolines are of immense interest (Figure 2.1).

Figure 2.1: Representative examples of Natural products and bioactive molecule containing substituted indoline and substituted tetrahydroquinoline scaffolds.
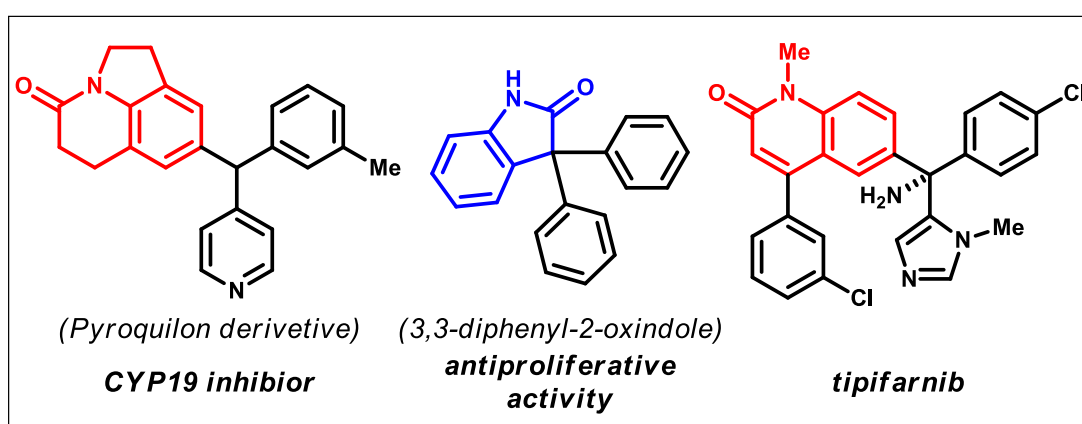
In this context, development of new methodology for the selective C–H functionalization of these molecules can give access to medicinally important scaffolds.[3] Significant efforts have been made over the last decade to develop efficient and practical strategies for the regioselective alkylation on the benzenoid nucleus of indolines[4–7] and tetrahydroquinolines.[8–10]

In this regard, the directing group assisted transition metal (Rh, Ru, Pd, Ir, and Co)-catalyzed activation of the proximal sp^2 C–H bond, i.e. C-7 of indolines,[11] and C-8 of tetrahydroquinolines,[12] are well documented. Recently, the Yu group has demonstrated elegant strategies to deliver *meta* functionalization of cyclic amines (indolines and tetrahydroquinolines) by utilizing a U-shaped template.[13] However, template assisted

para-functionalization of cyclic amines is still underdeveloped as it is associated with certain limitations such as regioselectivity (*ortho* and *para* products) (Figure 2.2a), chemoselectivity and reactivity (mono- and di-alkylation) (Figure 2.2b).[14,15] Consequently, the development of efficient synthetic methodology to access those molecules overcoming the regio- and chemo-selectivity issues is a challenging task.

Figure 2.2: Regio- and chemo-selectivity challenges between C-6 and C-8 functionalization of tetrahydroquinoline.
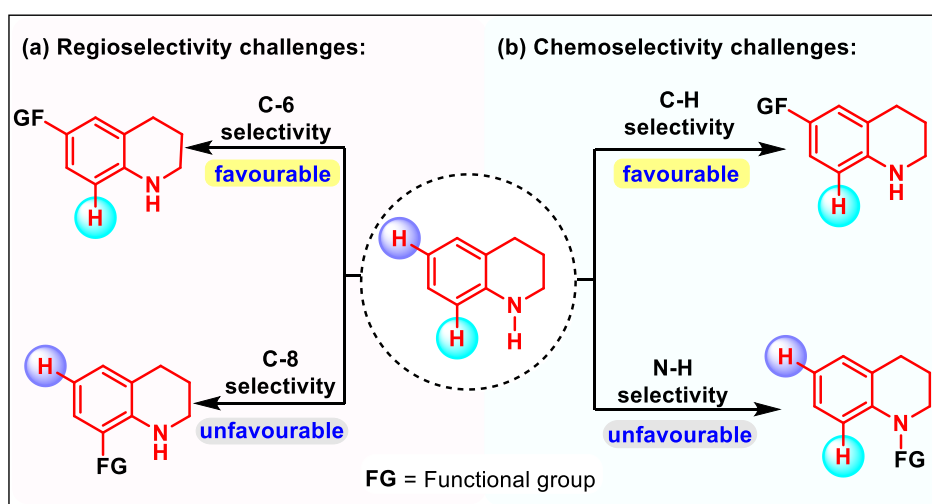
Considering the significance of selective functionalization, we have explored the selective C-5 and C-6 alkylation of indolines and tetrahydroquinolines, respectively, through Lewis acid assisted alkylation reaction. The developed alkylation reaction works efficiently in a regioselective manner under transition metal free conditions.

2.3 RESULTS AND DISCUSSION

We decided to try a new substrate combination which has never been explored before. Hence, we chose 5-methoxyisatin **1a** and tetrahydroquinoline **2a** (Table 2.1) as the model substrates to test the hypothesis. Accordingly, the reaction of **1a** with **2a** was tested under Lewis acid conditions. Gratifyingly, under the influence of the catalytic quantity of In(OTf)$_3$ in 1,4-dioxane, at 80 °C for 6 h, the selective C-6 functionalization of

tetrahydroquinoline occurred smoothly resulting in the desired product **3aa** in 55% isolated yield (Table 2.1, entry 1). Next, a series of solvents such as DMSO, DMF, MeOH, DCM and DCE were tested using In(OTf)$_3$ (Table 2.1, entries 2–6). Among them, DCE produced a better yield of **3aa**, 79%. So, we kept DCE as the optimized solvent and varied other parameters for further optimization. When we screened other Lewis acids such as ZnCl$_2$, AlCl$_3$ and Bi(OTf)$_3$, the yield of **3aa** was improved to 83% with Bi(OTf)$_3$ (Table 2.1).

Table 2.1. Optimization of the reaction conditions[a]
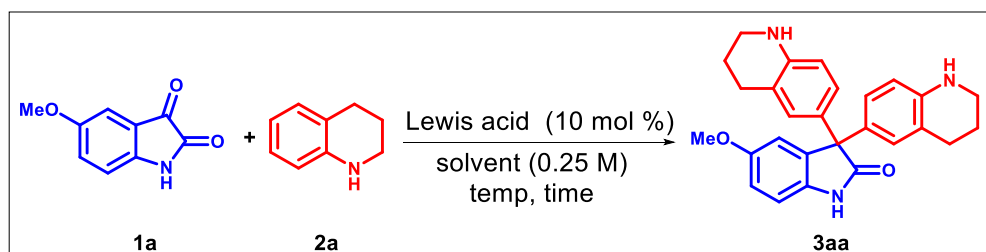
entry	2a (equiv)	Lewis acid	Solvent	Temp.	Time	Yield (%)[b]
1	2.5	In(OTf)$_3$	1,4-dioxane	80 °C	6 h	59 (55)[c]
2	2.5	In(OTf)$_3$	DMSO	80 °C	6 h	nr
3	2.5	In(OTf)$_3$	DMF	80 °C	6 h	56
4	2.5	In(OTf)$_3$	MeOH	80 °C	6 h	67
5	2.5	In(OTf)$_3$	DCM	80 °C	6 h	64
6	2.5	In(OTf)$_3$	DCE	80 °C	6 h	79
7	2.5	ZnCl$_2$	DCE	80 °C	6 h	58
8	2.5	AlCl$_3$	DCE	80 °C	6 h	39
9	2.5	Bi(OTf)$_3$	DCE	80 °C	6 h	83
10	**2.5**	**Bi(OTf)$_3$**	**DCE**	**80 °C**	**8 h**	**96(92)[c]**
11[d]	2.5	Bi(OTf)$_3$	DCE	80 °C	8 h	55
12	2.5	Bi(OTf)$_3$	DCE	60 °C	6 h	79(73)[c]
13	2.5	Bi(OTf)$_3$	DCE	100 °C	6 h	48
14	2.5	Bi(OTf)$_3$	DCE	rt	6 h	11
15	2	Bi(OTf)$_3$	DCE	80 °C	8 h	68
16	2.8	Bi(OTf)$_3$	DCE	80 °C	8 h	75

[a]Reaction conditions: **1a** (0.1 mmol), **2a** (2.5 equiv.), Lewis acid (10 mol %), and solvent (0.25 M), rt to 80 °C, 6–8 h. [b]NMR yield. [c]Isolated yields. [d]Bi(OTf)$_3$ (5 mol %).

entries 7–9). Interestingly, further improvement of the product yield to 96% was observed on increasing the reaction time to 8 h (Table 2.1, entry 10). Then we reduced the catalyst loading from 10 mol % to 5 mol %, but the yield of **3aa** decreased to 55% (Table 1, entry 11). Therefore, we fixed the catalyst loading to 10 mol % and varied the temperature. However, at reduced or increased temperature such as 60 °C, 100 °C and room temperature (Table 1, entries 12–14) the yields of **3aa** dropped to 79%, 48% and 11%, respectively. Moreover, to understand the influence of the number of equivalents of quinolines, we tested the reaction with 2 and 2.8 equivalents of **2a** and observed a decrease in the yield of **3aa** (Table 2.1, entries 15 & 16) in both cases. This indicates that 2.5 equivalents of **2a** are essential for this reaction. Thus, 10 mol % of Bi(OTf)$_3$, with DCE as the solvent at 80 °C for 8 h were found to be the optimized conditions (Table 2.1, entry 10).

With the optimized reaction conditions in hand, the viability of the C-6 functionalization of quinoline derivatives **2** was tested with various substituted and unsubstituted isatins **1** in both protected and unprotected forms (Scheme 2.1). The C-6 functionalization of **2a** with N–H isatin **1b** gave a 69% isolated yield of the arylated product (Scheme 2.1, **3ba**). When C5-trifluoromethoxy isatin was used, the yield of the product **3ca** increases to 72%. Then C5-halo substituted oxindoles were used, and 65% and 59% yields of the respective products were observed (Scheme 2.1, **3da** & **3ea**). Upon taking the dihalo substituted isatin, good yield of the product **3fa** (62%) was obtained, but when C7-methyl isatin was taken as the substrate, the yield of the product **3ga** decreased to 41%. Then we decided to check the effect of *N*-protection on isatin. Interestingly, the yield (67%) did not change much with *N*-acetyl isatin (Scheme 2.1, **3ha**). However, the yields (77% & 75%) of the arylated adduct improved with both *N*-benzyl and *N*-methyl isatins (Scheme 2.1,

Scheme 2.1: Scope of the isatins and tetrahydroquinolines in a two-component system

Crystal structure of **3aa**, CCDC = 2041963

3aa, 92%

3ba, 69%

3ca, 72%

3da, 65%

3ea, 59%

3fa, 62%

3ga, 41%

3ha, 67%

3ia, 77%

3ja, 75%

3ka, 80%

3ib, 76%

3jb, 60%

3kb, 97%

Analogous Substrate

3b', 42%

3b'', Trace
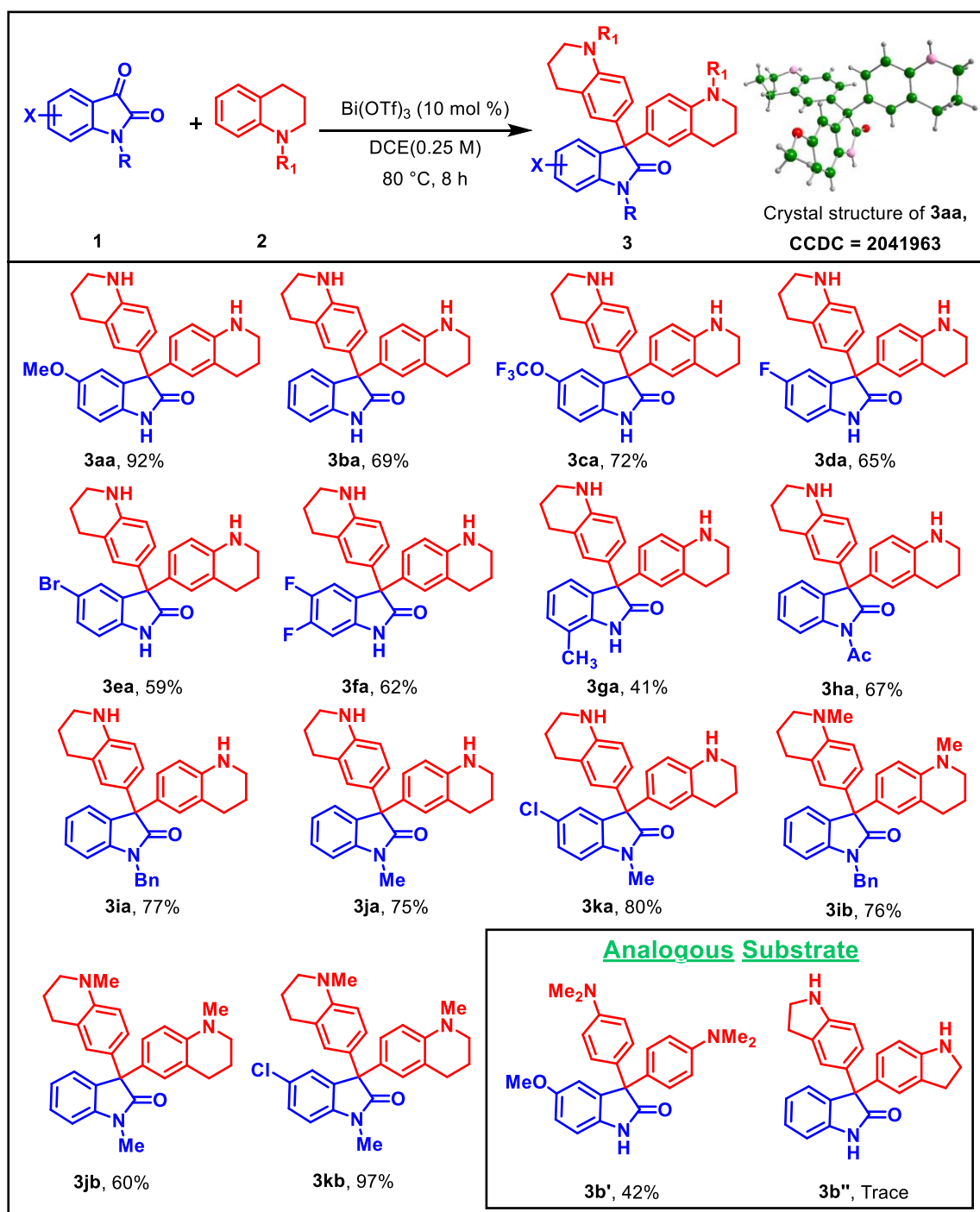
[a]Reaction conditions: **1** (0.1 mmol), **2** (2.5 equiv.), Bi(OTf)$_3$ (10 mol %), and DCE (0.25 M), 80 °C, 8 h.

3ia & **3ja**). Next, we tested the effect of a halo group on *N*-methyl isatin that led to further improvement of yield, 80% (Scheme 2.1, **3ka**). From the above set of experiments, it can be concluded that the reaction works well irrespective of the nature of the substituent present on the benzenoid ring of isatin. Furthermore, we have screened the effect of *N*-protection on both tetrahydroquinoline and isatin derivatives. In these cases, we obtained good to excellent yields of the products (Scheme 2.1, **3ib, 3jb** & **3kb**). Overall, this reaction worked well with a broad range of substrates. Then we applied our developed protocol to other cyclic amine substrates such as aniline and indoline. The *N*-protected aniline with 5-methoxy isatin gave the product **3b′** with 42% yield and indoline with isatin gave the product **3b″** in a trace amount. So, the above study reveals the broader scope of this developed methodology.

Scheme 2.2: Scope of the isatins and tetrahydroquinolines in a three-component system and its oxidized product.
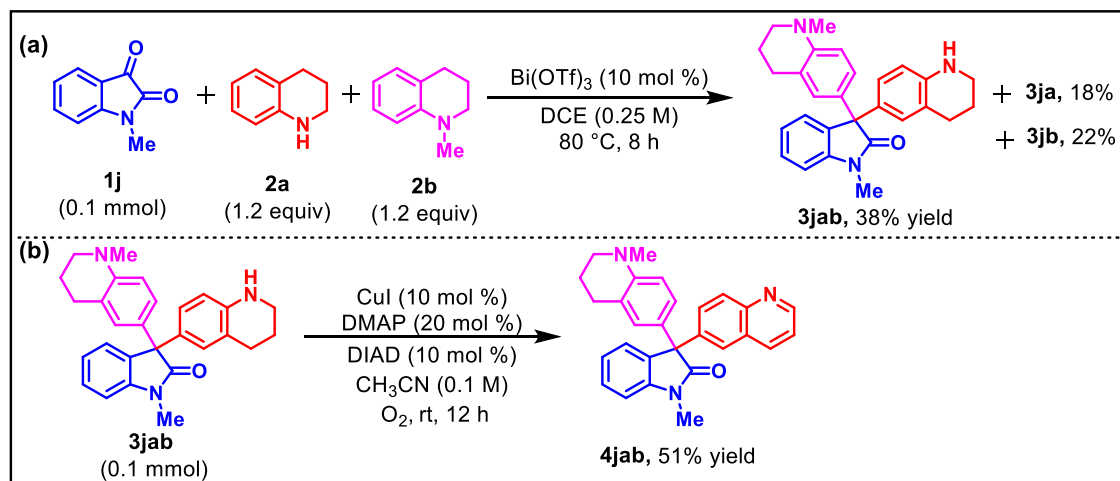
Having successfully demonstrated the utility of this protocol for the synthesis of a variety of symmetrically arylated products, we were interested in examining the scope of this protocol for the synthesis of an unsymmetrically arylated product as well.[16] Accordingly, we tested this protocol with two different tetra-hydroquinolines (**2a** and **2b**) with *N*-methylisatin. To our delight, we obtained a 38% yield of an unsymmetrically arylated

product (Scheme 2.2a, **3jab**) along with the symmetrical products **3ja** (18%) and **3jb** (22%). To further enhance the scope of the products through this methodology, we oxidized the obtained unsymmetrically arylated products following a procedure reported in the literature.[17] A reasonable yield of the respective oxidized product was obtained (Scheme 2.2b, **4jab**).

Synthesis of molecules containing all carbon quaternary centers is always a challenging task in organic synthesis. Indeed, the generation of a quaternary carbon stereo center is even more challenging. Herein, we have successfully synthesized the compounds bearing a quaternary stereo center.[18] In addition, our protocol provides an opportunity to synthesize various analogs of biologically important symmetrical and unsymmetrical 3,3′-bis-heteroaryl-2-oxindoles, which were not accessed before.

Scheme 2.3: Plausible mechanism for regioselective C-6 functionalization of tetrahydroquinoline.
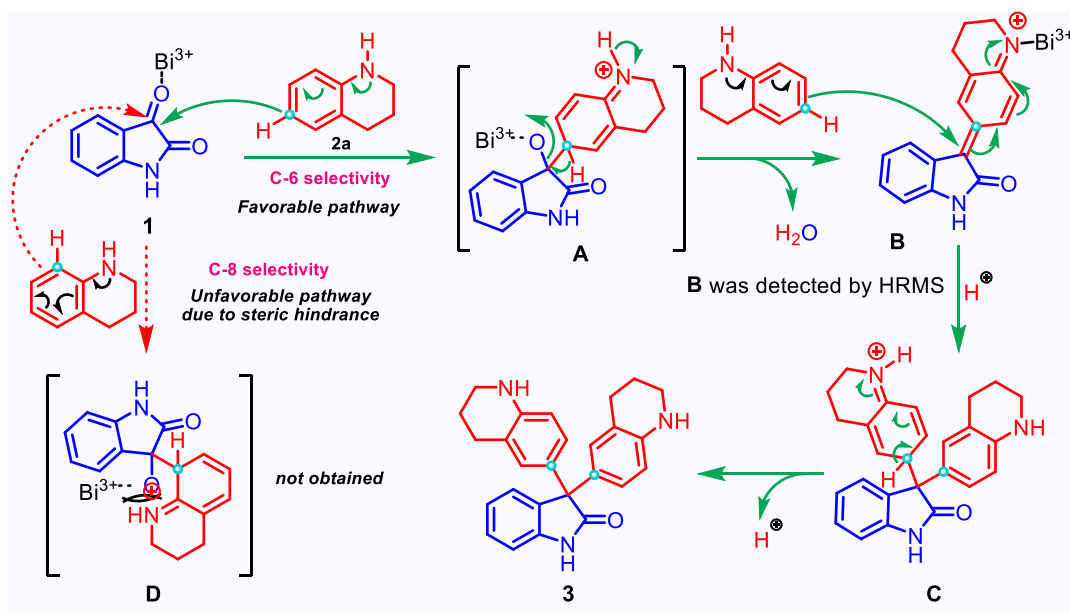
Based on the above experiments and literature precedence[19] a plausible mechanism is depicted in Scheme 2.3. Coordination of bismuth to the keto-carbonyl group of isatin **1** increases the electrophilicity so much so that the C-6 position of tetrahydroquinoline **2**

undergoes electrophilic attack by carbonyl carbon of isatin and forms intermediate A. Even though the C-8 position of tetrahydroquinoline is also capable of undergoing a similar electrophilic attack, we did not observe any product derived from this mode of attack, possibly due to steric reasons as shown below (intermediate **D**). Deprotonation and elimination of hydroxide from intermediate **A** lead to a quinoid type of intermediate **B** (detected by HRMS) which reacts with another molecule of tetrahydroquinoline at the C-6 position and forms Sigma complex **C** which then undergoes deprotonation to regain aromaticity giving rise to biarylated product **3**.

We intended to further demonstrate the scope of this methodology for the synthesis of another biologically important class of molecules such as 5-substituted indoline and 6-substituted tetrahydroquinoline derivatives **6** (Scheme 2.4a) for which trichloroacetimidate **5** was taken as the alkylating agent.[20] Hence, **2b** and **5a** were subjected to the optimized reaction conditions. As expected, we obtained the C-6 alkylated product in a very good yield of 85% (Scheme 2.4a, **6ba**). Also, with *N*-mesyl and *N*-tosyl tetrahydroquinolines **2c** and **2d**, the respective alkylated products were obtained in good yields (Scheme 2.4a, **6ca** & **6db**). Similarly, *N*-protected indolines **2e** and **2f** also resulted in excellent yields (88% & 93%) of their respective alkylated products (Scheme 4a, **6eb** & **6fa**).

To test the robustness of this methodology we designed a substrate, which could potentially undergo intramolecular Friedel–Crafts alkylation in addition to intermolecular alkylation. When compound **2g** was allowed to react with **5a** and **5b** under the standard conditions, to our delight, it underwent chemoselective alkylation furnishing good yields 67% & 61% of their respective intermolecular alkylation products (Scheme 2.4a, **6ga** & **6gb**).

Scheme 2.4: Scope of remote C–H functionalization of cyclic amines & DDQ oxidation.
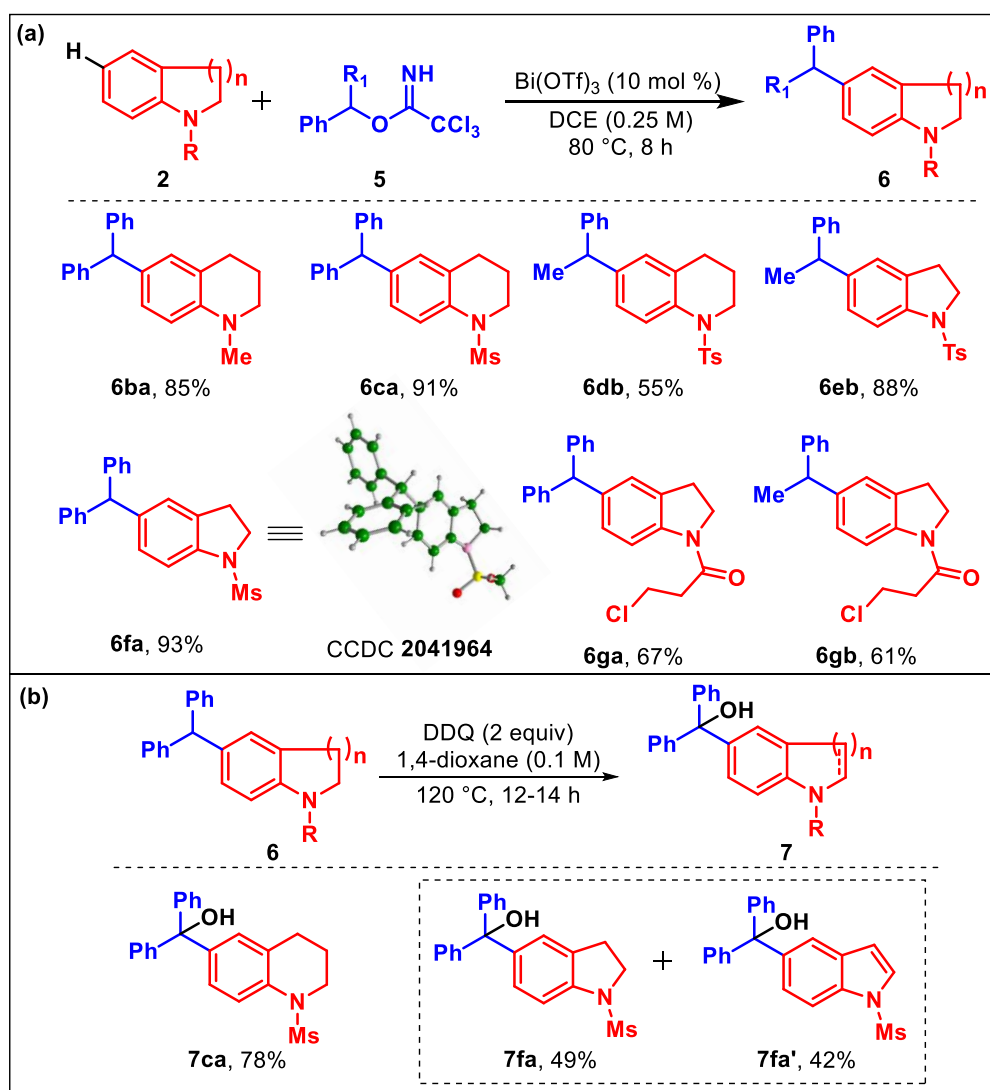
(a) Reaction conditions for products **6**: **2** (0.1 mmol), **5** (1.5 equiv.), Bi(OTf)$_3$ (10 mol %), and DCE (0.25 M), 80 °C, 8 h; (b) Reaction conditions for products **7**: **6** (0.1 mmol), DDQ (2 equiv.), and 1,4-dioxane (0.1 M), 120 °C, 12–14 h.

In order to diversify the product library, products **6** were oxidized using DDQ. Interestingly, it was found that triarylmethane carbon was oxidized to tertiary alcohol in both cases (Scheme 2.4b, **7ca** & **7fa**) and in indoline case, we obtained both hydroxylation and aromatization products (Scheme 2.4b, **7fa** & **7fa′**) with 2 equivalents

Scheme 2.5: Application of the methodology.

(a) 1 gram scale reaction for the synthesis of biaryl oxindole 3:

(b) 1 gram scale reaction for the synthesis of C-5 substituted indoline 6:

(c) Synthetic approach for the CYP19 inhibitor analogue:

(d) Synthetic approach for the CYP19 inhibitor:

Detected by *HRMS,* [M+H]$^+$ m/z calcd: 355.1805, found: 355.1780
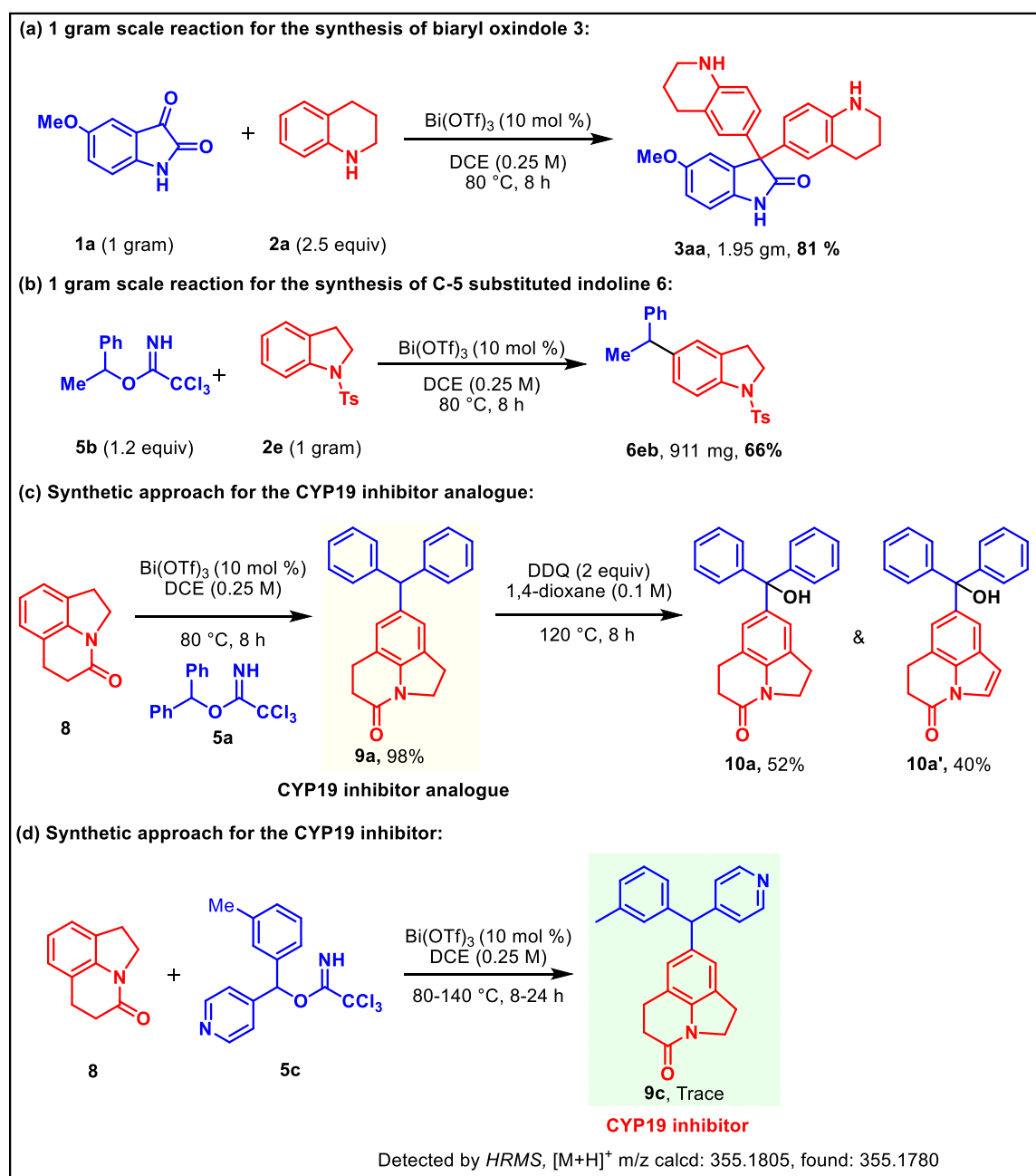
Reaction conditions: (a) 1 g scale reaction for synthesis of biaryloxindole **3**; (b) 1 g scale reaction for the synthesis of C-5 substituted indoline **6**; (c) 1st step = **8** (0.1 mmol), **5a** (1.5 equiv.), Bi(OTf)$_3$ (10 mol %), and DCE (0.25 M), 80 °C, 8 h; 2nd step = **9a** (0.1 mmol), DDQ (2 equiv.), and 1,4-dioxane (0.1 M), 120 °C, 8 h; (d) **8** (0.1 mmol), **5c** (1.5 equiv.), Bi(OTf)$_3$ (10 mol %), DCE (0.25 M), 80–140 °C, 8–24 h.

of DDQ. Apparently, it is clear that the hydroxylation step seems to be faster as compared to the aromatization of indoline to indole.

To show the efficiency of our protocol, we performed gram scale reaction for the synthesis of the biaryl oxindole and distal C–H functionalized product of tetrahydroquinoline and indoline. When 1 g 5-methoxy isatin **1a** was reacted with **2a**, it gave the product **3aa** with 81% yield (1.95 g) (Scheme 2.5a). The *N*-tosyl indoline **2e** (1 g) on reaction with **5b** gave the product **6eb** with 66% yield (911 mg) (Scheme 2.5b). Hence the methodology is very much efficient in a large scale. Then to show more applications of this methodology we have synthesized molecules with close similarity to potent drug candidates such as the CYP19 inhibitor. Intramolecular alkylation of **2g** in the presence of AlCl$_3$ at 140 °C gave the intramolecular alkylation product **8**, which under the standard conditions along with **5a** resulted in the C-5 alkylated product in 98% yield (Scheme 2.5c, **9a**). The molecule **9a** is analogous to the drug candidate, CYP19 inhibitor. Oxidation of **9a** with 2 equivalents of DDQ led to the formation of two products (Scheme 2.5c, **10a** & **10a′**). With further interest, we tried to synthesize the CYP19 inhibitor molecule by reacting pyridin-4-yl(m-tolyl) methyl 2,2,2-trichloroacetimidate **5c** with **8**, where a trace amount of product **9c** was found which was detected by HRMS.

2.4 CONCLUSION

In summary, we have developed bismuth catalyzed regioselective C-6 alkylation of tetrahydroquinolines with isatin derivatives. Both symmetrical and unsymmetrically arylated product of isatin derivatives were prepared in good to excellent yields. Bismuth is found to be the best catalyst choice because it is less toxic, works under low catalyst loading and allows hydrocompatibility (substrates with free OH/NH bonds). We have also developed C-6 and C-5 alkylation of tetrahydroquinolines and indolines, respectively, using trichloroacetimidates for the first time, where we attempted to synthesize the CYP-

19 inhibitor and its analogues. We have demonstrated numerous applications of this methodology for the synthesis of drug-like molecules.

2.5 EXPERIMENTAL SECTION

Reactions were performed using oven dried Borosil seal-tube glass vials with Teflon-coated magnetic stirring bars under a N_2 atmosphere. A syringe was used to transfer the solvents and liquid reagents. Dioxane, DMF, MeOH, DCM, DCE, and CH_3CN were distilled and dried over calcium hydride. All other solvents such as hexane, EtOAc, DMSO, THF, diethyl ether, and acetone was used as received. Column chromatography was performed by using 100–200 and 230–400 mesh size silica gel from Acme Synthetic Chemicals Company. A gradient elution was performed by using distilled petroleum ether and ethyl acetate. TLC plates were detected under UV light at 254 nm. ^{1}H NMR and ^{13}CNMR spectra were recorded on Bruker AV 400 and 700 MHz spectrometers and a JEOL 400 MHz spectrometer using $CDCl_3$ as the deuterated solvent.[21] Chemical shifts (δ) are reported in ppm relative to the residual solvent ($CHCl_3$) signal (δ = 7.26 for ^{1}H NMR and δ = 77.36 for ^{13}C NMR). Data for ^{1}H NMR spectra are reported as follows: chemical shift (multiplicity, coupling constants, and number of hydrogen). Abbreviations are as follows: s (singlet), d (doublet), t (triplet), q (quartet), quint (quintet), m (multiplet), dd (double doublet), br (broad signal), and J (coupling constants) in Hz (hertz). High-resolution mass spectrometry (HRMS) data were recorded using a micro-TOF Q-II mass spectrometer using methanol as solvent. IR spectra were recorded on a FTIR system and values are reported in frequency of absorption (cm^{-1}). Digital melting point apparatus is used to record the melting points. Reagents and starting materials were purchased from Sigma Aldrich, Alfa Aesar, TCI, Avra, Spectrochem and other commercially available sources and were used without further purification unless otherwise noted.

2.5.1 General procedure for the synthesis of *N*-acetyl isatin (1h):

1-Acetylindoline-2,3-dione was prepared according to a previously reported procedure.[22] Isatin (1.7 mmol) was suspended in acetic anhydride (10 mL) in a round bottom flask with a stir bar. Then 1 drop of H_2SO_4 was added to it and the reaction mixture was heated at reflux for 5 minutes at 140 °C. After the completion of reaction determined by TLC analysis, the reaction mixture was diluted with H_2O and saturated aqueous $NaHCO_3$ and worked up with EtOAc and the organic layer was washed with brine solution and dried over Na_2SO_4 and evaporated. Column chromatography gave the pure product as a yellow solid (82% yield).

2.5.2 General procedure for the synthesis of *N*-alkyl isatin (1i–1k):

N-Protected isatins were prepared according to a previously reported procedure.[23–29] Isatin (1 equiv., 3.4 mmol) was dissolved in DMF (5 mL) solvent under a N_2 atmosphere and the mixture was taken in an oven-dried round-bottom flask equipped with a magnetic stir bar at room temperature. To this reaction mixture NaH (1.2 equiv., 4.1 mmol) was added portion-wise at 0 °C. Then alkyl halide (1.2 equiv., 4.1 mmol) was added to the solution in a dropwise manner through a syringe. The reaction mixture was allowed to stir

for 2 h at 0 °C and then it was stirred at rt for 12 h. After the completion of reaction as monitored by TLC analysis, the reaction mixture was quenched with slow addition of water and then diluted with 10 mL of DCM. The organic layer was separated, dried over anhydrous Na_2SO_4 and concentrated in a rotary evaporator under vacuum. The crude products were purified by flash chromatography on silica gel (30% EtOAc/petroleum ether) to afford the desired product.

2.5.3 General procedure for the synthesis of *N*-methyl tetrahydroquinolines (2b):
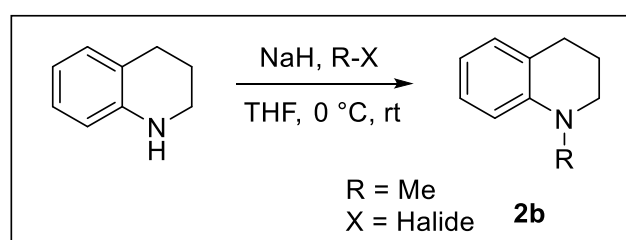
N-methyl tetrahydroquinolines were prepared according to a previously reported procedure.[30] Tetrahydroquinoline (1 equiv., 7.5 mmol) was dissolved in THF (10 mL) solvent under a N_2 atmosphere and the mixture was taken in an oven-dried round-bottom flask equipped with a magnetic stir bar at rt. To the reaction mixture, NaH (1.2 equiv., 9.0 mmol) was added portion-wise at 0 °C. Then alkyl halide (1.2 equiv., 9.0 mmol) was added to the solution in a dropwise manner through a syringe. The reaction mixture was allowed to stir for 16 h at rt. It was quenched with slow addition of water and then diluted with 10 mL of EtOAc upon completion of reaction. The organic layer was separated, dried over anhydrous Na_2SO_4 and concentrated in the rotary evaporator under vacuum. The crude products were purified by column chromatography to give the pure product **2b** as a colorless liquid.
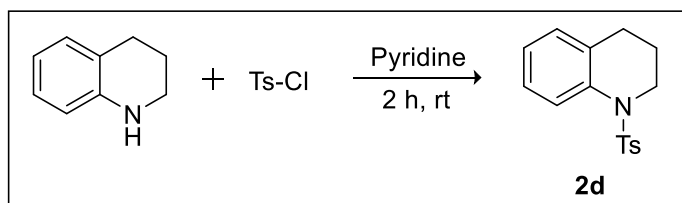
2.5.4 General procedure for the synthesis of *N*-mesyl tetrahydroquinoline (2c):

N-Mesyl tetrahydroquinoline was prepared according to a previously reported procedure.[31] Tetrahydroquinoline (1000 mg, 7.5 mmol) was dissolved in 5 mL dry
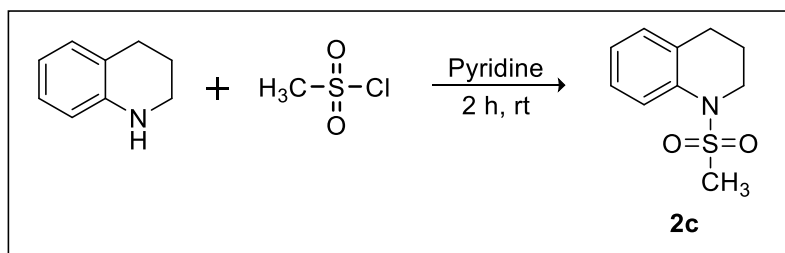
pyridine and methanesulfonyl chloride (1.2 equiv., 9.0 mmol) was dropped in 2 portions under N_2. The reaction mixture was stirred for 2 h at room temperature and an intense red colour developed. When the reaction was complete as determined by TLC, the crude reaction mixture was poured into 100 mL of cold 0.5 M HCl and extracted twice with 50 mL DCM. The organic phase was evaporated and the evaporation residue was purified by passing through a silica plug. The product eluted in 7/3 PE/EtOAc, while all of the pink polar byproduct was retained on silica. The product **2c** was obtained as a brown solid (85% yield).

2.5.5 General procedure for the synthesis of *N*-tosyl tetrahydroquinoline (2d):

N-Tosyl tetrahydroquinoline was prepared according to a previously reported procedure.[32] To a solution of tetrahydroquinoline (1 equiv.) in pyridine was added TsCl (1.2 equiv.). It was stirred at rt for 2 h. When the reaction was complete as monitored by TLC, the pyridine was evaporated under reduced pressure. To the obtained crude product, H_2O was added followed by DCM solvent. After the separation of the organic layer, the water layer was extracted with 30 mL DCM. The combined organic layer was dried over anhydrous Na_2SO_4, filtered, evaporated and the evaporation residue was purified *via* column

chromatography on silica gel (eluent: petroleum ether/ethyl acetate) to give the desired product **2d** as a white solid (84% yield).

2.5.6 General procedure for the synthesis of *N*-tosyl indoline (2e):
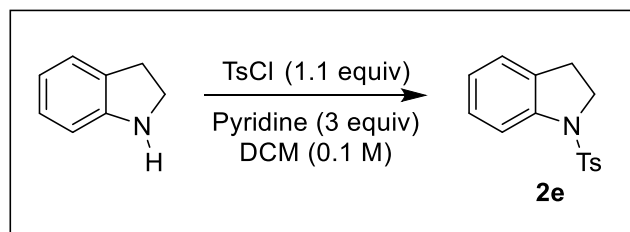
N-Tosyl indoline was prepared according to a previously reported procedure.[33] To a solution of the indoline (1.0 equiv.) in DCM (0.1 M) were added pyridine (3.0 equiv.) and p-toluenesulfonyl chloride (1.1 equiv.) and the resulting solution was stirred at room temperature for 16 h. Upon completion of reaction confirmed by TLC check, H_2O was added. The phases were separated and the aqueous layer was extracted with DCM (3×10 mL). The combined organic layers were washed with 1 M HCl and brine. Then the organic solvent was dried over anhydrous Na_2SO_4 and filtered and evaporated under reduced pressure. The evaporation residue was purified on silica gel to give the product **2e** as a white solid (76% yield).
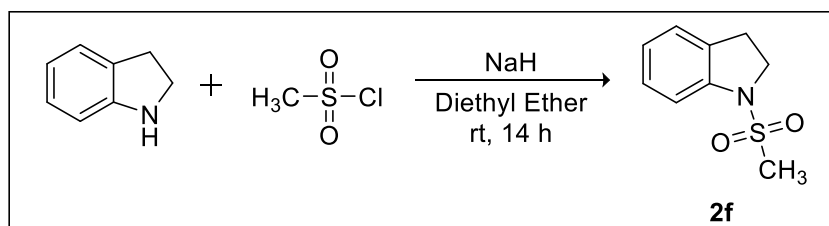
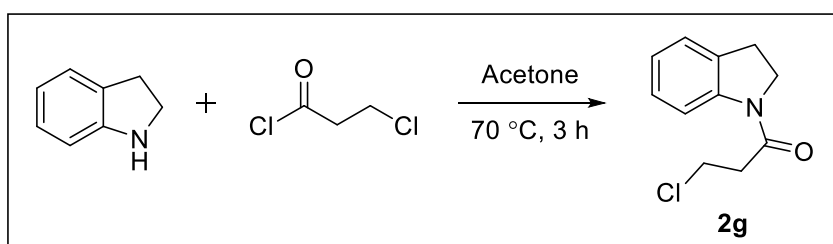### 2.5.7 General procedure for the synthesis of *N*-mesyl indoline (2f):

N-Mesyl indoline was prepared according to a previously reported procedure.[34] In a 100 mL two-neck round bottom flask, NaH (1.3 equiv.) was taken under a N_2-atmosphere and to it dry hexane was added, so that it dissolved the grease present in NaH and then hexane was decanted through a syringe. Then indoline (1 equiv.) in diethyl ether (5 mL) was

added slowly after the addition of dry ether (3 mL) (under ice cold conditions). Then it was washed with 2 mL dry ether and left for stirring for 30 minutes. Then methane sulfonyl chloride in diethyl ether was added to it and washed with 5 mL ether under ice cold conditions. After being stirred at room temperature for 14 h, the reaction was quenched with saturated aqueous NH$_4$Cl (10 mL), and extracted with DCM (3 × 10 mL). The combined organic phases were washed with brine (10 mL), dried over anhydrous Na$_2$SO$_4$ and concentrated under reduced pressure. Purification by column chromatography on silica gel (hexane : ethyl acetate = 3 : 1) afforded the pure product (67% yield) as a light brown solid, Rf = 0.3 (20% EtOAc in hexane).

2.5.8 General procedure for *N*-acylation of indoline (2g):

3-Chlorodihydro-indolyl propanone was prepared according to a previously reported procedure.[35] To a solution of indoline (4.0 g, 0.03 mol) in acetone (100 mL) in a round bottomed flask was added 3-chloro-propionyl chloride (4.7 g, 0.04 mol). After heating the mixture at 70 °C in an oil bath for 3 h, the solvent was removed under vacuum. The resulting residue was dissolved in DCM and washed with water and brine. The organic layer was dried over Na$_2$SO$_4$, filtered, and concentrated to give the product **2g** as a brown solid (7.0 g, 99% yield).

2.5.9 General procedure for the synthesis of trichloroacetimidate (5):

Trichloroacetimidate was prepared according to a previously reported procedure.[36] Acetophenol or benzophenol (1 equiv.) was taken in a round bottom flask with a stir bar
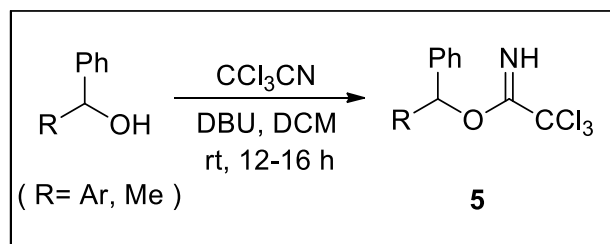
and to that DCM (0.32 M) was added through a syringe. Then DBU (0.02 equiv.) was added to the reaction mixture and kept at 0 °C by putting ice. After stirring for 5 min, trichloroacetonitrile (10 equiv.) was added to the reaction mixture slowly and left to stir for 10 min under cold conditions. Then after bringing it to room temperature, it was allowed to stir for 16 h. After the reaction completion, the reaction mixture was rota-evaporated and column chromatography (5% basified with Et$_3$N) gave the pure product **5**.
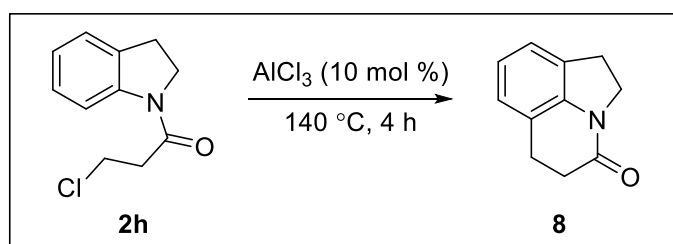
2.5.10 General procedure for the synthesis of pyrroloquinolinone (8):

Tetrahydropyrroloquinolinone was prepared according to a previously reported procedure.[37] A molten mixture of 3-chloro-dihydro-indolyl propanone (44.5 g, 212 mmol) and AlCl$_3$ (149 g, 1.12 mol) was taken in a round bottom flask and refluxed at 140 °C in a preheated oil bath for 4 h. Upon completion of reaction, it was cooled to 0 °C and then a mixture of water/ice (500 g) was added to decompose excess AlCl$_3$. The resulting solution was extracted with EtOAc (3 × 200 ml), followed by drying over MgSO$_4$. Removal of the solvent gave a yellow solid, which was purified by flash chromatography (EtOAc : hexane = 2 : 5, Rf = 0.15) to give the product as a white solid (25.7 g, 70% yield).

2.5.11 General procedure for the synthesis of biaryl oxindole *via* 2-component reaction (3):
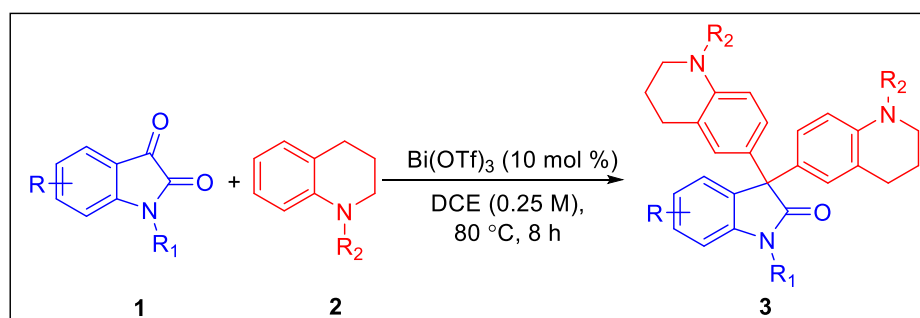
Isatin derivative **1** (1 equiv., 0.3 mmol) was dissolved in DCE (0.25 M) solvent under a N$_2$ atmosphere in an oven-dried sealed tube equipped with a magnetic stir bar at room temperature. A catalytic amount of Bi(OTf)$_3$ (10 mol %) was added to the reaction mixture followed by the addition of tetrahydroquinoline derivative **2** (2.5 equiv., 0.6 mmol). The reaction mixture was allowed to stir at 80 °C in a pre-heated aluminium block until the reaction completed. The reaction mixture was quenched with and diluted with EtOAc after the completion of reaction (monitored by TLC). The reaction mixture was then passed through Celite and evaporated. The evaporation residue was purified by column chromatography (200–400 mesh silica, basified with 5% Et$_3$N) to give the pure product **3**.
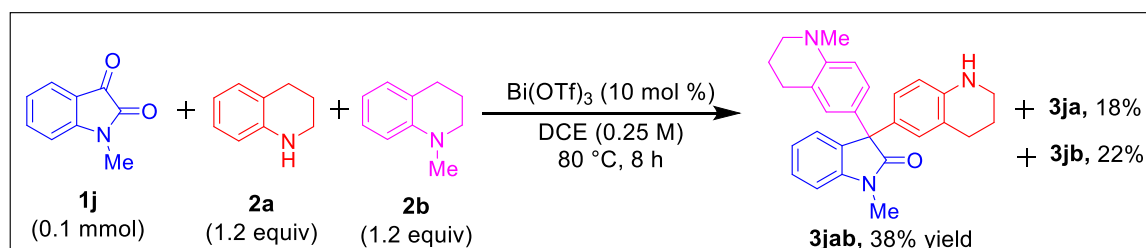
2.5.12 Procedure for the synthesis of biaryl oxindole *via* 3-component reaction (3jab):


N-methyl satin derivative **1j** (1 equiv., 0.3 mmol) was dissolved in DCE (1 mL) solvent under a N$_2$ atmosphere in an oven-dried sealed tube flask equipped with a magnetic stir

bar at room temperature. A catalytic amount of Bi(OTf)$_3$ (10 mol %) was added to the solution of the starting material and then tetrahydroquinoline **2a** (1.2 equiv., 0.34 mmol) and another derivative of tetrahydroquinoline **2b** (1.2 equiv., 0.34 mmol) were added to the reaction mixture. The reaction mixture was allowed to stir at 80 °C in a preheated aluminium block until the reaction completed. It was quenched and diluted with EtOAc after the completion of reaction (monitored by TLC). The reaction mixture was then passed through Celite and the solvent was evaporated. The evaporation residue was purified by column chromatography (200–400 mesh silica, basified with 5% Et$_3$N) to give the pure product.

2.5.13 General procedure for the synthesis of oxidized product 4jab:
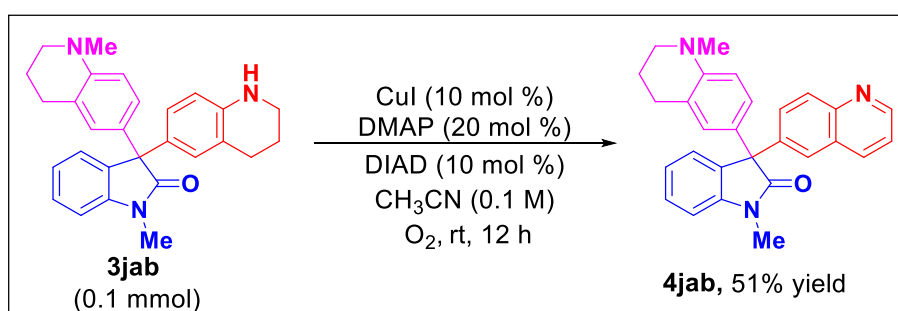
The oxidised product of biaryl oxindole **3jab** was prepared according to a previously reported procedure.[38] Biaryl oxindole derivative **3jab** (1 equiv., 0.1 mmol) was dissolved in CH$_3$CN (1.5 mL) solvent under an O$_2$ atmosphere and the mixture was taken in an oven-dried round bottom flask equipped with a magnetic stir bar at room temperature. Then copper iodide (0.1 equiv., 0.01 mmol) and DIAD (0.1 equiv., 0.01 mmol) were added followed by the addition of DMAP (20 mol %) to this reaction mixture. The reaction mixture was allowed to stir at room temperature until the reaction completed. The reaction mixture was quenched and diluted with EtOAc after the completion of reaction (monitored by TLC). The reaction mixture was then passed through Celite and

the solvent was evaporated. The crude mixture was purified by column chromatography (200–400 mesh silica, basified by 5% Et$_3$N) to give the pure product **4jab**.

2.5.14 General procedure for the synthesis of the remote C–H functionalized product of tetrahydroquinolines & indolines (6):
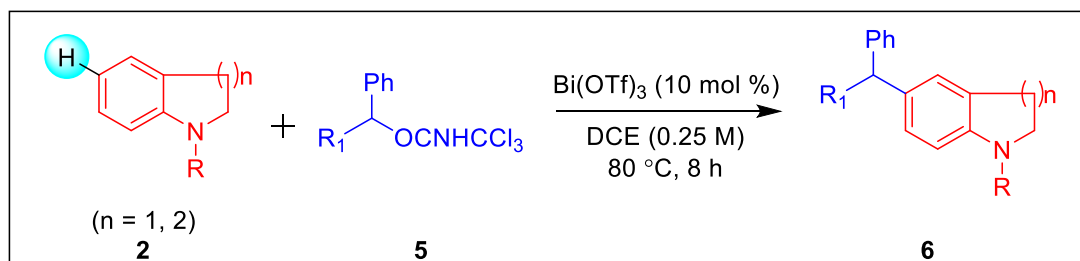
The compound **2** (1 equiv., 0.43 mmol) was dissolved in DCE (0.2 M) solvent under a N$_2$ atmosphere in an oven-dried sealed tube flask equipped with a magnetic stir bar at room temperature. Then a catalytic amount of Bi(OTf)$_3$ (10 mol %) was added to the solution of the starting material and then trichloroacetimidate derivative **5** (1.2 equiv.) was added to this reaction mixture. The reaction mixture was allowed to stir at 80 °C in a pre-heated aluminium block until the reaction completed. The reaction mixture was quenched and diluted with EtOAc after the completion of reaction (monitored by TLC). The reaction mixture was then passed through Celite and the solvent was evaporated. The crude products were purified by column chromatography (200–400 mesh silica) to give the pure product **6**.

2.5.15 General procedure for oxidation of 6 to 7:
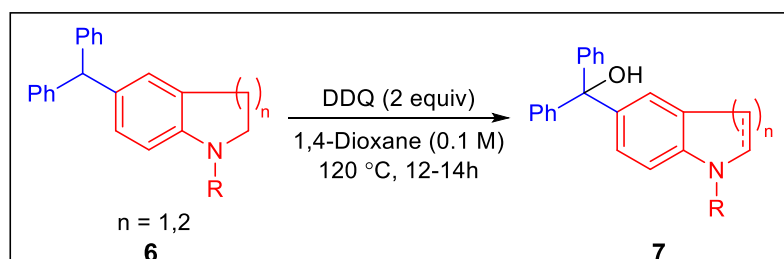
The oxidized product of **6** was prepared according to a previously reported procedure.[39] The compound **6** (1 equiv.) was dissolved in dioxane (0.1 M) solvent under a N$_2$ atmosphere and the mixture was taken in an oven-dried sealed tube flask equipped with a magnetic stir bar at room temperature. Then a catalytic amount of DDQ (2 equiv.) was added to the solution of the starting material and then the reaction mixture was allowed to stir at 120 °C in a pre-heated aluminium block until the reaction completed. The reaction mixture was quenched and diluted with EtOAc after the completion of reaction (monitored by TLC). The reaction mixture was then passed through Celite and the solvent was evaporated. The crude products were purified by column chromatography (200–400 mesh silica) to give the pure product **7**.

2.5.16 General procedure for the synthesis of the CYP19 inhibitor (9c) & its analogue (9a):
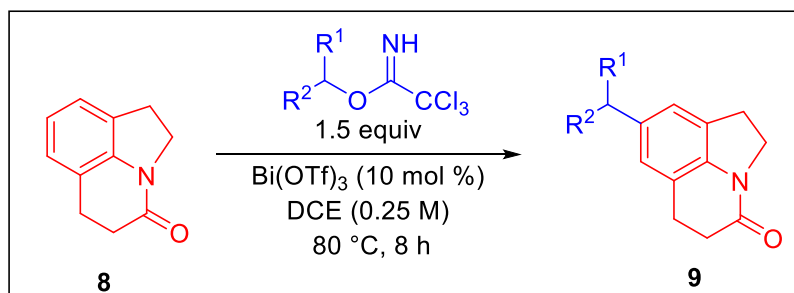
Tetrahydropyrroloquinolinone **8** (40 mg, 0.23 mmol) was dissolved in DCE (0.25 M) under a N$_2$ atmosphere in an oven-dried sealed tube equipped with a magnetic stir bar at room temperature. An amidate derivative (1.5 equiv., 0.35 mmol) was added to the reaction mixture followed by the addition of a catalytic amount of Bi(OTf)$_3$ (10 mol %). The reaction mixture was allowed to stir at 80 °C in a preheated aluminium block until the reaction completed. The reaction mixture was quenched and diluted with EtOAc after the completion of reaction (monitored by TLC) and then it was passed through Celite and

evaporated. The crude products were purified by column chromatography (200–400 mesh silica) to give the pure product.

2.5.17 General procedure for the synthesis of 10a & 10a′:

The product **9a** (50 mg, 0.15 mmol) was taken in an oven-dried sealed tube equipped with a magnetic stir bar and subjected to DDQ (2 equiv., 0.3 mmol) in dioxane solvent (0.1 M). The reaction mixture was allowed to stir at 120 °C in a pre-heated aluminium block for 8 h and it was quenched and diluted with EtOAc after the completion of reaction (monitored by TLC) and then it was passed through Celite and evaporated. The crude products were purified by column chrom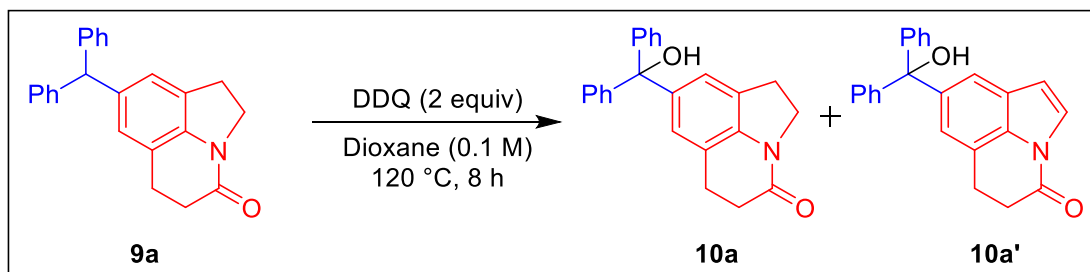atography (200–400 mesh silica) to give the pure products **10a** as a white solid (27 mg, 52% yield) and **10a′** as a brown solid (20 mg, 40% yield).

2.5.18 Detection of Intermediate B:
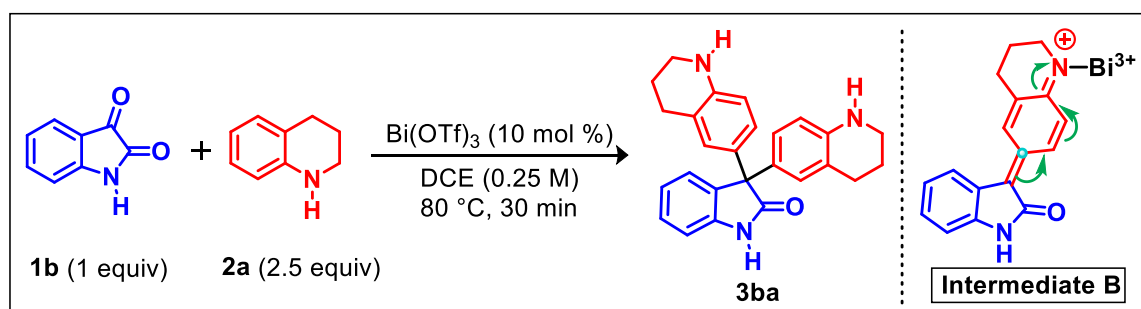
To a pre-dried sealed tube equipped with a magnetic stir bar under N_2, isatin **1b** (1 equiv, 0.01 mmol), tetrahydroquinoline **2a** (2.5 equiv, 0.03 mmol) were taken followed by addition of DCE (0.25 M) solvent. Then catalytic amount of Bi(OTf)$_3$ (10 mol %) was added to the reaction mixture. The reaction was allowed to stir at

80 °C in a pre-heated aluminium block for 30 minutes. After 30 min the reaction mixture was cooled to room temperature and quenched with EtOAc:Methanol (50:50) solvents. Then it is passed through a short celite pad and the solvent was evaporated under reduced pressure and the crude was submitted for HRMS in methanol.

Intermediate HRMS: HRMS (ESI) m/z: M+Na]$^+$ Calcd for $C_{17}H_{14}BiNaN_2O^{4+}$:494.0802, Found: 494.0750
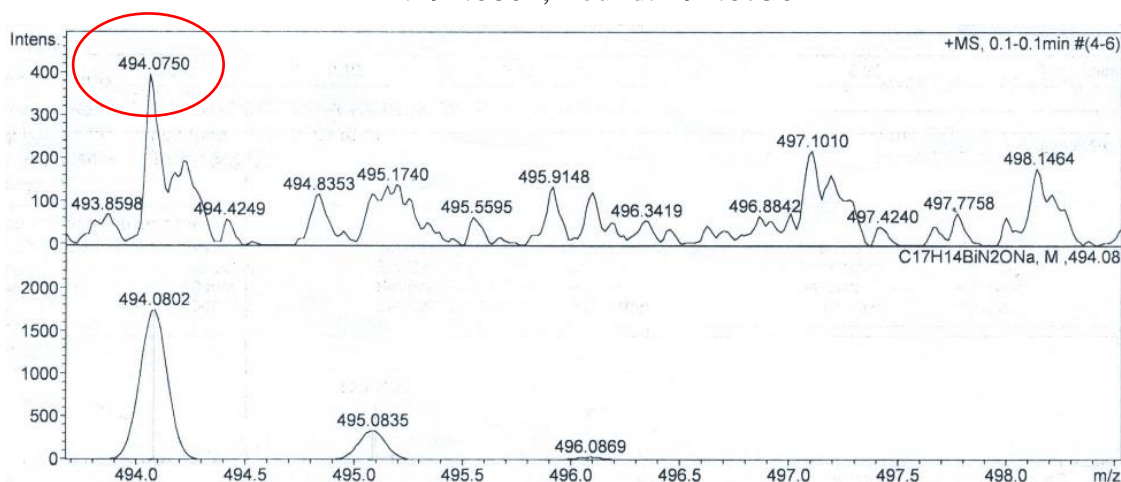
2.5.19 Attempted Synthesis of CYP-19 inhibitor and its HRMS data:
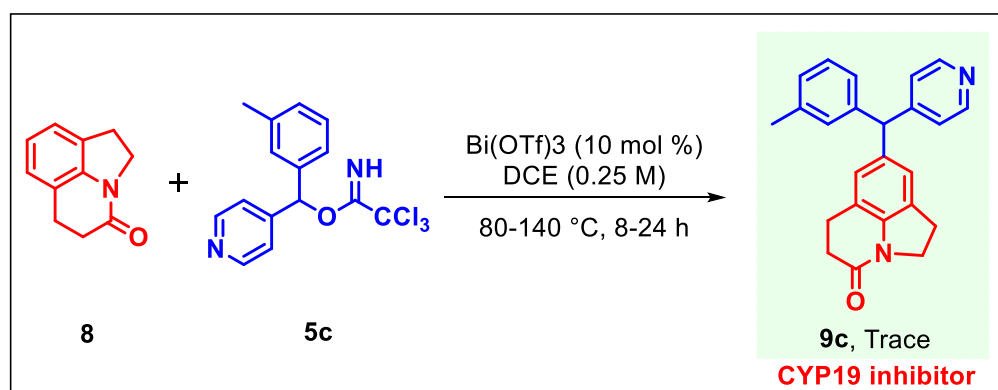
Tetrahydropyrroloquinolinone (**8**, 24 mg, 0.14 mmol) was dissolved in DCE (0.25 M) under N$_2$ atmosphere in an oven-dried sealed tube equipped with a magnetic stir bar at room temperature. pyridin-4-yl(m-tolyl)methyl 2,2,2-trichloroacetimidate **5c** (1.5 equiv, 0.21 mmol) was added to the reaction mixture followed by addition of catalytic amount of Bi(OTf)$_3$ (10 mol %). The reaction mixture was allowed to stir at 80 °C in a pre-heated aluminium block for 8-24h. Then the reaction mixture was quenched and diluted with EtOAc and it was passed

through celite and evaporated. The crude mixture was submitted for HRMS in methanol from which formation of **9c** was detected and it is formed in trace amount.

HRMS (ESI) m/z: $[M+H]^+$ Calcd for $C_{24}H_{23}N_2O$: 355.1805; Found: 355.1780.
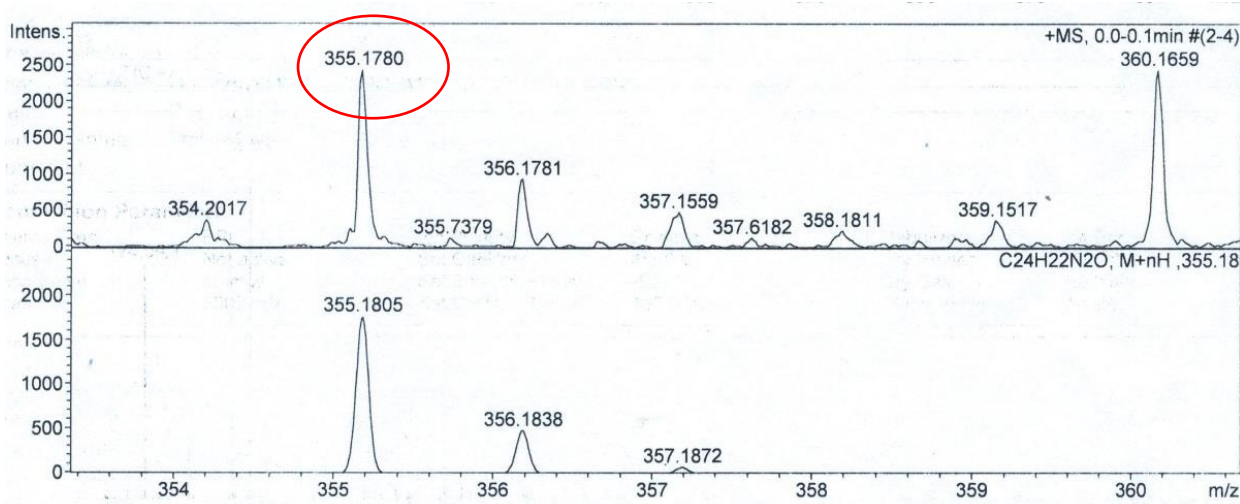
2.5.20 Experimental characterization data of starting materials:

Starting materials **1h**,[22] **1i-1k,**[23-29] **2b**,[30] **2c**,[31] **2d**,[32] **2e**,[33] **2f**,[34] **2g**,[35] **5a-5c**,[36] and **8**[37] were synthesized according to the previously reported procedures and the spectroscopic data were identical to those.

2.5.21 Experimental characterization data of products:

5-methoxy-3,3-bis(1,2,3,4-tetrahydroquinolin-6-yl)indolin-2-one (3aa):
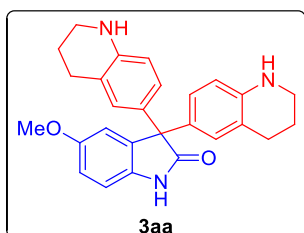
Physical state: white solid (44.2 mg for 0.11 mmol scale, 92%). m.p.: 118–120 °C. R_f: 0.3 (50% EtOAc/hexane). ^{1}H NMR (400 MHz, CDCl$_3$): δ 8.03 (s, 1H), 6.86–6.79 (m, 6H), 6.71 (dd, J_1 = 8.4 Hz, J_2 = 2.4 Hz, 1H), 6.38 (d, J = 8.8 Hz, 2H), 3.73 (s, 3H), 3.26 (t, J = 5.2 Hz, 4H), 2.67 (t, J = 6.0 Hz, 4H), 1.88 (quint, J = 6 Hz, 4H). ^{13}C {^{1}H} NMR (100 MHz, CDCl$_3$): δ 181.1, 156.1, 144.1, 136.9, 133.8, 130.5, 129.7, 127.3, 121.6, 114.4, 113.6, 112.5, 110.4, 62.5, 56.1, 42.3, 27.4, 22.4. IR (KBr,

cm^{-1}): 3384, 3157, 2925, 1698, 1611, 1508, 1302. HRMS (ESI) m/z: [M + H]$^+$ calcd for C$_{27}$H$_{28}$N$_3$O$_2$: 426.2176; found: 426.2173.

3,3-bis(1,2,3,4-tetrahydroquinolin-6-yl)indolin-2-one (3ba):
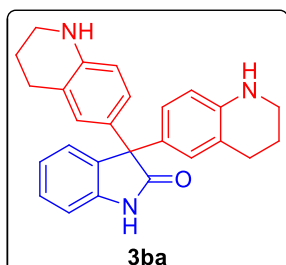
Physical state: light yellow solid (37 mg for 0.14 mmol scale, 69%). m.p.: 190-197 °C. R$_f$: 0.2 (50% EtOAc/hexane). ^{1}H NMR (400 MHz, CDCl$_3$): δ 8.21 (s, 1H), 7.19-7.16 (m, 2H), 7.01 (t, J = 7.6 Hz, 1H), 6.91-6.84 (m, 5H), 6.38-6.36 (m, 2H), 3.25 (t, J = 5.6 Hz, 4H), 2.66 (t, J = 6.4 Hz, 4H), 1.88 (quint, J = 6.0 Hz, 4H). ^{13}C {^{1}H} NMR (100 MHz, CDCl$_3$): δ 181.2, 144.0, 140.3, 135.5, 130.5, 129.7, 127.9, 127.3, 126.5, 122.9, 121.6, 114.4, 110.1, 62.0, 42.3, 27.3, 22.4. IR (KBr, cm^{-1}): 3402, 3022, 2836, 1703, 1653, 1510. HRMS (ESI) m/z: [M+H]$^+$ Calcd for C$_{26}$H$_{26}$N$_3$O: 396.2070; Found: 396.2084.

3,3-bis(1,2,3,4-tetrahydroquinolin-6-yl)-5-(trifluoromethoxy) indolin-2-one (3ca):
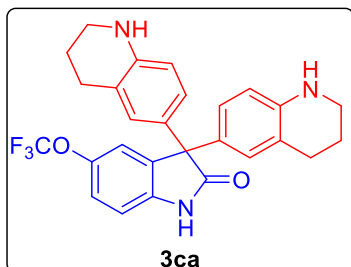
Physical State: white solid solid (75 mg for 0.22 mmol scale, 72%). m.p.: 157-162 °C. R$_f$: 0.5 (30% EtOAc/hexane). ^{1}H NMR (400 MHz, CDCl$_3$): δ 9.42 (s, 1H), 7.04-7.01 (m, 2H), 6.84-6.81 (m, 5H), 6.37 (d, J = 8.4 Hz, 2H), 3.24 (t, J = 5.6 Hz, 4H), 2.65 (t, J = 6.4 Hz, 4H), 1.87 (quint, J = 6.4 Hz, 4H). ^{13}C {^{1}H} NMR (100 MHz, CDCl$_3$): δ 182.1, 144.8, 144.3, 139.4, 137.0, 129.5, 127.1, 122.1, 121.5, 120.45, 119.6, 114.4, 111.0, 62.5, 42.2, 27.3, 22.3. IR (KBr, cm^{-1}): 3390, 2930, 2843, 1716, 1699, 1615,1510. 1218, 823. HRMS (ESI) m/z: [M+H]$^+$ Calcd for C$_{27}$H$_{25}$F$_3$N$_3$O$_2$: 480.1893; Found: 480.1896.

5-fluoro-3,3-bis(1,2,3,4-tetrahydroquinolin-6-yl)indolin-2-one (3da):
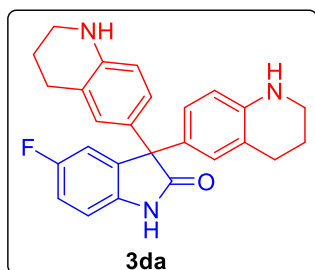
Physical State: pale yellow solid (49 mg for 0.18 mmol scale, 65%). m.p.: 110-120 °C. R_f: 0.3 (50% EtOAc/hexane). ^{1}H NMR (400 MHz, CDCl$_3$): δ 9.16 (s, 1H), 6.91-6.78 (m, 7H), 6.38-6.36 (m, 2H), 3.25 (t, $J = 5.6$ Hz, 4H), 2.66 (t, $J = 6.4$ Hz, 4H), 1.87 (quint, $J = 6.4$ Hz, 4H). ^{13}C {^{1}H} NMR (100 MHz, CDCl$_3$): δ 181.9, 159.3 (d, $J_{C-F} = 239.0$ Hz), 144.3, 137.1 (d, $J_{C-F} = 8$ Hz), 136.4 (d, $J_{C-F} = 2$ Hz), 129.8, 129.5, 127.2, 121.6, 114.4, 114.3 (d, $J_{C-F} = 23$ Hz), 114.0 (d, $J_{C-F} = 25$ Hz), 110.9 (d, $J_{C-F} = 8$ Hz), 62.6, 42.2, 27.3, 22.3. IR (KBr, cm^{-1}): 3402, 2926, 2841, 1702, 1510, 1485, 793. HRMS (ESI) m/z: [M+H]$^+$ Calcd for C$_{26}$H$_{25}$FN$_3$O: 414.1976; Found: 414.2010.

**5-bromo-3,3-bis(1,2,3,4-tetrahydroquinolin-6-yl)indolin-2-one (3ea):**

Physical State: yellow solid (62 mg for 0.22 mmol scale, 59%). m.p.: 140-145 °C. R_f: 0.2 (40% EtOAc/hexane). ^{1}H NMR (400 MHz, CDCl$_3$): δ 8.46 (s, 1H), 7.31.7.27 (m, 2H), 6.82-6.77 (m, 5H), 6.39-6.37 (m, 2H), 3.26 (t, $J = 5.6$ Hz, 4H), 2.67 (t, $J = 6.4$ Hz, 4H), 1.89 (quint, $J = 6.4$ Hz, 4H). ^{13}C {^{1}H} NMR (100 MHz, CDCl$_3$): δ 181.0, 144.4, 139.4, 137.6, 130.8, 129.6, 129.56, 129.5, 127.2, 121.6, 115.5, 114.4, 111.7, 62.3, 42.3, 27.4, 22.4. IR (KBr, cm^{-1}): 3380, 3105, 2809, 1704, 1580, 1509, 738. HRMS (ESI) m/z: [M+H]$^+$ Calcd for C$_{26}$H$_{25}$BrN$_3$O: 474.1176; Found: 474.1148.

5,6-difluoro-3,3-bis(1,2,3,4-tetrahydroquinolin-6-yl)indolin-2-one (3fa):
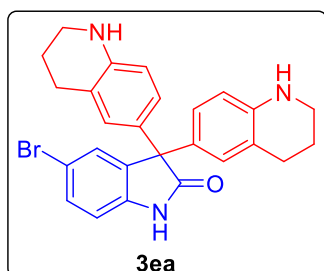

Physical State: yellow solid (71 mg for 0.27 mmol scale, 62%). m.p.: 175-180 °C. R_f: 0.1 (30% EtOAc/hexane). ^{1}H NMR (400 MHz, CDCl$_3$): δ 8.77 (s, 1H), 6.985 (dd, J_1 = 9.6 Hz, J_2 = 7.6 Hz, 1H), 6.82 – 6.79 (m, 4H), 6.73 (dd, J_1 = 9.6 Hz, J_2 = 6.4 Hz, 1H), 6.38 (d, J = 8.0 Hz, 2H), 3.26 (t, J = 5.6 Hz, 4H), 2.67 (t, J = 6.4 Hz, 4H), 1.89 (quint, J = 6.4 Hz, 4H). ^{13}C {^{1}H} NMR (100 MHz, CDCl$_3$): δ 182.3, 171.6, 150.1, 146.9, 144.4, 136.6, 131.0, 129.5, 129.4, 127.1, 121.6, 115.4, 114.4, 100.6, 62.3, 42.2, 27.3, 22.2, (60.7, 21.4, 14.5 = EtOAc peaks). IR (KBr, cm^{-1}): 3399, 2929, 2841, 1716, 1630, 1612, 1503, 1184, 798. HRMS (ESI) m/z: [M+H]$^+$ Calcd for C$_{26}$H$_{24}$F$_2$N$_3$O: 432.1882; Found: 432.1812.

7-methyl-3,3-bis(1,2,3,4-tetrahydroquinolin-6-yl)indolin-2-one (3ga):
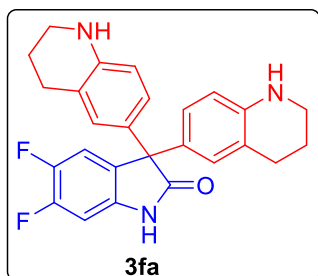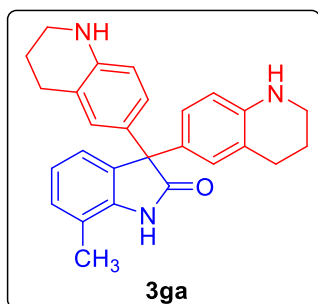
Physical State: yellow solid (52 mg for 0.31 mmol scale, 41%). m.p.: 240-245 °C. R_f: 0.2 (30% EtOAc/hexane). ^{1}H NMR (400 MHz, CDCl$_3$): δ 8.50

(s, 1H), 7.03-6.98 (m, 2H), 6.94-6.90 (m, 1H), 6.86-6.84 (m, 4H), 6.36 (d, J = 8.8 Hz, 2H), 3.25 (t, J = 5.6 Hz, 4H), 2.66 (t, J = 6.4 Hz, 4H), 2.25 (s, 3H), 1.88 (quint, J = 6.4 Hz, 4H). ^{13}C {^{1}H} NMR (100 MHz, CDCl$_3$): δ 182.0, 144.0, 139.2, 135.0, 130.6, 129.7, 129.1, 127.3, 123.9, 122.6, 121.4, 119.6, 114.3, 62.4, 42.3, 27.3, 22.4, 16.9. IR (KBr, cm^{-1}): 2957, 2856, 1699, 1611, 1508, 1464, 1301, 810, 732. HRMS (ESI) m/z: [M+H]$^+$ Calcd for C$_{27}$H$_{28}$N$_3$O: 410.2227; Found: 410.2169.

1-acetyl-3,3-bis(1,2,3,4-tetrahydroquinolin-6-yl)indolin-2-one (3ha):

3ha
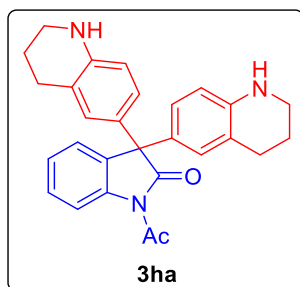
Physical State: colourless liquid (31 mg for 0.11 mmol scale, 67%). R_f : 0.2 (30% EtOAc/hexane). ^{1}H NMR (400 MHz, CDCl$_3$): δ 8.29 (d, J = 8.4 Hz, 1H), 7.32-7.28 (m, 1H), 7.18 (d, J = 4.4 Hz, 2H), 6.80-6.75 (m, 4H), 6.36 (d, J = 8.4 Hz, 2H), 3.26 (t, J = 5.6 Hz, 4H), 2.69-2.64 (m, 7H), 1.89 (quint,

J = 6.0 Hz, 4H). ^{13}C {^{1}H} NMR (100 MHz, CDCl$_3$): δ 180.1, 171.8, 144.4, 139.5, 134.0, 130.1, 129.7, 128.2, 127.4, 126.1, 125.5, 121.4, 116.9, 114.2, 62.1, 42.2, 27.4, 27.2, 22.3. IR (KBr, cm^{-1}): 3405, 3126, 2928, 1709, 1611, 1511. HRMS (ESI) m/z: [M+H]$^+$ Calcd for C$_{28}$H$_{28}$N$_3$O$_2$: 438.2176; Found: 438.2166.

1-benzyl-3,3-bis(1,2,3,4-tetrahydroquinolin-6-yl)indolin-2-one (3ia):

3ia
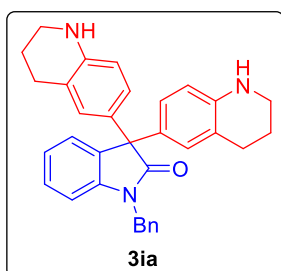
Physical State: yellow solid (31.5 mg for 0.08 mmol scale, 77%). m.p.: 82-88 °C. R$_f$: 0.4 (50% EtOAc/hexane). ^{1}H NMR (400 MHz, CDCl$_3$): δ 7.28-7.22 (m, 6H), 7.11-7.09 (m, 1H), 7.01-6.97 (m, 1H), 6.84 (s, 4H), 6.73-6.71 (m, 1H), 6.36 (d, J = 7.2 Hz, 2H), 4.96 (s, 2H), 3.25 (br, 4H), 2.66 (br, 4H), 1.89-

1.88 (m, 4H). ^{13}C {^{1}H} NMR (100 MHz, CDCl$_3$): δ 179.1, 144.1, 142.3, 136.5, 134.9, 130.8, 129.7, 129.0, 127.73, 127.72, 127.6, 127.2, 126.1, 122.9, 121.5, 114.3, 109.5, 61.6, 44.2, 42.3, 27.4, 22.4. IR (KBr, cm^{-1}): 3389, 2924, 2838, 1701, 1608, 1509. HRMS (ESI) m/z: [M+H]$^+$ Calcd for C$_{33}$H$_{32}$N$_3$O: 486.2540; Found: 486.2533.

1-methyl-3,3-bis(1,2,3,4-tetrahydroquinolin-6-yl)indolin-2-one (3ja):

3ja
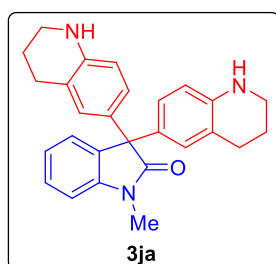
Physical State: pale solid (38 mg for 0.12 mmol scale, 75%). m.p.: 278-280 °C. R$_f$: 0.13 (30% EtOAc/hexane). ^{1}H NMR (400 MHz, CDCl$_3$): δ 7.26-7.21 (m, 2H), 7.04 (t, J = 7.2 Hz,

1H), 6.87-6.81 (m, 5H), 6.35-6.33 (m, 2H), 3.76 (br, 2H), 3.25-3.22 (m, 7H), 2.65 (t, J = 6.4 Hz, 4H), 1.87 (p, J_1 = 5.6 Hz, 4H). ^{13}C {^1H} NMR (100 MHz, CDCl$_3$): δ 179.1, 144.1, 143.3, 134.8, 130.7, 129.6, 127.9, 127.2, 126.2, 122.8, 121.4, 114.2, 108.4, 61.5, 42.3, 27.4, 26.9, 22.4. IR (KBr, cm^{-1}): 3409, 2839, 2925, 1703, 1606, 1511, 1275. HRMS (ESI) m/z: [M+H]$^+$ Calcd for C$_{27}$H$_{28}$N$_3$O: 410.2227; Found: 410.2246.

5-chloro-1-methyl-3,3-bis(1,2,3,4-tetrahydroquinolin-6-yl) indolin-2-one (3ka):
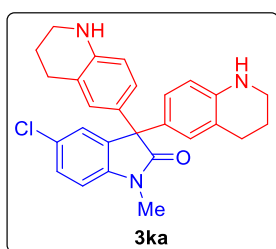
Physical State: pink solid (36 mg for 0.10 mmol scale, 80%). m.p.: 195-200 °C. R$_f$: 0.3 (40% EtOAc/hexane). ^1H NMR (400 MHz, CDCl$_3$): δ 7.23 (dd, J_1 = 8.0 Hz, J_2 = 2.0 Hz, 1H), 7.18 (d, J = 2.0 Hz, 1H), 6.79-6.77 (m, 5H), 6.37-6.35 (m, 2H), 3.27-3.24 (m, 7H), 2.67 (t, J = 6.4 Hz, 4H), 1.89 (quint, J = 5.6 Hz, 4H). ^{13}C {^1H} NMR (100 MHz, CDCl$_3$): δ 178.7, 144.3, 141.9, 136.5, 130.0, 129.5, 128.2, 127.9, 127.2, 126.5, 121.5, 114.3, 109.4, 61.8, 42.3, 27.4, 27.0, 22.4. IR (KBr, cm^{-1}): 3365, 2923, 2836, 1706, 1610, 1514, 811. HRMS (ESI) m/z: [M+H]$^+$ Calcd for C$_{27}$H$_{27}$ClN$_3$O: 444.1837; Found: 444.1780.

1-benzyl-3,3-bis(1-methyl-1,2,3,4-tetrahydroquinolin-6-yl) indolin-2-one (3ib):
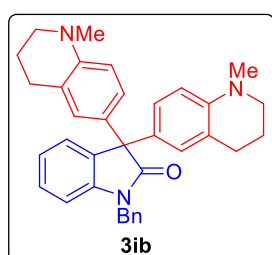
Physical State: white solid (82 mg for 0.21 mmol scale, 76%). m.p.: 117-122 °C. R$_f$: 0.5 (20% EtOAc/hexane). ^1H NMR (400 MHz, CDCl$_3$): δ 7.28-7.24 (m, 6H), 7.11 (dt, J_1 = 7.6 Hz, J_2 = 1.2 Hz, 1H), 7.00 (dd, J_1 = 7.6 Hz, J_2 = 1.2 Hz, 1H), 6.95 (dd, J_1 = 8.8 Hz, J_2 = 2.4 Hz, 2H), 6.87 (d, J = 2.4 Hz, 2H), 6.71 (d, J = 7.6 Hz, 1H), 6.48 (d, J = 8.4 Hz, 2H), 4.96 (s, 2H), 3.17 (t, J = 6 Hz, 4H), 2.84 (s, 6H), 2.67 (t, J = 6.4 Hz, 4H), 1.92 (quint, J = 6.4 Hz, 4H). ^{13}C {^1H} NMR (100 MHz, CDCl$_3$): δ 179.1, 146.0, 142.4, 136.6, 135.0, 129.9, 129.1, 129.0, 127.7, 127.6, 127.4, 126.2, 122.9, 122.88, 110.9, 109.5, 61.4, 51.5, 44.2, 39.4, 28.2, 22.7. IR (KBr, cm^{-1}): 2927, 2855, 1713,

1608, 1506, 1323, 1207. HRMS (ESI) m/z: [M+H]$^+$ Calcd for $C_{35}H_{36}N_3O$: 514.2818; Found: 514.2853.

1-methyl-3,3-bis(1-methyl-1,2,3,4-tetrahydroquinolin-6-yl) indolin-2-one (3jb):
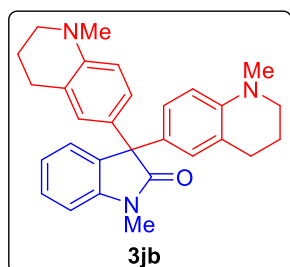
Physical State: brown solid (32.5 mg for 0.12 mmol scale, 60%). m.p.: 150-165 °C. R$_f$: 0.6 (30% EtOAc/hexane). ^{1}H NMR (700 MHz, CDCl$_3$): δ 7.18-7.16 (m, 2H), 6.96 (t, J = 7.7 Hz, 1H), 6.84 (d, J = 8.4 Hz, 2H), 6.79-6.77 (m, 3H), 6.39 (d, J = 8.4 Hz, 2H), 3.18 (s, 3H), 3.09 (t, J = 5.6 Hz, 4H), 2.75 (s, 6H), 2.59 (t, J = 7 Hz, 4H), 1.84 (quint, J = 6.3 Hz, 4H). ^{13}C {^{1}H} NMR (175 MHz, CDCl$_3$): δ 179.1, 146.0, 143.3, 134.9, 129.8, 129.0, 127.8, 127.4, 126.2, 122.9, 122.8, 110.8, 108.4, 61.4, 51.5, 39.4, 28.2, 26.9, 22.7. IR (KBr, cm^{-1}): 3130, 2927, 1709, 1606, 1510. HRMS (ESI) m/z: [M+H]$^+$ Calcd for $C_{29}H_{32}N_3O$: 438.2540; Found: 438.2511.

5-chloro-1-methyl-3,3-bis(1-methyl-1,2,3,4-tetrahydroquinolin-6-yl)indolin-2-one (3kb):
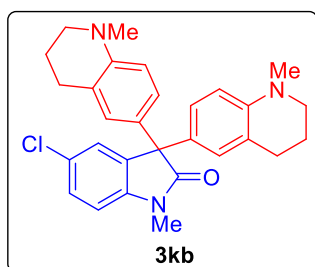
Physical State: white solid (47 mg for 0.10 mmol scale, 97%). m.p.: 110-112 °C. R$_f$: 0.2 (50% EtOAc/hexane). ^{1}H NMR (400 MHz, CDCl$_3$): δ 7.23-7.19 (m, 2H), 6.89-6.86 (m, 2H), 6.81-6.76 (m, 3H), 6.46 (d, J = 8.4 Hz, 2H), 3.23 (s, 3H), 3.18 (t, J = 6.0 Hz, 4H), 2.84 (s, 6H), 2.67 (t, J = 6.4 Hz, 4H), 1.92 (quint, J = 6.0 Hz, 4H). ^{13}C {^{1}H} NMR (100 MHz, CDCl$_3$): δ 178.7, 146.2, 141.9, 136.5, 129.0, 128.9, 128.1, 127.9, 127.3, 126.5, 123.0, 110.8, 109.3, 61.6, 51.5, 39.3, 28.2, 27.0, 22.7. IR (KBr, cm^{-1}): 2928, 2817, 1717, 1608, 1510, 806. HRMS (ESI) m/z: [M+H]$^+$ Calcd for $C_{29}H_{31}ClN_3O$: 472.2150; Found: 472.2167.

3,3-bis(4-(dimethylamino)phenyl)-5-methoxyindolin-2-one (3b'):
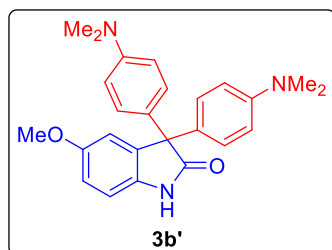
Physical State: yellow solid (17 mg for 0.10 mmol scale, 42%). m.p.: 247-250 °C. R_f: 0.4 (40% EtOAc/hexane). ^{1}H NMR (400 MHz, CDCl$_3$): δ 8.90 (s, 1H), 7.15 (d, J = 8.8 Hz, 4H), 6.82 (d, J = 8.4 Hz, 1H), 6.79 (d, J = 2.4 Hz, 1H), 6.70 (dd, J_1 = 8.4 Hz, J_2 = 2.4 Hz, 1H), 6.65 (J = 8.8 Hz, 4H), 3.78 (s, 3H), 2.90 (s, 12H). ^{13}C {^{1}H} NMR (100 MHz, CDCl$_3$): δ 181.5, 156.0, 149.9, 136.6, 134.1, 130.0, 129.4, 113.4, 112.7, 112.67, 110.7, 62.4, 56.0, 40.9. IR (KBr, cm^{-1}): 2922, 2850, 1717, 1516, 1489, 1288, 1246, 1030. HRMS (ESI) m/z: [M+H]$^+$ Calcd for C$_{25}$H$_{28}$N$_3$O$_2$: 402.2176; Found: 402.2171.

2,2'',3,3''-tetrahydro-1H,1''H-[5,3':3',5''-terbenzo[*b*]pyrrol]-2'(1'*H*)-one (3b''):

The crude reaction mixture was subjected to HRMS and a trace amount of the product **3b″** was observed. HRMS (ESI) m/z: [M+H]$^+$ Calcd for C$_{24}$H$_{22}$N$_3$O: 368.1757; Found: 368.1728.

1-methyl-3-(1-methyl-1,2,3,4-tetrahydroquinolin-6-yl)-3-(1,2,3,4-tetrahydroquinolin-6-yl)indolin-2-one (3jab):
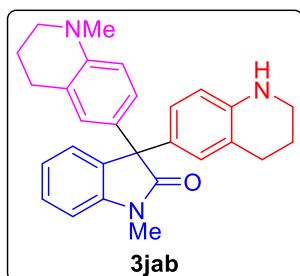
Physical State: pale yellow solid (30 mg for 0.19 mmol scale, 38%). m.p.: 119-120 °C. R_f: 0.3 (30% EtOAc/hexane). ^{1}H NMR (400 MHz, CDCl$_3$): δ 7.27-7.22 (m, 2H), 7.04 (t, J = 7.6 Hz, 1H), 6.91 (dd, J_1 = 8.4 Hz, J_2 = 2.4 Hz, 1H), 6.87-6.81 (m, 4H), 6.46 (d, J = 8.4 Hz, 1H), 6.36-6.34 (m, 1H), 3.25-3.23 (m, 5H), 3.16 (t, J = 6.0 Hz, 2H), 2.83 (s, 3H), 2.66 (t, J = 6.4 Hz, 4H), 1.95-1.84 (m, 4H). ^{13}C {^{1}H} NMR (100 MHz, CDCl$_3$): δ 179.1, 146.0, 144.0, 143.3, 134.8, 130.8, 129.8, 129.6,

129.0, 127.8, 127.4, 127.2, 126.2, 122.9, 122.8, 121.4, 114.3, 110.8, 108.4, 61.4, 51.5, 42.3, 39.4, 28.2, 27.3, 26.9, 22.7, 22.4. IR (KBr, cm^{-1}): 2925, 2835, 1707, 1607, 1510. HRMS (ESI) m/z: [M+H]$^+$ Calcd for C$_{28}$H$_{30}$N$_3$O: 424.2383; Found: 424.2376.

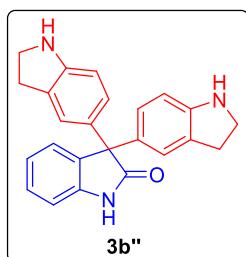## 1-methyl-3-(1-methyl-1,2,3,4-tetrahydroquinolin-6-yl)-3-(quinolin-6-yl)indolin-2-one (4jab):
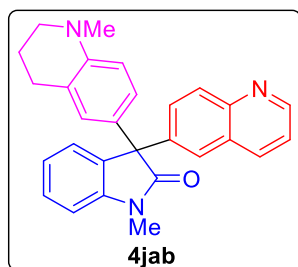
Physical State: pale yellow solid (20 mg for 0.09 mmol scale, 51%). m.p.: 105-110 °C. R$_f$: 0.2 (50% EtOAc/hexane). ^{1}H NMR (400 MHz, CDCl$_3$): δ 8.86 (d, J = 2.8 Hz, 1H), 8.07-8.01 (m, 2H), 7.72-7.67 (m, 2H), 7.36-7.31 (m, 3H), 7.10 (t, J = 8.0 Hz, 1H), 6.95-6.90 (m, 2H), 6.84 (d, J = 1.6 Hz, 1H), 6.48 (d, J = 8.4 Hz, 1H), 3.32 (s, 3H), 3.19 (t, J = 5.6 Hz, 2H), 2.85 (s, 3H), 2.66 (t, J = 6.4 Hz, 2H), 1.93 (quint, J = 6.0 Hz, 2H). ^{13}C {^{1}H} NMR (100 MHz, CDCl$_3$): δ 178.2, 150.7, 147.8, 146.4, 143.4, 141.1, 136.7, 133.5, 130.9, 129.8, 129.0, 128.6, 128.5, 128.2, 127.4, 127.0, 126.3, 123.2, 123.1, 121.5, 110.9, 108.9, 64.0, 51.5, 39.3, 28.2, 27.0, 22.6. IR (KBr, cm^{-1}): 3160, 2927, 1686, 1608, 1511, 1401. HRMS (ESI) m/z: [M+H]$^+$ Calcd for C$_{28}$H$_{26}$N$_3$O: 420.2070; Found: 420.2092.

pyridin-4-yl(m-tolyl)methyl 2,2,2-trichloroacetimidate (5c):
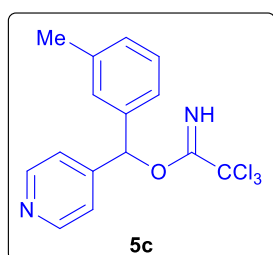
Physical State: yellow liquid (82 mg for 0.25 mmol scale, 95%). R$_f$: 0.4 (30% EtOAc/hexane). ^{1}H NMR (400 MHz, CDCl$_3$): δ 8.60-8.58 (m, 2H), 8.49 (s, 1H), 7.35-7.34 (m, 2H), 7.28-7.21 (m, 3H), 7.15-7.13 (m, 1H), 6.86 (s, 1H), 2.34 (s, 3H). ^{13}C {^{1}H} NMR (100 MHz, CDCl$_3$): δ 161.3, 150.2, 149.0, 138.8, 138.4, 129.8, 128.9, 128.1, 124.5, 121.5, 91.5, 80.2, 21.7. IR (KBr, cm^{-1}): 3028, 2922, 1688, 1599, 1412, 1289, 1068, 795. HRMS (ESI) m/z: [M+H]$^+$ Calcd for C$_{15}$H$_{14}$Cl$_3$N$_2$O: 343.0166; Found: 343.0160.

6-benzhydryl-1-methyl-1,2,3,4-tetrahydroquinoline (6ba):
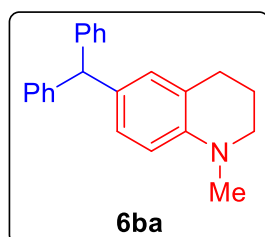
Physical State: colourless solid (36 mg for 0.14 mmol scale, 85%). m.p.: 108-111 °C. R_f: 0.2 (5% EtOAc/hexane). ^{1}H NMR (400 MHz, CDCl$_3$): δ 7.27-7.22 (m, 4H), 7.19-7.11 (m, 6H), 6.76 (d, J = 8.0 Hz, 1H), 6.71 (s, 1H), 6.50 (d, J = 8.4 Hz, 1H), 5.40 (s, 1H), 3.17 (t, J = 5.6 Hz, 2H), 2.84 (s, 3H), 2.67 (t, J = 6.4 Hz, 2H), 1.94 (quint, J = 6.4 Hz, 2H). ^{13}C {^{1}H} NMR (100 MHz, CDCl$_3$): δ 145.5, 145.1, 131.9, 130.2, 129.8, 128.5, 128.2, 126.3, 123.0, 111.0, 56.4, 51.6, 39.5, 28.1, 22.8. IR (KBr, cm^{-1}): 3134, 1636, 1510, 1401. HRMS (ESI) m/z: [M+H]$^+$ Calcd for C$_{23}$H$_{24}$N: 314.1903; Found: 314.1901.

6-benzhydryl-1-(methylsulfonyl)-1,2,3,4-tetrahydroquinoline (6ca):
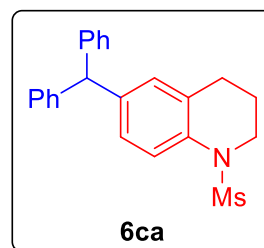
Physical State: yellow solid (44 mg for 0.13 mmol scale, 91%). m.p.: 94-96 °C. R_f: 0.4 (20% EtOAc/hexane). ^{1}H NMR (400 MHz, CDCl$_3$): δ 7.60 (d, J = 8.8 Hz, 1H), 7.29 (t, J = 7.6 Hz, 4H), 7.21 (t, J = 7.6 Hz, 2H), 7.11 (d, J = 7.2 Hz, 4H), 6.94-6.91 (m, 1H), 6.88 (s, 1H), 5.46 (s, 1H), 3.81-3.78 (m, 2H), 2.90 (s, 3H), 2.76 (t, J = 6.8 Hz, 2H), 1.97 (quint, J = 6.8 Hz, 2H). ^{13}C {^{1}H} NMR (100 MHz, CDCl$_3$): δ 143.9, 140.3, 135.4, 130.8, 129.6, 129.1, 128.6, 128.1, 126.6, 122.6, 56.4, 46.7, 38.9, 27.4, 22.5. IR (KBr, cm^{-1}): 1491, 1344, 1155, 975, 753. HRMS (ESI) m/z: [M+Na]$^+$ Calcd for C$_{23}$H$_{23}$NO$_2$SNa: 400.1342; Found: 400.1331.

6-(1-phenylethyl)-1-tosyl-1,2,3,4-tetrahydroquinoline (6db):
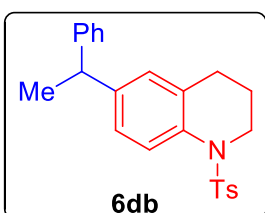
Physical State: white solid (15 mg for 0.07 mmol scale, 55%). m.p.: 120-130 °C. R_f: 0.3 (20% EtOAc/hexane). ^{1}H NMR (400 MHz, CDCl$_3$): δ 7.67 (d, J = 8.4 Hz, 1H), 7.47 (d, J = 8.4 Hz, 2H),

7.31-7.27 (m, 2H), 7.20-7.16 (m, 5H), 7.06-7.04 (m, 1H), 6.83 (s, 1H), 4.07 (q, J = 7.2 Hz, 1H), 3.78-3.75 (m, 2H), 2.41-2.37 (m, 5H), 1.61-1.56 (m, 5H). ^{13}C {^{1}H} NMR (100 MHz, CDCl$_3$): δ 146.7, 143.7, 143.2, 137.3, 135.2, 130.7, 129.9, 128.7, 128.5, 127.9, 127.4, 126.4, 126.1, 125.0, 46.8, 44.5, 27.0, 22.2, 21.92, 21.9. IR (KBr, cm^{-1}): 3025, 2920, 2872, 1598, 1493, 1341, 1163. HRMS (ESI) m/z: [M+Na]$^+$ Calcd for C$_{24}$H$_{25}$NO$_2$SNa: 414.1498; found: 414.1488.

5-(1-phenylethyl)-1-tosylindoline (6eb):
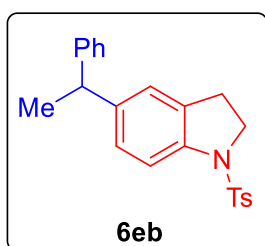
Physical State: white solid (36 mg for 0.11 mmol scale, 88%). m.p.: 101-104 °C. R$_f$: 0.3 (20% EtOAc/hexane). ^{1}H NMR (400 MHz, CDCl$_3$): δ 7.65 (d, J = 8.4 Hz, 2H), 7.52 (d, J = 8.4 Hz, 1H), 7.26 (t, J = 7.6 Hz, 2H), 7.21-7.15 (m, 5H), 7.06 (dd, J_1 = 8.0 Hz, J_2 = 0.8 Hz, 1H), 6.90 (s, 1H), 4.06 (q, J = 7.2 Hz, 1H),

3.87 (t, J = 8.4 Hz, 2H), 2.80 (t, J = 8.4 Hz, 2H), 2.35 (s, 3H), 1.57 (d, J = 7.2 Hz, 3H). ^{13}C {^{1}H} NMR (100 MHz, CDCl$_3$): δ 146.7, 144.3, 142.4, 140.4, 134.3, 132.3, 129.9, 128.7, 127.8, 127.6, 127.2, 126.4, 124.6, 115.0, 50.4, 44.6, 28.2, 22.3, 21.8. IR (KBr, cm^{-1}): 3133, 1636, 1401, 1165, 1106. HRMS (ESI) m/z: [M+H]$^+$ Calcd for C$_{23}$H$_{24}$NO$_2$S: 378.1522; found: 378.1525.

5-benzhydryl-1-(methylsulfonyl)indoline (6fa):

Physical State: colourless white solid (47 mg for 0.14 mmol scale, 93%). m.p.: 98-102 °C. R$_f$: 0.2 (20% EtOAc/hexane). ^{1}H NMR (400 MHz, CDCl$_3$): δ 7.30 (m, 5H), 7.24-7.19 (m, 2H), 7.10 (d, J = 7.6 Hz, 4H), 6.96-6.94 (m, 2H), 5.49 (s, 1H), 3.95 (t, J = 8.4 Hz, 2H), 3.07 (t, J = 8.4 Hz, 2H), 2.85 (s, 3H). ^{13}C {^{1}H} NMR (100 MHz, CDCl$_3$): δ 144.1, 140.7, 140.0, 131.7, 129.7, 129.5, 128.7, 126.7, 126.6, 113.7, 56.6, 50.9, 34.8,

28.3. IR (KBr, cm^{-1}): 3371, 3023, 2927, 1696, 1485, 1347, 1160. HRMS (ESI) m/z: [M+Na]$^+$ Calcd for C$_{22}$H$_{21}$NO$_2$SNa: 386.1185; Found: 386.1185.

1-(5-benzhydrylindolin-1-yl)-3-chloropropan-1-one (6ga):
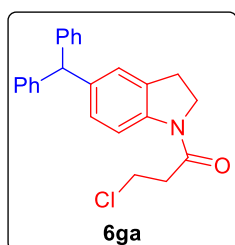
Physical State: brown solid (36 mg for 0.14 mmol scale, 67%). m.p.: 168-172 °C. R$_f$: 0.4 (20% EtOAc/hexane). ^{1}H NMR (700 MHz, CDCl$_3$): δ 8.05 (d, J = 8.4 Hz, 1H), 7.21-7.17 (m, 4H), 7.14-7.12 (m, 2H),7.02 (d, J = 7.7 Hz, 4H), 6.89 (d, J = 8.4 Hz, 1H), 6.85 (s, 1H), 5.43 (s, 1H), 3.96 (t, J = 8.4 Hz, 2H), 3.81 (t, J = 7.0 Hz, 2H), 3.05

(t, J = 8.4 Hz, 2H), 2.80 (t, J = 7.0 Hz, 2H). ^{13}C {^{1}H} NMR (175 MHz, CDCl$_3$): δ 167.9, 144.3, 141.4, 140.2, 131.7, 129.7, 129.1, 128.6, 126.6, 125.8, 117.1, 56.7, 48.5, 39.7, 39.0, 28.3. IR (KBr, cm^{-1}): 3131, 1661, 1487, 1401, 1115. HRMS (ESI) m/z: [M+H]$^+$ Calcd for C$_{24}$H$_{23}$ClNO: 376.1463; Found: 376.1464.

3-chloro-1-(5-(1-phenylethyl)indolin-1-yl)propan-1-one (6gb):
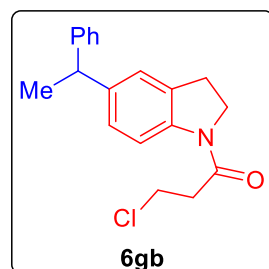
Physical State: light yellow solid (18 mg for 0.09 mmol scale, 61%). m.p.: 152-156 °C. R$_f$: 0.3 (20% EtOAc/hexane). ^{1}H NMR (400 MHz, CDCl$_3$): δ 8.13 (d, J = 8.4 Hz, 1H), 7.29-7.28 (m, 2H), 7.21-7.17 (m, 3H), 7.09 (d, J = 8.4 Hz, 1H), 7.01 (s, 1H), 4.14-4.10 (m, 1H), 4.05 (t, J = 8.4 Hz, 2H), 3.90 (t, J = 6.8 Hz, 2H), 3.16 (t, J = 8.4 Hz, 2H), 2.89 (t, J = 6.8 Hz, 2H), 1.61 (d, J = 7.2 Hz, 3H). ^{13}C {^{1}H} NMR (100 MHz, CDCl$_3$): δ 167.8, 156.1, 146.8, 142.8, 131.7, 128.7, 127.9, 127.1, 126.4, 124.2, 117.2, 48.5, 44.7, 39.8, 39.0, 28.3, 22.3. IR (KBr, cm^{-1}): 3133, 1650, 1490, 1402, 1287, 1114. HRMS (ESI) m/z: [M+Na]$^+$ Calcd for C$_{19}$H$_{20}$ClNONa: 336.1126; Found: 336.1117.

(1-(methylsulfonyl)-1,2,3,4-tetrahydroquinolin-6-yl)diphenyl methanol (7ca):

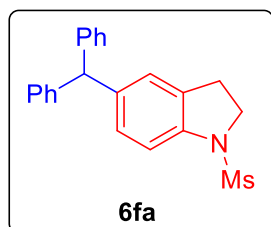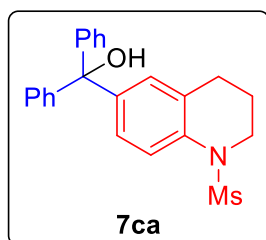Physical State: white solid (16 mg for 0.05 mmol scale, 78%). m.p.: 150-160 °C. R_f: 0.2 (30% EtOAc/hexane). ^{1}H NMR (400 MHz, CDCl$_3$): δ 7.53 (d, J = 8.8 Hz, 1H), 7.26-7.18 (m, 10H), 7.04 (d, J = 1.2 Hz, 1H), 6.94 (dd, J_1 = 8.8 Hz, J_2 = 2.0 Hz, 1H), 3.72 (t, J = 6.0 Hz, 2H), 2.83 (s, 3H), 2.71 (t, J = 6.4 Hz, 2H), 1.93-1.87 (m, 2H). ^{13}C {^{1}H} NMR (175 MHz, CDCl$_3$): δ 147.0, 143.1, 136.2, 129.3, 128.6, 128.3, 128.1, 127.7, 127.0, 121.9, 81.9, 46.8, 39.0, 27.7, 22.5. IR (KBr, cm^{-1}): 3134, 1636, 1492, 1401, 1338, 1151. HRMS (ESI) m/z: [M+Na]$^+$ Calcd for C$_{23}$H$_{23}$NO$_3$SNa: 416.1291; Found: 416.1294.

(1-(methylsulfonyl)indolin-5-yl)diphenylmethanol (7fa):
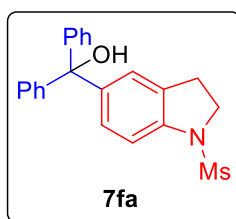
Physical State: white solid (15 mg for 0.08 mmol scale, 49%). m.p.: 155-160 °C. R_f -value: 0.2 (30% EtOAc/hexane). ^{1}H NMR (400 MHz, CDCl$_3$): δ 7.27-7.18 (m, 11H), 7.10 (s, 1H), 7.00 (d, J = 8.4 Hz, 1H), 3.90 (t, J = 8.4 Hz, 2H), 3.02 (t, J = 8.4 Hz, 2H), 2.80 (s, 3H). ^{13}C {^{1}H} NMR (100 MHz, CDCl$_3$): δ 147.1, 143.0, 141.4, 131.3, 128.32, 128.3, 128.1, 127.7, 125.4, 113.0, 82.1, 50.9, 34.9, 28.3. IR (KBr, cm^{-1}): 3500, 1483, 1443, 1338, 1242, 1151. HRMS (ESI) m/z: [M+Na]$^+$ Calcd for C$_{22}$H$_{21}$NO$_3$SNa: 402.1134; Found: 402.1131.

(1-(methylsulfonyl)-1H-indol-5-yl)diphenylmethanol (7fa'):
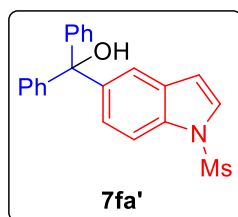
Physical State: light yellow solid (13 mg for 0.08 mmol scale, 42%). m.p.: 90-93 °C. R_f: 0.4 (30% EtOAc/hexane). ^{1}H NMR (400 MHz, CDCl$_3$): δ 7.75 (d, J = 8.8 Hz, 1H), 7.43 (d, J = 1.2 Hz, 1H), 7.35 (d, J = 3.6 Hz, 1H), 7.28-7.18 (m, 11H), 6.55 (d, J = 3.6 Hz, 1H), 3.02 (s, 3H). ^{13}C {^{1}H} NMR (175 MHz, CDCl$_3$): δ 147.3, 142.9, 134.2, 130.5,

128.33, 128.3, 127.7, 126.8, 125.6, 121.3, 112.7, 109.5, 82.4, 41.2. IR (KBr, cm^{-1}): 3516, 3150, 1401, 1360, 1164, 1141. HRMS (ESI) m/z: [M+Na]$^+$ Calcd for C$_{22}$H$_{19}$NO$_3$SNa: 400.0978; Found: 400.0810.

8-benzhydryl-5,6-dihydro-1H-pyrrolo[3,2,1-ij]quinolin-4(2H)-one (9a):
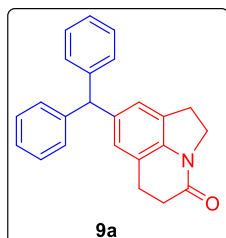
Physical State: light yellow solid (76 mg for 0.23 mmol scale, 98%). m.p.: 105-110 °C. R$_f$: 0.5 (30% EtOAc/hexane). ^{1}H NMR (400 MHz, CDCl$_3$): δ 7.28 (t, J = 7.6 Hz, 4H), 7.23-7.18 (m, 2H), 7.11 (d, J = 7.6 Hz, 4H), 6.82 (s, 1H), 6.75 (s, 1H), 5.48 (s, 1H), 4.04 (t, J = 8.8 Hz, 2H), 3.09 (t, J = 8.4 Hz, 2H), 2.86 (t, J = 7.6 Hz, 2H), 2.63 (t, J = 7.6 Hz, 2H). ^{13}C {^{1}H} NMR (100 MHz, CDCl$_3$): δ 167.8, 144.3, 140.0, 139.8, 129.6, 129.2, 128.6, 126.9, 126.6, 124.6, 120.1, 56.9, 45.6, 31.9, 28.0, 24.7. IR (KBr, cm^{-1}): 3056, 2928, 1615, 1490, 1382, 1154. HRMS (ESI) m/z: [M+H]$^+$ Calcd for C$_{24}$H$_{22}$NO: 340.1696; Found: 340.1711.

8-(pyridin-3-yl(m-tolyl)methyl)-5,6-dihydro-1H-pyrrolo[3,2,1-ij]quinolin-4(2H)-one (9c):
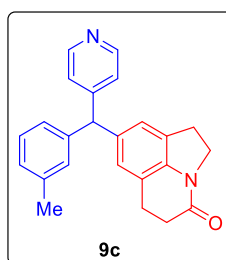
The crude reaction mixture was submitted for HRMS giving the product **9c** in trace amount. HRMS (ESI) m/z: [M+H]$^+$ Calcd for C$_{24}$H$_{23}$N$_2$O: 355.1805; Found: 355.1780.

8-(hydroxydiphenylmethyl)-5,6-dihydro-1H-pyrrolo[3,2,1-ij]quinolin-4(2H)-one (10a):
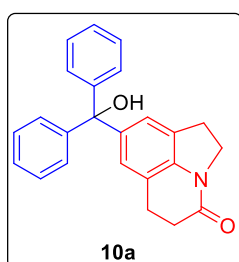
Physical State: white solid (27 mg for 0.15 mmol scale, 52%). m.p.: 140-145 °C. R$_f$: 0.3 (70% EtOAc/hexane). ^{1}H NMR (400 MHz, CDCl$_3$): δ 7.35-7.27 (m, 10H), 6.97 (s, 1H), 6.93 (s, 1H),

4.07 (t, J = 8.8 Hz, 2H), 3.13 (t, J = 8.8 Hz, 2H), 2.90 (t, J = 7.6 Hz, 2H), 2.77 (s, 1H), 2.66 (t, J = 7.6 Hz, 2H). ^{13}C {^{1}H} NMR (100 MHz, CDCl$_3$): δ 168.0, 147.4, 143.0, 140.9, 128.8, 128.4, 128.2, 127.7, 125.7, 123.5, 119.7, 82.4, 45.8, 32.0, 28.1, 24.9. IR (KBr, cm^{-1}): 3134, 1645, 1494, 1400. HRMS (ESI) m/z: [M+H]$^+$ Calcd for C$_{24}$H$_{22}$NO$_2$: 356.1645; Found: 356.1661.

8-(hydroxydiphenylmethyl)-5,6-dihydro-4H-pyrrolo[3,2,1-ij]quinolin-4-one (10a'):
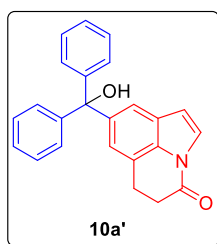
Physical State: brown solid (20 mg for 0.15 mmol scale, 40%). m.p.: 138-142 °C. R$_f$ 0.1 (70% EtOAc/hexane). ^{1}H NMR (400 MHz, CDCl$_3$): δ 7.67 (d, J = 3.2 Hz, 1H), 7.35-7.27 (m, 11H), 7.16 (s, 1H), 6.61 (d, J = 3.6 Hz, 1H), 3.21 (t, J = 7.6 Hz, 2H), 2.99 (t, J = 7.6 Hz, 2H), 2.87 (s, 1H). ^{13}C {^{1}H} NMR (100 MHz, CDCl$_3$): δ 166.9, 147.5, 143.5, 134.9, 129.0, 128.5, 128.3, 127.6, 122.3, 122.1, 120.0, 119.2, 110.6, 82.7, 32.9, 24.7. IR (KBr, cm^{-1}): 3406, 3141, 2919, 2850, 1685, 1467, 1399. HRMS (ESI) m/z: [M+Na]$^+$ Calcd for C$_{24}$H$_{19}$NO$_2$Na: 376.1308; Found: 376.1314.

NMR spectra of 5-methoxy-3,3-bis(1,2,3,4-tetrahydroquinolin-6-yl)indolin-2-one
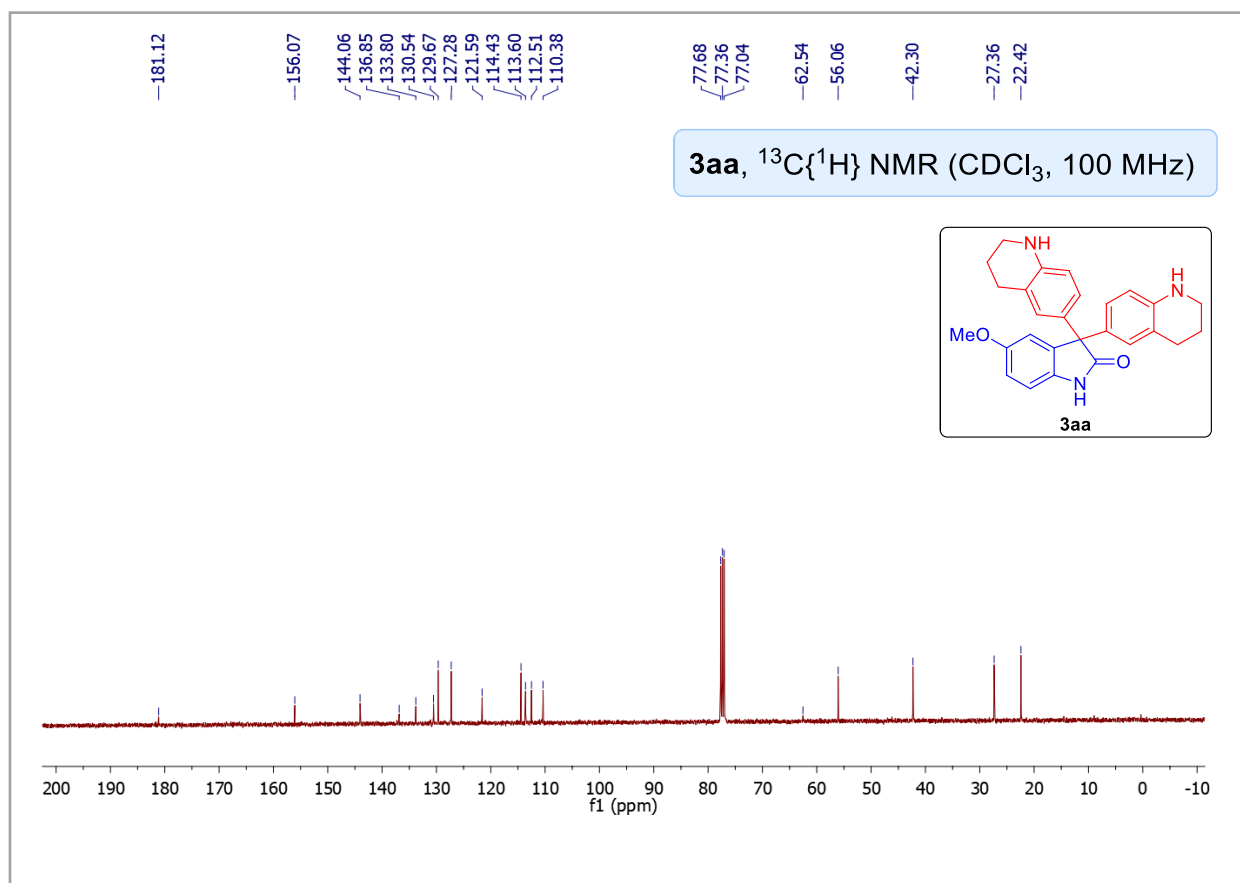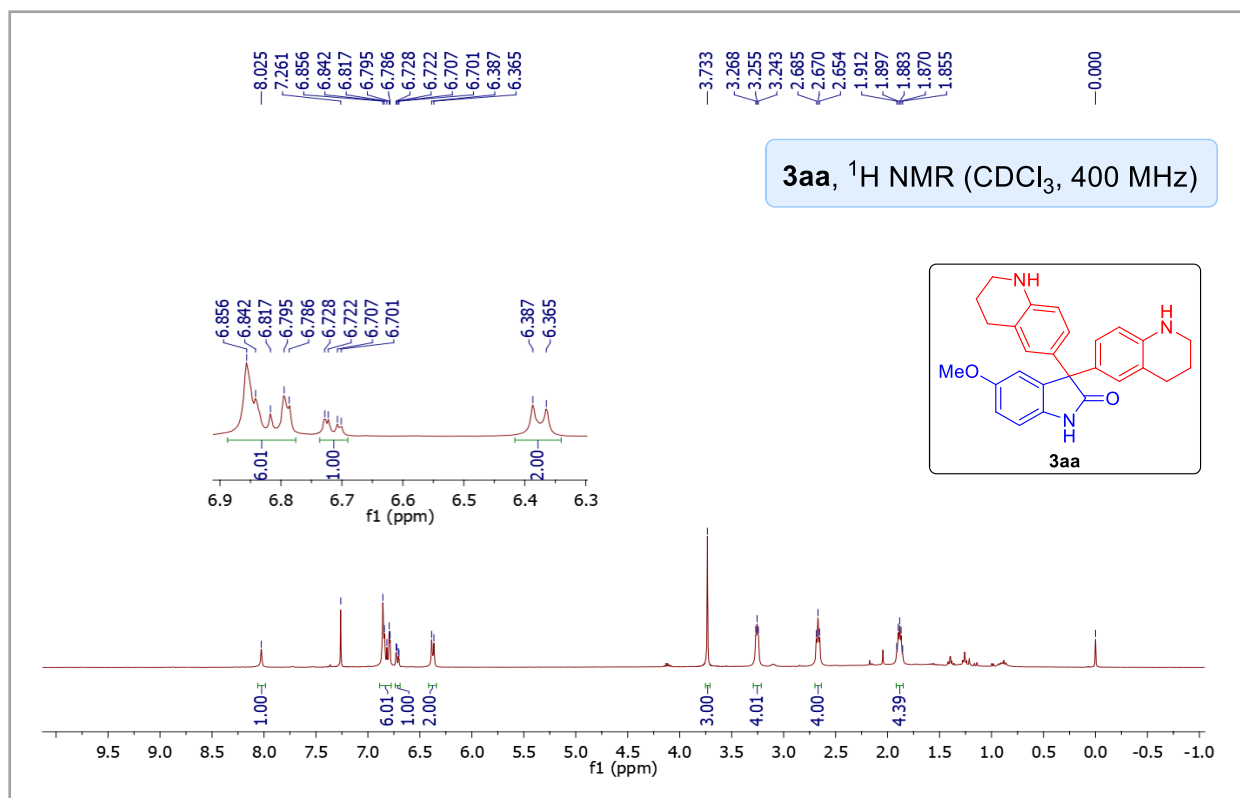
(3aa):

3aa, ^{1}H NMR (CDCl$_3$, 400 MHz)

3aa, ^{13}C{^{1}H} NMR (CDCl$_3$, 100 MHz)

NMR spectra of 1-methyl-3-(1-methyl-1,2,3,4-tetrahydroquinolin-6-yl)-3-(1,2,3,4-tetrahydroquinolin-6-yl)indolin-2-one (3jab):

3jab, ^{1}H NMR (CDCl$_3$, 400 MHz)

3jab, ^{13}C{^{1}H} NMR (CDCl$_3$, 100 MHz)

NMR spectra of 1-methyl-3-(1-methyl-1,2,3,4-tetrahydroquinolin-6-yl)-3-(quinolin-6-yl)indolin-2-one (4jab):

4jab, ^{1}H NMR (CDCl$_3$, 400 MHz)

4jab, ^{13}C {^{1}H} NMR (CDCl$_3$, 100 MHz)
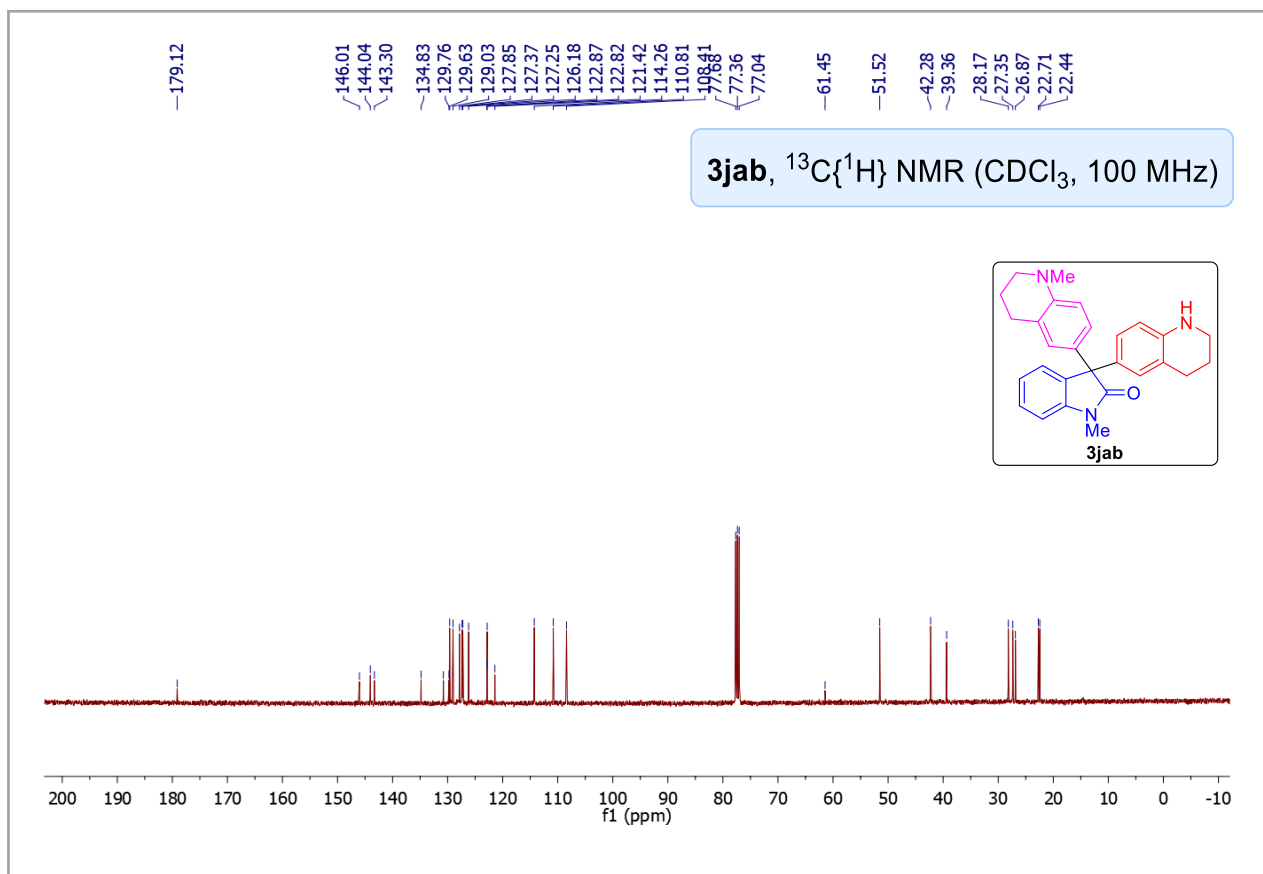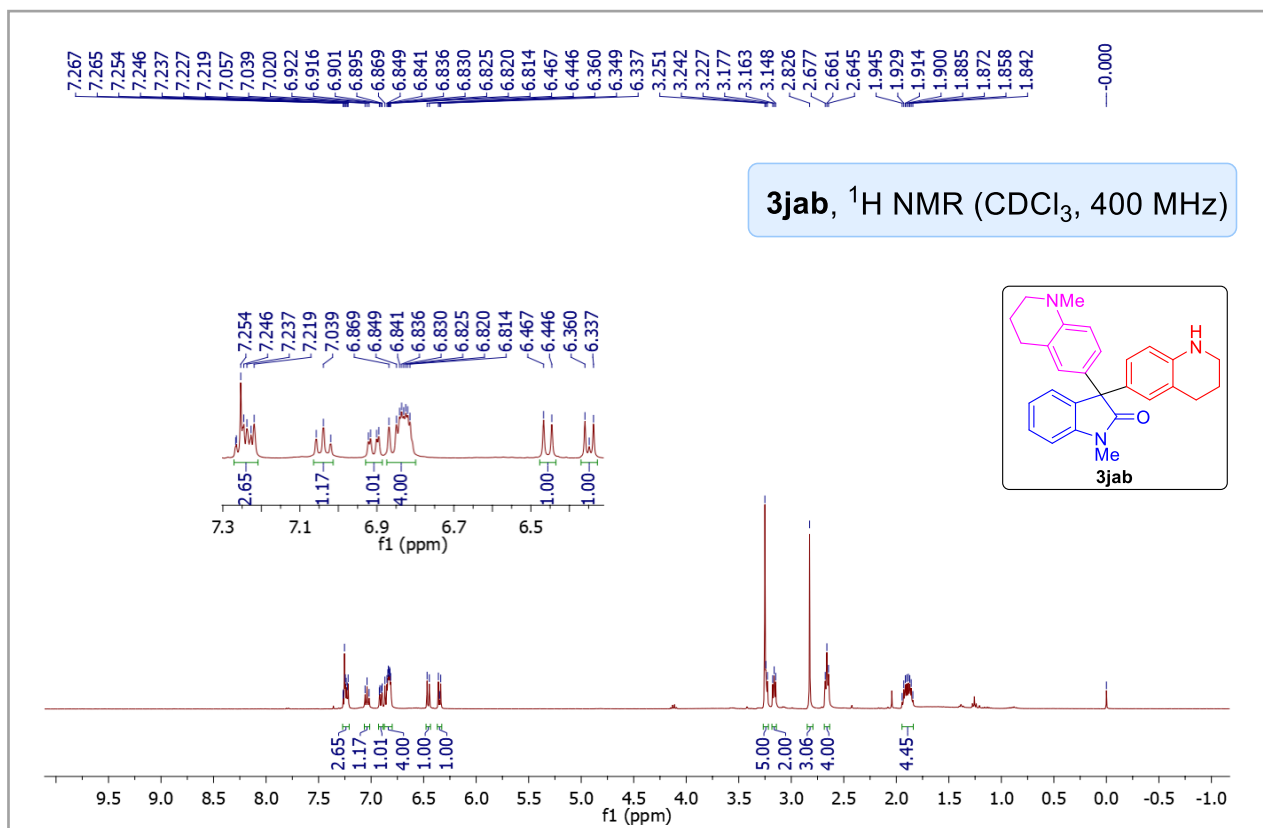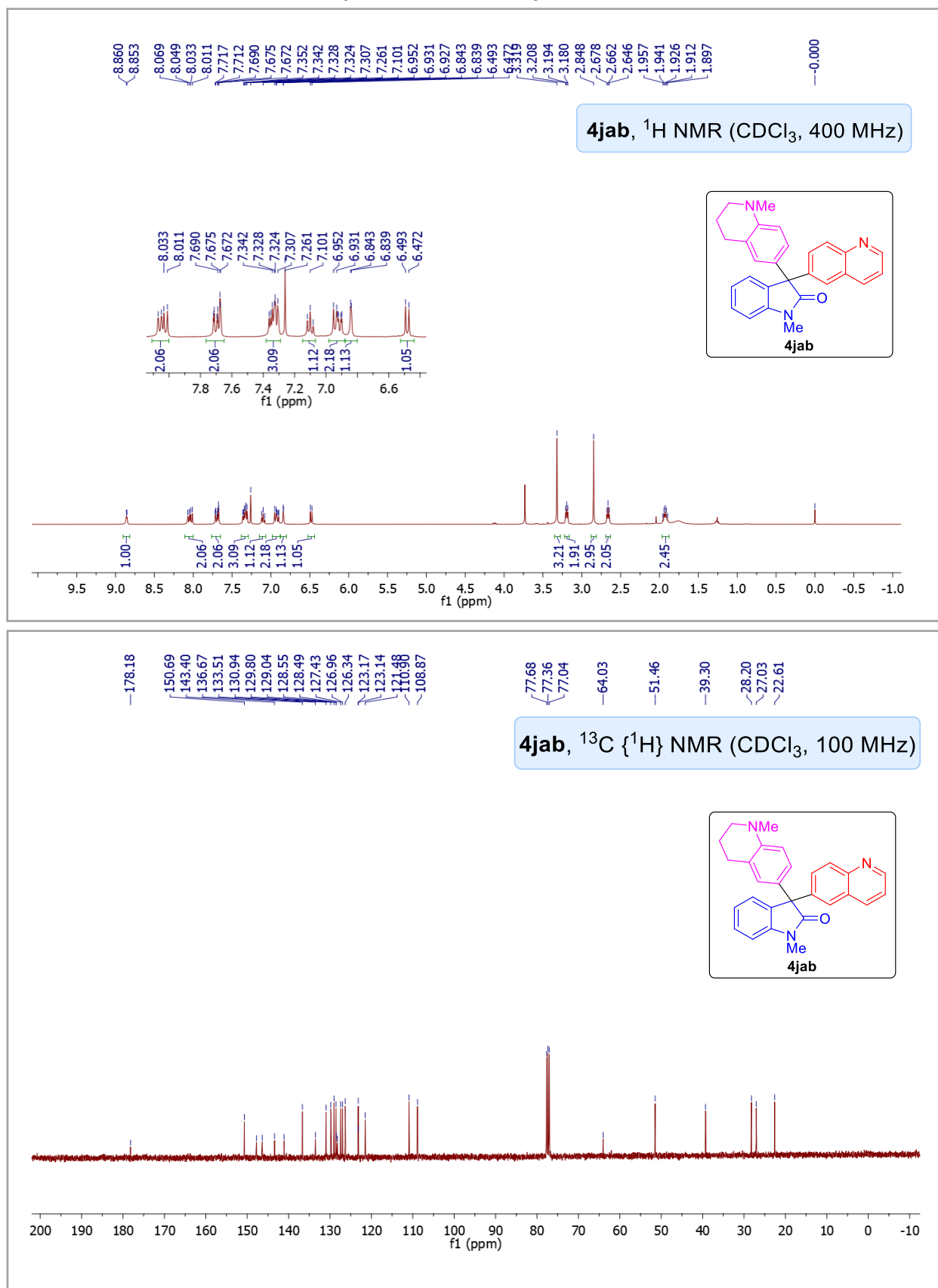
NMR spectra of 1-(5-Benzhydrylindolin-1-yl)-3-chloropropan-1-one (6ga):

6ga, ^{1}H NMR (CDCl$_3$, 700 MHz)

6ga, ^{13}C{^{1}H} NMR (CDCl$_3$, 176 MHz)
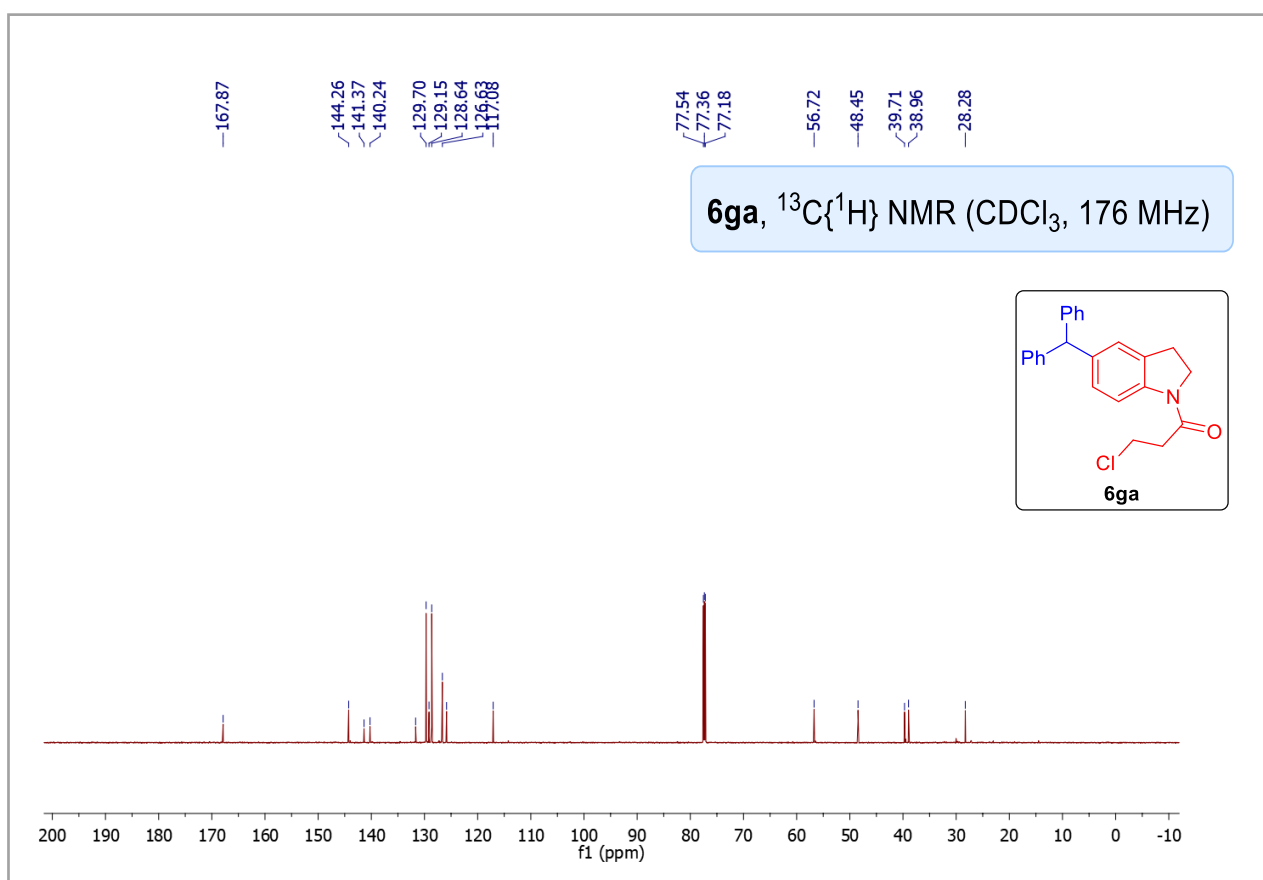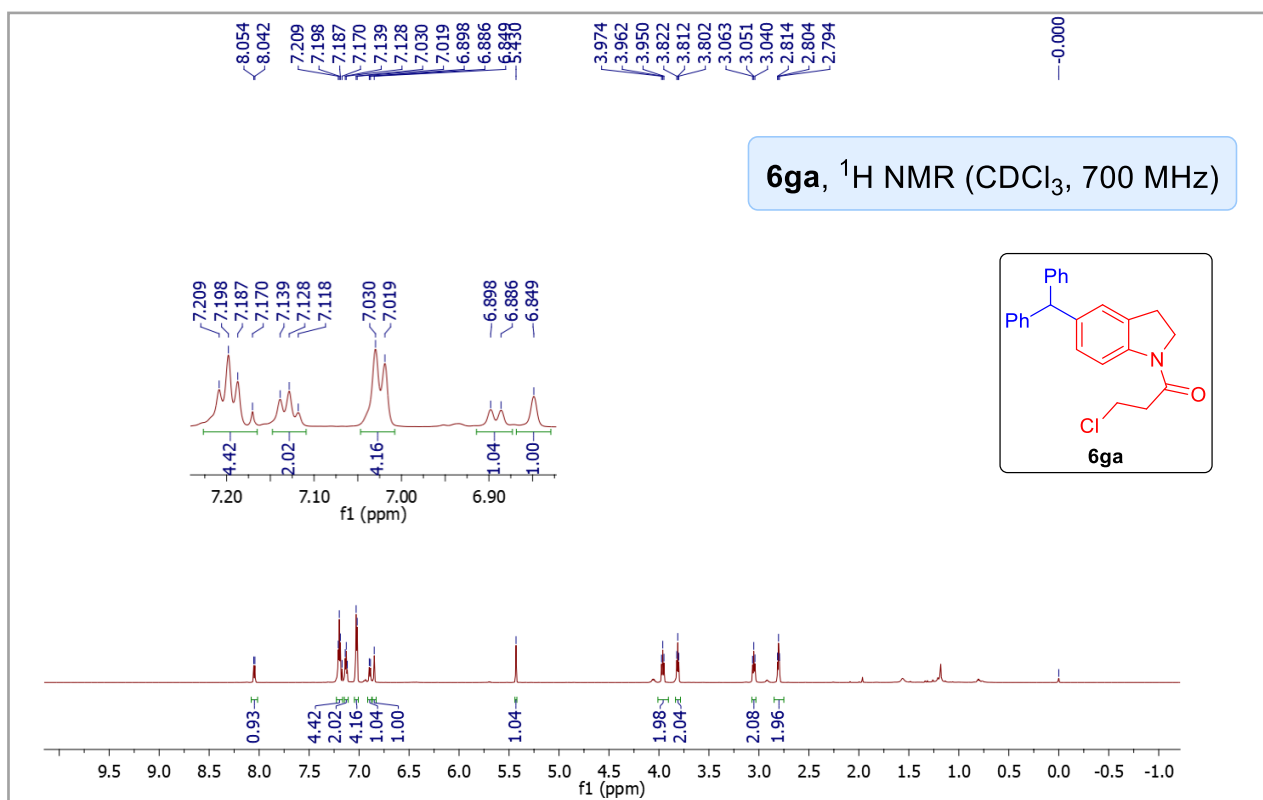
NMR spectra of 8-(Hydroxydiphenylmethyl)-5,6-dihydro-4H-pyrrolo[3,2,1-ij]-quinolin-4-one (10a′):

10a', ^{1}H NMR (CDCl$_3$, 400 MHz)

10a', ^{13}C {^{1}H} NMR (CDCl$_3$, 100 MHz)

Crystal Structure of 3aa

3aa   CCDC **2041963**

ORTEP diagram of **3aa** with 50% ellipsoid probability

Crystal Structure of 6fa

6fa CCDC **2041964**

ORTEP diagram of **6fa** with 50% ellipsoid probability
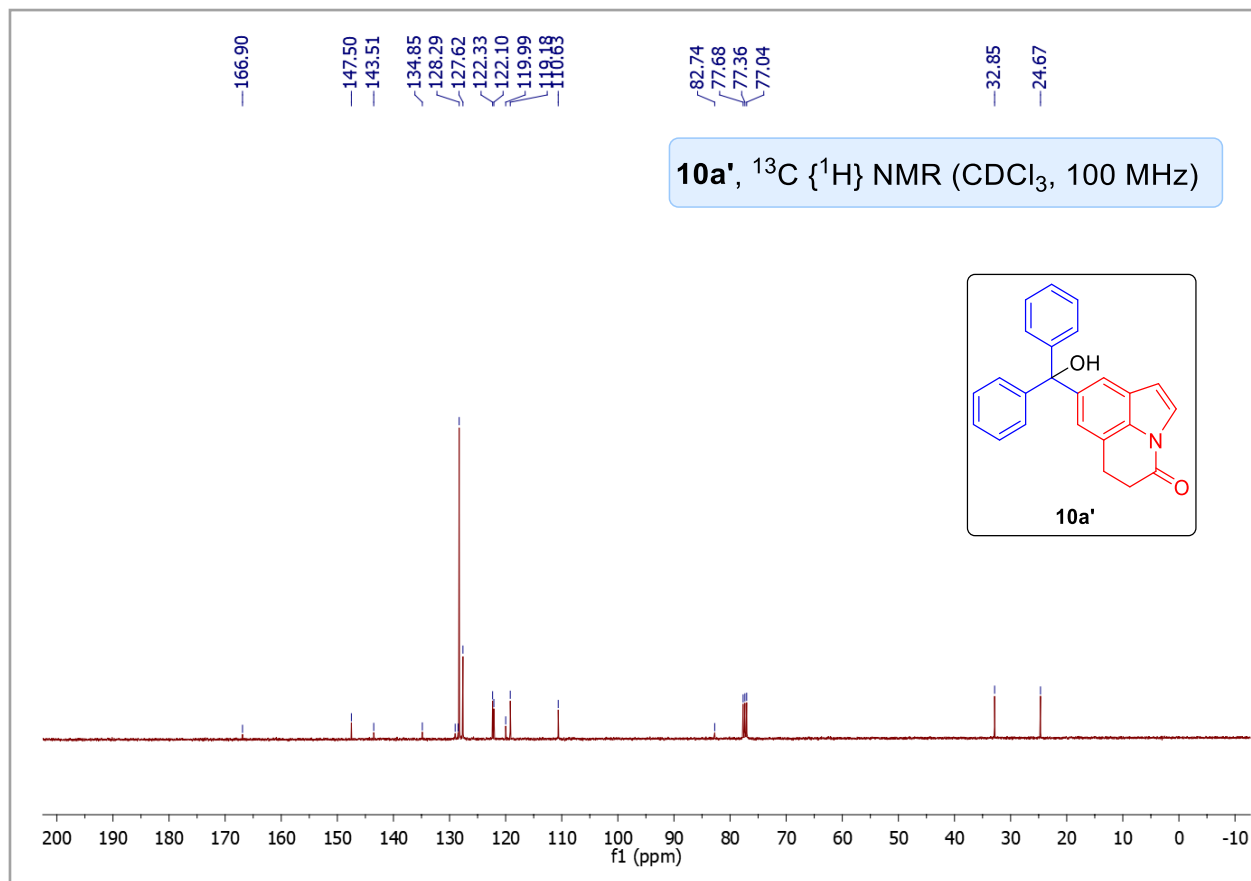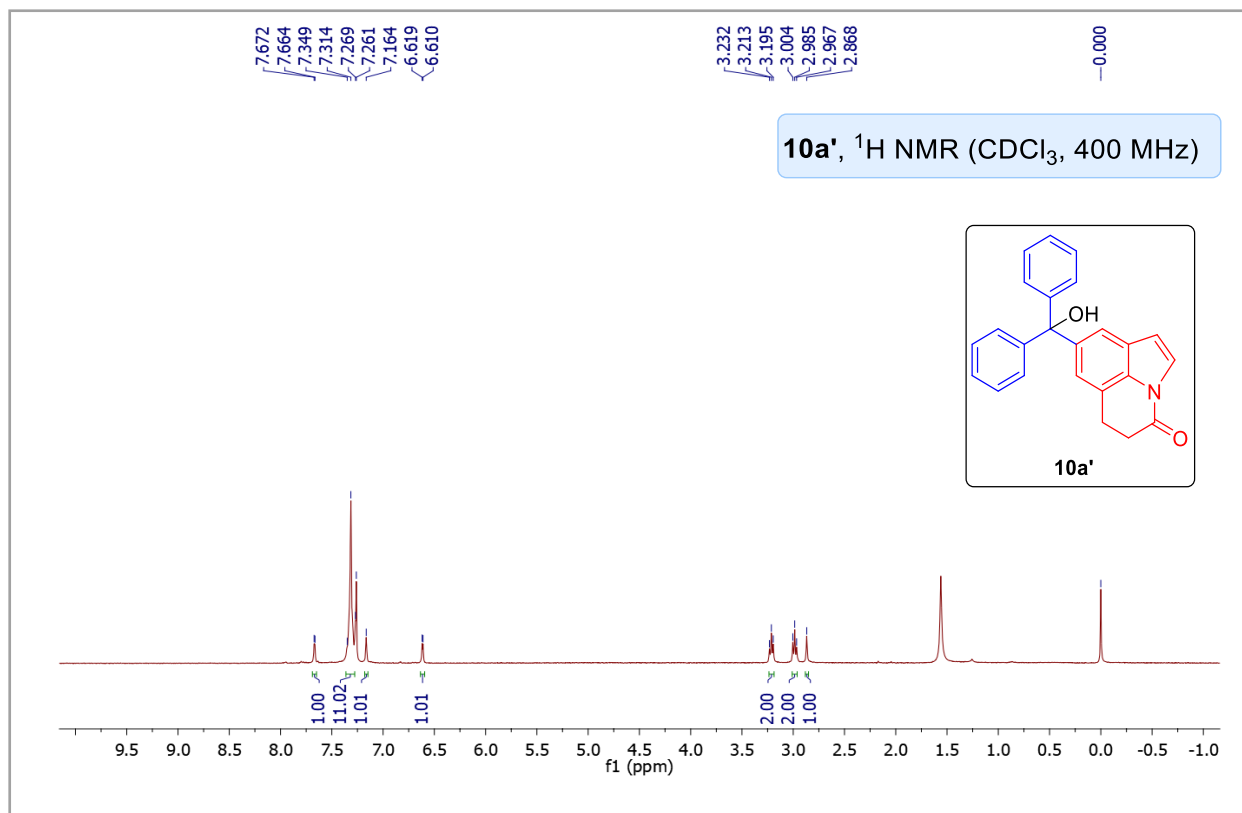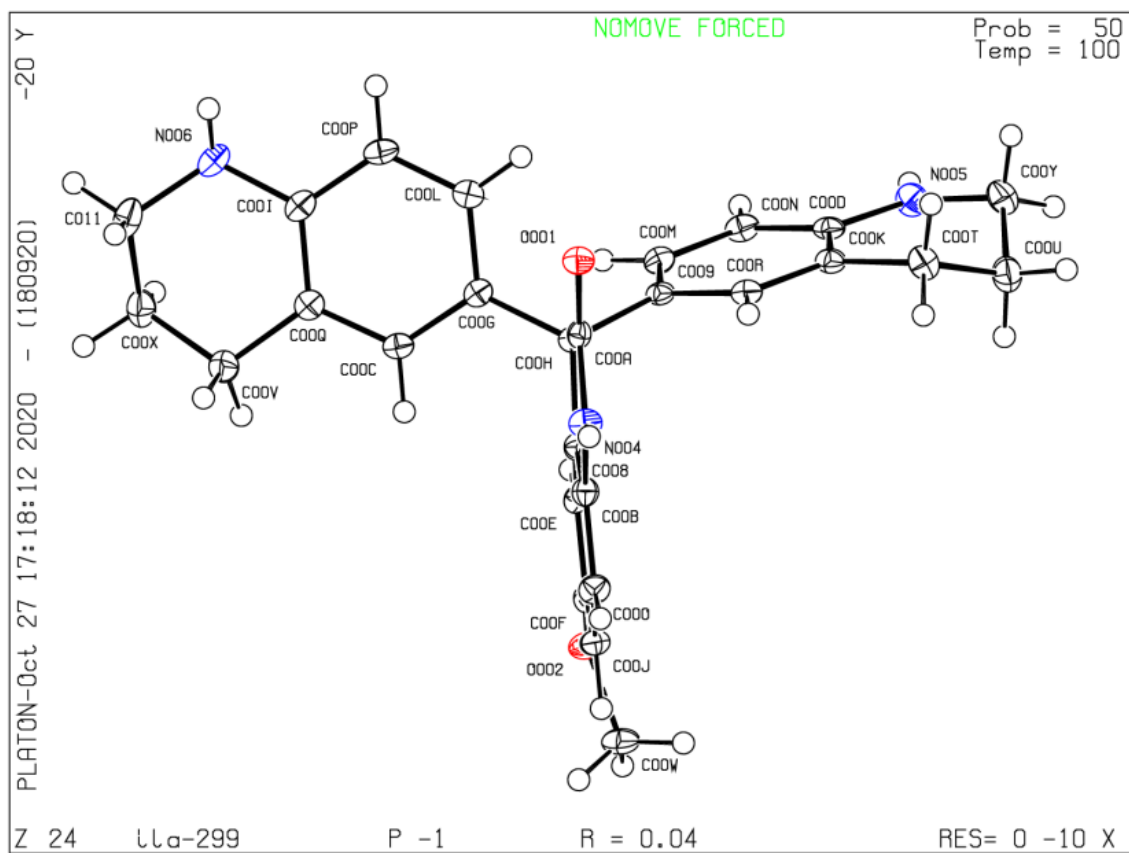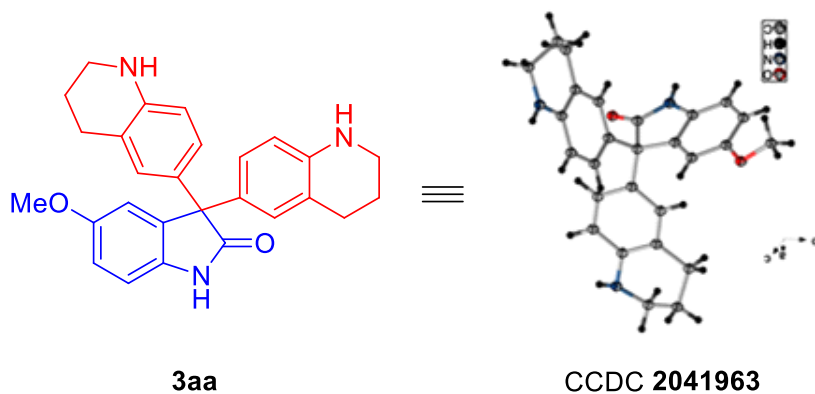
2.6 REFERENCES

1. (a) McCormick, J. L.; McKee, T. C.; Cardellina, J. H.; Boyd, M. R. HIV Inhibitory Natural Products. 26. Quinoline Alkaloids from Euodia roxburghiana. *J. Nat. Prod.* **1996**, *59*, 469–471. (b) Gul, W.; Hamann, M. T. Indole alkaloid marine natural products: An established source of cancer drug leads with considerable promise for the control of parasitic, neurological and other diseases. *Life Sci.* **2005**, *78*, 442–453. (c) Ruiz-Sanchis, P.; Savina, S. A.; Albericio, F.; Alvarez, M. Structure, Bioactivity and Synthesis of Natural Products with Hexahydropyrrolo[2,3-*b*]indole. *Chem. - Eur. J.* **2011**, *17*, 1388–1408. (d) Garg, Y.; Gahalawat, S.; Pandey, S. K. An enantioselective approach to 2-alkyl substituted tetrahydroquinolines: total synthesis of (+)-angustureine. *RSC Adv.* **2015**, *5*, 38846-38850. (e) Muthukrishnan, I.; Sridharan, V.; Menéndez, J. C. Progress in the chemistry of tetrahydroquinolines. *Chem. Rev.* **2019**, *119*, 5057−5191.

2. (a) Lucas, S.; Negri, M.; Heim, R.; Zimmer, C.; Hartmann, R. W. Fine-Tuning the Selectivity of Aldosterone Synthase Inhibitors: Structure–Activity and Structure–Selectivity Insights from Studies of Heteroaryl Substituted 1,2,5,6-Tetrahydropyrrolo[3,2,1-*ij*]quinolin-4-one Derivatives. *J. Med. Chem.* **2011**, *54*, 2307−2319. (b) Beattie, D. E.; Crossley, R.; Curran, A. C. W.; Dixon, G. T.; Hill, D. G.; Lawrence, A. E.; Shepherd, R. G. 5, 6, 7, 8-Tetrahydroquinolines. 4. Antiulcer and antisecretory activity of 5, 6, 7, 8-tetrahydroquinolinenitriles and-thioamides. *J. Med. Chem.* **1977**, *20*, 714–718. (c) Su, D.-S.; Lim, J. J.; Tinney, E.; Wan, B.-L.; Young, M. B.; Anderson, K. D.; Rudd, D.; Munshi, V.; Bahnck, C.; Felock, P. J.; Lu, M.; Lai, M.-T.; Touch, S.; Moyer, G.; DiStefano, D. J.; Flynn, J. A.; Liang, Y.; Sanchez, R.; Prasad, S.; Yan, Y.; Perlow-Poehnelt, R.; Torrent, M.;

Miller, M.; Vacca, J. P.; Williams, T. M.; Anthony, N. J. Substituted tetrahydroquinolines as potent allosteric inhibitors of reverse transcriptase and its key mutants. *Bioorg. Med. Chem. Lett.* **2009**, *19*, 5119–5123.

3. Cernak, T.; Dykstra, K. D.; Tyagarajan, S.; Vachal, P.; Krska, S. W. The medicinal chemist's toolbox for late stage functionalization of drug-like molecules. *Chem. Soc. Rev.* **2016**, *45*, 546–576.

4. Park, J.; Mishra, N. K.; Sharma, S.; Han, S.; Shin, Y.; Jeong, T.; Oh, J. S.; Kwak, J. H.; Jung, Y. H.; Kim, I. S. Mild Rh(III)-Catalyzed C7-Allylation of Indolines with Allylic Carbonates. *J. Org. Chem.* **2015**, *80*, 1818–1827.

5. Premi, C.; Dixit, A.; Jain, N. Palladium-Catalyzed Regioselective Decarboxylative Alkylation of Arenes and Heteroarenes with Aliphatic Carboxylic Acids. *Org. Lett.* **2015**, *17*, 2598–2601.

6. Han, S. H.; Choi, M.; Jeong, T.; Sharma, S.; Mishra, N. K.; Park, J.; Oh, J. S.; Kim, W. J.; Lee, J. S.; Kim, I. S. Rhodium-Catalyzed C–H Alkylation of Indolines with Allylic Alcohols: Direct Access to *β*-Aryl Carbonyl Compounds. *J. Org. Chem.* **2015**, *80*, 11092–11099.

7. Pan, S.; Ryu, N.; Shibata, T. Iridium(I)-Catalyzed Direct C–H Bond Alkylation of the C-7 Position of Indolines with Alkenes. *Adv. Synth. Catal.* **2014**, *356*, 929–933.

8. (a) Chen, C.-C.; Hong, B.-C.; Li, W.-S.; Chang, T.-T.; Lee, G.-H. Synthesis Of Biologically Active Bis(Indolyl)Methane Derivatives by Bisindole Alkylation of Tetrahydroisoquinolines with Visible-Light Induced Ring-Opening Fragmentation. *Asian J. Org. Chem.* **2017**, *6*, 426–431. (b) Yuan, C.; Zhu, L.; Chen, C.; Chen, X.; Yang, Y.; Lan, Y.; Zhao, Y. Ruthenium(II)-enabled *para*-selective C–H

difluoromethylation of anilides and their derivatives. *Nat. Commun.* **2018**, *9*, 1189–1198.

9. Liu, Z.; Vidovic, D. Michael Additions Catalyzed by a *β*-Diketiminate-Supported Aluminum Complex. *J. Org. Chem.* **2018**, *83*, 5295–5300.

10. Kumar, N. S.; Kumar, R. N.; Rao, L. C.; Muthineni, N.; Ramesh, T.; Babu, N. J.; Meshram, H. M. Acid-Catalyzed Protocol for the Synthesis of Novel 6-Substituted Tetrahydroquinolines by Highly Regioselective C6-Functionalization of Tetrahydroquinolines with Chromene Hemiacetals or *β*-Nitrostyrenes. *Synth.* **2017**, *49*, 3171–3182.

11. (a) Zhou, X.; Yu, S.; Qi, Z.; Kong, L.; Li, X. Rhodium(III)-Catalyzed Mild Alkylation of (Hetero)Arenes with Cyclopropanols *via* C–H Activation and Ring Opening. *J. Org. Chem.* **2016**, *81*, 4869–4875. (b) Wu, Y.; Yang, Y.; Zhou, B.; Li, Y. Iridium(III)-Catalyzed C-7 Selective C−H Alkynylation of Indolines at Room Temperature. *J. Org. Chem*. **2015**, 8*0*, 1946−1951. (c) Banjare, S. K.; Chebolu, R.; Ravikumar, P. C. Cobalt-Catalyzed Hydroarylation of Michael Acceptors with Indolines Directed by a Weakly Coordinating Functional Group. *Org. Lett.* **2019**, *21*, 4049–4053. (d) Ertugrul, B.; Kilic, H.; Lafzi, F.; Saracoglu, N. Access to C5-Alkylated Indolines/Indoles *via* Michael-Type Friedel−Crafts Alkylation Using Aryl-Nitroolefins. *J. Org. Chem*. **2018**, *83*, 9018−9038. (e) Zhang, W.; Xu, G.; Qiu, L.; Sun, J. Gold-catalyzed C5-alkylation of indolines and sequential oxidative aromatization: access to C5-functionalized indoles. *Org. Biomol. Chem.* **2018**, *16*, 3889–3892.

12. (a) Sharma, R.; Kumar, I.; Kumar, R.; Sharma, U. RhodiumCatalyzed Remote C-8 Alkylation of Quinolines with Activated and Unactivated Olefins: Mechanistic Study and Total Synthesis of EP4 Agonist. *Adv. Synth. Catal.* **2017**, *359*, 3022–

3028. (b) Chen, C.; Pan, Y.; Zhao, H.; Xu, X.; Luo, Z.; Cao, L.; Xi, S.; Li, H.; Xu, L. Ruthenium(II)-Catalyzed Regioselective C-8 Hydroxylation of 1,2,3,4-Tetrahydroquinolines. *Org. Lett*. **2018**, *20*, 6799−6803.

13. (a) Tang, R. Y.; Li, G.; Yu, J. Q. Conformation-induced remote meta-C–H activation of amines. *Nature,* **2014**, *507*, 215–220. (b) Wang, P.; Farmer, M. E.; Huo, X.; Jain, P.; Shen, P.-X.; Ishoey, M.; Bradner, J. E.; Wisniewski, S. R.; Eastgate, M. D.; Yu, J.-Q. Ligand-Promoted *Meta*-C–H Arylation of Anilines, Phenols, and Heterocycles. *J. Am. Chem. Soc*. **2016**, *138*, 9269–9276.

14. (a) Fujisawa, T.; Ito, T.; Fujimoto, K.; Shimizu, M.; Wynberg, H.; Staring, E. G. J. Facile synthesis of (S)-*β*-hydroxy-*β*-trichloromethylated aromatic ketones by the regioselective ring cleavage of chiral *β*-trichloromethyl-*β*-propiolactone under the Friedel-Crafts conditions. *Tetrahedron Lett***. 1997**, *38*, 1593-1596. (b) Bartolucci, S.; Bartoccini, F.; Righi, M.; Piersanti, G. Direct, Regioselective, and Chemoselective Preparation of Novel Boronated Tryptophans by Friedel–Crafts Alkylation. *Org. Lett.* **2012**, *14*, 600−603.

15. (a) Babu, K. N.; Kinthada, L. K.; Ghosh, K.; Bisai, A. Highly chemoselective synthesis of dimeric 2-oxindoles with a C-3/C-5′ linkage *via* Friedel–Crafts alkylations of 2-oxindoles with 3-hydroxy-2-oxindoles. *Org. Biomol. Chem*. **2015**, *13*, 10641–10655. (b) Fujita, S.; Watanabe, H.; Katagiri, A.; Yoshida, H.; Arai, M. Nitrogen and oxygen-doped metal-free carbon catalysts for chemoselective transfer hydrogenation of nitrobenzene, styrene, and 3-nitrostyrene with hydrazine. *J. Mol. Catal*. *A: Chem.* **2014**, *393*, 257−262.

16. Ahadi, S.; Moafi, L.; Feiz, A.; Bazgir, A. Three-component synthesis of new unsymmetrical oxindoles *via* Friedel–Crafts type reaction. *Tetrahedron*, **2011**, *67*, 3954–3958.

17. Jung, D.; Kim, M. H.; Kim, J. Cu-Catalyzed Aerobic Oxidation of Di-*tert*-butyl Hydrazodicarboxylate to Di-*tert*-butyl Azodicarboxylate and Its Application on Dehydrogenation of 1,2,3,4-Tetrahydroquinolines under Mild Conditions. *Org. Lett.* **2016**, *18*, 6300−6303.

18. Uddin, M. K.; Reignier, S. G.; Coulter, T.; Montalbetti, C.; Grånäs, C.; Butcher, S.; Krog-Jensen, C.; Felding, J. Syntheses and antiproliferative evaluation of oxyphenisatin derivatives. *Bioorg. Med. Chem. Lett.* **2007**, *17*, 2854−2857.

19. (a) Jana, U.; Maiti, S.; Biswas, S. An FeCl₃-catalyzed highly C3-selective Friedel–Crafts alkylation of indoles with alcohols. *Tetrahedron Lett*. **2007**, *48*, 7160–7163. (b) Ghosh, S.; Kinthada, L. K.; Bhunia, S.; Bisai, A. Lewis acid-catalyzed Friedel–Crafts alkylations of 3-hydroxy-2-oxindole: an efficient approach to the core structure of azonazine. *Chem. Commmun.* **2012**, *48*, 10132−10134. (c) Xiang, B.; Xu, T.-F.; Wu, L.; Liu, R.-R.; Gao, J.-R.; Jia, Y.-X. Lewis Acid Catalyzed Friedel−Crafts Alkylation of Alkenes with Trifluoropyruvates. *J. Org. Chem.* **2016**, *81*, 3929–3935.

20. Wallach, D. R.; Chisholm, J. D. Alkylation of Sulfonamides with Trichloroacetimidates under Thermal Conditions. *J. Org. Chem.* 2016, **81**, 8035−8042.

21. Gottlieb, H. E.; Kotlyar, V.; Nudelman, A. NMR chemical shifts of common laboratory solvents as trace impurities. *J. Org. Chem.* **1997**, *62*, 7512−7515.

22. Castelo-Branco, F. S.; de Lima, E. C.; Domingos, J. L. de O.; Pinto, A. C.; Lourenço, M. C. S.; Gomes, K. M.; Costa-Lima M. M.; Araujo-Lima, C. F.; Aiub, C. A. F.; Felzenszwalb, I.; Costa, T. E. M. M.; Penido,C.; Henriques, M. G.; Boechat, N. New hydrazides derivatives of isoniazid against Mycobacterium

tuberculosis: Higher potency and lower hepatocytotoxicity. *Eur. J. Med. Chem.* **2018**, *146*, 529−540.

23. Wu, Z.; Fang, X.; Leng, Y.; Yao, H.; Lin, A. Indium-mediated Palladium-catalyzed Allylic Alkylation of Isatins with Alkynes. *Adv. Synth. Catal.* **2018**, *360*, 1289–1295.

24. Ryu, H.; Seo, J.; Ko, H. M. Synthesis of Spiro[oxindole-3,2'-pyrrolidine] Derivatives from Benzynes and Azomethine Ylides through 1,3-Dipolar Cycloaddition Reactions. *J. Org. Chem.* **2018**, *83*, 14102–14109.

25. Buxton, C, S.; Blackemore, D. C.; Bower, J. F. Reductive Coupling of Acrylates with Ketones and Ketimines by a Nickel-Catalyzed Transfer-Hydrogenative Strategy. *Angew. Chem. Int. Ed.* **2017**, *56*, 13824–13828.

26. Satish, G.; Ilangovan, A. Direct Amidation of 2′-Aminoacetophenones Using I2-TBHP: A Unimolecular Domino Approach toward Isatin and Iodoisatin. *J. Org. Chem.* **2014**, *79*, 4984–4991.

27. Mamuye, A. D.; Monticelli, S.; Castoldi, L.; Holzer, W.; Pace, V. Eco-friendly chemoselective *N*-functionalization of isatins mediated by supported KF in 2-MeTHF. *Green. Chem.* **2015**, *17*, 4194–4197.

28. Lee, Y. C.; Patil, S.; Golz, C.; Strohmann, C.; Ziegler, S.; Kumar, K.; Waldmann, H. A ligand directed divergent catalytic approach to establish structural and functional scaffold diversity. *Nature Communications* **2017**, *8*, 14043–14054.

29. Roman, R.; Mateu, N.; Lopez, I.; Medio-Simon, M.; Fustero, S.; Barrio, P. Vinyl Fluorides: Competent Olefinic Counterparts in the Intramolecular Pauson-Khand Reaction. *Org. Lett.* **2019**, *21*, 2569–2573.

30. Kobayashi, K.; Fuchimoto, Y.; Hayashi, K.; Mano, M.; Tanmatsu, M.; Morikawa, O.; Konishi, H. A Convenient Synthesis of 3-(1-Aminoalkyl)quinolin-2(*1H*)-one Derivatives. *Synthesis* **2005**, *16*, 2673–2676.

31. a) Huang, Y. Q.; Song, H. J.; Liu, Y. X.; Wang, Q. M. Dehydrogenation of *N*-Heterocycles by Superoxide Ion Generated through Single-Electron Transfer. *Chem. - Eur. J.* **2018**, *24*, 2065−2069. (b) Silva, S. B. L.; Della Torre, A.; Ernesto de Carvalho, J.; Ruiz, A. L. T. G.; Silva, L. F., Jr. Seven-Membered Rings through Metal-Free Rearrangement Mediated by Hypervalent Iodine. *Molecules* **2015**, *20*, 1475−1494.

32. Rodriguez, A. L.; Zhou, Y.; Williams, R.; Weaver, C. D.; Vinson, P. N.; Dawson, E. S.; Steckler, T.; Lavreysen, H.; Mackieg, C.; Bartolome, J. M.; Macdonald, G. J.; Daniels, J. S.; Niswender, C. M.; Jones, C. K.; Conn, P. J.; Lindsley, C. W.; Stauffer, S. R. Discovery and SAR of a novel series of non-MPEP site mGlu5 PAMs based on an aryl glycine sulfonamide scaffold. *Bioorg. Med. Chem. Lett.* **2012**, *22*, 7388−7392.

33. Ortgies, S; Breder, A. Selenium-Catalyzed Oxidative C(sp^2)–H Amination of Alkenes Exemplified in the Expedient Synthesis of (*Aza-*)Indoles. *Org. Lett.* **2015**, *17*, 2748–2751.

34. Jiao, L.-Y.; Oestreich, M. Oxidative Palladium(II)-Catalyzed C-7 Alkenylation of Indolines. *Org. Lett.* **2013**, *15*, 20, 5374–5377.

35. Awasthi, A. K.; Cho, S. S. Y.; Graham, J. M.; Nikam, S. S. Fused tricyclic heterocycles for the treatment of schizophrenia. U. S. Patent WO 2008/015516 A1 07 February **2008**.

36. Ali, I. A. I.; El Ashry, E. S. H.; Schmidt, R. R. Protection of Hydroxy Groups with Diphenylmethyl and 9-FluorenylTrichloroacetimidates - Effect on Anomeric Stereocontrol. *Eur. J. Org. Chem.* **2003**, 4121–4131.

37. Yin, L.; Lucas, S.; Maurer, F.; Kazmaier, U.; Hu, Q.; Hartmann, R. W. Novel Imidazol-1-ylmethyl Substituted 1,2,5,6-Tetrahydropyrrolo[3,2,1-*ij*]quinolin-4-ones as Potent and Selective CYP11B1 Inhibitors for the Treatment of Cushing's Syndrome. *J. Med. Chem.* **2012**, *55*, 6629–6633.

38. Jung, D.; Kim, M. H.; Kim, J. Cu-Catalyzed Aerobic Oxidation of Di-*tert*-butyl Hydrazodicarboxylate to Di-*tert*-butyl Azodicarboxylate and Its Application on Dehydrogenation of 1,2,3,4-Tetrahydroquinolines under Mild Conditions. *Org. Lett.* **2016**, *18*, 6300−6303.

39. Bergman, J.; Carlsson, R.; Misztal, S. The reaction of some indoles and indolines with 2,3-dichloro-5,6-dicyano-1,4-benzoquinone. *Acta chim. Scand.* **1976,** *30B*, 853–862.

Chapter 3

Introduction to C–H bond Activation

Chapter 3

Introduction to C–H bond Activation
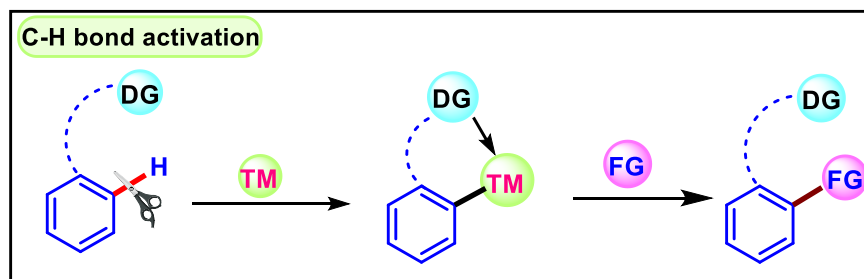
3.1 ABSTRACT

The transition metal catalyzed C–H bond activation has been used as an efficient method to construct C-C bonds on a heterocyclic moiety. The directed C–H activation provides more complex molecules of importance in pharmaceuticals with good selectivity and specificity. In transition metal catalyzed C–H bond activation reaction, the use of 3d transition metal catalyst has received significant attention in recent years as compared to 4d and 5d metal. It is because of their low cost, unique reactivity profiles, and high earth crust abundance. Among the first row-transition metals, nickel catalysts have drawn considerable attention from the scientific community because of its ability to exhibit variable oxidation states which enables catalytic reactions that are mechanistically distinct from other metals. Thus, synthetic transformations that utilize nickel as the catalyst is highly desirable.

3.2 INTRODUCTION

Synthesis of organic molecules that has application in agriculture and medicine is essential to upholding human life.[1] Electrophilic substitution reactions mainly relies on the electronics of the molecule. But some of the major challenges with this approach is that it has poor regioselectivity and requirement of stoichiometric amount of Lewis acid catalyst

which generates a lot of by-products.[2] Despite improvements in regioselectivity and use of catalytic amounts of catalyst for electrophilic aromatic substitution, a novel approach was still required for C–H functionalization. Later, cross-coupling reactions gained popularity in organic synthesis due to their ease of use and selectivity.[3] C(sp^2)–X bonds can be converted into C-C bonds[4] using suitable metal-catalyzed coupling techniques such as Suzuki-Miyaura coupling, Sonogashira coupling, Kumada coupling, Heck reaction, Negishi coupling and Stille cross-coupling, etc. However, these cross-coupling processes have the limitation that it need pre-functionalized substrates. The utilization of the C–H bond as a functional group for synthetic transformations is an appealing alternative to pre-functionalized substrates (C–X). It avoids tedious functional group conversions and substantially lowers the by-products. In this context, the activation and functionalization of inert C–H bonds *via* transition metal catalysis has grown significantly.[5] Even though virtually it was looking impossible to carry out the inert C–H bond functionalization reaction through metal-catalyzed C–H bond activation in the beginning of this century. This C–H bond activation is associated with few major challenges like (i) high bond dissociation energy (BDE),[6] (ii) non-polar nature of this bond which makes the bond less reactive.[7] However, during the past two decades, it has developed into one of the most explored researched fields, thereby expanding the boundaries of synthetic and organometallic chemistry.[8] In addition, metal-catalyzed C–H functionalization has become a potent technique because it is easy to makes valuable carbon-carbon (C–C) and carbon-hetero (like C–N, C–O) bonds.[9] With all of these developments, the C–H bond activation method has developed into an alternative, and step-economical strategy than the older classical synthesis. There are two possible paths for C–H bond activation: (i) non-directed and (ii) directed.

3.3 NON-DIRECTED C–H ACTIVATION

In non-directed C–H bond activation approach, the arene C–H bond is directly functionalized in the presence of a metal catalyst. However, it is a challenging task to synthesize the desired product with good regio selectivity because of the availability of chemically similar C–H bond in the arene motif (Figure 3.1).

Figure 3.1: Non-directed C–H bond functionalization
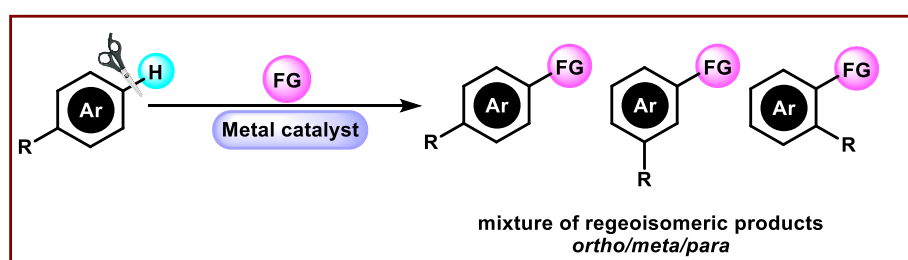
A highly selective *para*-olefination of *N,N*-dialkylanilines using a palladium/molybdovanadophosphoric acid catalyst was reported by the Obara group in 2012 (Scheme 3.1).[10] Despite the *ortho*/*para*-directing nature of *N,N*-dialkylaniline,

Scheme 3.1: Palladium catalyzed non-directed C–H functionalization
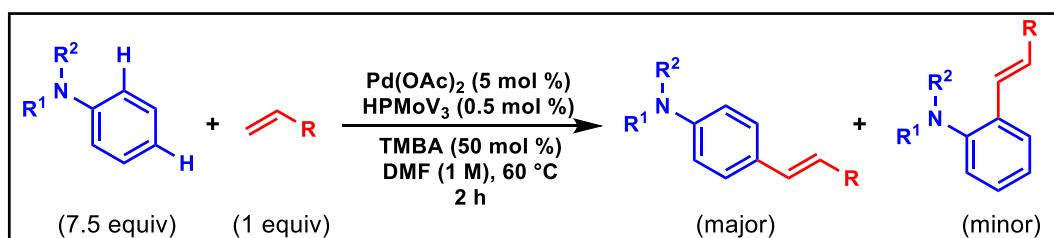
Extremely *para* selective functionalization was achieved over *ortho*-functionalisation. This remarkable selectivity is a result of combining an *ortho N,N*-dialkyl unit with a sterically bulky TMB (trimethyl benzoate) ligand. Although they achieved extremely *para*-selective olefination, the synthetic applicability of this technology makes it unsuitable for large-scale applications because excess arene (>7 equiv) must be utilised to improve the C–H metalation phase.

Limitations of non-directed C–H functionalizations: Although there are numerous publications on the non-directed functionalization of inert C–H bonds, they all have certain limitations such as:

(i) Functionalizations are heavily biassed in favour of reactive or electronically rich arenes (i.e., electronically poor arenes are less reactive).

(ii) The nature of the substituent or functional group present in the (arene) molecule completely determines the regioselectivity of C–H functionalization.

(iii) Very poor regioselectivity between *ortho*/*para*-functionalization (especially when an electron-donating group is present in the arene ring)

In order to address the aforementioned problems, a novel approach known as directed C–H bond activation has emerged. This enables highly regioselective functionalization of inert C–H bonds.[11]

3.4 DIRECTED C–H ACTIVATION

Substrates having functional groups, such as imine, amine, amide, and carbonyl groups, can coordinate with transition metals. By giving its free lone pair of electrons to the transition metal's unoccupied *d*-orbitals, these coordinating atoms (N, O, S, and P) chelate with the metal (Figure 3.2). As a result, the metal is now directed by the substrate towards the proximal C–H bond, where it engages in an agostic interaction (a 3c–2e transition state) with the proximal C–H bonds.

Figure 3.2: Schematic representation of directed C–H bond activations
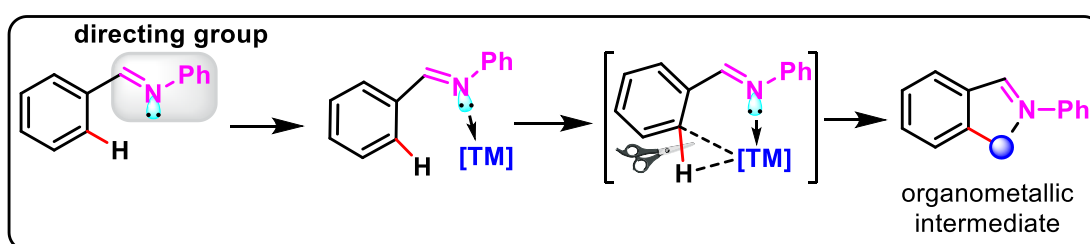
This agostic interaction results from synergistic σ-donation of the C–H bond to the vacant metal d-orbital and backbonding by the metal orbital. This interaction results in the formation of an organometallic intermediate with a reactive carbon-metal bond. This process is called as directed C–H bond activation. This organometallic species can couple with an appropriate coupling partner to produce a new C–C and C–hetero (halide, N, O, S, B) bonds.

The overall process of directed C–H functionalization could be better explained from a general catalytic cycle that proceeds through four stages (Figure 3.3).

Stage 1: The active transition metal catalyst first chelated by the directing group's σ-donor atom, which produces an organometallic intermediate **I** {**C**-[**M**]} through agostic interaction with the proximal C–H bond.

Stage 2: The intermediate **I** undergo functionalization with a secondary substrate (coupling partner), resulting in the intermediate **II**, where the substrate and the coupling partner are both linked to the metal catalyst **[C-M-R]**.

Figure 3.3: General catalytic cycle for directed C–H functionalization
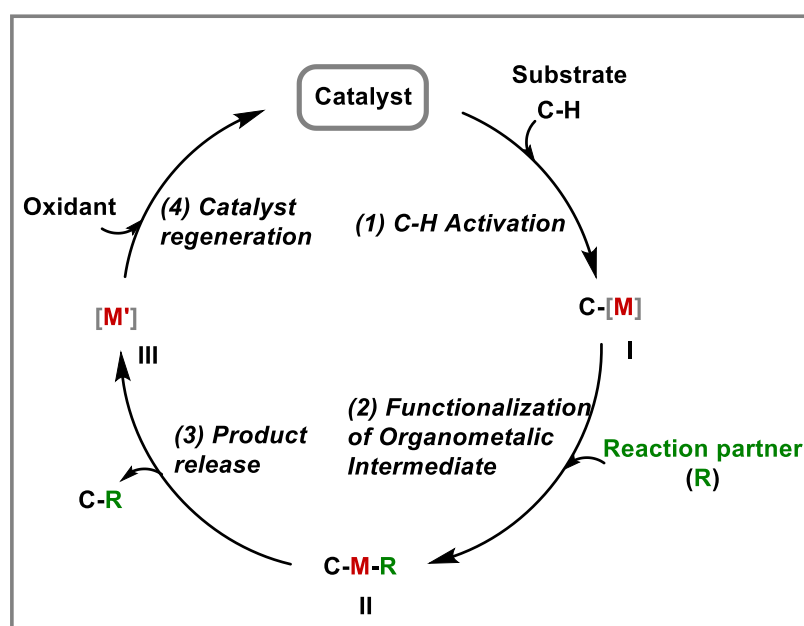
Stage 3: When the substrate and coupling partner coupled with each other, the final product **(C-R)** and reduced metal catalyst **[M′]** are produced.

Stage 4: Regeneration of the catalyst from the reduced catalyst using copper/silver salts, molecular oxygen, and organic oxidants is involved.

3.5 DIFFERENT MODES INVOLVED IN C–H ACTIVATION:

Six different modes of C–H bond activations have been documented in the literature.[12,13] Those are

(1) *Oxidative addition* **(OA):**
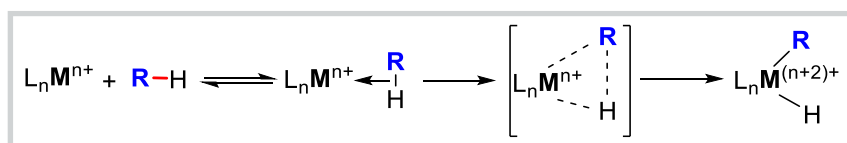
Metals in their low oxidation state (metal centers with a lot of electrons) commonly show this kind of mechanism for C–H activation. The metal interacts strongly and synergistically with the σ-C–H bond during this step. The bond order of the C–H bond is then lowered by a $d\pi$-backdonation to the σ*- C–H orbital. This results in a homolytic bond cleavage. This procedure results in a two-unit rise in the coordination number as well as oxidation number of metal. An aryl/alkyl ligand and a hydride are present in the oxidized metal core (organometallic species).

(2) *Aromatic electrophilic substitution* **(SEAr):**
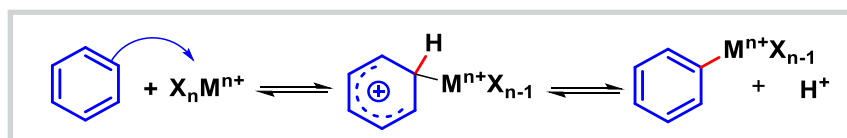
The transition metals are generally electron deficient in presence of vacant d-orbitals which creates Lewis acidic character on metal center. Hence, they act as electrophiles and undergo aromatic electrophilic substitution type reaction. The electrophilic metal center and the π-

electron cloud of substrate interact electronically during this activation phase. Without changing the oxidation state of the metal, this approach results in the formation of a new C(aryl)-M bond. The vicinal C(aryl)-H bond has a substantial rise in acidity, and re-aromatization can cause it to lose its proton. This mode of functionalization observed with electron rich arenes.

(3) *σ-Bond metathesis* (σBM):

$$R{-}H \ + \ X_nM^{n+}{-}R^1 \ \longrightarrow \ \left[\begin{array}{c} X_nM^{n+}\text{- - - -}R^1 \\ \vdots \qquad \vdots \\ R\text{- - - -}H \end{array} \right] \ \longrightarrow \ X_nM^{n+}{-}R + \ R^1{-}H$$
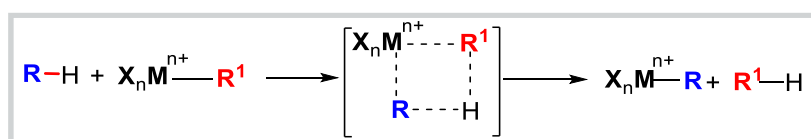
High oxidation state metals (metals with less electrons) are best suited for this kind of activation process. Through a four membered transition state, the inert C–H bond undergoes concerted metathesis (exchange) with the metal-ligand sigma bond. Without the involvement of any metal hydride species, a new C–H bond and M–C bond are formed during this activation process. The oxidation state of metal center is unaltered during the entire process.

(4) *Single electron transfer* (SET):

$$R{-}H \ + \ L_nM^{n+} \ \xrightarrow{SET} \ L_nM^{(n+1)+}{-}H \ + \ R^\bullet \ \xrightarrow{SET} \ L_nM^{(n+2)+}\begin{array}{c} R \\ \diagdown \\ H \end{array}$$
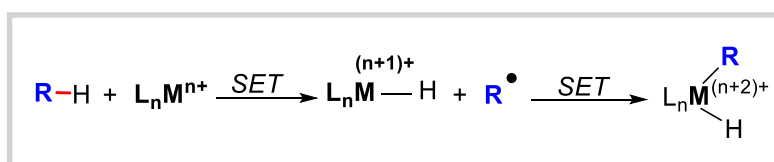
This C–H bond activation method uses two elementary events, each requiring one electron, to transfer two electrons. Through the homolytic cleavage of the C–H bond, a metal-hydride species and a carbon-centered radical are first produced. The aryl/alkyl hydride metal oxidized species is then produced by a recombination process between the metal center and the radical. Such reactions occur quite frequently with catalyst systems made up of Ni, Cu, Fe and Mn. The radical intermediate produced during the reaction can be confirmed by employing radical scavengers.

(5) *Concerted metalation deprotonation* **(CMD):**
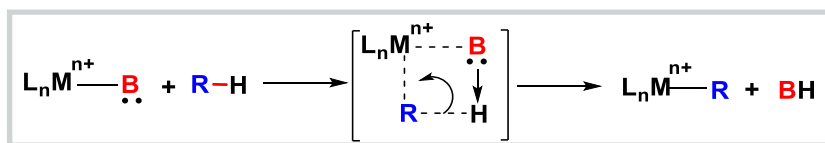
For late transition metals in high oxidation states (metal centers with less electrons), such as Ir(III), Pd(II), Ru(II), and Rh(III), this type of C–H activation process is favored. The C–H bond needs to be in close proximity to the metal center for this process to occur, and this is often made possible by the presence of a directing group. The metal center has a coordinated base that actively promotes the coordinated deprotonation of the C–H bond as the C–M bond is formed. The deprotonation by the coordinated base and M–C bond formation occurs in a concerted manner.

(6) *Base-assisted intramolecular electrophilic substitution* **(BIES):**
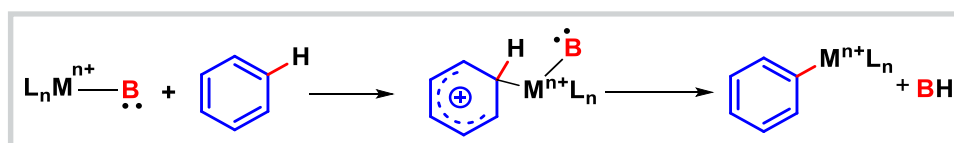
This mode of activation is similar to electrophilic aromatic substitution type reaction. But the only difference is the presence of a base in the coordination sphere of the metal center. This process is favored for electron rich aromatic substrates.

3.6 IMPORTANCE OF 1ST ROW TRANSITION METAL IN C–H ACTIVATION

For C–H bond functionalization, noble metals like ruthenium,[14] palladium,[15] rhodium,[16] and iridium[17] have been widely employed. These metals are less sustainable, nevertheless, due to their high prices and low natural abudance.[18] Utilising first-row 3d-transition metals provides a cost-effective and environmentally friendly alternative to their higher congeners. The first-row transition metals have substantial natural abundance, making the catalytic process economical. The number of publications in the development of C–H bond functionalization by using 3d metals is depicted in Figure 3.4.[19] Among the 3d metals,

nickel has emerged as a versatile and efficient metal[20] catalyst for C–H activation because it has low cost, ready availability and uniqueness in the reactivity. The reactivity of nickel is comparable to that of 2nd and 3rd-row metal catalysts and it is isoelectronic to Pd and Pt (which is well explored in C–H activation). As such nickel as the catalyst in organic transformation is underdeveloped, hence exploring the reactivity of this catalyst may lead to unusual transformation. While Pd is commonly detected in 0 and +2 oxidation states (in some cases +3 and +4), and Pt is more readily available in +4 oxidation states, Ni is typically observed not only in 0 and +2 but also in +1 and +3. The oxidative addition of low-valent Ni (Ni(0) or Ni(I)) prefers the SET process, in contrast to the oxidative insertion of Pd(0) into organohalides. Ni is also more nucleophilic because of its smaller size, located in the third row.

Figure 3.4: 3d-transition metals in C–H bond functionalization.
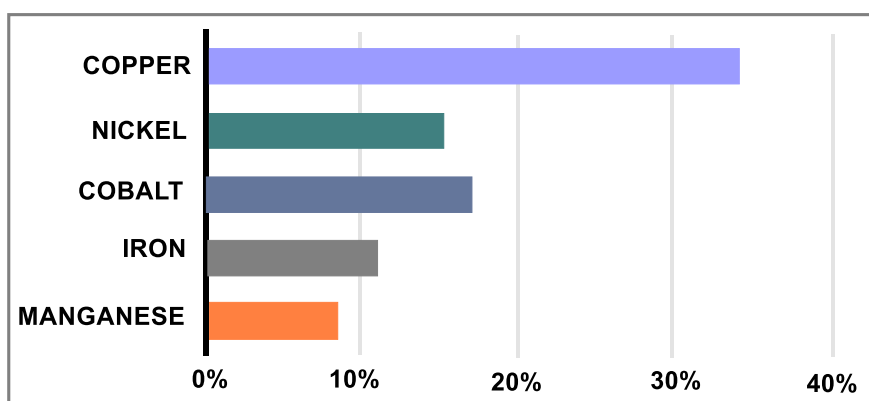
The affinity of nickel for catalysis makes it possible for reactions that are mechanistically unique from those involving other metals. Therefore, Ni was found to be very useful in inert bond C–O, C–H, C-C and C–N activation because of which new exciting and innovative achievements are expected. Generally, the C–H bond functionalization with nickel catalyst have been accomplished by making use of strongly coordinating atoms, such

as nitrogen (e.g., pyridine, pyrimidine, aminoquinoline), are known as strong σ-donors (Scheme 3.2).[21]

Scheme 3.2: C–H functionalization *via* strongly coordinating directing group
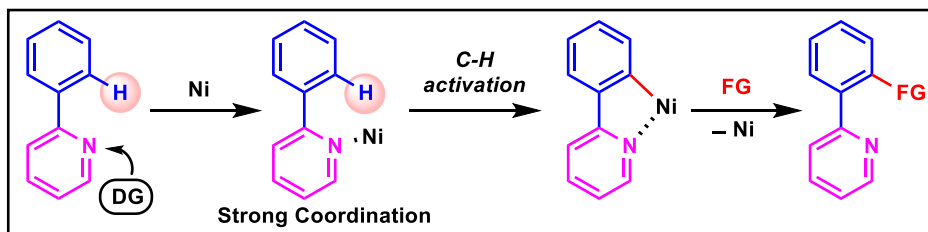
3.7 Reports of C–H activation with Nickel

The directing group assisted Ni-catalyzed C–H functionalization are discovered by many groups. With the aid of an 8-aminoquinoline directing group and a $Ni(OTf)_2$/PPh_3 catalytic system (Scheme 3.3a), Chatani reported the C–H alkylation of aromatic amides with alkyl halides in 2013.[22] A wide range of amides have been used as substrates for this reaction, and various functional groups on the aromatic backbone and alkyl halides were well tolerated. Later, other groups like Akermann,[23,24] Sundararaju,[25] Punji,[26] demonstrated C–H alkylation of the arene ring using various alkylating agents.

Several groups have demonstrated C–H arylation reactions using nickel as a catalyst. In this regard, the 2-(pyridine-2-yl)isopropylamine (PIP) directing group was used by the Shi group in 2016 to find the Ni-catalyzed arylation of $C(sp^2)$–H bonds in aromatic amides with arylboron reagents.[27] Shi also reported employing arylsilanes and a PIP directing group to arylate aromatic and heteroaromatic amides (Scheme 3.3b).[28] An easy way to get rid of this directing group is to use a nitrosylation/hydrolysis process. Additionally, by using a range of substrates, Chatani,[29] Hoover,[30] Punji,[31] and others have identified the C–H arylation of the arene ring. In 2016, Balaraman developed an effective approach for the C–H alkynylation of aromatic amides with alkynyl bromides[32] utilising $Ni(OTf)_2$ and an 8-

aminoquinoline moiety (Scheme 3.3c). Shi,[33] Ackermann,[34] Punji,[35] and other groups have also studied the alkenylation of aromatic substrates.

Scheme 3.3 Reports of C–H functionalization in Nickel catalyst
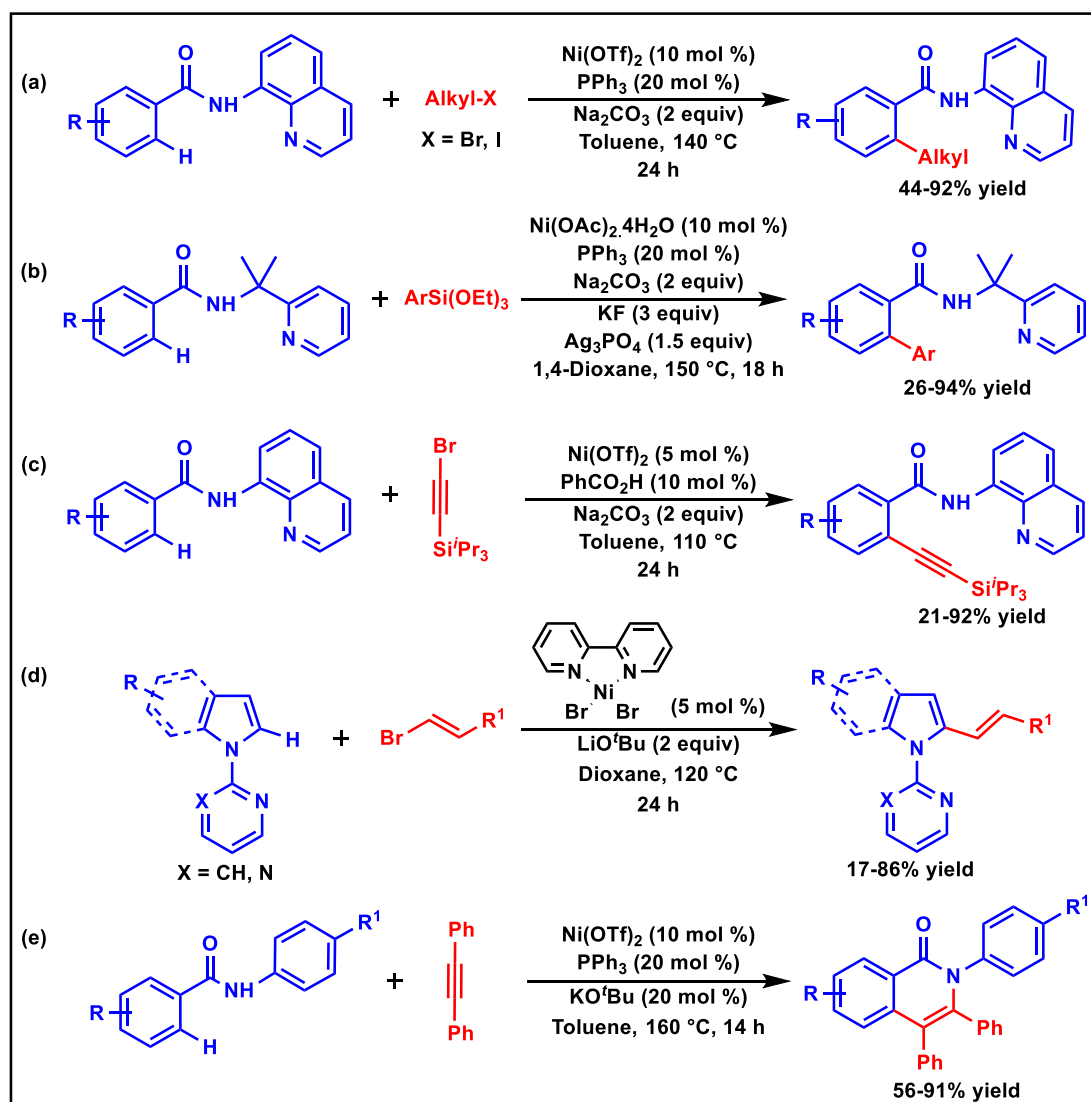
There have been numerous reports of nickel catalyst-aided alkenylation of C–H bonds.[36] Using (phen)NiBr$_2$ catalyst, the Punji group developed the regioselective alkenylation of C–H bonds of derivatives of indoles with alkenyl bromides (Scheme 3.2d).[37] According to preliminary mechanistic investigations, the process only uses one electron transfer (SET) pathway and the C–H activation serves as the rate-determining step. Studies using electron

paramagnetic resonance (EPR) and X-ray photoelectron spectroscopy (XPS) show that the reaction follows a Ni(I)/Ni(III) route.

In 2017 Chatani group introduced reaction of aromatic amides with alkynes catalyzed by nickel in the presence of KO^{t}Bu which involves C–H/N–H oxidative annulation to give 1(2H)-isoquinolinones.[38] The use of a catalytic quantity of a strong base, such as KO^{t}Bu is the key to success of the reaction (Scheme 3.2e).

3.8 CONCLUSION

In this chapter, we have discussed the transition metal-catalyzed C–H bond activation which has been used as an efficient method to construct C–C, C–N, C–X bonds on a heterocyclic moiety. The need of preactivated starting materials in the cross coupling reaction led to the discovery of non-directed C–H functionalizations, which worked well in many transformations. Even though non-directed C–H functionalization is more eco-friendly, it is also associated with major issues like (i) reactivity is highly biased with electronically rich arenes and (ii) very poor regioselectivity. This gave rise to a directed C–H bond activation functionalization strategy, free from these limitations. Directed C–H activation enables the synthesis of more complex molecules of importance in medicinal chemistry and pharmaceuticals. In transition metal catalyzed C–H bond activation reaction, the use of 3d transition metal catalyst has received considerable attention in recent years as compared to 4d and 5d metal. It is because of their low cost, unique reactivity profiles, and high earth crust abundance. Among the first row-transition metals, nickel (Ni) catalysts have drawn considerable attention by the scientific community because of its ability to exhibit variable oxidation states which enables catalytic reactions that are mechanistically distinct from other metals. Considering all this, we got inspired to explore the reactivity of Nickel catalyst in C–H as well as C–N activation/functionalisation area.

3.9 REFERENCES

1. (a) Nicolaou, K. C.; Bulger, P. G.; Sarlah, D. Palladium-catalyzed cross-coupling reactions in total synthesis. *Angew. Chem., Int. Ed.* **2005**, *44*, 4442–4489. (b) Magano, J.; Dunetz, J. R. Large-Scale Applications of Transition Metal-Catalyzed Couplings for the Synthesis of Pharmaceuticals. *Chem. Rev.* **2011**, *111*, 2177-2250. (c) Ruiz-Castillo, P.; Buchwald, S. L. Applications of Palladium-Catalyzed C−N Cross-Coupling Reactions. *Chem. Rev.* **2016**, *116*, 12564–12649.

2. Larock, R. C. Comprehensive organic transformations: a guide to functional group preparations; *Wiley-VCH*: **1999**. DOI: 10.1002/9781118662083. Online ISBN: 9781118662083.

3. (a) Miyaura, N.; Suzuki, A. Palladium-catalyzed cross-coupling reactions of organoboron compounds. *Chem. Rev.* **1995**, *95*, 2457-2483. (b) De Meijere, A., Diederich, F., Eds.; Metal Catalyzed Cross-Coupling Reactions. *Wiley-VCH: Weinheim*, **2004**.

4. (a) Miyaura, N.; Yamada, K.; Suzuki, A. A New Stereospecific Cross-Coupling by the Palladium-Catalyzed Reaction of 1-Alkenylboranes with 1-Alkenyl or 1-Alkynyl Halides. *Tetrahedron Lett.* **1979**, *20*, 3437–3440. (b) Miyaura, N.; Suzuki, A. Stereoselective Synthesis of Arylated (*E*)-Alkenes by the Reaction of Alk-1-Enylboranes with Aryl Halides in the Presence of Palladium Catalyst. *J. Chem. Soc., Chem. Commun.* **1979**, 866–867. (c) Thorand, S.; Krause, N. Improved Procedures for the Palladium-Catalyzed Coupling of Terminal Alkynes with Aryl Bromides (Sonogashira Coupling). *J. Org. Chem.* **1998**, *63*, 8551–8553.

5. (a) Ding, K.; Dai, L.-X. Transition Metal-Catalyzed C–H Functionalization: Synthetically Enabling Reactions for Building Molecular Complexity. Organic Chemistry-Breakthroughs and Perspectives; *Wiley-VCH:* Weinheim, **2012** (b) Yu, J.-Q.; Shi, Z. C–H Activation. Topics in Current Chemistry; *Springer-Verlag: Heidelberg*, **2010**; Vol. 292.

6. Roudesly, F.; Oble, J.; Poli, G. Metal-Catalyzed C–H Activation/ Functionalization: The Fundamentals. *J. Mol. Catal. A: Chem.* **2017**, *426*, 275-296.

7. Bordwell, F. G. Equilibrium Acidities in Dimethyl Sulfoxide Solution. *Acc. Chem. Res.* **1988**, *21*, 456–463. (b) M. B. Smith, March's Advanced Organic Chemistry, *Wiley, New York, 7th Edn,* **2013**, pp. 314–318.

8. (a) Chen, Z.; Rong, M.-Y.; Nie, J.; Zhu, X.-F.; Shi, B.-F.; Ma, J.-A. Catalytic alkylation of unactivated $C(sp^3)$–H bonds for $C(sp^3)$–$C(sp^3)$ bond formation. *Chem. Soc. Rev*. **2019**, *48*, 4921–4942. (b) Abrams, D. J.; Provencher, P. A.; Sorensen, E. J. Recent Applications of C–H Functionalization in Complex Natural Product Synthesis. *Chem. Soc. Rev.* **2018**, *47*, 8925–8967. (c) Liu, C.; Yuan, J.; Gao, M.; Tang, S.; Li, W.; Shi, R.; Lei, A. Oxidative Coupling between Two Hydrocarbons: An Update of Recent C–H Functionalizations. *Chem. Rev.* **2015**, *115*, 12138–12204.

9. (a) Cernak, T.; Dykstra, K. D.; Tyagarajan, S.; Vachal, P.; Krska, S. W. The Medicinal Chemist's Toolbox for Late Stage Functionalization of Drug-Like Molecules. *Chem. Soc. Rev.* **2016**, *45*, 546–576. (b) Wencel-Delord, J.; Glorius, F. C–H Bond Activation Enables the Rapid Construction and Late-Stage Diversification of Functional Molecules. *Nat. Chem.* **2013**, *5*, 369–375. (c) Okamoto, K.; Zhang, J.; Housekeeper, J. B.; Marder, S. R.; Luscombe, C. K. C–H Arylation Reaction: Atom Efficient and Greener Syntheses of π-Conjugated Small Molecules and Macromolecules for Organic Electronic Materials. *Macromolecules* **2013**, *46*, 8059–8078.

10. Mizuta, Y.; Obora, Y.; Shimizu, Y.; Ishii, Y. *para*-Selective Aerobic Oxidative C–H Olefination of Aminobenzenes Catalyzed by Palladium/Molybdovanadophosphoric acid/2,4,6-Trimethylbenzoic Acid System. *ChemCatChem* **2012**, *4*, 187–191.

11. (a) Godula, K.; Sames, D. C–H Bond Functionalization in Complex Organic Synthesis. *Science* **2006**, *312*, 67–72. (b) Yamaguchi, J.; Yamaguchi, A. D.; Itami, K. C–H Bond Functionalization: Emerging Synthetic Tools for Natural Products and Pharmaceuticals. *Angew. Chem., Int. Ed.* **2012**, *51*, 8960–9009. (c) McMurray, L.; O'Hara, F.; Gaunt, M. J. Recent Developments in Natural Product Synthesis Using Metal-Catalysed C–H Bond Functionalisation. *Chem. Soc. Rev.* **2011**, *40*, 1885–1898. (d) He, R.; Huang, Z.-T.; Zheng, Q.-Y.; Wang, C. Isoquinoline Skeleton Synthesis *via* Chelation-Assisted C−H Activation. *Tetrahedron Lett.* **2014**, *55*, 5705–5713.

12. (a) Gallego. D.; Baquero E. A. Recent Advances on Mechanistic Studies on C–H Activation Catalyzed by Base Metals. *Open. Chem.* **2018**, *16*, 1001–1058. (b) Balcells, D.; Clot, E.; Eisenstein, O. C–H Bond Activation in Transition Metal Species from a Computational Perspective. *Chem. Rev.* **2010**, *110*, 749–823.

13. (a) Xavier, E. S.; De Alemeida, W. B.; da Silva, J. C. S.; Rocha, W. R. C–H Bond Activation of Methane Promoted by (η^5-Phospholyl)Rh(CO)$_2$: A Theoretical Perspective *Organometallics* **2005**, *24*, 2262–2268. (b) Myers, A. G.; Tanaka, D.; Mannion, M. R. Development of a decarboxylative palladation reaction and its use in a Heck-type olefination of arene carboxylates. *J. Am. Chem. Soc.* **2002**, *124*, 11250–11251. (c) Zhang, C.; Tang, C.; Jiao, N. Recent advances in copper-catalyzed dehydrogenative functionalization *via* a single electron transfer (SET) process. *Chem. Soc. Rev.* **2012**, *41*, 3464–3484. (d) Ruan, Z.; Ghorai, D.; Zanoni, G.; Ackermann, L. Nickel-catalyzed C–H activation of purine bases with alkyl halides. *Chem. Commun.* **2017**, *53*, 9113−9116. (e) Jagtap, R. A.; Verma, S. K.; Punji, B. MnBr$_2$ Catalyzed Direct and Site-Selective Alkylation of Indoles and Benzo[h]quinoline. *Org. Lett.* **2020**, *22*, 4643–4647. (f) Jagtap, R. A.; Samal, P. P.; Vinod, C. P.; Krishnamurty, S.; Punji, B. Iron-Catalyzed C(sp^2)−H Alkylation of Indolines and Benzo[*h*]quinoline with Unactivated Alkyl Chlorides through Chelation Assistance. *ACS Catal.* **2020**, *10*, 7312–7321. (g) Lafrance, M.; Rowley, C. N.; Woo, T. K.; Fagnou, K. Catalytic Intermolecular Direct Arylation of Perfluorobenzenes. *J. Am. Chem. Soc.* **2006**, *128*, 8754−8756. (h) C. Tirler and L. Ackermann, Ruthenium(II)-catalyzed cross-dehydrogenative C–H alkenylations by triazole assistance. *Tetrahedron*, **2015**, *71*, 4543–4551.

14. (a) Duarah, G.; Kaishap, P. P.; Begum, T.; Gogoi, S. Recent Advances in Ruthenium(II)-Catalyzed C–H Bond Activation and Alkyne Annulation Reactions. *Adv. Synth. Catal.* **2019**, *361*, 654–672. (b) Arockiam, P. B.; Bruneau, C.; Dixneuf, P. H. Ruthenium(II)-Catalyzed C–H Bond Activation and Functionalization. *Chem. Rev.* **2012**, *112*, 5879–5918.

15. (a) Ramachandiran, K.; Sreelatha, T.; Lakshmi, N. V. T.; Babu, T. H.; Muralidharan, D.; Perumal, P. T. Palladium Catalyzed C–H Activation and its Application to Multi-bond Forming Reactions. *Curr. Org. Chem*. **2013**, *17*, 2001. (b) Li, H.; Li, B.-J.; Shi, Z. - J. Challenge and progress: palladium-catalyzed sp^3 C–H activation. *Catal. Sci. Technol.* **2011**, *1*, 191–206.

16. (a) Yang, Z.; Yu, J.-T.; Pan, C. Recent advances in rhodium-catalyzed C(sp^2)–H (hetero)arylation. *Org. Biomol. Chem*. **2021**, *19*, 8442–8465. (b) Colby, D. A.; Bergman, R. G.; Ellman, J. A. Rhodium-Catalyzed C–C Bond Formation *via* Heteroatom-Directed C–H Bond Activation. *Chem. Rev.* **2010**, *110*, 624–655.

17. (a) Nishimura, T. Iridium-Catalyzed Hydroarylation *via* C–H Bond Activation. *Chem. Rec.* **2021**, *21*, 3532-3545. (b) Wu, X.; Sun, S.; Yu, J.- T.; Cheng, J. Recent Applications of α-Carbonyl Sulfoxonium Ylides in Rhodium and Iridium-Catalyzed C–H Functionalizations. *Synlett* **2019**, *30*, 21–29.

18. Dalton, T.; Faber, T.; Glorius, F. C–H Activation: Toward Sustainability and Applications. *ACS Cent. Sci.* **2021**, *7*, 245–261.

19. Gandeepan, P.; Müller, T.; Zell, D.; Cera, G.; Warratz, S.; Ackermann, L. 3d Transition Metals for C–H Activation. *Chem. Rev.* **2019**, *119*, 2192-2452.

20. (a) Su, B.; Cao, Z.-C.; Shi, Z.-J. Exploration of Earth-Abundant Transition Metals (Fe, Co, and Ni) as Catalysts in Unreactive Chemical Bond Activations. *Acc. Chem. Res.* **2015**, *48*, 886– 896. (b) Zhou, J.-Y.; Tian, R.; Zhu, Y.-M. Nickel-Catalyzed Selective Decarbonylation of α-Amino Acid Thioester: Aminomethylation of Mercaptans. *J. Org. Chem.* **2021**, *86*, 12148–12157.

21. Khake, S. M.; Chatani, N. Chelation-Assisted Nickel-Catalyzed C–H Functionalizations. *Trends Chem.* **2019**, *1*, 524−539.

22. Aihara, Y. and Chatani, N. Nickel-catalyzed direct alkylation of C–H bonds in benzamides and acrylamides with functionalized alkyl halides *via* bidentate-chelation assistance. *J. Am. Chem. Soc.* **2013**, *135*, 5308–5311.

23. Song, W.; Lackner, S.; Ackermann, L. Nickel-Catalyzed C–H Alkylations: Direct Secondary Alkylations and Trifluoroethylations of Arenes. *Angew. Chem., Int. Ed.* **2014**, *53*, 2477–2480.

24. Ruan, Z.; Ghorai, D.; Zanoni, G.; Ackermann, L. Nickelcatalyzed C–H activation of purine bases with alkyl halides. *Chem. Commun.* **2017**, *53*, 9113−9116.

25. Barsu, N.; Kalsi, D.; Sundararaju, B. Carboxylate Assisted Ni-Catalyzed C–H Bond Allylation of Benzamides. *Chem. - Eur. J.* **2015**, *21*, 9364–9368.

26. Soni, V.; Jagtap, R. A.; Gonnade, R. G.; Punji, B. Unified Strategy for Nickel-Catalyzed C-2 Alkylation of Indoles through Chelation Assistance. *ACS Catal.* **2016**, *6*, 5666–5672.

27. Liu, B.; Zhang, Z.-Z.; Li, X.; Shi, B.-F. Nickel(II)-Catalyzed Direct Arylation of Aryl C–H Bonds with Aryl-Boron Reagents Directed by a Removable Bidentate Auxiliary. *Org. Chem. Front.* **2016**, *3*, 897–900.

28. Zhao, S.; Liu, B.; Zhan, B.-B.; Zhang, W.-D.; Shi, B.-F. Nickel-Catalyzed *Ortho*-Arylation of Unactivated (Hetero)aryl C–H Bonds with Arylsilanes Using a Removable Auxiliary. *Org. Lett.* **2016**, *18*, 4586–4589.

29. Yokota, A.; Aihara, Y.; Chatani, N. Nickel(II)-Catalyzed Direct Arylation of C–H Bonds in Aromatic Amides Containing an 8-Aminoquinoline Moiety as a Directing Group. *J. Org. Chem.* **2014**, *79*, 11922–11932.

30. Honeycutt, A.P. and Hoover, J.M. Nickel-catalyzed oxidative decarboxylative (hetero)arylation of unactivated C–H bonds: Ni and Ag synergy. *ACS Catal.* **2017**, 7, 4597–4601.

31. Jagtap, R. A.; Soni, V.; Punji, B. Expeditious and Solvent-Free Nickel-Catalyzed C–H Arylation of Arenes and Indoles. *ChemSusChem* **2017**, *10*, 2242– 2248.

32. Landge, V. G.; Shewale, C. H.; Jaiswal, G.; Sahoo, M. K.; Midya, S. P.; Balaraman, E. Nickel-Catalyzed Direct Alkynylation of $C(sp^2)$–H Bonds of Amides: An "Inverse Sonogashira Strategy" to *Ortho*-Alkynylbenzoic Acids. *Catal. Sci. Technol.* **2016**, *6*, 1946–1951.

33. Liu, Y.-J.; Liu, Y.-H.; Yan, S.-Y.; Shi, B.-F. A Sustainable and Simple Catalytic System for Direct Alkynylation of $C(sp^2)$–H Bonds with Low Nickel Loadings. *Chem. Commun.* **2015**, *51*, 6388–6391.

34. Ruan, Z.; Lackner, S.; Ackermann, L. Nickel-catalyzed C–H alkynylation of anilines: expedient access to functionalized indoles and purine nucleobases. *ACS Catal.* **2016**, *6*, 4690–4693.

35. Khake, S. M.; Soni, V.; Gonnade, R. G.; Punji, B. A general nickel-catalyzed method for C–H bond alkynylation of heteroarenes through chelation assistance. *Chem. - Eur. J.* **2017**, 23, 2907–2914.

36. (a) Liu, Y.-J.; Zhang, Z.-Z.; Yan, S.-Y.; Liu, Y.-H.; Shi, B.-F. Ni(II)/BINOL-Catalyzed Alkenylation of Unactivated $C(sp^3)$-H Bonds. *Chem. SCommun.* **2015**, *51*, 7899–7902. (b) Li, M.; Yang, Y.; Zhou, D.; Wan, D.; You, J. Nickel-Catalyzed Addition-Type Alkenylation of Unactivated, Aliphatic C–H Bonds with Alkynes: A Concise Route to Polysubstituted *γ*-Butyrolactones. *Org. Lett.* **2015**, *17*, 2546–2549. (c) Lin, C.; Chen, Z.; Liu, Z.; Zhang, Y. Nickel-Catalyzed Stereoselective Alkenylation of $C(sp^3)$-H Bonds with Terminal Alkynes. *Org. Lett.* **2017**, *19*, 850–853.

37. Jagtap, R. A.; Vinod, C. P.; Punji, B. Nickel-Catalyzed Straightforward and Regioselective C–H Alkenylation of Indoles with Alkenyl Bromides: Scope and Mechanistic Aspect. *ACS Catal.* **2019**, *9*, 431–441.

38. Obata, A.; Ano, Y.; Chatani, N. Nickel-Catalyzed C–H/N–H Annulation of Aromatic Amides with Alkynes in the Absence of a Specific Chelation System. *Chem. Sci.* **2017**, *8*, 6650–6655.

Chapter 4

Synthesis and Photophysical Study of Hetero-polycyclic and

Carbazole Motif: Nickel-Catalyzed Chelate Assisted Cascade
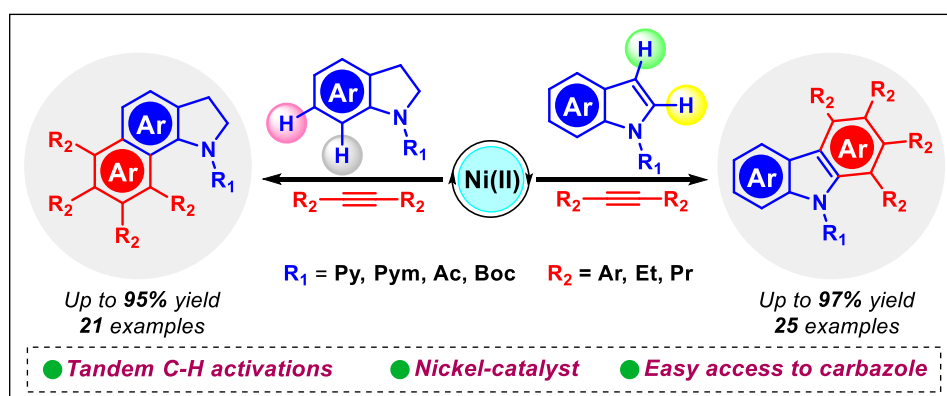
C-H Activations/Annulations

Chapter 4

Synthesis and Photophysical Study of Hetero-polycyclic and Carbazole Motif: Nickel-Catalyzed Chelate Assisted Cascade C-H Activations/Annulations

4.1 ABSTRACT: Herein, nickel catalyzed synthesis of polyarylcarbazole through sequential C-H bond activations has been described. Regioselective indole C2/C3 functionalization has been achieved in presence of indole C(7)-H which is quite challenging. Further, this approach also gives easy access to building heteropolycyclic motif through C6/C7 C-H functionalization of indoline. This methodology is not only limited to aromatic internal alkynes as coupling partners, aliphatic alkynes have also shown good tolerance. Notably, during the optimization we have observed the catalytic enhancement with sodium iodide as an additive. We have also studied the photophysical properties of these highly conjugated molecules.

4.2 INTRODUCTION

The incisive and efficient synthesis of hetero-polycyclic structures has attracted significant interest due to their large consumption as agrochemicals, pharmaceuticals, and organic functional materials.[1] Indole and indoline are very important from medicinal point of view,

and also their core skeletons has been existing in many natural products.[2,3] Indole derived carbazole moiety is known to show bioactivity such as antimalarial, antiviral, and antitumor property.[4] Carbazole moiety is also known to possess many interesting optical properties and hence it is used in organic light-emitting diodes (OLEDs), organic photovoltaic devices (OPVs), and organic field effect transistors (OFETs).[5] Therefore, the synthesis and photophysical study of these heterocycle motifs (indole, indoline and carbazole) is considered very important. In this regard, the C(7)-H functionalization of indoline has been achieved using noble transition metal catalysts[6] such as Ru, Rh, Pd, and Ir which are expensive and their natural abundance in the earth crust is comparatively lower than base metals.

In the recent decade, the development of earth abundant first-row transition metal catalyzed reactions are gaining significant interest, owing to its cost effectiveness, abundance and eco-friendly nature.[7] A paradigm shift has been observed towards the development of 3d transition metal catalyzed indole and indoline C-H bond functionalizations.[8] In this regard, copper catalyzed selective indoline C-7 selenation, thiolation and C-O bond formation has been reported by Ackermann and Koley *et. al* respectively (Figure 3.1, 1a).[9] Punniyamurthy and Punji groups have also exploited the strong coordinating ability of pyrimidine directing group, where they have successfully demonstrated indoline C-7 arylation and alkylation using earth abundant first row transition metal cobalt and iron catalyst respectively.[10] Recently, Ravikumar *et. al.* has developed methodologies on selective C-7 alkenylation, alkylation and hydroarylation of indoline using cobalt catalyst.[11] Remarkably, there are only a few reports on first-row transition metal cobalt and manganese catalyzed regioselective C-2 alkenylation of indole using alkynes as a reacting partner (Figure 4.1, 1b).[12] However, there is no report on nickel catalyzed cascade functionalization of indoline C6/C7 and indole C2/C3 C-H bonds. Herein, we are introducing a novel approach to

synthesize highly substituted indoline C-6/C-7 derived hetero-polycyclic motif, wherein for the first-time nickel catalyst has been used for this transformation (Figure 4.1, 2a). Interestingly, this methodology also gives easy access to carbazole molecules which are useful in pharmaceutical industries and material chemistry (Figure 4.1, 2b).

Figure 4.1: C-H functionalization of indole and indoline using 1st row transition metals.
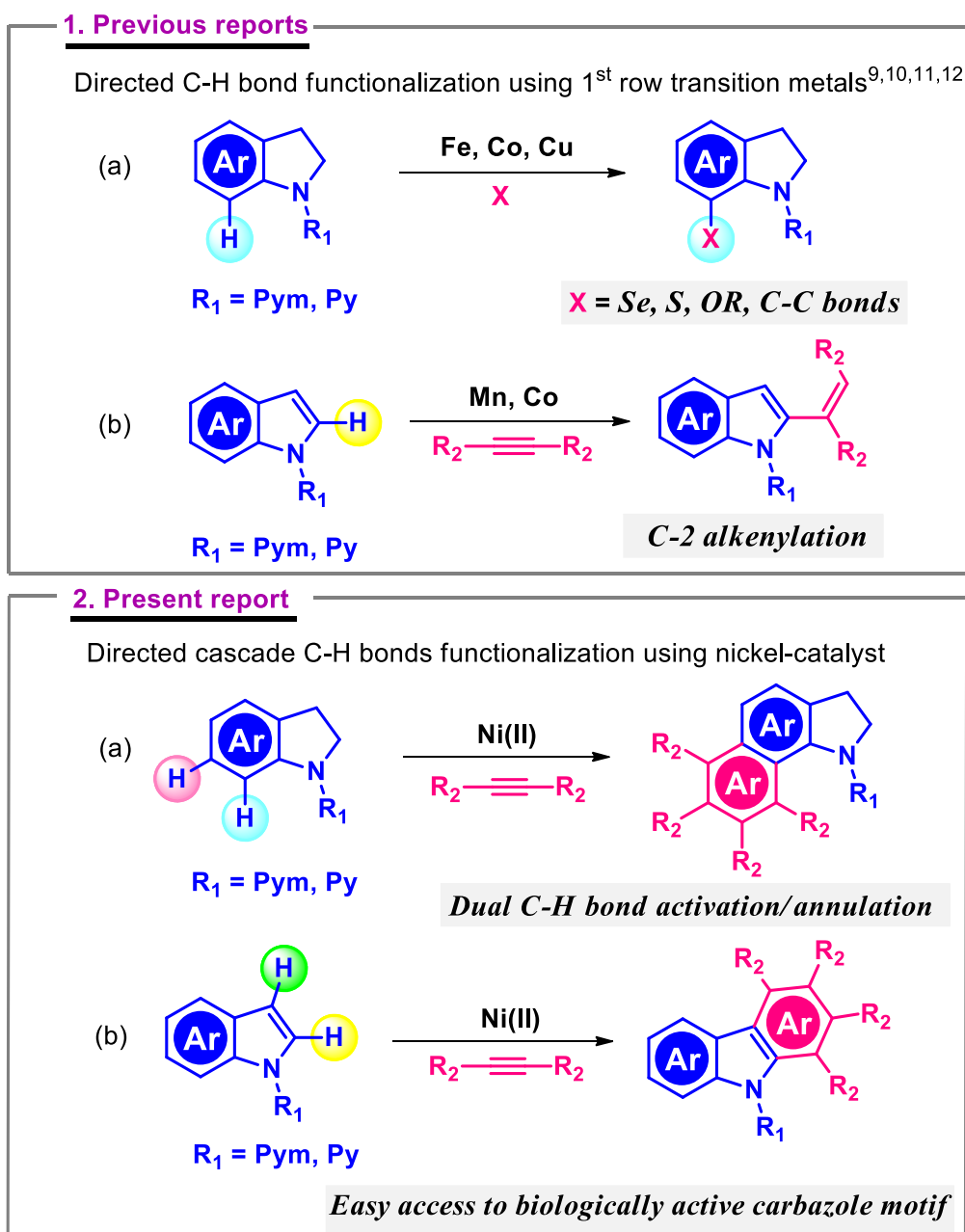

Most importantly, Ni(II)-catalyzed cascade C-H bond functionalization[13a] are not widely explored as compared to rhodium[13b-c] and palladium[14] on indole and indolines. Whereas we

have observed efficient catalytic activity of nickel catalyst for these conversions (Figure 3.1, 2a,b).

4.3 RESULTS AND DISCUSSION

Our investigation on catalytic hetero-polycyclization began with *N*-pyrimidyl indoline **1a** (0.1 mmol, 1 equiv) and diphenylacetylene **2a** (0.4 mmol, 4 equiv) as the model systems. At first, the various chlorinated, fluorinated, and polar protic solvent was screened in the presence of Ni(II)-catalyst (10 mol %), PPh$_3$ ligand (20 mol %), at 140 ºC (Table 4.1, entry 1-3). However, none of them were effective for this reaction. Further, we have screened several nonpolar solvents such as benzene, xylene, toluene, TFT, 1,4-dioxane, and polar solvent THF (Table 4.1, entry 4-9). To our delight, toluene worked well giving 66% of the desired product **3aa**. Benzene and THF did not show any reactivity. As ligand plays a very crucial role in Nickel-based transformation, we envisaged varying different phosphine ligands. A series of phosphine ligand with different electronic and steric properties have been screened (Table 4.1, entry 10-15). No superior result was observed, indicating triphenylphosphine as the optimal ligand for this transformation. In order to increase the product yield, other nickel catalysts such as NiBr$_2$, Ni(acac)$_2$, and Ni(cod)$_2$ were employed, they all failed to show any improved reactivity (Table 4.1, entry 16-18). Further, to accelerate the reactivity and enhance the product yield, 50 mol % of additive was added to the reaction. Among them, carbonate/bicarbonate additives cease the reactivity resulting in no reaction (Table 4.1, entry 19-20), whereas acetate decreases the yield of the desired adduct to 11% (Table 4.1, entry 21). A sudden hike in the product yield was observed when sodium iodide was used as an additive giving 82% yield of **3aa** (Table 4.1, entry 22). However, a detrimental effect on product yield was observed with other iodide salts such as KI, and CuI (Table 4.1, entry 23-24). The reaction performed without catalyst resulted in no reaction (Table 4.1, entry 25).

Table 4.1: Optimization of the reaction conditions[a]
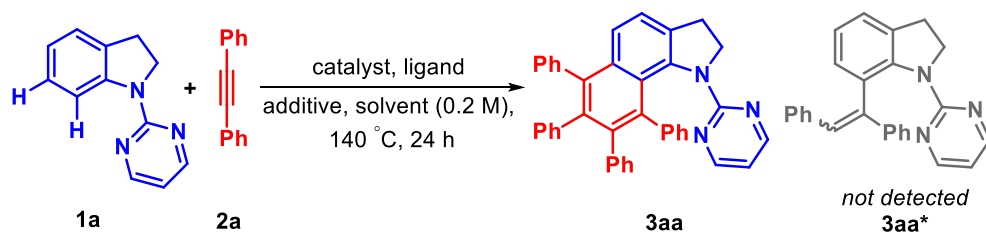
entry	solvent	ligands	catalyst	additive	3aa yield (%)[b]
1	DCE	PPh$_3$	Ni(OTf)$_2$	-	0
2	TFE	PPh$_3$	Ni(OTf)$_2$	-	0
3	MeOH	PPh$_3$	Ni(OTf)$_2$	-	0
4	benzene	PPh$_3$	Ni(OTf)$_2$	-	0
5	o-xylene	PPh$_3$	Ni(OTf)$_2$	-	43
6	toluene	PPh$_3$	Ni(OTf)$_2$	-	66
7	trifluoro toluene	PPh$_3$	Ni(OTf)$_2$	-	39
8	1, 4-dioxane	PPh$_3$	Ni(OTf)$_2$	-	32
9	THF	PPh$_3$	Ni(OTf)$_2$	-	0
10	toluene	PMe$_3$	Ni(OTf)$_2$	-	18
11	toluene	PCy$_3$	Ni(OTf)$_2$	-	56
12	toluene	dppm	Ni(OTf)$_2$	-	34
13	toluene	dppe	Ni(OTf)$_2$	-	48
14	toluene	dppf	Ni(OTf)$_2$	-	0
15	toluene	bipy	Ni(OTf)$_2$	-	0
16	toluene	PPh$_3$	NiBr$_2$	-	31
17	toluene	PPh$_3$	Ni(acac)$_2$	-	23
18	toluene	PPh$_3$	Ni(cod)$_2$	-	14
19	toluene	PPh$_3$	Ni(OTf)$_2$	Na$_2$CO$_3$	0
20	toluene	PPh$_3$	Ni(OTf)$_2$	NaHCO$_3$	0
21	toluene	PPh$_3$	Ni(OTf)$_2$	NaOAc	11
22	**toluene**	**PPh$_3$**	**Ni(OTf)$_2$**	**NaI**	**82**
23	toluene	PPh$_3$	Ni(OTf)$_2$	KI	49
24	toluene	PPh$_3$	Ni(OTf)$_2$	CuI	34
25	toluene	PPh$_3$	-	NaI	0
26	toluene	-	Ni(OTf)$_2$	-	39
27	toluene	-	Ni(OTf)$_2$	NaI	66
28	toluene	PPh$_3$	NiI$_2$	-	52
29	toluene	PPh$_3$	Ni(OTf)$_2$	NaI	75[c], 70[d]
30	— screening of directing groups:				
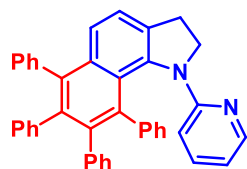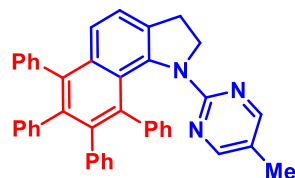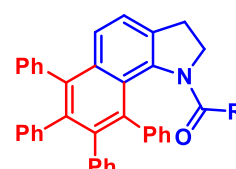
3ba, 93%   **3ca**, 30%   R = Me, **3da**, nr   R = O^{t}Bu, **3ea**, nd

[a]Reaction conditions: **1a** (0.10 mmol), **2a** (4 equiv), Ni(OTf)$_2$ (10 mol %), ligands (20 mol %), base (50 mol %), solvents (0.2 M), 140 °C, 24 h. [b]isolated yield. [c]time = 20 h, [d]temperature = 120 °C.

The reaction without ligand and additive gave 39% yield of product (Table 4.1, entry 26), whereas without ligand 66% yield has been observed (Table 4.1, entry 27). This implies that catalyst, ligand and additive are important for this transformation. Since Ni(OTf)$_2$ and NaI is working well for this transformation, we presumed that the NiI$_2$ might be forming inside the reaction. Therefore, we have taken NiI$_2$ as catalyst instead of Ni(OTf)$_2$ and NaI (Table 4.1, entry 28). However, we observed lower yield of the product **3aa** which indicates the superior role of Ni(OTf)$_2$ and NaI combination. Such enhancement of yield by iodide salts has been reported earlier.[15a] There could some secondary counter ion effects influencing this reaction, which is not clear to us yet. Moreover, possibility of counter ion/ligand exchange [from Ni(OTf)$_2$ to Ni(OTf)I] cannot be ruled out. Thus, for this developed protocol 10 mol % Ni(OTf)$_2$, in combination with 20 mol % of PPh$_3$, 50 mol % of NaI in 0.2 M toluene for 24 h was found as optimized reaction condition. Decreasing the time and temperature resulted in a decrease in product yield **3aa** (Table 4.1, entry 29). Further, the role of directing group was examined. By changing the directing group from pyrimidine to pyridine, the yield of the desired product increased to 93% (Table 4.1, entry 30). This can be attributed to the fact that the presence of an extra nitrogen in the directing group could poison the catalyst, decreasing the reactivity and yield. Furthermore, yield of the product **3ca** has drastically decreased to 30% when *p*-me pyrimidine was chosen as directing group. Also, the effect of weak chelating directing group has been tested and found ineffective for this reaction.[15b] This implies that a strong donor directing group is necessary for this transformation.[15c]

With the optimized reaction condition in hand, we have examined various substrate scope of 1-(pyridin-2-yl)indoline **1b** with diphenylacetylene **2a** (Scheme 4.1). Delightfully, this protocol is quite general with many structurally and electronically diverse compounds. With methyl substituent at C(2)-position of substrate, it furnished the respective product

3fa (62%) in good yields. However, C(4)-halo group substituted indoline gave the respective desired products in high yields (**3ga** 84%, **3ha** 89%, **3ia** 86%). Indoline substrate containing -Me and -OMe group at C(5) position gave the products with good to excellent yields (**3ja**, 78% & **3ka,** 95%). In contrast, the electron withdrawing group such as CN, NO$_2$, substitution at C(5)-position failed to deliver the desired product, even at high
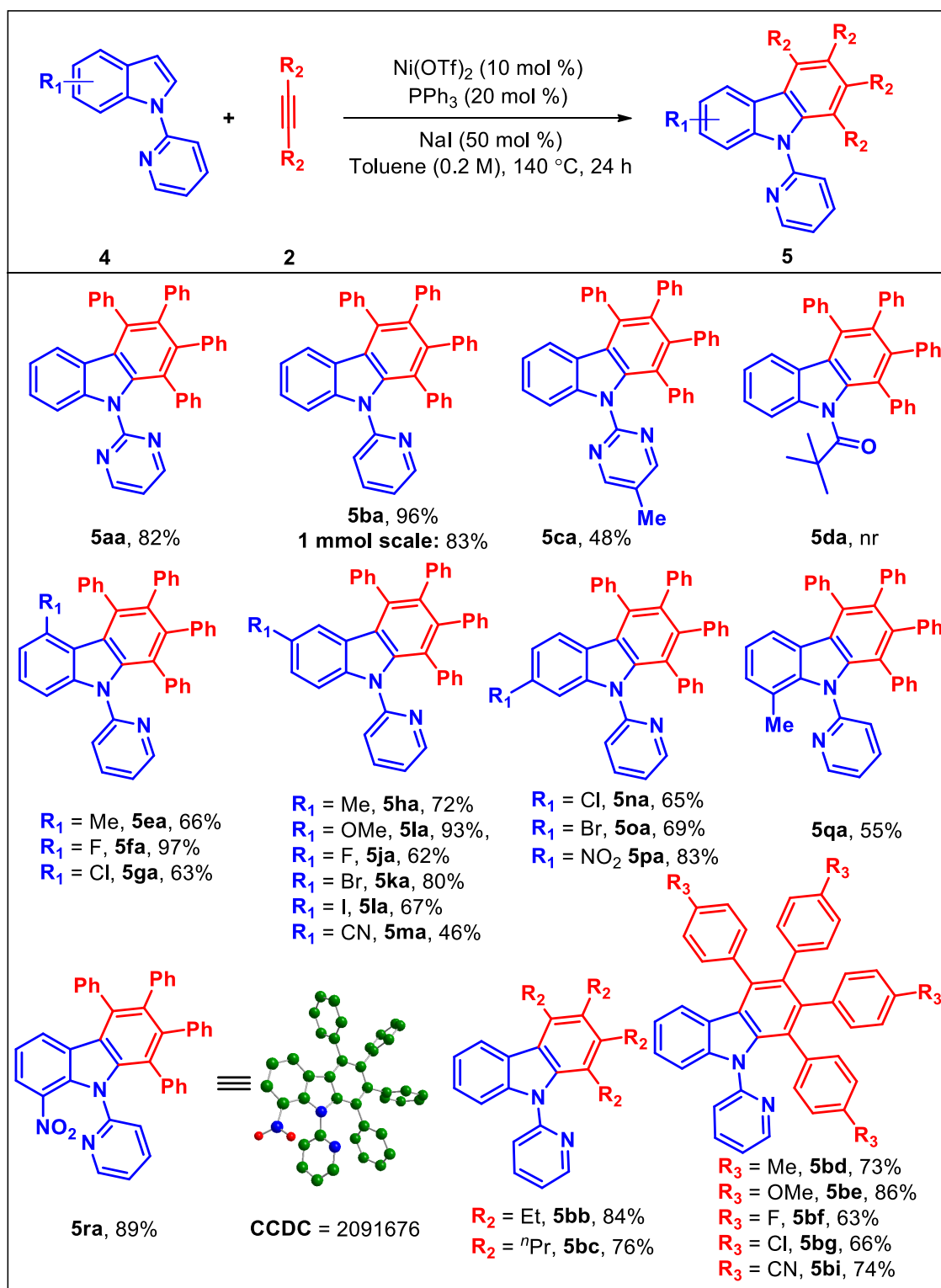
Scheme 4.1: Substrate scope for the synthesis of 3[a,b]
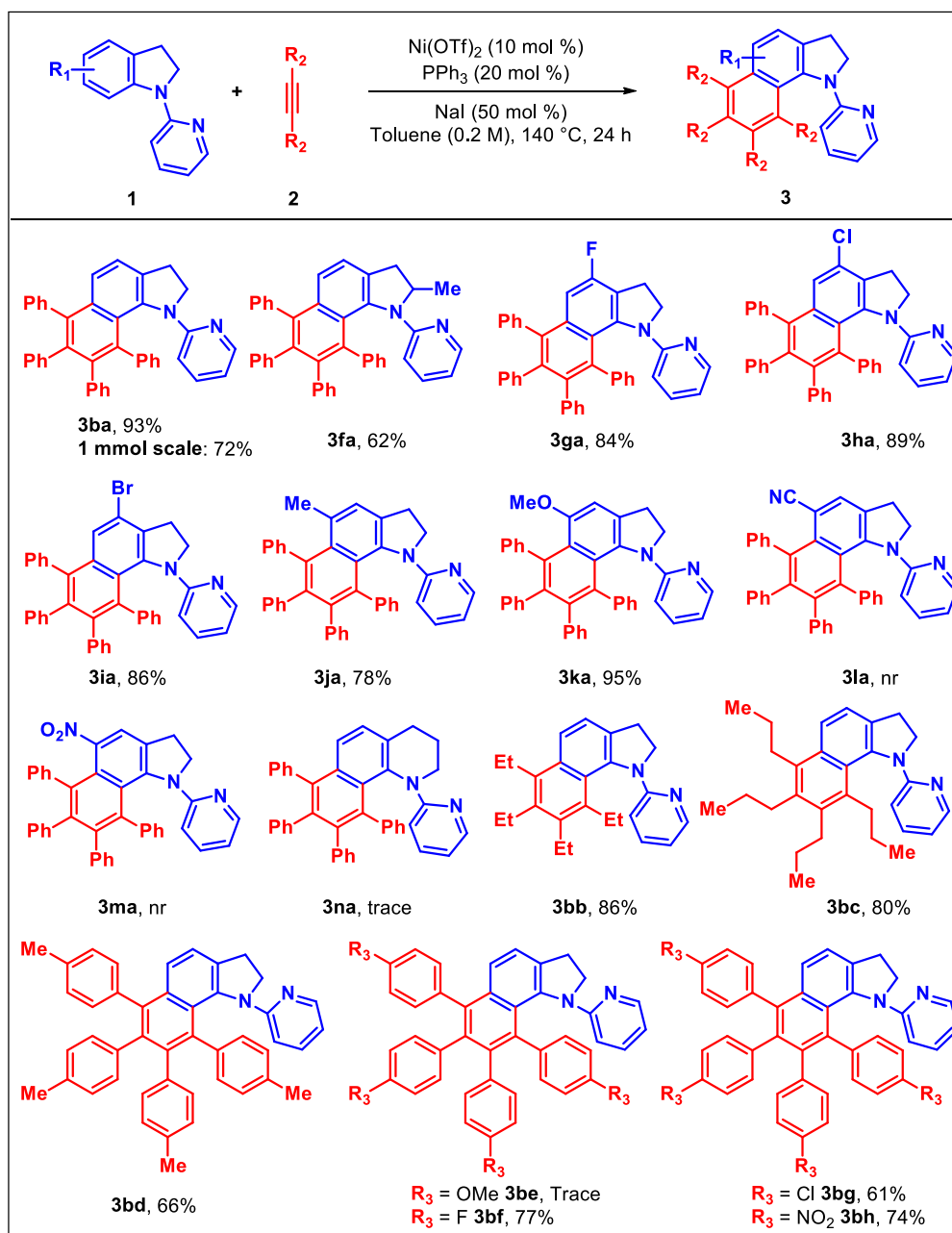
temperature (**3la**, **3ma**). This might be due to the decrease in the nucleophilicity of M-C bond in presence of electron withdrawing groups, making it less reactive towards alkyne in intermediate **B** (Scheme 4.4). Further, when we changed the substrate from indoline to tetrahydroquinoline, it gave only a trace amount of product (**3na**). Such precedence is reported in the literature as well.[15d] After screening various substituted indoline, further the generality of aliphatic internal alkynes **2b-c** were explored. In both cases we obtained very good yields (**3bb, 3bc**). Substituted diphenylacetylene **2d-h** were also examined under optimized reaction conditions. The reacting partner diphenylacetylene with electron-donating and electron-withdrawing substituents were well-tolerated, with significant reactivity giving the corresponding annulated product (**3bd, 3bf−3bh)** in good yields. Whereas, the 1,2-bis(4-methoxyphenyl)ethyne **2e** was less reactive towards insertion of the M-C bond. Thereby, it gave only trace amount of the product (**3be**).

Further we intended to demonstrate the scope of this methodology for the synthesis of another important class of molecules i.e.; carbazoles (Scheme 4.2). To our delight, when *N*-pyrimidinyl indole **4a** was subjected to our standard reaction condition, the desired product **5aa** in 82% yield was obtained, whereas with *N*-pyridyl indole, enhanced yield of the desired product **5ba** was obtained. Indole bearing 5-methylpyrimidinyl directing group afforded the product with moderate yield (**5ca**, 48%) and the *N*-Boc-protected indole substrate failed to give the desired product (**5da**, nr). As the *N*-pyridyl directing group delivered the best yield of the desired annulated product **5**, we chose *N*-pyridyl as the directing group to explore the substrate scope. Various substituted indoles were tested and found compatible under standard reaction condition (Scheme 4.2). In case of C(4) substituted indoles, a significant difference of reactivity was observed.
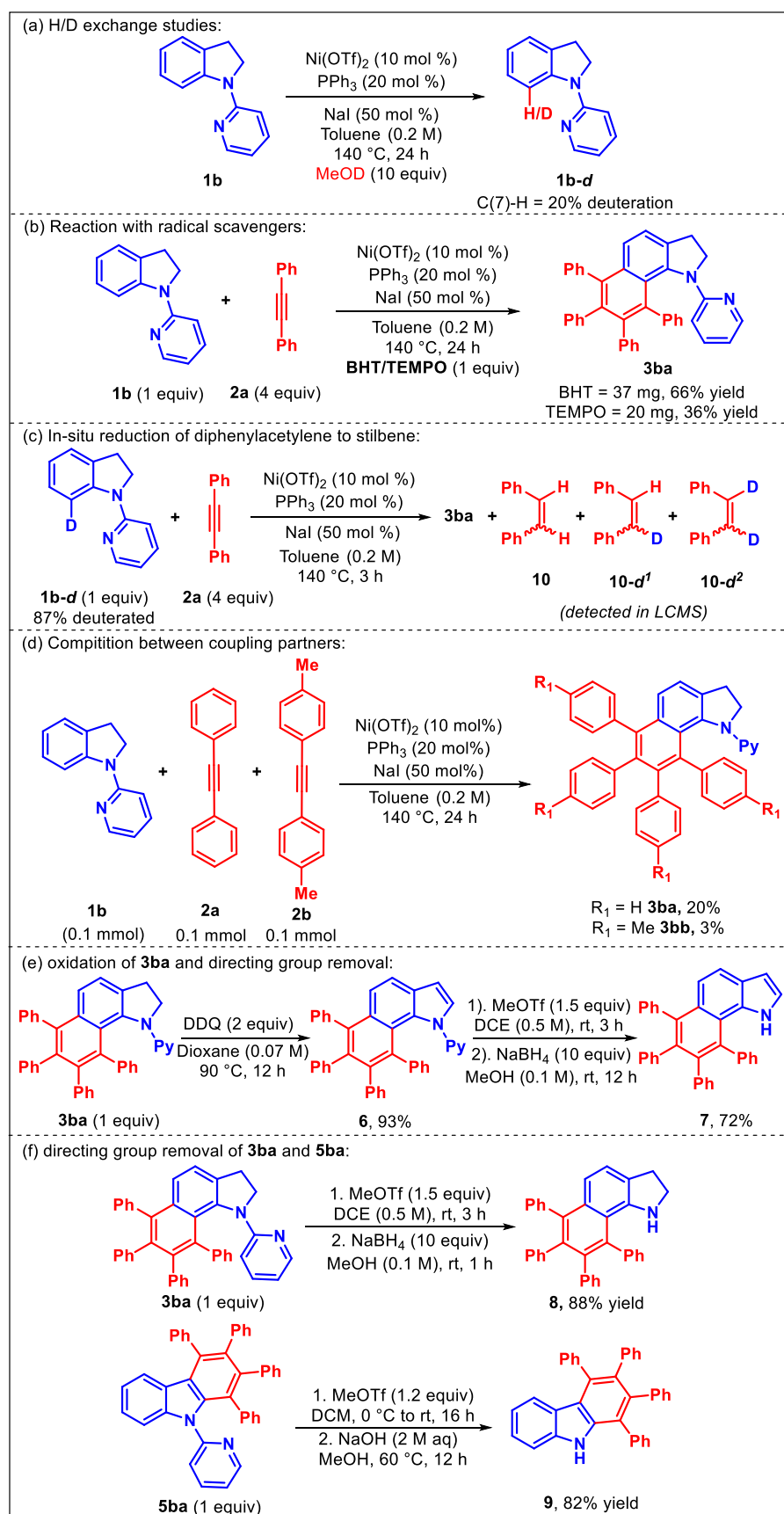
Scheme 4.2: Substrate scope for the synthesis of 5[a,b]

5aa, 82%

5ba, 96%
1 mmol scale: 83%

5ca, 48%

5da, nr

R$_1$ = Me, 5ea, 66%
R$_1$ = F, 5fa, 97%
R$_1$ = Cl, 5ga, 63%

R$_1$ = Me, 5ha, 72%
R$_1$ = OMe, 5la, 93%,
R$_1$ = F, 5ja, 62%
R$_1$ = Br, 5ka, 80%
R$_1$ = I, 5la, 67%
R$_1$ = CN, 5ma, 46%

R$_1$ = Cl, 5na, 65%
R$_1$ = Br, 5oa, 69%
R$_1$ = NO$_2$ 5pa, 83%

5qa, 55%

5ra, 89%

CCDC = 2091676

R$_2$ = Et, 5bb, 84%
R$_2$ = ^{n}Pr, 5bc, 76%

R$_3$ = Me, 5bd, 73%
R$_3$ = OMe, 5be, 86%
R$_3$ = F, 5bf, 63%
R$_3$ = Cl, 5bg, 66%
R$_3$ = CN, 5bi, 74%

[a]Reaction conditions: **1b** (0.2 mmol), **2a** (0.8 mmol), Ni(OTf)$_2$ (10 mol %), PPh$_3$ (20 mol %), NaI (50 mol %), toluene (0.2 M), 140 °C, 24 h. [b]Isolated yields. . [c]Isolated yield of 1 mmol scale reaction.

The C(4) methyl-substituted indole is less prone to react giving product **5ea** in 66% yield, whereas fluoro-substituted substrate reacted efficiently to give the desired product **5fa** in 97% yield. Further, the chloro-substitution at C(4)-position of indole gave the product **5ga** in 63% yield. The substituent variations at C(5)-position of *N*-pyridyl indole also led to the products in good to excellent yields (Scheme 4.2, **5ha**-**5ma**).The 5-methyl indole gave the product **5ha** in 72% yield, whereas, 5-methoxy indole delivered the product **5ia** in excellent yield (93%). In addition to this, the halo substitution at C(5)-position also led to the products with good yield (**5ja** 62%, **5ka** 80% & **5la** 67%). However, the cyano substitution gave the desired product **5ma** in moderate yield 46%. Furthermore, the variation of substitution at C(6) & C(7) position of the substrate were screened which resulted good to very good yield of the products (Scheme 4.2, **5na**-**5ra**). The structure of **5ra** was confirmed from single crystal X-ray analysis. Further, the aliphatic internal alkynes have given desired products in good yields (Scheme 4.2, **5bb**, **5bc**). Various diphenylacetylene with electron-donating and electron-withdrawing substituents were well tolerated, furnishing the corresponding annulated product in very good yields (Scheme 4.2, **5bd-5bg**, **5bi**).

To gain comprehensive information regarding reaction mechanism, some control experiments have been performed (Scheme 4.3). A deuterium exchange study was carried out using *N*-pyridyl indoline **1b** in the absence of coupling partner **2a** under the optimized reaction conditions, 20% deuteration at C(7)-H position, suggests that the first step might be a reversible step (Scheme 4.3a).

Scheme 4.3: Mechanistic Studies, Synthetic Utility

(a) H/D exchange studies:

Ni(OTf)$_2$ (10 mol %)
PPh$_3$ (20 mol %)

NaI (50 mol %)
Toluene (0.2 M)
140 °C, 24 h
MeOD (10 equiv)

1b

1b-d
C(7)-H = 20% deuteration

(b) Reaction with radical scavengers:

Ni(OTf)$_2$ (10 mol %)
PPh$_3$ (20 mol %)
NaI (50 mol %)

Toluene (0.2 M)
140 °C, 24 h
BHT/TEMPO (1 equiv)

1b (1 equiv)   2a (4 equiv)

3ba
BHT = 37 mg, 66% yield
TEMPO = 20 mg, 36% yield

(c) In-situ reduction of diphenylacetylene to stilbene:

Ni(OTf)$_2$ (10 mol %)
PPh$_3$ (20 mol %)

NaI (50 mol %)
Toluene (0.2 M)
140 °C, 3 h

3ba +

1b-d (1 equiv)   2a (4 equiv)
87% deuterated

10   10-d^1 10-d^2
(detected in LCMS)

(d) Compitition between coupling partners:

Ni(OTf)$_2$ (10 mol%)
PPh$_3$ (20 mol%)
NaI (50 mol%)

Toluene (0.2 M)
140 °C, 24 h

1b   2a   2b
(0.1 mmol) 0.1 mmol 0.1 mmol

R$_1$ = H 3ba, 20%
R$_1$ = Me 3bb, 3%

(e) oxidation of 3ba and directing group removal:

DDQ (2 equiv)
Dioxane (0.07 M)
90 °C, 12 h

1). MeOTf (1.5 equiv)
DCE (0.5 M), rt, 3 h
2). NaBH$_4$ (10 equiv)
MeOH (0.1 M), rt, 12 h

3ba (1 equiv)   6, 93%   7, 72%

(f) directing group removal of 3ba and 5ba:

1. MeOTf (1.5 equiv)
DCE (0.5 M), rt, 3 h
2. NaBH$_4$ (10 equiv)
MeOH (0.1 M), rt, 1 h

3ba (1 equiv)   8, 88% yield

1. MeOTf (1.2 equiv)
DCM, 0 °C to rt, 16 h
2. NaOH (2 M aq)
MeOH, 60 °C, 12 h

5ba (1 equiv)   9, 82% yield

reaction of **1b-*d*** and diphenylacetylene **2a** (Scheme 4.3c) was detected in LCMS (*LCMS (ESI) m/z* of stilbene: [M+H]$^+$ Calcd for $C_{14}H_{12}$: 181.1; Found: 181.1). This result suggests the crucial role of diphenylacetylene **2a** acting as a coupling partner as well as organic oxidant to carry forward the catalytic processes. A competition experiment was performed and it was observed the electron poor alkyne is giving good yield than electron rich alkyne (Scheme 4.3d). To diversify the products formed, we subjected **3ba** to DDQ oxidation,[16] which delivered the oxidized product **6** with 93% yield (Scheme 4.3e). Deprotection[17] of the oxidized product **6** in the presence of MeOTf, NaBH$_4$ and DCE solvent, delivered directing group free annulated product **7** (72% yield) (Scheme 4.3e). Under the same reaction condition, deprotection of **3ba** and **5ba** have been performed, which led to the formation of product **8** (88%) and **9** (82%) with free *N-H* group (Scheme 4.3f).

Based on above mechanistic studies and literature findings,[18] a plausible catalytic cycle for the synthesis of **3** as well as for **5** was depicted in scheme 4.4. For the synthesis of product **3,** initially, the Ni(II)-catalyst undergoes ligand exchange to generate the active Ni(II)-catalyst (Scheme 4.4a). Then indoline **1** coordinates with active Ni(II)-catalyst to give intermediate **A** through concerted metallation–deprotonation (CMD) pathway. Then, alkyne **2** coordinates with intermediate **A** and gives intermediate **B**. Migratory insertion of alkyne forms the intermediate **C**. Then, second C-H bond activation leads to the formation of five-membered cyclic intermediate **D**. Further, alkyne insertion followed by reductive eliminations delivers the desired product **3** along with the formation of L$_2$Ni(0) intermediate **F**. Then, the oxidative addition of L$_2$Ni(0) **F** species into C-H bond of substrate **1** gives intermediate **G**. Reduction of alkyne and protodemetallation regenerates active-intermediate **A** for the next catalytic cycle.

Scheme 4.4: Plausible mechanism

(a) cascade C-H functionalization of *N*-pyridyl indoline:
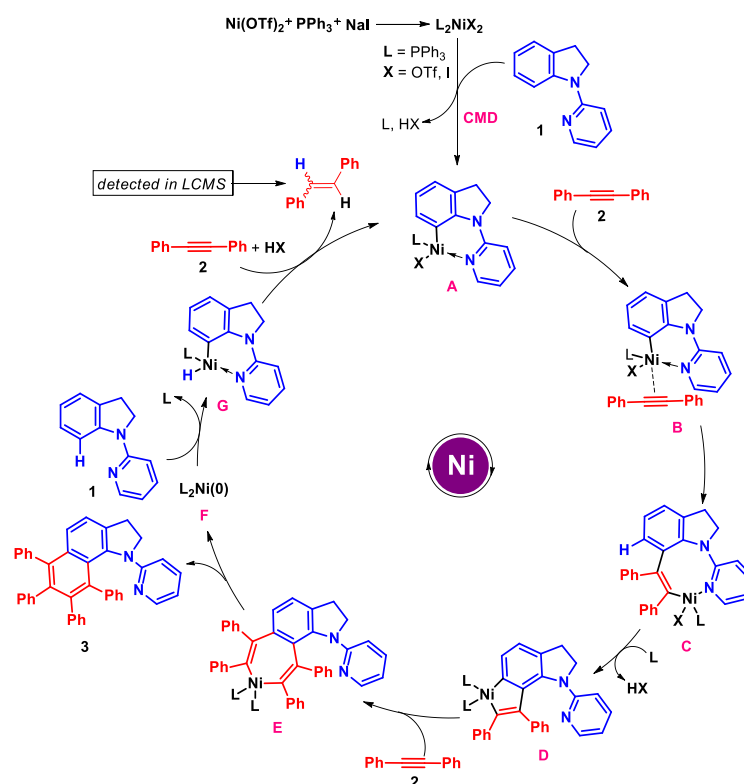
(b) Cascade C-H functionalization of N-pyridyl indole:
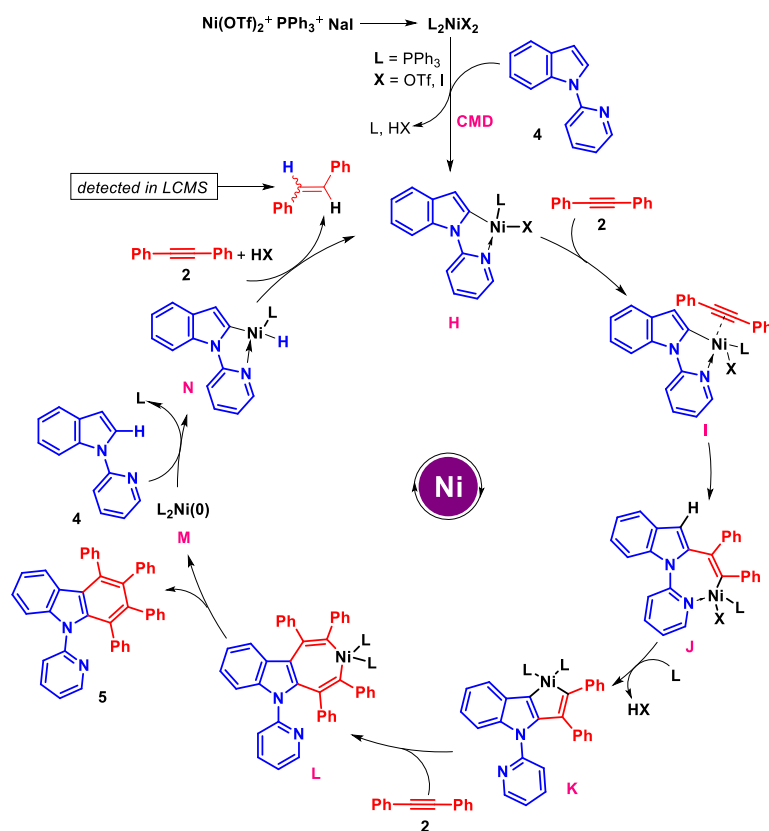
For the synthesis of carbazole product **5**, initially indole **4** coordinates with Ni(II)-catalyst to give intermediate **H** (Scheme 4.4b) through concerted metallation–deprotonation (CMD) pathway. Then, alkyne **2** coordinates with intermediate **H** and gives intermediate **I**. Migratory insertion of alkyne forms the intermediate **J**. Then, second C-H bond activation leads to the formation of five-membered cyclic intermediate **K**. Further, alkyne insertion followed by reductive eliminations delivers the desired product **5** along with the formation of L$_2$Ni(0) intermediate **M**. Then, the oxidative addition of L$_2$Ni(0) **M** species into C-H bond of substrate **4** gives intermediate **N**. Reduction of alkyne (stilbene detected in HRMS) and protodemetallation regenerates active-intermediate **H** for the next catalytic cycle.

Figure 4.2: Photophysical Studies

(a) Absorption, Emission & lifetime Spectra of 3ba in CH$_2$Cl$_2$ Solution

(b) Absorption, Emission & lifetime Spectra of 5ba in CH$_2$Cl$_2$ Solution
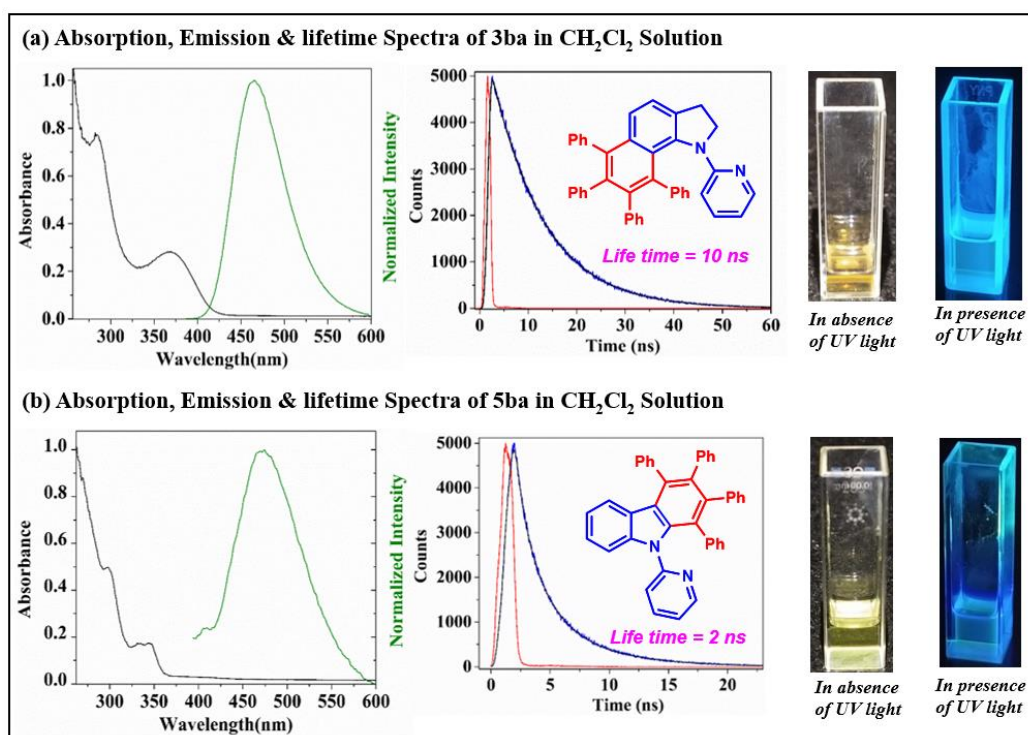
To demonstrate the utility of highly conjugated motifs in material chemistry, we have investigated some photophysical studies (Figure 4.2a-b). Generally, highly π-conjugated systems exhibit interesting optical properties. These polyaromatic heterocycles have the potential as optical material, therefore photophysical property of **3ba** and **5ba** was

investigated in solution state at room temperature and the corresponding absorption/emission spectrum were shown in Figure 4.2. The samples were recorded in dichloromethane solvent. The fluorescence spectra of **3ba** (Figure 4.2a) and **5ba** (Figure 4.2b) show emission maxima at 465 nm & 474 nm respectively. It is found that the product **3ba** shows higher lifetime (10 ns) in excited state than that of the product **5ba** (2 ns). These molecules indicate prominent fluorescent properties, which can be further applicable for optoelectronics such as light-emitting diodes (OLEDs) and organic field-effect transistors (OFETs) in material science.[19]

4.4 CONCLUSION

In summary, we have successfully developed a Ni-catalyzed methodology to access π-conjugated polycyclic heteroaromatic scaffolds *via* C−H bond activation of indoline/indole. Herein, we have introduced an approach to synthesize C-6 & C-7 derived hetero-polycyclic indoline motif, where nickel has been used as a catalyst for the first time. Interestingly, this methodology gives easy access to carbazole molecule which are highly desirable in pharmaceutical industries. In addition, sodium iodide plays a crucial role that enhances the catalytic potential of nickel. Most importantly, photophysical studies of the products have been performed, the results indicate that it can have wide application in material chemistry.

4.5 EXPERIMENTAL SECTION[20]

Reactions were performed using oven dried borosil seal-tube glass vial with Teflon-coated magnetic stirring bars under N_2 atmosphere. Column chromatography was done by using 100-200 and 230-400 mesh size silica gel of Acme synthetic chemicals company. A gradient elution was performed by using distilled petroleum ether and ethyl acetate. TLC plates were detected under UV light at 254 nm. ^{1}H NMR, ^{13}C NMR & ^{19}F NMR were recorded on Bruker AV 400 and 700 MHz spectrometers using $CDCl_3$ as the deuterated

solvent.[21] Chemical shifts (δ) are reported in ppm relative to the residual solvents (CHCl$_3$)

signal (δ = 7.26 for ^{1}H NMR and δ = 77.36 for ^{13}C NMR). Data for ^{1}H NMR spectra are

reported as follows: chemical shift (multiplicity, coupling constants, number of hydrogen).

Abbreviations are as follows: s (singlet), d (doublet), t (triplet), q (quartet), quint (quintet),

m (multiplet), dd (double doublet), br (broad signal), J (coupling constants) in Hz (hertz).

High-Resolution Mass Spectrometry (HRMS) data was recorded using micro TOF Q-II

mass spectrometer using methanol as solvent. IR spectra were recorded on a FTIR system

and values are reported in frequency of absorption (cm^{-1}). Melting point was performed

using Stuart[TM] melting point apparatus SMP10. X-ray analysis was conducted using Rigaku

Smartlab X-ray diffractometer, Steady-state absorption and emission spectra are recorded

using a Jasco V-730 spectrophotometer and Shimadzu RF-6000 fluorescence

spectrophotometer (Shimadzu Corporation), respectively. For emission spectra, samples

were excited at 375 nm at SCS, NISER. For the measurement of time-resolved

fluorescence, a time-correlated single-photon counting (TCSPC) spectrometer (Edinburgh,

OB920) was used. Reagents and starting materials were purchased from Sigma Aldrich,

Alfa Aesar, TCI, Avra, Spectrochem and other commercially available sources and used

without further purification unless otherwise noted.

4.5.1 General procedure for reduction of indoles to indolines:[22]
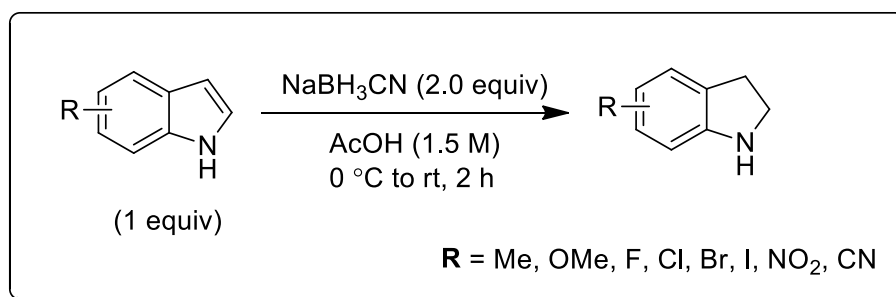
To a solution of indole (40 mmol, 1 equiv) in acetic acid (1.5 M, 27 mL) was added in

portions sodium cyanoborohydride (80 mmol, 2 equiv) at 0 °C, and the mixture was stirred

at room temperature. After 2 h, water (50 mL) was added at 0 °C, and the mixture was basified with NaOH (5 N aqueous solution). The organic material was extracted with CH_2Cl_2 (100 mL × 3), washed with brine, dried over anhydrous $MgSO_4$, and concentrated using a rotary evaporator to give crude reaction mixture. The column chromatography gives the pure product.

4.5.2 General procedure for the preparation of *N*-protected indolines and indoles:[23]

(a) 1-(pyrimidin-2-yl)indolines were prepared by following the reported procedure[23a]
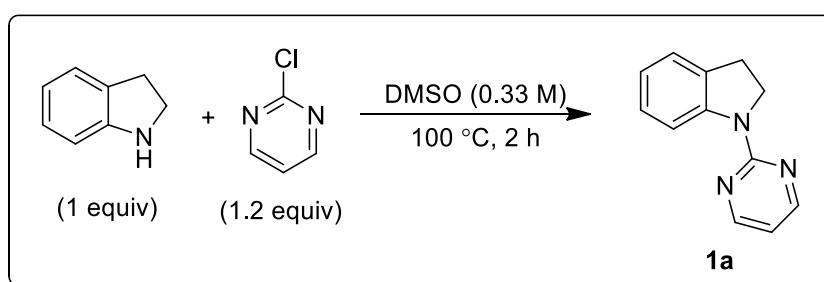
To a well-stirred solution of indoline (4.2 mmol, 1 equiv) in DMSO (0.33 M, 13 mL) at room temperature was added 2-chloropyrimidine (5 mmol, 1.2 equiv). The reaction was refluxed at 100 °C for 2 h. After 2 h, the reaction flask was cooled to room temperature. After completion of the reaction (as monitored by TLC analysis), it is cooled to room temperature and worked up with cold water. The product was extracted with EtOAc (3 x 20 mL) and dried over anhydrous Na_2SO_4. The organic phase was concentrated in vacuum to obtain the crude mixture which was further purified by column chromatography (using 5% ethyl acetate/hexane) giving the product as white solid (99% yield).

(b) 1-(pyridin-2-yl)indolines were prepared by following the reported procedure[23b]
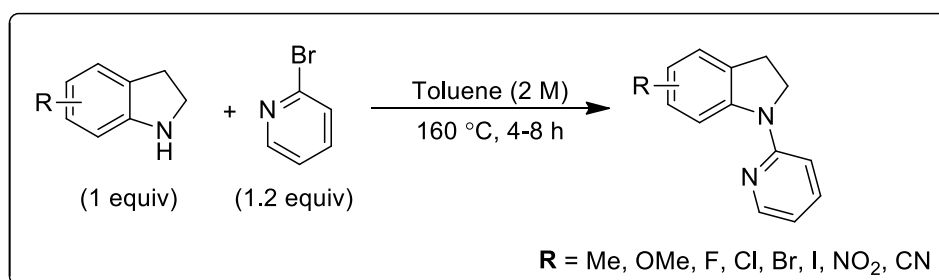
To an oven dried 25 mL round bottom flask charged with indoline (8.4 mmol, 1 equiv) were added 2-bromopyridine (10 mmol, 1.2 equiv) and toluene (2 M, 4.2 mL) under air at room temperature. The reaction was stirred at 160 °C for 8 h. The reaction mixture was diluted with EtOAc and washed with a saturated NaHCO₃ solution. The organic solution was dried over anhydrous Na₂SO₄. The organic phase was concentrated in vacuum to obtain the crude mixture which was further purified by column chromatography (using 5% EtOAc/hexane) giving the pure product.

(c) General and modified procedure for preparation of 1-(pyridin-2-yl)-1H-indole:[23c,d]
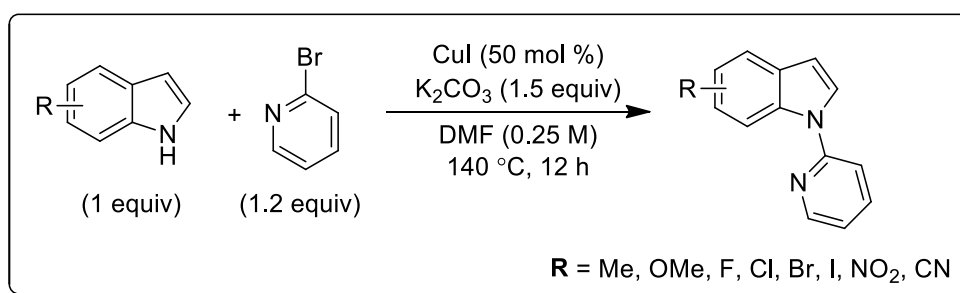
N-pyridyl indoles were prepared by following the reported procedure. To an oven dried 25 mL sealed tube charged with a stirring bar, indole (1.7 mmol, 1 equiv), copper iodide (0.86 mmol, 0.5 equiv), K₂CO₃ (2.6 mmol, 1.5 equiv) were added sequentially under nitrogen atmosphere. Then 2-bromopyridine (1.9 mmol, 1.1 equiv) was added to the reaction mixture followed by addition of DMF solvent (0.25 M). The reaction was allowed to stir at 140 °C in a pre-heated aluminum block until the reaction completed. After completion of the reaction (as monitored by TLC analysis), it is cooled to room temperature and worked up with cold water. The product was extracted with EtOAc (3 x 20 mL) and dried over anhydrous Na₂SO₄. The organic phase was concentrated in vacuum to obtain the crude mixture which was further purified by column chromatography (using 5% EtOAc/hexane) giving the pure product.

4.5.3 General procedure for preparation of internal alkynes:[24]

Symmetrical alkynes **2b, 2c, 2d, 2e, 2f** and **2i** were prepared following the reported literature procedure.
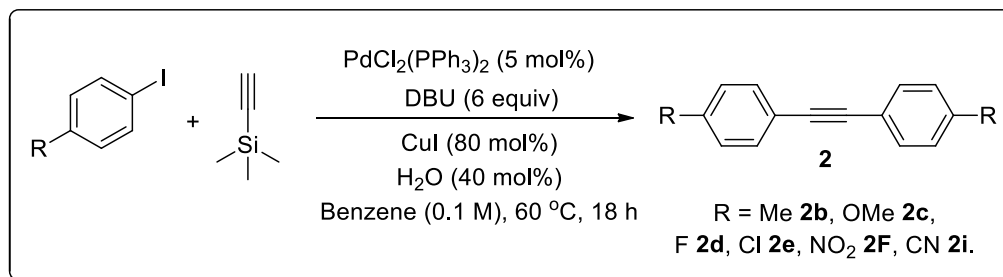
To an oven dried sealed tube charged with a stirring bar, dry benzene (0.1 M), aryl iodide (2.8 equiv), trimethylsilylacetylene (1 equiv), PdCl$_2$(PPh$_3$)$_2$ (4.5 mol %), CuI (80 mol %), DBU (6 equiv) and distilled water (40 mol %) were added sequentially under nitrogen atmosphere. The solution was stirred at rt for 20-30 minute and then kept it in a pre-heated aluminum block at 60 °C for 15-20 h. After completion of the reaction (as monitored by TLC analysis), the reaction mixture was quenched with 10% HCl (10 mL). Then the crude mixture was extracted with EtOAc and washed with saturated NaCl. After drying over anhydrous Na$_2$SO$_4$, the crude mixture was purified by column chromatography using EtOAc/hexane mixture on silica gel to furnish the pure product.

4.5.4 General reaction procedure for C(6)-H & C(7)-H activation of 1-(pyridin-2-yl)indolines with diphenyl acetylene as coupling partner:
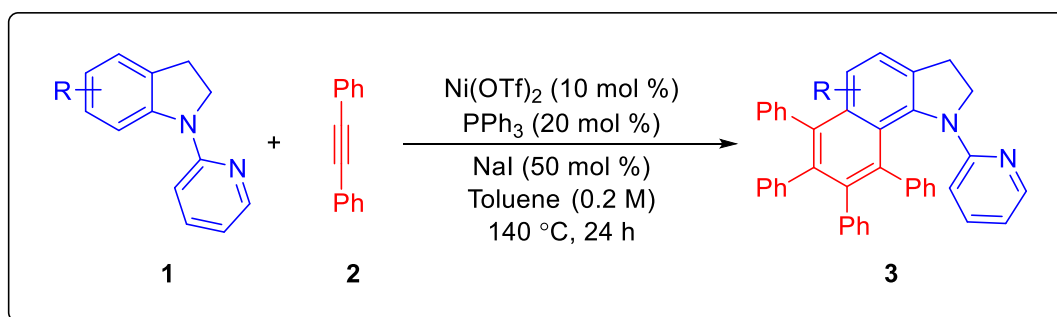
To an oven dried sealed tube charged with a stirring bar under N$_2$ atmosphere, the 1-(pyridin-2-yl)indoline **1** (0.1 mmol), diphenylacetylene **2** (4 equiv), PPh$_3$ (20 mol %), NaI (50 mol %) were added and sealed. The sealed tube was high-vacuumed and refilled with N$_2$. Then Ni(OTf)$_2$ (10 mol %) and degassed toluene solvent (0.2 M) were added to the reaction mixture inside the glove box. Then the sealed tube was taken out of the glove box and reaction mixture was vigorously stirred at 140 °C on preheated aluminum block for 24 h. After 24 h (upon completion of reaction as monitored by TLC analysis), the reaction mixture was cooled to room temperature and diluted with EtOAc or DCM and passed through a short celite pad. The solvent was evaporated under reduced pressure and the residue was purified by column chromatography using EtOAc/hexane mixture on silica gel to give the pure product **3**.

4.5.5 General reaction procedure for C(2)-H & C(3)-H activation of 1-(pyridin-2-yl)-1H-indole with diphenyl acetylene as coupling partner:
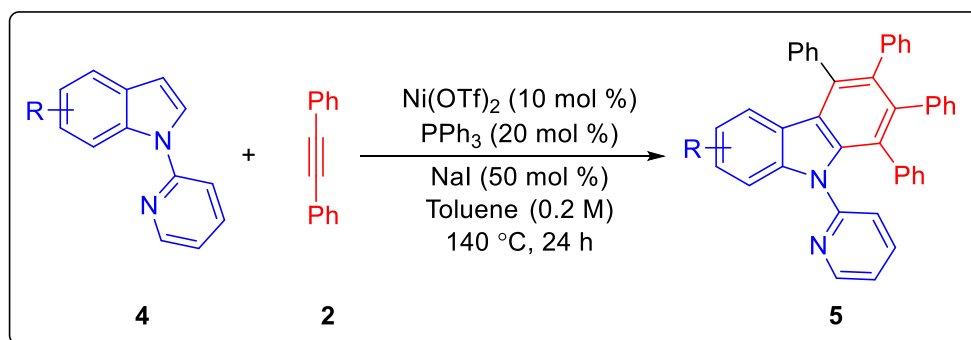
To an oven dried sealed tube charged with a stirring bar under N$_2$ atmosphere, the 1-(pyridin-2-yl)-1H-indole **4** (0.1 mmol), diphenylacetylene **2** (4 equiv), PPh$_3$ (20 mol %), NaI (50 mol %), were added and sealed. The sealed tube was high-vacuumed and refilled with N$_2$. Then Ni(OTf)$_2$ (10 mol %) and degassed toluene solvent (0.2 M) were added to the reaction mixture inside the glove box. Then the sealed tube was taken out of the glove box and reaction mixture was vigorously stirred at 140 °C on preheated aluminium block

for 24 h. After 24 h (upon completion of reaction as monitored by TLC analysis), the reaction mixture was cooled to room temperature and diluted with EtOAc or DCM and passed through a short celite pad. The solvent was evaporated under reduced pressure and the residue was purified by column chromatography using EtOAc/hexane mixture on silica gel to give the pure product **5**.

### 4.5.6 Detection of deuterated-Stilbene in the reaction:
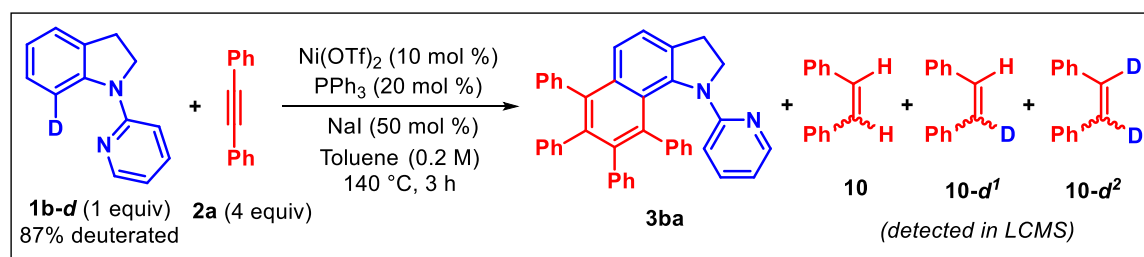
To an oven dried sealed tube charged with a stirring bar under N_2 atmosphere, **1b-d** (10 mg, 0.05 mmol), diphenylacetylene **2a** (36 mg, 0.20 mmol), PPh$_3$ (20 mol %), NaI (50 mol %) were added. The sealed tube was high-vacuumed and refilled with N_2. Then toluene (0.2 M, 0.3 mL) was added to the reaction mixture. The Ni(OTf)$_2$ (10 mol %) was added to the reaction mixture inside the glove box. Then the reaction mixture was vigorously stirred at 140 °C on preheated aluminium block for the 3 h. After 3 h, the reaction mixture was cooled to room temperature and diluted with EtOAc and passed through a short celite pad. The solvent was evaporated under reduced pressure and the residue was submitted for LCMS in methanol from which formation of deuterated stilbenes (**10**, **10-d^1**, **10-d^2**) was detected along with the formation of product **3ba**.

(a) LCMS (ESI) m/z of **10:** [M+H]$^+$ Calcd for $C_{14}H_{12}$: 181.1; Found: 181.1.

(b) LCMS (ESI) m/z of **10-d^1:** [M+H]$^+$ Calcd for $C_{14}H_{11}D$: 182.1; Found: 182.1.

(c) LCMS (ESI) m/z of **10-d^2:** [M+H]$^+$ Calcd for $C_{14}H_{10}D_2$: 183.1; Found: 183.1.
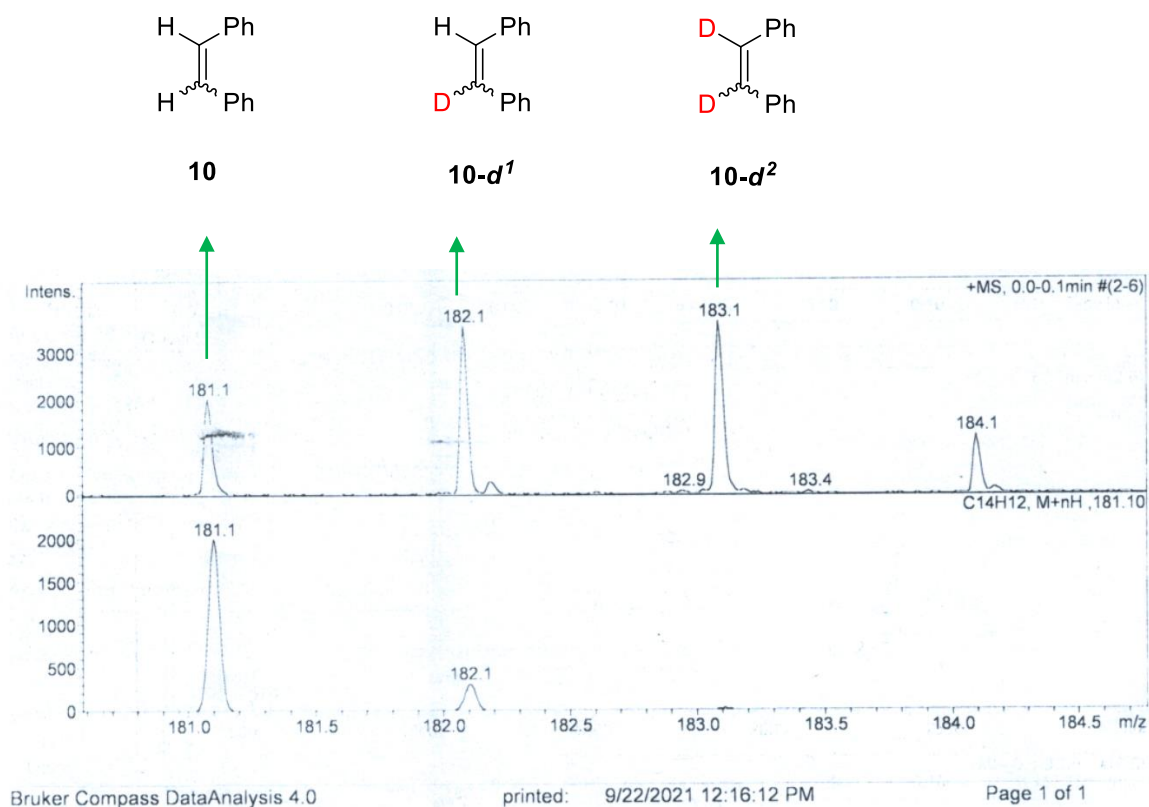
4.5.7 DDQ oxidation of 3ba:[16]
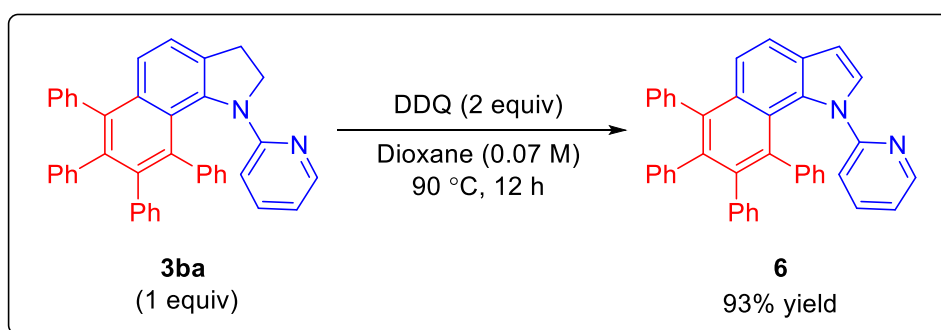
To an oven dried sealed tube charged with a stirring bar under N_2 atmosphere, the compound **3ba** (55 mg, 1 equiv, 0.1 mmol), DDQ (50 mg, 2 equiv, 0.22 mmol) were added followed by addition of 1,4-dioxane (0.07 M, 1.6 mL) solvent. The reaction mixture was vigorously stirred at 90 °C on preheated aluminium block for the 12 h. After 12 h (upon completion of reaction as monitored by TLC analysis), the reaction mixture was cooled to room temperature and diluted with EtOAc. The solvent was evaporated under reduced pressure and the residue was purified by column chromatography using EtOAc/hexane mixture on silica gel to give the pure product **6** (51 mg, 93% yield).

4.5.8 Directing group removal of 6:[17]
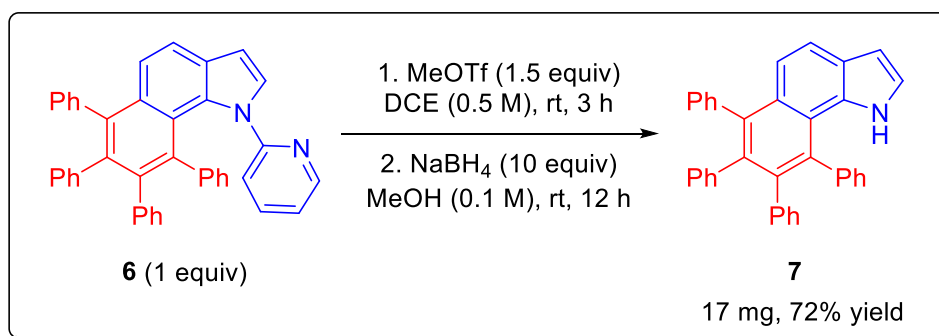
To an oven dried sealed tube charged with a stirring bar under N_2 atmosphere, the compound **6** (26 mg, 0.05 mmol, 1 equiv) was added followed by addition of DCE (0.5 M, 0.1 mL) solvent. The reaction mixture was cooled to 0 °C and then MeOTf (9 µL, 0.07 mmol, 1.5 equiv) was added to the reaction mixture over 1 min under cold condition. Then the reaction mixture was stirred for 3 h at rt. After 3 h, MeOH (0.1 M, 0.5 mL), $NaBH_4$ (19 mg, 0.5 mmol, 10 equiv) were added to the reaction mixture at 0 °C, which was further stirred for 12 h at rt. The resulting mixture was quenched with saturated aqueous NH_4Cl (2 mL) solution and concentrated in vacuum. The aqueous layer was extracted with EtOAc (5 mL) and the organic layer was dried on anhydrous $MgSO_4$ and concentrated in vacuum. The residue was purified by column chromatography using EtOAc/hexane mixture on silica gel to give the pure product **7** (17 mg, 72% yield).

4.5.9 Further annulation of compound 6:

To an oven dried sealed tube charged with a stirring bar under N_2 atmosphere, tetraphenyl-1-(pyridin-2-yl)-1H-benzo[g]indole **6** (0.1 mmol), diphenylacetylene **2a** (4 equiv), PPh_3 (20 mol %), NaI (50 mol %), were added and sealed. The sealed tube was high-vacuumed and refilled with N_2. Then $Ni(OTf)_2$ (10 mol %) and degassed toluene solvent (0.2 M) were added to the reaction mixture inside the glove box. Then the sealed tube was taken out of the glove box and reaction mixture was vigorously stirred at 140 °C on preheated

aluminium block for 24 h. After 24 h, we didn't observe formation of the product (even upon keeping for longer time and on higher temperature).
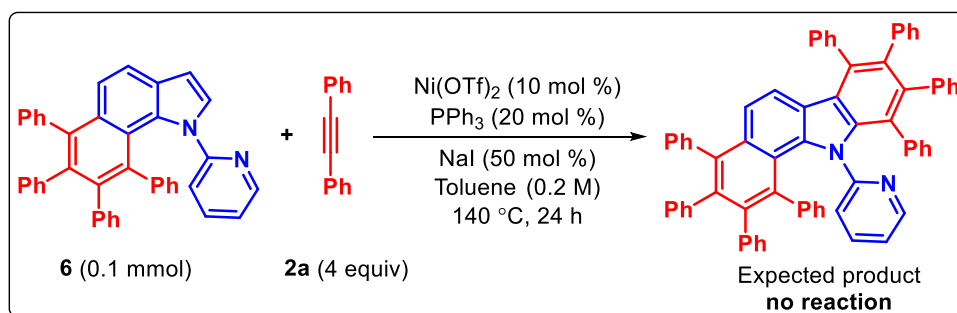

For the further confirmation, the reaction mixture was cooled to room temperature and diluted with EtOAc or DCM and passed through a short celite pad. The solvent was evaporated under reduced pressure and the residue was purified by column chromatography using EtOAc/hexane mixture on silica gel, where we have recovered 92% starting material **6**.

4.5.10 Unsuccessful coupling partners:

4.5.11 Experimental characterization data of products:

6,7,8,9-tetraphenyl-1-(pyrimidin-2-yl)-2,3-dihydro-1H-benzo[g]indole (3aa):
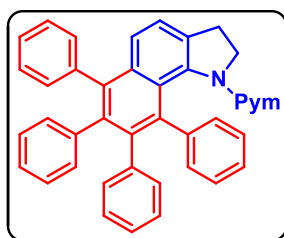
Physical State: green solid (45 mg for 0.10 mmol scale, 82% yield). m.p.: 108-112 °C. R_f-value: 0.3 (10% EtOAc/hexane). ^{1}H NMR (CDCl$_3$, 400 MHz): δ 8.01 (br, 2H), 7.48 (d, J = 7.6 Hz, 1H), 7.42-7.40 (m, 1H), 7.35-7.28 (m, 2H), 7.18-7.09 (m, 4H), 7.02-6.99 (m, 2H), 6.93-6.77 (m, 6H), 6.72 (q, J = 6.8 Hz, 2H), 6.57 (d, J = 7.2 Hz, 1H), 6.48 (t, J = 4.8 Hz, 1H), 6.42 (d, J = 7.6 Hz, 1H), 6.33 (t, J = 7.6 Hz, 1H), 6.09 (d, J = 8.0 Hz, 1H), 4.53-4.49 (m, 1H), 4.09-4.01 (m, 1H), 3.40-3.31 (m, 1H), 2.93-2.87 (m, 1H). ^{13}C{^{1}H} NMR (CDCl$_3$, 100 MHz): δ 161.7, 157.6, 156.8, 141.2, 140.9, 140.7, 140.1, 139.7,

139.3, 138.9, 138.6, 136.3, 133.4, 133.1, 132.5, 132.1, 131.9, 131.7, 131.6 (2C), 131.5, 127.9, 127.5, 126.7 (2C), 126.6 (2C), 126.5, 125.9, 125.6, 125.4, 125.3, 124.2, 124.0, 122.7, 112.6, 53.7, 30.6. IR (KBr, cm^{-1}): 3439, 3053, 2984, 1601, 1264. HRMS (ESI) m/z: [M+H]$^+$ Calcd for C$_{40}$H$_{30}$N$_3$: 552.2434; Found: 552.2414.

**6,7,8,9-tetraphenyl-1-(pyridin-2-yl)-2,3-dihydro-1H-benzo[g]indole (3ba)**:
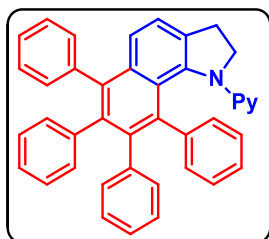
Physical State: yellow solid (51 mg for 0.10 mmol scale, 93% yield). m.p.: 126-130 °C. R$_f$ -value: 0.4 (10% EtOAc/hexane). ^{1}H NMR (CDCl$_3$, 400 MHz): δ 7.82 (d, J = 4.8 Hz, 1H), 7.44 (d, J = 7.6 Hz, 1H), 7.38-7.30 (m, 3H), 7.19-7.11 (m, 5H), 7.01 (d, J = 8.8 Hz, 2H), 6.92 (d, J = 7.6 Hz, 1H), 6.83-6.69 (m, 7H), 6.58-6.53 (m, 2H), 6.42 (d, J = 7.6 Hz, 1H), 6.23 (t, J = 7.6 Hz, 2H), 5.94 (d, J = 7.6 Hz, 1H), 4.32-4.27 (m, 1H), 4.13-4.05 (m, 1H), 3.37-3.28 (m, 1H), 2.89 (q, J = 8.4 Hz, 1H). ^{13}C{^{1}H} NMR (CDCl$_3$, 100 MHz): δ 147.4, 141.1, 140.8, 140.7, 140.2, 139.2, 138.8, 138.7, 136.2, 136.1, 136.0, 133.7, 133.4, 132.1, 131.9, 131.8, 131.7, 131.6, 131.5, 128.0, 127.6, 126.8, 126.7, 126.5, 125.8, 125.7, 125.5, 125.3, 124.5, 124.0, 123.2, 115.3, 111.7, 54.8, 30.4. IR (KBr, cm^{-1}): 3440, 3053, 2986, 1652, 1260. HRMS (ESI) m/z: [M+K]$^+$ Calcd for C$_{41}$H$_{30}$N$_2$K: 589.2046; Found: 589.2053.

1-(5-methylpyrimidin-2-yl)-6,7,8,9-tetraphenyl-2,3-dihydro-1H-benzo[g]indole (3ca):
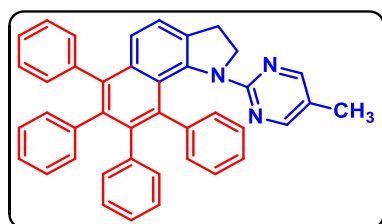
Physical State: yellow solid (17 mg for 0.10 mmol scale, 30% yield). m.p.: 115-120 °C. R$_f$ -value: 0.3 (30% EtOAc/hexane). ^{1}H NMR (CDCl$_3$, 400 MHz): δ 7.87 (s, 2H), 7.48 (d, J = 7.6 Hz, 1H), 7.40-7.28 (m, 3H), 7.18-7.10 (m, 4H), 7.02-6.99 (m, 2H), 6.93-6.76 (m, 6H), 6.75-6.69 (m, 2H), 6.56 (d, J = 7.6 Hz, 1H), 6.42 (d, J = 7.6 Hz, 1H), 6.28 (t, J = 7.6 Hz, 1H), 6.06 (d, J = 7.6 Hz, 1H), 4.47-4.42 (m, 1H), 4.10-4.02 (m, 1H), 3.40-3.31 (m, 1H), 2.92-2.86 (m, 1H), 2.07 (s, 3H). ^{13}C{^{1}H} NMR (CDCl$_3$, 100 MHz): δ 160.7, 157.4, 156.9, 141.3, 141.0, 140.9, 140.8, 140.6 (2C),

139.6, 139.4, 139.0, 138.6, 136.4, 133.5, 133.0, 132.6, 132.2, 132.0, 131.9, 131.8, 131.7, 131.5, 127.9, 127.5, 126.9, 126.7 (2C), 126.6, 126.5, 126.4, 125.8, 125.6, 125.5, 125.4, 125.2, 125.15, 124.2, 123.9, 122.8, 121.3, 54.1, 30.6, 15.1. IR (KBr, cm^{-1}): 3440, 3054, 2923, 2359, 1636, 1381. HRMS (ESI) m/z: [M+H]$^+$ Calcd for $C_{41}H_{32}N_3$: 566.2591; Found: 566.2567.

2-methyl-6,7,8,9-tetraphenyl-1-(pyridin-2-yl)-2,3-dihydro-1H-benzo[g]indole (3fa):
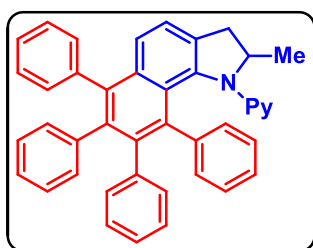
Physical State: yellow solid (35 mg for 0.10 mmol scale, 62% yield). m.p.: 165–174 °C. R$_f$-value: 0.2 (5% EtOAc/hexane). ^{1}H NMR (CDCl$_3$, 400 MHz): δ 7.85 (dd, J_1 = 4.8 Hz, J_2 = 1.6 Hz, 1H), 7.46 (d, J = 7.6 Hz, 1H), 7.40-7.30 (m, 3H), 7.19-7.07 (m, 5H), 7.01 (t, J = 8.0 Hz, 2H), 6.92-6.89 (m, 1H), 6.85-6.68 (m, 7H), 6.58-6.54 (m, 2H), 6.42 (d, J = 7.6 Hz, 1H), 6.22 (t, J = 7.6 Hz, 1H), 6.16 (d, J = 8.0 Hz, 1H), 5.94 (d, J = 8.0 Hz, 1H), 4.51 (br, 1H), 3.49 (q, J = 8.0 Hz, 1H), 2.52 (d, J = 15.6 Hz, 1H), 1.42 (d, J = 6.8 Hz, 3H). ^{13}C{^{1}H} NMR (CDCl$_3$, 100 MHz): δ 159.3, 147.4, 141.2, 140.9, 140.8, 140.3, 139.9, 139.2, 138.7, 138.6, 136.3, 133.8, 133.3, 132.3, 132.2, 131.9, 131.7, 131.6 (2C), 131.5, 127.9, 127.5, 126.8, 126.6, 126.4, 125.9, 125.5, 125.4, 125.2, 124.6, 123.94, 123.9, 123.7, 115.7, 111.5, 63.3, 37.6, 22.1. IR (KBr, cm^{-1}): 3440, 2077, 1636, 1600, 1264. HRMS (ESI) m/z: [M+H]$^+$ Calcd for $C_{42}H_{33}N_2$: 565.2638; Found: 565.2614.

4-fluoro-6,7,8,9-tetraphenyl-1-(pyridin-2-yl)-2,3-dihydro-1H-benzo[g]indole (3ga):
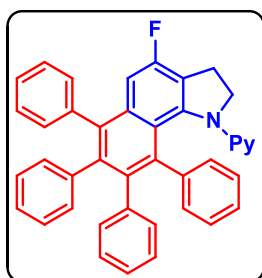
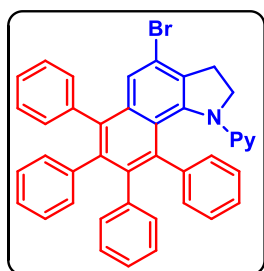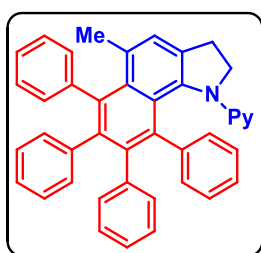Physical State: yellow solid (48 mg for 0.10 mmol scale, 84% yield). m.p.: 200–210 °C. R$_f$-value: 0.3 (20% EtOAc/hexane). ^{1}H NMR (CDCl$_3$, 400 MHz): δ 7.86-7.84 (m, 1H), 7.43 (d, J = 7.6 Hz, 1H), 7.32 (dt, J_1 = 7.6 Hz, J_2 = 1.2 Hz, 1H), 7.20-7.11 (m, 5H), 7.01-6.99 (m, 3H), 6.91 (dt, J_1 = 7.6 Hz, J_2 = 1.2 Hz, 1H), 6.82-

6.69 (m, 7H), 6.60-6.55 (m, 2H), 6.40 (dd, J_1 = 7.6 Hz, J_2 = 1.2 Hz, 1H), 6.24-6.18 (m, 2H), 5.91 (d, J = 8.0 Hz, 1H), 4.29-4.25 (m, 1H), 4.19-4.11 (m, 1H), 3.33-3.24 (m, 1H), 3.03-2.96 (m, 1H). $^{13}C\{^1H\}$ NMR (CDCl$_3$, 100 MHz): δ 158.9, 158.0 (d, J_{C-F} = 243.3 Hz), 147.5, 144.8 (d, J_{C-F} = 8.0 Hz), 141.0, 140.6, 140.3, 139.7, 139.4 (d, J_{C-F} = 2.0 Hz), 138.7 (2C), 138.6, 136.4 (2C), 135.05 (d, J_{C-F} = 8.0 Hz), 132.2, 132.1, 131.7 (2C), 131.6, 131.4 (3C), 128.1, 127.8, 126.9, 126.8, 126.7, 126.5, 125.9, 125.7, 125.6, 125.4, 124.3, 121.8 (d, J_{C-F} = 23.0 Hz), 120.4 (d, J_{C-F} = 1.0 Hz), 116.1, 112.1, 107.7 (d, J_{C-F} = 21.0 Hz), 55.4, 26.7. ^{19}F NMR (CDCl$_3$, 376 MHz): δ -118.9. IR (KBr, cm^{-1}): 3442, 2099, 1626, 1264, 1027, 737. HRMS (ESI) m/z: [M+K]$^+$ Calcd for C$_{41}$H$_{29}$FN$_2$K: 607.1952; Found: 607.1954.

4-chloro-6,7,8,9-tetraphenyl-1-(pyridin-2-yl)-2,3-dihydro-1H-benzo[g]indole (3ha):
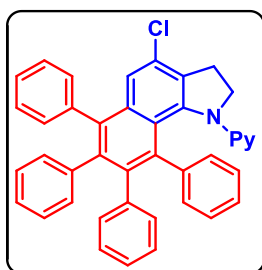
Physical State: yellow solid (52 mg for 0.10 mmol scale, 89% yield). m.p.: 175-180 °C. R$_f$-value: 0.2 (10% EtOAc/hexane). ^1H NMR (CDCl$_3$, 400 MHz): δ 7.85-7.83 (m, 1H), 7.42 (d, J = 8.0 Hz, 1H), 7.35-7.31 (m, 2H), 7.18 (tt, J_1 = 7.6 Hz, J_2 = 1.2 Hz, 1H), 7.15-7.11 (m, 4H), 7.00-6.97 (m, 2H), 6.91 (t, J = 7.6 Hz, 1H), 6.82-6.68 (m, 7H), 6.60-6.54 (m, 2H), 6.40-6.38 (m, 1H), 6.22 (t, J = 7.6 Hz, 1H), 6.17 (d, J = 8.4 Hz, 1H), 5.91-5.88 (m, 1H), 4.25-4.10 (m, 2H), 3.36-3.27 (m, 1H), 3.05-2.98 (m, 1H). $^{13}C\{^1H\}$ NMR (CDCl$_3$, 100 MHz): δ 158.8, 147.4, 143.1, 140.9, 140.5, 140.3, 140.0, 139.7, 138.6, 138.5, 136.5, 136.3, 134.8, 132.0 (2C), 131.8, 131.7, 131.6, 131.4, 129.4, 128.1, 127.8, 126.9, 126.8, 126.7, 126.5, 125.9, 125.8, 125.6, 125.4, 124.3, 122.7, 121.7, 116.0, 112.0, 54.6, 29.9. IR (KBr, cm^{-1}): 3441, 3090, 2376, 1634, 1323, 700. HRMS (ESI) m/z: [M+H]$^+$ Calcd for C$_{41}$H$_{30}$ClN$_2$: 585.2092; Found: 585.2108.

4-bromo-6,7,8,9-tetraphenyl-1-(pyridin-2-yl)-2,3-dihydro-1H-benzo[g]indole (3ia):

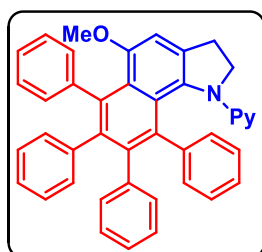Physical State: yellow solid (54 mg for 0.10 mmol scale, 86% yield). m.p.: 170-180 °C. R_f-value: 0.3 (10% EtOAc/hexane). ^{1}H NMR (CDCl$_3$, 400 MHz): δ 7.84 (d, J = 4.8 Hz, 1H), 7.50 (s, 1H), 7.42 (d, J = 7.6 Hz, 1H), 7.33 (t, J = 7.6 Hz, 1H), 7.20-7.11 (m, 5H), 6.99-6.96 (m, 2H), 6.91 (t, J = 7.6 Hz, 1H), 6.82-6.68 (m, 7H), 6.59-6.53 (m, 2H), 6.38 (d, J = 7.6 Hz, 1H), 6.22 (t, J = 7.6 Hz, 1H), 6.16 (d, J = 8.0 Hz, 1H), 5.88 (d, J = 8.0 Hz, 1H), 4.23-4.08 (m, 2H), 3.36-3.26 (m, 1H), 3.03-2.96 (m, 1H). ^{13}C{^{1}H} NMR (CDCl$_3$, 176 MHz): δ 158.8, 147.5, 142.6, 141.2, 140.8, 140.6, 140.5, 140.4, 140.0, 139.9, 139.7, 139.6, 138.6, 138.4, 138.2, 136.9, 136.5, 136.4 (2C), 136.3, 135.4, 135.1, 132.6, 132.0 (2C), 131.9 (2C), 131.8, 131.7, 131.6, 131.5 (2C), 131.4 (2C), 128.1 (2C), 127.8, 127.7, 126.9, 126.8, 126.7, 126.5, 125.9 (2C), 125.8, 125.6, 125.4, 124.3, 122.5, 122.0, 118.4, 116.0 (2C), 111.8, 111.7, 91.7, 35.6, 31.9. IR (KBr, cm^{-1}): 3439, 3053, 2928, 1601, 1264, 895, 738. HRMS (ESI) m/z: [M+H]$^+$ Calcd for C$_{41}$H$_{30}$BrN$_2$: 629.1587; Found: 629.2319.

5-methyl-6,7,8,9-tetraphenyl-1-(pyridin-2-yl)-2,3-dihydro-1H-benzo[g]indole (3ja):

Physical State: brown solid (44 mg for 0.10 mmol scale, 78% yield). m.p.: 140–142 °C. R_f-value: 0.4 (10% EtOAc/hexane). ^{1}H NMR (CDCl$_3$, 400 MHz): δ 7.83 (d, J = 4.0 Hz, 1H), 7.24-7.22 (m, 2H), 7.20-7.07 (m, 4H), 7.02-6.96 (m, 2H), 6.88-6.70 (m, 10H), 6.60 (d, J = 7.6 Hz, 1H), 6.54 (t, J = 6.0 Hz, 1H), 6.39 (d, J = 7.6 Hz, 1H), 6.25 (t, J = 7.2 Hz, 2H), 5.91 (d, J = 8.0 Hz, 1H), 4.35 (d, J = 10.0 Hz, 1H), 4.03 (q, J = 11.2 Hz, 1H), 3.34-3.25 (m, 1H), 2.91-2.85 (m, 1H), 1.91 (s, 3H). ^{13}C{^{1}H} NMR (CDCl$_3$, 100 MHz): δ 147.4, 143.3, 141.2, 140.8, 139.9, 139.6, 139.3, 139.1, 138.6, 136.2, 136.1, 132.8, 132.5, 132.3, 132.1, 132.0, 131.9, 131.7, 131.6, 131.5, 127.8, 127.2, 126.7, 126.6, 126.5, 126.4

(2C), 125.9, 125.8, 125.2, 124.7, 124.3, 117.2, 114.8, 110.7, 53.9, 30.3, 25.6. IR (KBr, cm^{-1}): 3441, 3021, 2084, 1635, 1329, 1216. HRMS (ESI) m/z: [M+Na]$^+$ Calcd for C$_{42}$H$_{32}$N$_2$Na: 587.2463; Found: 587.2451.

5-methoxy-6,7,8,9-tetraphenyl-1-(pyridin-2-yl)-2,3-dihydro-1H-benzo[g]indole (3ka):

Physical State: yellow liquid (55 mg for 0.10 mmol scale, 95% yield. R$_f$-value: 0.5 (10% EtOAc/hexane). ^{1}H NMR (CDCl$_3$, 400 MHz): δ 7.82 (d, J = 4.0 Hz, 1H), 7.25-7.23 (m, 1H), 7.18-7.10 (m, 4H), 7.02-6.95 (m, 2H), 6.93-6.89 (m, 2H), 6.86-6.68 (m, 9H), 6.56 (d, J = 7.2 Hz, 1H), 6.52 (t, J = 6.0 Hz, 1H), 6.39 (d, J = 6.0 Hz, 1H), 6.25-6.17 (m, 2H), 5.93 (d, J = 8.0 Hz, 1H), 4.34 (t, J = 8.6 Hz, 1H), 4.03-3.95 (m, 1H), 3.35 (s, 3H), 3.33-3.26 (m, 1H), 2.84 (q, J = 8.8 Hz, 1H). ^{13}C{^{1}H} NMR (CDCl$_3$, 100 MHz): δ 155.2, 144.4, 141.0, 140.8, 140.6, 139.4, 138.9, 137.3, 136.3, 135.7, 133.7, 132.0, 131.9, 131.8, 131.4, 130.3, 129.9, 126.6 (2C), 126.4 (2C), 126.3, 125.8, 125.2 (2C), 125.1, 125.0, 124.4, 124.1, 114.7, 111.1, 106.0, 56.7, 54.3, 31.2. IR (KBr, cm^{-1}): 3445, 3054, 2365, 1590, 1382. HRMS (ESI) m/z: [M+Na]$^+$ Calcd for C$_{42}$H$_{32}$N$_2$ONa: 603.2412; Found: 603.2390.

6,7,8,9-tetraethyl-1-(pyridin-2-yl)-2,3-dihydro-1H-benzo[g] indole (3bb):
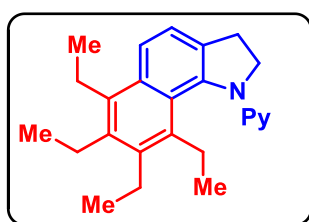
Physical State: colorless liquid (31 mg for 0.10 mmol scale, 86% yield). R$_f$-value: 0.5 (10% EtOAc/hexane). ^{1}H NMR (CDCl$_3$, 400 MHz): δ 8.30 (d, J = 3.6 Hz, 1H), 7.85 (d, J = 8.4 Hz, 1H), 7.38 (d, J = 8.4 Hz, 1H), 7.18-7.14 (m, 1H), 6.67 (t, J = 6.8 Hz, 1H), 6.06 (d, J = 8.4 Hz, 1H), 5.09-5.04 (m, 1H), 4.27-4.19 (m, 1H), 3.30-3.21 (m, 1H), 3.15-3.09 (m, 2H), 3.06-2.99 (m, 1H), 2.90-2.74 (m, 5H), 2.69-2.60 (m, 1H), 1.34 (t, J = 7.6 Hz, 3H), 1.29 (t, J = 7.6 Hz, 3H), 1.16 (t, J = 7.6 Hz, 3H), 0.87 (t, J = 7.6 Hz, 3H). ^{13}C{^{1}H} NMR (CDCl$_3$, 100 MHz): δ 161.2, 148.3, 141.5, 139.8, 137.5, 137.0, 135.9, 135.8, 132.6, 132.2, 124.5, 122.1, 121.9, 115.3, 109.8, 54.5, 30.2, 23.4, 22.8, 22.7, 22.4,

16.8, 16.7, 16.0 (2C). IR (KBr, cm^{-1}): 3420, 2964, 1589, 1375. HRMS (ESI) m/z: [M+H]$^+$ Calcd for C$_{25}$H$_{31}$N$_2$: 359.2482; Found: 359.2487.

6,7,8,9-tetrapropyl-1-(pyridin-2-yl)-2,3-dihydro-1H-benzo[g] indole (3bc):
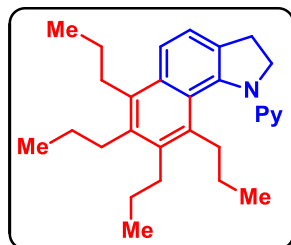
Physical State: yellow liquid (33 mg for 0.10 mmol scale, 80% yield). R$_f$-value: 0.6 (10% EtOAc/hexane). ^{1}H NMR (CDCl$_3$, 400 MHz): δ 8.30 (d, J = 4.4 Hz, 1H), 7.79 (d, J = 8.4 Hz, 1H), 7.35 (d, J = 8.4 Hz, 1H), 7.18-7.14 (m, 1H), 6.67 (t, J = 6.0 Hz, 1H), 6.06 (d, J = 8.4 Hz, 1H), 5.10-5.05 (m, 1H), 4.23-4.15 (m, 1H), 3.30-3.21 (m, 1H), 3.07-2.92 (m, 3H), 2.89-2.83 (m, 1H), 2.77-2.64 (m, 4H), 2.58-2.50 (m, 1H), 1.76-1.60 (m, 4H), 1.57-1.44 (m, 2H), 1.40-1.20 (m, 2H), 1.15-1.09 (m, 6H), 1.01 (t, J = 7.2 Hz, 3H), 0.74 (t, J = 7.2 Hz, 3H). ^{13}C{^{1}H} NMR (CDCl$_3$, 100 MHz): δ 161.1, 148.3, 141.6, 138.8, 136.9, 136.6, 134.7, 134.3, 132.4, 132.3, 124.9, 122.1, 121.7, 115.2, 109.7, 54.4, 33.3, 32.5, 32.3, 31.6, 30.2, 25.8, 25.7, 25.1, 25.0, 15.4, 15.3, 15.2, 14.7. IR (KBr, cm^{-1}): 3441, 2955, 2928, 1653, 1589, 1374. HRMS (ESI) m/z: [M+H]$^+$ Calcd for C$_{29}$H$_{39}$N$_2$: 415.3108; Found: 415.3115.

1-(pyridin-2-yl)-6,7,8,9-tetra-p-tolyl-2,3-dihydro-1H-benzo [g]indole (3bd):
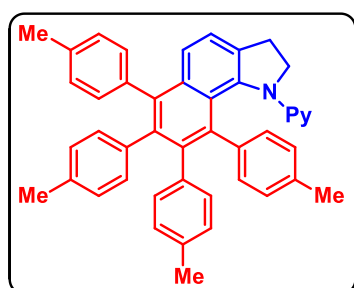

Physical State: pale white solid (40 mg for 0.10 mmol scale, 66% yield). m.p.: 264–266 °C, R$_f$ -value: 0.3 (10% EtOAc/hexane). ^{1}H NMR (CDCl$_3$, 400 MHz): δ 7.81 (dd, J = 5.2 Hz, J = 1.2 Hz, 1H), 7.31-7.25 (m, 3H), 7.12-7.05 (m, 2H), 6.99 (dd, J = 7.6 Hz, J = 1.6 Hz, 1H), 6.94-6.85 (m, 4H), 6.73-6.67 (m, 2H), 6.62 (d, J = 8.0 Hz, 1H), 6.83-6.49 (m, 3H), 6.43 (d, J = 7.6 Hz, 1H), 6.28 (dd, J = 7.6 Hz, J = 1.6 Hz, 1H), 6.19 (d, J = 8.4 Hz, 1H), 6.00 (d, J = 7.2 Hz, 1H), 5.80 (dd, J = 7.6 Hz, J = 1.6 Hz, 1H), 429 (t, J = 10.0 Hz, 1H), 4.13-4.03 (m, 1H), 3.35-3.25 (m, 1H), 2.86 (q, J = 8.4 Hz, 1H), 2.30 (s, 3H), 2.11 (s, 3H), 2.09 (s, 3H), 2.07

(s, 3H). $^{13}C\{^1H\}$ NMR (CDCl$_3$, 100 MHz): δ 139.1, 138.9, 138.2, 137.8, 135.8, 135.6, 134.5, 134.4, 134.0, 133.8, 133.0, 132.2, 131.9, 131.8, 131.5, 131.4, 131.3, 131.3, 131.2, 128.7, 128.2, 127.5, 127.4, 127.1, 126.5, 124.6, 123.2, 122.8, 115.0, 54.9, 30.3, 21.5, 21.5, 21.4, 21.3. IR (KBr, cm^{-1}): 3438, 3053, 2923, 2351, 1642, 1434. HRMS (ESI) m/z: [M+H]$^+$ Calcd for C$_{45}$H$_{39}$N$_2$: 607.3108; Found: 607.3092.

6,7,8,9-tetrakis(4-fluorophenyl)-1-(pyridin-2-yl)-2,3-dihydro-1H-benzo[g]indole (3bf):
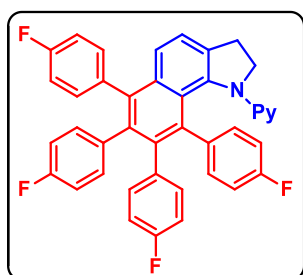
Physical State: yellow solid (48 mg for 0.10 mmol scale, 77% yield). m.p.: 160-170 °C. R$_f$-value: 0.3 (5% EtOAc/hexane). ^{1}H NMR (CDCl$_3$, 400 MHz): δ 7.87 (d, J = 4.4 Hz, 1H), 7.40-7.30 (m, 3H), 7.17-7.01 (m, 3H), 6.93-6.82 (m, 4H), 6.75-6.72 (m, 1H), 6.66 (t, J = 8.4 Hz, 1H), 6.61-6.45 (m, 5H), 6.33 (t, J = 6.4 Hz, 1H), 6.18 (d, J = 8.4 Hz, 1H), 5.97-5.93 (m, 1H), 5.88-5.85 (m, 1H), 4.22-4.10 (m, 2H), 3.41-3.31 (m, 1H), 2.94-2.88 (m, 1H). $^{13}C\{^1H\}$ NMR (CDCl$_3$, 100 MHz): δ 162.2, (d, J_{C-F} = 121.4 Hz), 161.7 (d, J_{C-F} = 3.5 Hz), 160.8 (d, J_{C-F} = 121.4 Hz), 160.3 (d, J_{C-F} = 3.5 Hz), 147.1, 141.3, 141.2 (d, J_{C-F} = 1.8 Hz), 139.3, 138.8, 137.9, 136.8 (d, J_{C-F} = 3.5 Hz), 136.7, 136.4 (d, J_{C-F} = 3.5 Hz), 136.25 (d, J_{C-F} = 3.5 Hz), 135.6, 134.5 (d, J_{C-F} = 1.8 Hz), 133.8, 133.5, 133.4, 133.3, 133.2 (2C), 133.1, 133.05, 133.0 (d, J_{C-F} = 3.5 Hz), 132.9 (2C), 132.8 (3C), 131.9, 128.6 (d, J_{C-F} = 14.1 Hz), 124.5, 123.7, 123.3, 115.8, 115.3, 115.1, 114.9, 114.8, 114.3, 114.2, 114.1, 114.0, 113.9, 112.9 (d, J_{C-F} = 22.9 Hz), 112.1, 111.2 (d, J_{C-F} = 22.9 Hz), 55.4, 30.4. ^{19}F NMR (CDCl$_3$, 376 MHz): δ -115.6, -116.7, -116.9. IR (KBr, cm^{-1}): 3430, 3045, 2926, 1602, 1264, 1157, 1094. HRMS (ESI) m/z: [M+H]$^+$ Calcd for C$_{41}$H$_{27}$F$_4$N$_2$: 623.2105; Found: 623.2056.

6,7,8,9-tetrakis(4-chlorophenyl)-1-(pyridin-2-yl)-2,3-dihydro-1H-benzo[g]indole

(3bg):
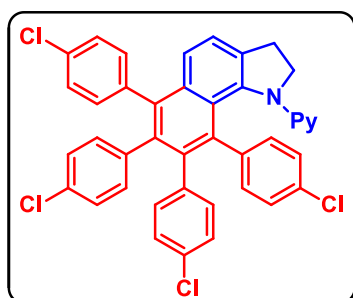
Physical State: yellow solid (42 mg for 0.10 mmol scale, 61% yield). m.p.: 200-210 °C. R_f -value: 0.4 (30% EtOAc/hexane). ^{1}H NMR (CDCl$_3$, 400 MHz): δ 7.86 (d, J = 3.6 Hz, 1H), 7.39-7.31 (m, 3H), 7.28-7.26 (m, 2H), 7.16-7.04 (m, 4H), 6.97-6.94 (m, 1H), 6.90-6.85 (m, 2H),

6.81-6.70 (m, 3H), 6.60 (dd, J_1 = 6.4 Hz, J_2 = 5.2 Hz, 1H), 6.46 (dd, J_1 = 8.4 Hz, J_2 = 2.0 Hz, 1H), 6.32 (dd, J_1 = 8.0 Hz, J_2 = 2.0 Hz, 1H), 6.21 (dd, J_1 = 8.4 Hz, J_2 = 2.0 Hz, 1H), 6.11 (d, J = 8.4 Hz, 1H), 5.81 (dd, J_1 = 8.4 Hz, J_2 = 2.0 Hz, 1H), 4.16-4.11 (m, 2H), 3.41-3.32 (m, 1H), 2.94-2.87 (m, 1H). ^{13}C{^{1}H} NMR (CDCl$_3$, 100 MHz): δ 159.1, 147.3, 141.5, 139.0, 138.7, 138.7, 138.6, 138.4, 137.1, 136.9, 136.5, 135.6, 133.8, 133.6, 133.2, 133.1, 133.0, 133.0, 132.9, 132.8, 132.6, 132.5, 132.0, 131.9, 128.6, 128.2, 127.6, 127.5, 127.4, 127.3, 126.0, 124.5, 124.3, 123.8, 123.2, 116.1, 112.3, 55.4, 30.4. IR (KBr, cm^{-1}): 3450, 2364, 2309, 1635, 1385, 736. HRMS (ESI) m/z: [M+H]$^+$ Calcd for C$_{41}$H$_{27}$Cl$_4$N$_2$: 687.0923; Found: 687.0896.

6,7,8,9-tetrakis(4-nitrophenyl)-1-(pyridin-2-yl)-2,3-dihydro 1H-benzo[g]indole (3bh):
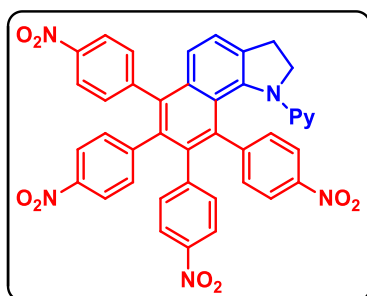
Physical State: yellow solid (54 mg for 0.10 mmol scale, 74% yield). m.p.: 295-300 °C. R_f -value: 0.35 (40% EtOAc/hexane). ^{1}H NMR (CDCl$_3$, 400 MHz): δ 8.26 (d, J = 8.4 Hz, 1H), 8.08-8.02 (m, 2H), 7.91-7.79 (m, 3H), 7.72-7.66 (m, 3H), 7.51 (d, J = 8.4 Hz ,1H), 7.38 (d, J = 8.4 Hz

,1H), 7.25-7.05 (m, 6H), 6.77-6.60 (m, 3H), 6.00 (d, J = 8.0 Hz ,2H), 4.23-4.15 (dd, J_1 = 10.8 Hz, J_2 = 10.4 Hz, 1H), 4.04 (br, 1H), 3.49-3.40 (m, 1H), 3.03-2.97 (dd, J_1 = 16.0 Hz, J_2 = 8.8 Hz, 1H). ^{13}C{^{1}H} NMR (CDCl$_3$, 100 MHz): δ 159.1, 147.4, 146.5, 146.4, 146.4,

146.2, 146.1, 145.0, 141.9, 138.4, 137.4, 136.4, 135.6, 135.3, 135.2, 133.0, 132.4, 132.4, 132.2, 132.1, 131.9, 131.8, 125.3, 124.1, 123.8, 123.5, 123.1, 123.0, 123.0, 122.8, 122.7, 121.3, 119.7, 117.0, 112.5, 55.9, 30.5. IR (KBr, cm^{-1}): 3440, 3056, 2690, 1635, 1522, 1348. HRMS (ESI) m/z: [M+H]$^+$ Calcd for $C_{41}H_{27}N_6O_8$: 731.1885; found: 731.1855.

**1,2,3,4-tetraphenyl-9-(pyrimidin-2-yl)-9H-carbazole (5aa):**
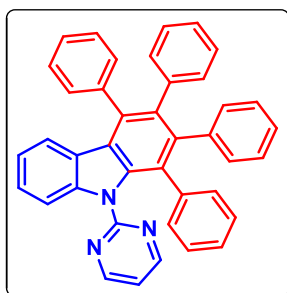
Physical State: brown solid (45 mg for 0.10 mmol scale, 82% yield). m.p.: 255–257 °C. R$_f$ -value: 0.4 (20% EtOAc/hexane). ^{1}H NMR (CDCl$_3$, 400 MHz): δ 8.30 (d, J = 4.8 Hz, 2H), 7.94 (d, J = 8.4 Hz, 1H), 7.33-7.26 (m, 6H), 6.99-6.94 (m, 3H), 6.86– 6.79 (m, 13H), 6.76 (t, J = 5.2 Hz, 1H), 6.71 (d, J = 7.6 Hz, 1H).

^{13}C{^{1}H} NMR (CDCl$_3$, 100 MHz): δ 152.1, 148.3, 142.5, 140.3, 140.1, 139.9, 139.6, 137.9, 137.0, 136.8, 136.2, 136.0, 134.5, 132.0, 131.7, 131.3, 130.5, 128.7 (2C), 128.7, 127.6, 127.5, 127.4, 126.9, 126.7, 126.1 (2C), 125.7 (2C), 125.2, 123.0, 122.6, 121.7, 119.8. IR (KBr, cm^{-1}): 3439, 2919, 1632, 1415. HRMS (ESI) m/z: [M+Na]$^+$ Calcd for $C_{40}H_{27}N_3Na$: 572.2097; Found: 572.2096.

1,2,3,4-tetraphenyl-9-(pyridin-2-yl)-9H-carbazole (5ba):
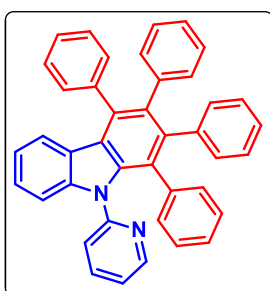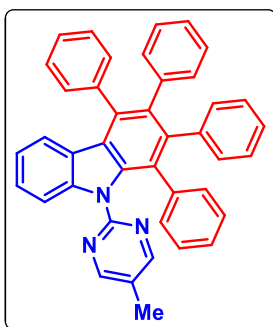

Physical State: brown solid (53 mg for 0.10 mmol scale, 96% yield). m.p.: 268–270 °C. R$_f$ -value: 0.5 (20% EtOAc/hexane). ^{1}H NMR (CDCl$_3$, 400 MHz): δ 8.28 (d, J = 4.0 Hz, 1H), 7.35–7.23 (m, 8H), 6.95-6.81 (m, 15H), 6.75-6.73 (m, 4H). ^{13}C{^{1}H} NMR (CDCl$_3$, 100 MHz): δ 151.9, 149.0, 143.1, 140.8, 140.6, 140.4, 140.1, 138.1, 137.7, 137.3, 135.9, 134.8, 132.1, 132.0, 131.6, 130.6, 128.3, 127.2, 127.1, 126.7 (2C), 126.2, 125.8, 125.4, 125.4, 125.0, 123.9, 123.2, 123.1, 122.7, 121.7, 120.6, 110.6. IR (KBr, cm^{-1}): 3445, 3053, 1588, 1274. HRMS (ESI) m/z: [M+Na]$^+$ Calcd for $C_{41}H_{28}N_2Na$: 571.2150; Found: 571.2167.

9-(5-methylpyrimidin-2-yl)-1,2,3,4-tetraphenyl-9H-carbazole (5ca):

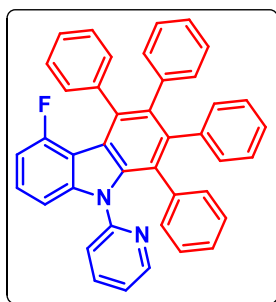Physical State: yellow solid (27 mg for 0.10 mmol scale, 48% yield). m.p.: 275-280 °C. R_f-value: 0.15 (5% EtOAc/hexane). ^{1}H NMR (CDCl$_3$, 400 MHz): δ 8.10 (s, 2H), 7.80 (d, J = 8.4 Hz, 1H), 7.34-7.24 (m, 6H), 6.97-6.92 (m, 3H), 6.87-6.78 (m, 13H), 6.73 (d, J = 8.0 Hz, 1H), 2.12 (s, 3H). ^{13}C{^{1}H} NMR (CDCl$_3$, 100 MHz): δ 157.8, 156.0, 142.1, 140.9, 140.6, 140.3, 140.0, 139.5, 137.6, 135.9 (2C), 135.9, 132.2, 132.1, 131.2, 130.7, 128.4, 127.3, 127.2, 126.9, 126.8, 126.4, 125.7, 125.5 (2C), 125.2, 124.8, 124.2, 122.7, 121.4, 111.3, 15.3. IR (KBr, cm^{-1}): 3444, 3054, 2986, 1634, 1264. HRMS (ESI) m/z: [M+H]$^+$ Calcd for C$_{41}$H$_{30}$N$_3$: 564.2434; Found: 564.2338.

5-methyl-1,2,3,4-tetraphenyl-9-(pyridin-2-yl)-9H-carbazole (5ea):
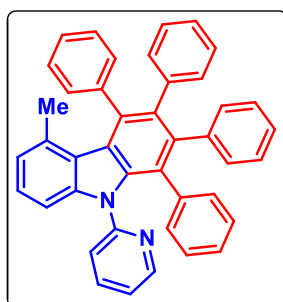
Physical State: yellow solid (37 mg for 0.10 mmol scale, 66% yield). Melting Point: 250-260 °C. R_f-value: 0.1 (5% EtOAc/hexane). ^{1}H NMR (CDCl$_3$, 400 MHz): δ 8.28 (d, J = 4.4 Hz, 1H), 7.34 (t, J = 7.6 Hz, 1H), 7.25 (br, 2H), 7.20 – 7.14 (m, 4H), 7.04 (d, J = 8.0 Hz, 1H), 6.96-6.91 (m, 2H), 6.86-6.82 (m, 6H), 6.77-6.73 (m, 10 H), 1.60 (s, 3H). ^{13}C{^{1}H} NMR (CDCl$_3$, 100 MHz): δ 152.3, 149.4, 144.3, 143.1, 141.5, 141.0, 140.0, 138.8, 138.3, 137.5, 135.8, 135.1, 134.6, 132.6, 132.3, 132.0, 131.8, 127.5, 127.1, 126.7, 126.65, 126.6, 126.2, 125.9, 125.3, 125.1, 124.8, 124.3, 124.2, 124.1, 122.8, 122.1, 108.1, 22.6. IR (KBr, cm^{-1}): 3440, 3053, 2986, 1635, 1273. HRMS (ESI) m/z: [M+H]$^+$ Calcd for C$_{42}$H$_{31}$N$_2$: 563.2482; Found: 563.2428.

5-fluoro-1,2,3,4-tetraphenyl-9-(pyridin-2-yl)-9H-carbazole (5fa):

Physical State: light yellow solid (55 mg for 0.10 mmol scale, 97% yield). Melting Point: 265-272 °C. R_f -value: 0.3 (20% EtOAc/hexane). ^{1}H NMR (CDCl$_3$, 400 MHz): δ 8.30 (d, J = 4.4 Hz, 1H), 7.34-7.17 (m, 6H), 7.00 (d, J = 8.0 Hz, 1H), 6.95 (t, J = 6.4 Hz, 1H), 6.91 (d, J = 8.0 Hz, 1H), 6.84-6.73 (m, 16H), 6.68 (dd, J_1 = 11.2 Hz, J_2 = 8.0 Hz, 1H). ^{13}C{^{1}H} NMR (CDCl$_3$, 176 MHz): δ 157.4 (d, J_{C-F} = 253.4 Hz), 151.9, 149.3, 145.6 (d, J_{C-F} = 8.8 Hz), 142.1 (d, J_{C-F} = 5.3 Hz), 141.1, 140.9 (2C), 140.7, 140.6, 137.9, 137.8, 137.6, 136.7, 135.9, 132.2, 131.9, 131.8, 131.1 (d, J_{C-F} = 3.5 Hz), 127.2 (2C), 127.1, 127.0, 126.9, 126.7 (2C), 126.5, 126.0, 125.5 (2C), 125.3, 124.9, 123.8, 122.4, 121.7 (d, J_{C-F} = 5.3 Hz), 111.7 (d, J_{C-F} = 19.4 Hz), 107.7 (d, J_{C-F} = 21.1 Hz), 106.5 (d, J_{C-F} = 3.5 Hz). ^{19}F NMR (CDCl$_3$, 376 MHz): δ -106.0. IR (KBr, cm^{-1}): 3440, 3053, 2986, 1436, 1273, 749. HRMS (ESI) m/z: [M+H]$^+$ Calcd for C$_{41}$H$_{28}$FN$_2$: 567.2231; Found: 567.2196.

5-chloro-1,2,3,4-tetraphenyl-9-(pyridin-2-yl)-9H-carbazole (5ga):
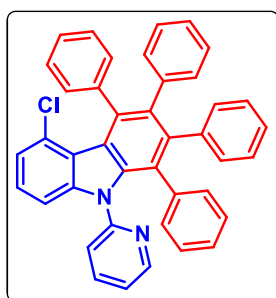
Physical State: yellow solid (37 mg for 0.10 mmol scale, 63% yield). m.p.: 250-255 °C. R_f -value: 0.3 (10% EtOAc/hexane). ^{1}H NMR (CDCl$_3$, 400 MHz): δ 8.30 (dd, J_1 = 5.2 Hz, J_2 = 1.2 Hz, 1H), 7.36-7.32 (m, 1H), 7.24-7.22 (m, 1H), 7.18-7.11 (m, 3H), 7.09-7.04 (m, 2H), 6.99-6.92 (m, 2H), 6.85-6.82 (m, 9H), 6.78-6.72 (m, 8H). ^{13}C{^{1}H} NMR (CDCl$_3$, 100 MHz): δ 151.9, 149.4, 145.3, 142.9, 141.3, 141.1, 140.9, 140.7, 140.6, 138.9, 138.0, 137.7, 136.6, 135.8, 132.3 (2C), 131.9, 131.7 (2C), 129.1, 127.4, 127.2, 126.9, 126.7, 126.6 (2C), 126.1, 125.5, 125.4, 125.2, 124.9, 124.3, 123.7, 122.5, 122.1, 121.5, 109.1. IR (KBr, cm^{-1}): 3440, 3053, 2986, 1635, 1261, 895. HRMS (ESI) m/z: [M+H]$^+$ Calcd for C$_{41}$H$_{28}$ClN$_2$: 583.1936; Found: 583.1933.

**6-methyl-1,2,3,4-tetraphenyl-9-(pyridin-2-yl)-9H-carbazole (5ha)**:
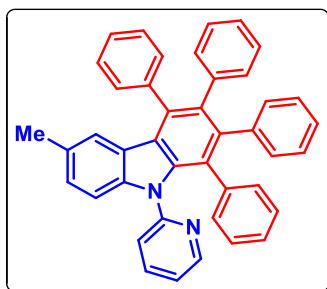
Physical State: pale white solid (40 mg for 0.10 mmol scale, 72% yield). m.p.: 243–245 °C. R_f -value: 0.5 (20% EtOAc/hexane). ^{1}H NMR (CDCl$_3$, 400 MHz): δ 8.25 (dd, J = 4.8 Hz, J = 1.2 Hz, 1H), 7.33-7.27 (m, 4H), 7.26-7.21 (m, 2H), 7.07 (dd, J = 8.4 Hz, J = 1.6 Hz, 1H), 6.90-6.81 (m, 15H), 6.74-6.73 (m, 3H), 6.49 (s, 1H), 2.20 (s, 3H). ^{13}C{^{1}H} NMR (CDCl$_3$, 100 MHz): δ 152.1, 148.9, 141.4, 140.9, 140.7, 140.5, 139.9, 138.3, 137.9, 137.2, 135.9, 134.6, 132.2, 132.1, 131.7, 131.6, 130.6, 129.8, 128.2, 127.4, 127.1, 127.0, 126.9, 126.7, 126.7, 125.8, 125.4, 125.3, 124.9, 124.0, 123.2, 123.0, 122.7, 121.5, 110.3, 21.8. IR (KBr, cm^{-1}): 3446, 2922, 1653, 1264, 698. HRMS (ESI) m/z: [M+Na]$^+$ Calcd for C$_{42}$H$_{30}$N$_2$Na: 585.2307; Found: 585.2288.

6-methoxy-1,2,3,4-tetraphenyl-9-(pyridin-2-yl)-9H-carbazole (5ia):
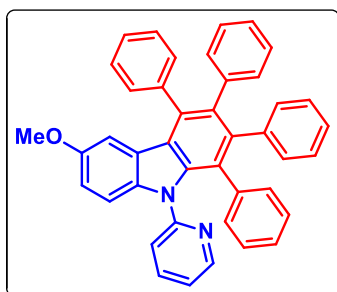
Physical State: brown solid (54 mg for 0.10 mmol scale, 93% yield). m.p.: 236–238 °C. R_f -value: 0.4 (20% EtOAc/hexane). ^{1}H NMR (CDCl$_3$, 400 MHz): δ 8.25 (dd, J = 4.8 Hz, J = 1.2 Hz, 1H), 7.38-7.31 (m, 4H), 7.28-7.22 (m, 3H), 6.92-6.81 (m, 15H), 6.75–6.72 (m, 3H), 6.17 (d, J = 2.4 Hz, 1H), 3.46 (s, 3H). ^{13}C{^{1}H} NMR (CDCl$_3$, 100 MHz): δ 154.3, 152.0, 148.9, 140.8, 140.6, 140.4, 140.0, 138.2, 138.1, 138.0, 137.2, 135.8, 134.5, 132.2, 132.1, 131.6, 130.8, 128.3, 127.2, 127.1, 126.8, 126.7, 125.9, 125.5, 125.1, 124.4, 123.2, 122.9, 121.5, 115.4, 111.5, 105.0, 55.5. IR (KBr, cm^{-1}): 3441, 3053, 3021, 1635, 1329, 1216. HRMS (ESI) m/z: [M+H]$^+$ Calcd for C$_{42}$H$_{31}$N$_2$O: 579.2431; Found: 579.2421.

6-fluoro-1,2,3,4-tetraphenyl-9-(pyridin-2-yl)-9H-carbazole (5ja):
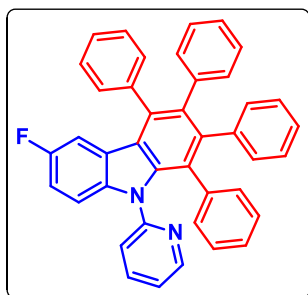
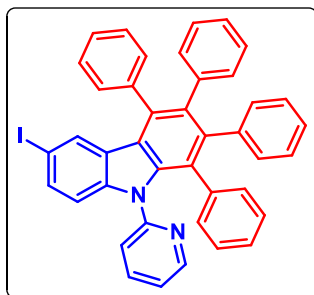Physical State: white solid (35 mg for 0.10 mmol scale, 62% yield). m.p.: 285-290 °C. R_f-value: 0.4 (20% EtOAc/hexane). ^{1}H NMR (CDCl$_3$, 400 MHz): δ 8.29 (d, J = 4.4 Hz, 1H), 7.32-7.25 (m, 7H), 7.01-6.74 (m, 18H), 6.40-6.37 (m, 1H). ^{13}C{^{1}H} NMR (CDCl$_3$, 100 MHz): δ 158.0 (d, J = 234.0 Hz), 151.8, 149.0, 140.8, 140.6, 140.4, 139.8, 139.4, 138.5, 137.9, 137.4, 136.1, 134.9, 132.1, 132.0, 131.5, 130.4, 128.5, 127.4, 127.3, 126.83, 126.8, 126.0, 125.5 (d, J = 3.0 Hz), 125.2, 124.5 (d, J = 10 Hz), 123.1, 122.8 (d, J = 3.0 Hz), 121.9, 113.9 (d, J = 25.0 Hz), 111.4 (d, J = 9.0 Hz), 108.4 (d, J = 25.0 Hz). ^{19}F NMR (CDCl$_3$, 376 MHz): δ -122.8. IR (KBr, cm^{-1}): 3440, 3054, 2986, 2305, 1635, 1261, 895. HRMS (ESI) m/z: [M+H]$^+$ Calcd for C$_{41}$H$_{28}$FN$_2$: 567.2231; Found: 567.2185.

6-bromo-1,2,3,4-tetraphenyl-9-(pyridin-2-yl)-9H-carbazole (5ka):
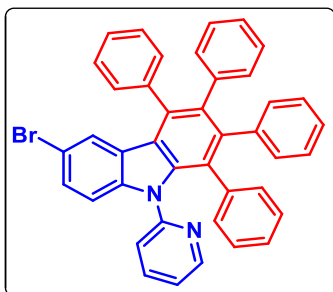
Physical State: light green solid (50 mg for 0.10 mmol scale, 80% yield). m.p.: 245-250 °C. R_f-value: 0.2 (5% EtOAc/hexane). ^{1}H NMR (CDCl$_3$, 400 MHz): δ 8.30 (dd, J_1 = 4.8 Hz, J_2 = 1.2 Hz, 1H), 7.33-7.28 (m, 3H), 7.22-7.17 (m, 4H), 7.00 (d, J = 8.4 Hz, 1H), 6.96-6.93 (m, 1H), 6.90 (d, J = 8.0 Hz, 1H), 6.86-6.73 (m, 15H), 6.71-6.66 (m, 1H). ^{13}C{^{1}H} NMR (CDCl$_3$, 100 MHz): δ 158.8, 156.3, 152.0, 149.3, 145.8, 145.7, 142.14, 142.1, 141.2, 140.9, 140.8, 138.0, 137.9, 137.6, 136.8, 135.9, 132.2, 131.9, 131.8, 131.14, 131.1, 127.2, 127.15, 127.1, 126.7, 126.68, 126.5, 126.0, 125.5, 125.3, 125.0, 123.9, 122.4, 121.8, 121.75, 111.9, 111.8, 107.8, 107.6, 106.6, 106.5. IR (KBr, cm^{-1}): 3441, 2084, 1636, 1383, 1329, 695. HRMS (ESI) m/z: [M+H]$^+$ Calcd for C$_{41}$H$_{28}$BrN$_2$: 627.1436; Found: 627.1414.

6-iodo-1,2,3,4-tetraphenyl-9-(pyridin-2-yl)-9H-carbazole (5la):

Physical State: brown solid (45 mg for 0.10 mmol scale, 67% yield). m.p.: 276–278 °C. R_f-value: 0.3 (20% EtOAc/hexane). ^{1}H NMR (CDCl$_3$, 400 MHz): δ 8.28 (dd, J = 5.2 Hz, J = 1.6 Hz, 1H), 7.49 (dd, J = 8.0 Hz, J = 2.0 Hz, 1H), 7.35-7.27 (m, 6H), 7.07 (d, J = 8.4 Hz, 1H), 6.97–7.92 (m, 2H), 6.88-6.80 (m, 13H), 6.76-6.73 (m, 3H). ^{13}C{^{1}H} NMR (CDCl$_3$, 100 MHz): δ 151.4, 149.0, 142.2, 140.9, 140.5, 140.3, 139.8, 137.8, 137.6, 137.4, 136.1, 135.1, 134.4, 132.0, 131.9, 131.6, 131.5, 130.3, 130.1, 128.5, 127.4, 127.2, 126.8, 126.7, 126.3, 126.0, 125.5, 125.1, 123.1, 122.1, 122.0, 112.7, 83.8. IR (KBr, cm^{-1}): 3440, 3054, 2923, 1599, 1380, 698. HRMS (ESI) m/z: [M+Na]$^+$ Calcd for C$_{41}$H$_{27}$IN$_2$Na: 697.1111; Found: 697.1116.

5,6,7,8-tetraphenyl-9-(pyridin-2-yl)-9H-carbazole-3-carbonitrile (5ma):
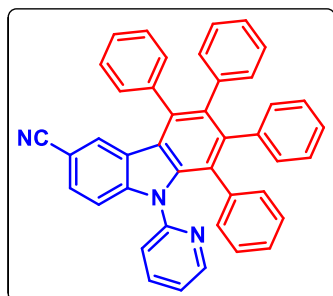
Physical State: brown solid (26 mg for 0.10 mmol scale, 46% yield). m.p.: 272–274 °C. R_f-value: 0.4 (20% EtOAc/hexane). ^{1}H NMR (CDCl$_3$, 400 MHz): δ 8.33-8.32 (m, 1H), 7.50-7.47 (m, 1H), 7.37-7.25 (m, 7H), 7.02-6.98 (m, 2H), 6.87-6.85 (m, 5H), 6.84-6.81 (m, 7H), 6.79-6.74 (m, 4H). ^{13}C{^{1}H} NMR (CDCl$_3$, 100 MHz): δ 150.9, 149.2, 144.7, 141.8, 140.2, 140.0, 139.4, 137.6, 137.4, 136.4, 136.0, 131.9, 131.8, 131.7, 131.5, 130.1, 129.4, 128.8, 127.9, 127.6, 127.3, 126.9, 126.9, 126.8, 126.2, 125.7, 125.5, 124.1, 123.4, 122.6, 121.9, 120.7, 111.5, 103.5. IR (KBr, cm^{-1}): 3441, 3055, 1601, 1383, 1299. HRMS (ESI) m/z: [M+H]$^+$ Calcd for C$_{42}$H$_{28}$N$_3$: 574.2278; Found: 574.2334.

7-chloro-1,2,3,4-tetraphenyl-9-(pyridin-2-yl)-9H-carbazole (5na):
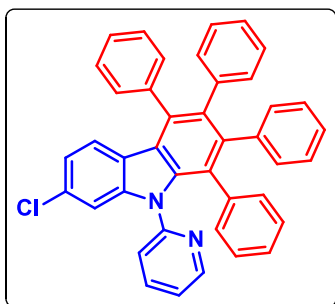
Physical State: yellow solid (38 mg for 0.10 mmol scale, 65% yield). m.p.: 278-281 °C. R_f-value: 0.5 (10% EtOAc/hexane). ^{1}H NMR (CDCl$_3$, 400 MHz): δ 8.30 (d, J = 4.4 Hz, 1H), 7.32-7.25 (m, 6H), 6.96-6.93 (m, 1H), 6.91-6.74 (m, 18H), 6.64 (d, J = 8.8 Hz, 1H). ^{13}C{^{1}H} NMR (CDCl$_3$, 100 MHz): δ 151.4,149.2, 143.6, 141.0, 140.6, 140.4, 140.1, 138.0, 137.9, 137.5, 135.9, 135.3, 132.1, 132.0 (2C), 131.8, 131.6, 130.5, 128.5, 127.3 (2C), 126.9, 126.8 (2C), 126.1, 125.6, 125.5, 125.2, 123.5, 123.2, 122.61, 122.6, 122.1, 121.2, 110.9. IR (KBr, cm^{-1}): 3421, 3053, 1601, 1273, 702. HRMS (ESI) m/z: [M+Na]$^+$ Calcd for C$_{41}$H$_{27}$ClN$_2$Na: 605.1755; Found: 605.1758.

7-bromo-1,2,3,4-tetraphenyl-9-(pyridin-2-yl)-9H-carbazole (5oa):
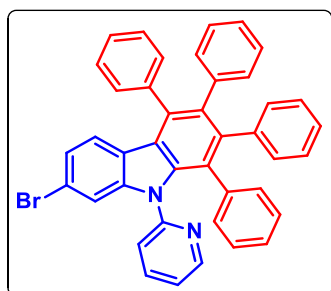
Physical State: yellow solid (43 mg for 0.10 mmol scale, 69% yield). Melting Point: 270-274 °C. R_f-value: 0.3 (20% EtOAc/hexane). ^{1}H NMR (CDCl$_3$, 400 MHz): δ 8.31 (d, J = 4.4 Hz, 1H), 7.62 (s, 1H), 7.31-7.22 (m, 9H), 6.97-6.94 (m, 1H), 6.87-6.74 (m, 14H), 6.45 (d, J = 8.4 Hz, 1H). ^{13}C{^{1}H} NMR (CDCl$_3$, 100 MHz): δ 151.4, 149.2, 143.9, 143.8, 140.9, 140.7, 140.6, 140.4, 140.1, 137.8, 137.5, 136.0, 135.9, 135.3, 132.1, 132.0, 131.5, 130.5 (2C), 129.7, 128.5, 127.31, 127.3, 126.8 (2C), 126.0, 125.6, 125.5, 125.2 (2C), 125.2, 124.1, 124.0, 123.8, 123.5, 123.2 (2C), 122.9, 122.6 (2C), 122.2, 120.0, 119.6, 113.8, 91.1. IR (KBr, cm^{-1}): 3053, 2986, 1601, 1264, 1154, 738. HRMS (ESI) m/z: [M+H]$^+$ Calcd for C$_{41}$H$_{28}$BrN$_2$: 627.1436; Found: 627.1413.

7-nitro-1,2,3,4-tetraphenyl-9-(pyridin-2-yl)-9H-carbazole (5pa):
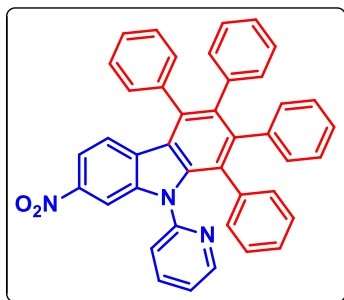
Physical State: yellow solid (49 mg for 0.10 mmol scale, 83% yield). m.p.: 296-298 °C. R_f-value: 0.2 (5% EtOAc/hexane). ^{1}H NMR (CDCl$_3$, 400 MHz): δ 8.34 (dd, J_1 = 4.8 Hz, J_2 = 1.2 Hz, 1H), 8.14 (d, J = 2.0 Hz, 1H), 7.83 (dd, J_1 = 8.8 Hz, J_2 = 2.0 Hz, 1H), 7.37-7.30 (m, 6H), 7.03-7.00 (m, 1H), 6.90-6.75 (m, 17H). ^{13}C{^{1}H} NMR (CDCl$_3$, 100 MHz): δ 150.8, 149.5, 146.0, 142.7, 142.1, 140.2, 139.92, 139.9, 139.6, 137.8, 137.3, 137.0, 136.0, 132.0, 131.7, 131.5, 130.3, 129.1, 128.7, 127.7, 127.4, 127.0, 126.9, 126.3, 125.82, 125.8, 125.6, 123.3, 122.7, 121.8, 115.9, 106.9. IR (KBr, cm^{-1}): 3943, 3688, 3420, 1518, 1421. HRMS (ESI) m/z: [M+H]$^+$ Calcd for C$_{41}$H$_{28}$N$_3$O$_2$: 594.2176; Found: 594.2149.

8-methyl-1,2,3,4-tetraphenyl-9-(pyridin-2-yl)-9H-carbazole (5qa):
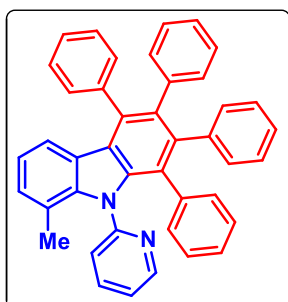
Physical State: yellow liquid (31 mg for 0.10 mmol scale, 55% yield). R_f-value: 0.5 (20% EtOAc/hexane). ^{1}H NMR (CDCl$_3$, 400 MHz): δ 8.25 (dd, J_1 = 4.8 Hz, J_2 = 2.0 Hz, 1H), 7.35-7.25 (m, 5H), 7.23-7.19 (m, 1H), 7.01-6.95 (m, 3H), 6.89–6.73 (m, 16H), 6.63 (d, J = 8.0 Hz, 1H), 1.66 (s, 3H). ^{13}C{^{1}H} NMR (CDCl$_3$, 100 MHz): δ 154.7, 148.5, 142.7, 140.8, 140.6, 140.5, 140.4, 140.0, 138.4, 136.8, 135.6, 134.5, 132.1, 131.7, 131.6, 130.6, 129.1, 128.3, 127.1, 127.0, 126.6, 126.6, 126.5, 126.2, 125.7, 125.6, 125.3, 124.9, 123.0, 122.7, 121.8, 120.8, 120.5, 19.6. IR (KBr, cm^{-1}): 3440, 3055, 1642, 1406. HRMS (ESI) m/z: [M+H]$^+$ Calcd for C$_{42}$H$_{31}$N$_2$: 563.2482; Found: 563.2497.

8-nitro-1,2,3,4-tetraphenyl-9-(pyridin-2-yl)-9H-carbazole (5ra):
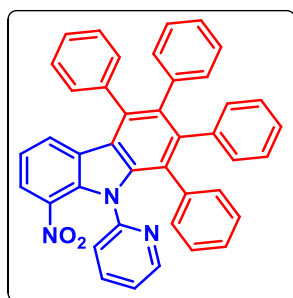
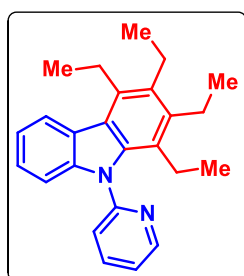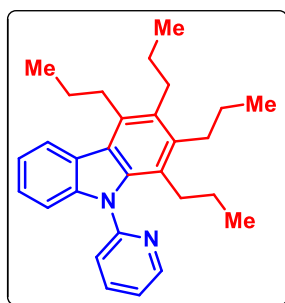Physical State: brown liquid (53 mg for 0.10 mmol scale, 89% yield). R_f -value: 0.4 (20% EtOAc/hexane). ^{1}H NMR (CDCl$_3$, 400 MHz): δ 8.18 (dd, J_1 = 5.2 Hz, J_2 = 1.2 Hz, 1H), 7.72 (p, J = 8.4 Hz, J = 4.0 Hz, 1H), 7.33-7.29 (m, 5H), 7.12-7.07 (m, 1H), 6.95–6.92 (m, 3H), 6.86-6.79 (m, 7H), 6.76-6.68(m, 9H).

^{13}C{^{1}H} NMR (CDCl$_3$, 100 MHz): δ 152.1, 148.3, 142.5, 140.3, 140.1, 139.9, 139.6, 137.9, 137.0, 136.8, 136.2, 136.0, 134.5, 132.0, 131.7, 131.3, 130.5, 128.7(2C), 127.6, 127.5, 127.4, 126.9, 126.7, 126.1, 126.1, 125.7, 125.6, 125.2, 123.0, 122.6, 121.7, 119.8. IR (KBr, cm^{-1}): 3440, 3055, 2923, 1590, 1378. HRMS (ESI) m/z: [M+H]$^+$ Calcd for C$_{41}$H$_{28}$N$_3$O$_2$: 594.2176; Found: 594.2179.

1,2,3,4-tetraethyl-9-(pyridin-2-yl)-9H-carbazole (5bb):

Physical State: colorless liquid (30 mg for 0.10 mmol scale, 84% yield). R_f -value: 0.5 (10% EtOAc/hexane). ^{1}H NMR (CDCl$_3$, 400 MHz): δ 8.69 (dd, J_1 = 4.8 Hz, J_2 = 1.6 Hz, 1H), 8.14 (d, J = 6.8 Hz, 1H), 7.91-7.87 (m, 1H), 7.44 (d, J = 8.0 Hz, 1H), 7.41-7.38 (m, 1H),

7.28-7.20 (m, 2H), 7.03 (d, J = 7.2 Hz, 1H), 3.30 (q, J = 7.6 Hz, 2H), 288-2.76 (m, 4H), 2.39 (q, J = 7.2 Hz, 2H), 1.44 (t, J = 7.2 Hz, 3H), 1.28 (t, J = 7.6 Hz, 3H), 1.20 (t, J = 7.2 Hz, 3H), 0.86 (t, J = 7.2 Hz, 3H). ^{13}C{^{1}H} NMR (CDCl$_3$, 100 MHz): δ 154.6, 150.1, 143.8, 139.6, 139.2, 138.5, 135.5, 133.2, 125.0, 124.4, 124.2, 124.0, 123.4, 122.7, 122.0, 120.6, 110.4, 77.4, 23.4, 22.7, 22.1, 21.4, 16.8, 16.5, 15.2, 14.7. IR (KBr, cm^{-1}): 3442, 3049, 2869, 1585, 1465, 1398. HRMS (ESI) m/z: [M+H]$^+$ Calcd for C$_{25}$H$_{29}$N$_2$: 357.2325; Found: 357.2321.

1,2,3,4-tetrapropyl-9-(pyridin-2-yl)-9H-carbazole (5bc):

Physical State: brown liquid (31 mg for 0.10 mmol scale, 76% yield). R_f-value: 0.6 (10% EtOAc/hexane). ^{1}H NMR (CDCl$_3$, 400 MHz): δ 8.70-8.68 (m, 1H), 8.04 (d, J = 7.2 Hz, 1H), 7.88 (td, J_1 = 7.6 Hz, J_2 = 2.0 Hz 1H), 7.43-7.38 (m, 2H), 7.27-7.19 (m, 2H), 7.02-7.00 (m, 1H), 3.20-3.16 (m, 2H), 2.75-2.64 (m, 4H), 2.26 (t, J = 8.4 Hz, 2H), 1.85-1.79 (m, 2H), 1.65-1.50 (m, 4H), 1.36-1.30 (m, 2H), 1.21 (t, J = 7.62 Hz, 3H), 1.10 (t, J = 7.2 Hz, 3H), 1.04 (t, J = 7.2 Hz, 3H), 0.50 (t, J = 7.2 Hz, 3H). ^{13}C{^{1}H} NMR (CDCl3, 100 MHz): δ 154.5, 150.1, 143.7, 139.2, 138.6, 138.5, 134.2, 132.3, 124.9, 124.5, 124.1, 123.2, 122.9, 122.5, 122.1, 120.5, 110.3, 32.9, 32.5, 31.9, 30.9, 25.8, 25.6, 24.0, 23.5, 15.4, 15.3, 15.1, 14.6. IR (KBr, cm^{-1}): 3441, 2956, 2927, 1635, 1465, 1397, 1345. HRMS (ESI) m/z: [M+H]$^+$ Calcd for C$_{29}$H$_{37}$N$_2$: 413.2951; Found: 413.2935.

9-(pyridin-2-yl)-1,2,3,4-tetra-p-tolyl-9H-carbazole (5bd):
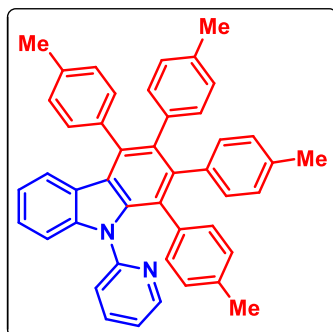
Physical State: brown solid (44 mg for 0.10 mmol scale, 73% yield). m.p.: 261–262 °C. R_f-value: 0.5 (20% EtOAc/hexane). ^{1}H NMR (CDCl$_3$, 400 MHz): δ 8.28 (dd, J_1 = 4.4 Hz, J_2 = 1.2 Hz, 1H), 7.30 (d, J = 8.4 Hz, 1H), 7.25-7.19 (m, 4H), 7.11 (d, J = 7.6 Hz, 2H), 6.94-6.90 (m, 2H), 6.77–6.62 (m, 12H), 6.51 (d, J = 8.0 Hz, 2H), 2.7 (s, 3H), 2.10-2.07 (m, 9H). ^{13}C{^{1}H} NMR (CDCl$_3$, 100 MHz): δ 152.1, 148.7, 143.0, 140.2, 137.9, 137.9, 137.8, 137.6, 137.0, 136.3, 135.9, 135.3, 135.0, 135.0, 134.4, 134.3, 131.9, 131.8, 131.4, 130.4, 129.0, 127.9, 127.4, 127.4, 125.9, 124.9, 124.1, 123.3, 123.2, 122.7, 121.1, 120.5, 110.5, 21.7, 21.4, 21.4, 21.3. IR (KBr, cm^{-1}): 3441, 1635, 1515, 1435, 1337, 1299. HRMS (ESI) m/z: [M+H]$^+$ Calcd for C$_{45}$H$_{37}$N$_2$: 605.2951; Found: 605.2896.

1,2,3,4-tetrakis(4-methoxyphenyl)-9-(pyridin-2-yl)-9H-carbazole (5be):
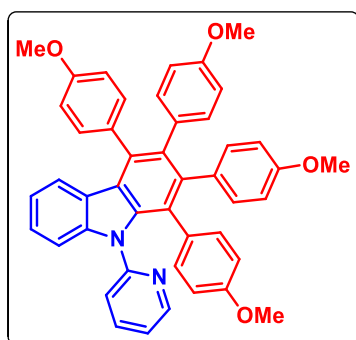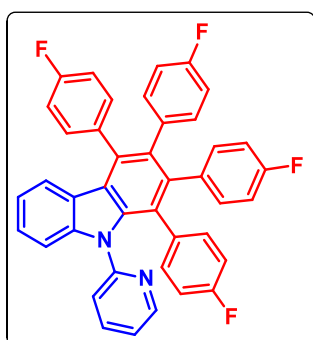

Physical State: yellow solid (58 mg for 0.10 mmol scale, 86% yield). m.p.: 271–273 °C. R_f -value: 0.3 (20% EtOAc/hexane). ^{1}H NMR (CDCl$_3$, 400 MHz): δ 8.31 (d, J = 4.4 Hz, 1H), 7.33-7.21 (m, 5H), 6.96-6.92 (m, 2H), 6.87-6.67 (m, 10H), 6.45-6.39 (m, 4H), 6.29 (d, J = 8.4 Hz, 2H),

3.84 (s, 3H) 3.64-3.61 (m, 9H). ^{13}C{^{1}H} NMR (CDCl$_3$, 100 MHz): δ 158.5, 157.5, 157.1, 157.0, 152.2, 148.8, 143.0, 140.2, 138.0, 137.1, 135.7, 135.1, 133.5, 133.4, 133.0, 133.0, 132.7, 132.5, 131.6, 130.8, 126.0, 124.8, 124.1, 123.4, 123.3, 122.7, 121.4, 120.6, 113.8, 112.8, 112.4, 112.3, 110.6, 55.4, 55.4, 55.2 (2C). IR (KBr, cm^{-1}): 3446, 3033, 2999, 1609, 1385. HRMS (ESI) m/z: [M+H]$^+$ Calcd for C$_{45}$H$_{37}$N$_2$O$_4$: 669.2748; Found: 669.2726.

1,2,3,4-tetrakis(4-fluorophenyl)-9-(pyridin-2-yl)-9H-carbazole (5bf):

Physical State: white solid (39 mg for 0.10 mmol scale) 63% yield). Melting Point: 291-297 °C. R_f -value: 0.3 (10% EtOAc/hexane). ^{1}H NMR (CDCl$_3$, 400 MHz): δ 8.30 (dd, J_1 = 4.8 Hz, J_2 = 1.2 Hz, 1H), 7.41 (dt, J_1 = 7.6 Hz, J_2 = 2 Hz, 1H), 7.30-7.26 (m, 4H), 7.07-7.02 (m, 3H), 7.00-6.96 (m, 1H), 6.93 (d, J = 7.6 Hz, 1H), 6.81-6.77 (m, 5H), 6.73-6.69 (m, 2H), 6.62

(t, J = 8.8 Hz, 2H), 6.57 (t, J = 8.8 Hz, 2H), 6.48 (t, J = 8.8 Hz, 2H). ^{13}C{^{1}H} NMR (CDCl$_3$, 100 MHz): δ 163.5, 162.4 (d, J = 19.3 Hz), 161.0, 159.9 (d, J = 17.3 Hz), 151.8, 149.4, 143.2, 139.3, 138.0, 137.6, 136.3 (dd, J_1 = 15.4 Hz, J_2 = 3.5 Hz), 136.0 (d, J = 3.5 Hz), 135.3, 134.1, 133.9 (d, J = 3.5 Hz), 133.3 (m), 133.0 (d, J = 7.8 Hz), 132.1 (d, J = 7.9 Hz), 126.6, 124.4, 123.6, 123.5, 123.4, 122.6, 122.2, 121.0, 115.8, 115.6, 114.5, 114.3 (m), 114.0 (m), 110.7. ^{19}F NMR (CDCl$_3$, 376 MHz): δ -115.0, -116.3, -116.8, -117.0. IR (KBr, cm^{-1}):

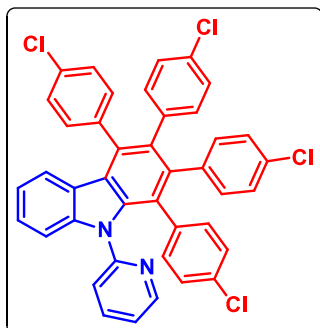3942, 3852, 3445, 1604, 1436, 1264. HRMS (ESI) m/z: [M+H]$^+$ Calcd for $C_{41}H_{25}F_4N_2$: 621.1948; Found: 621.1923.

1,2,3,4-tetrakis(4-chlorophenyl)-9-(pyridin-2-yl)-9H-carbazole (5bg):

Physical State: solid (45 mg for 0.10 mmol scale, 66% yield). m.p.: 252–254 °C R_f-value: 0.4 (20% EtOAc/hexane). ^{1}H NMR (CDCl$_3$, 400 MHz): δ 8.29 (dd, J_1 = 4.8 Hz, J_2 = 1.2 Hz, 1H), 7.42 (dt, J_1 = 7.6 Hz, J_2 = 2.0 Hz, 1H), 7.34-7.32 (m, 2H), 7.29 (dd, J_1 = 6.8 Hz, J_2 = 1.2 Hz, 1H), 7.26-7.22 (m, 4H),

7.08–7.05 (m, 1H), 7.01-6.97 (m, 1H), 6.92-6.85 (m, 5H), 6.80 (d, J = 8.0 Hz, 1H), 6.77-6.74 (m, 5H) 6.70-6.67 (m, 2H). ^{13}C{^{1}H} NMR 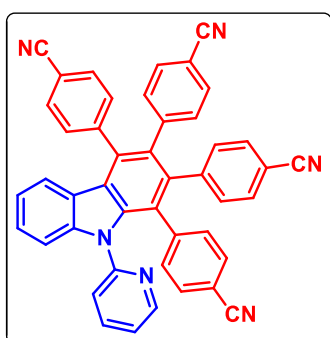(CDCl$_3$, 100 MHz): δ 151.6, 149.5, 143.1, 138.6, 138.6, 138.5, 138.3, 138.0, 137.7, 136.2, 135.0, 133.5, 133.4, 133.1, 133.0, 132.7, 132.3, 132.1, 132.0, 131.8, 129.0, 127.6, 127.5, 127.5, 126.8, 124.1, 123.4, 123.3, 122.6, 122.1, 121.1, 110.7. IR (KBr, cm^{-1}): 3440, 2349, 1634, 1435, 1014. HRMS (ESI) m/z: [M+H]$^+$ Calcd for $C_{41}H_{25}Cl_4N_2$: 685.0766; Found: 685.0729.

4,4',4'',4'''-(9-(pyridin-2-yl)-9H-carbazole-1,2,3,4-tetrayl) tetrabenzonitrile (5bi):

Physical State: light pink solid (48 mg for 0.10 mmol scale, 74% yield). m.p.: 280-285 °C. R_f-value: 0.3 (10% EtOAc/hexane). ^{1}H NMR (CDCl$_3$, 400 MHz): δ 8.25 (dd, J_1 = 4.4 Hz, J_2 = 1.2 Hz, 1H), 7.70-7.65 (m, 3H), 7.55-7.48 (m, 2H), 7.45-7.43 (m, 2H), 7.38 (t, J = 8.4 Hz, 1H), 7.25 (d, J = 3.2 Hz, 1H), 7.20 (d, J = 8.0 Hz, 2H), 7.12-7.09 (m, 3H), 7.06-7.03 (m, 2H), 6.97-6.93 (m, 4H),

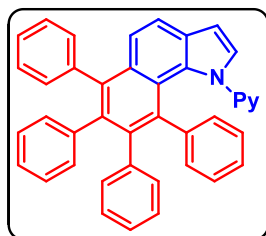6.87 (d, J = 8.0 Hz, 2H), 6.70 (d, J = 8.0 Hz, 1H). ^{13}C{^{1}H} NMR (CDCl$_3$, 100 MHz): δ 151.1, 150.1, 144.3, 144.1, 144.0, 143.3, 142.2, 138.1, 137.8, 137.4, 134.7, 132.8, 132.5, 132.4 (2C), 132.3 (3C), 132.1, 132.1, 131.5, 131.4, 131.3, 128.9, 128.8, 127.8, 123.9, 123.7, 123.3, 123.0, 122.5, 122.4, 121.9, 118.7, 118.6, 118.5 (2C), 112.4, 111.0 (2C), 110.8. IR

(KBr, cm^{-1}): 3441, 2922, 1393, 1184. HRMS (ESI) m/z: [M+H]$^+$ Calcd for C$_{45}$H$_{25}$N$_6$: 649.2135; Found: 649.2106.

6,7,8,9-tetraphenyl-1-(pyridin-2-yl)-1H-benzo[g]indole (6):

Physical State: white solid (51 mg for 0.10 mmol scale, 93% yield). m.p.: 275-280 °C. R$_f$ -value: 0.2 (5% EtOAc/hexane). ^{1}H NMR (CDCl$_3$, 400 MHz): δ 8.05 (d, J = 4.0 Hz, 1H), 7.63 (d, J = 8.4 Hz, 1H), 7.40 (d, J = 8.8 Hz, 1H), 7.34 (t, J = 8.0 Hz, 1H), 7.25-7.19 (m, 6H), 6.91 (t, J = 6.4 Hz, 1H), 6.84-6.57 (m, 17H). ^{13}C{^{1}H} NMR (CDCl$_3$, 100 MHz): δ 154.4, 148.7, 141.3, 141.1, 141.0, 140.9, 140.6, 139.6, 139.5, 137.9, 134.6, 131.84, 131.8, 131.7 (2C), 131.3, 130.1, 127.7, 126.9, 126.7 (2C), 126.6, 125.5, 125.4, 125.3, 125.2, 123.0, 121.7, 120.9, 120.7, 117.2, 106.6. IR (KBr, cm^{-1}): 3439, 2986, 1601, 1264. HRMS (ESI) m/z: [M+H]$^+$ Calcd for C$_{41}$H$_{29}$N$_2$: 549.2325; Found: 549.2292.

6,7,8,9-Tetraphenyl-1H-benzo[g]indole (7):
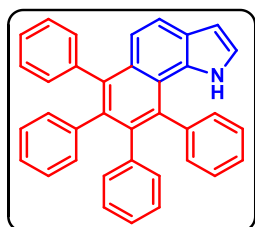
Physical State: white solid (17 mg for 0.05 mmol scale, 72% yield). m.p.: 270−280 °C. R$_f$ -value: 0.7 (10% EtOAc/hexane). ^{1}H NMR (CDCl$_3$, 400 MHz): δ 7.65 (d, J = 8.8 Hz, 1H), 7.36-7.32 (m, 7H), 7.24 (d, J = 4.4 Hz, 4H), 7.20-7.17 (m, 1H), 6.87-6.80 (m, 11H), 6.55 (s, 1H). ^{13}C{^{1}H} NMR (CDCl$_3$, 176 MHz): δ 141.9, 141.1, 141.0, 140.6, 139.7, 139.2, 137.3, 134.2, 131.8, 131.7, 131.6, 131.3, 130.8, 129.5, 128.9, 127.8 (2C), 126.8 (2C), 126.6, 125.6, 125.5, 125.4, 122.7, 121.4, 120.6, 120.3, 103.3. IR (KBr, cm^{-1}): 3456, 3055, 1366, 1264. HRMS (ESI) m/z: [M+H]$^+$ Calcd for C$_{36}$H$_{26}$N: 472.2060; Found: 472.2060.

6,7,8,9-tetraphenyl-2,3-dihydro-1H-benzo[g]indole (8):
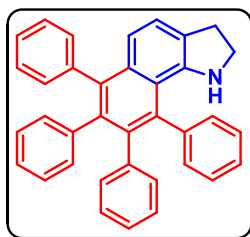
Physical State: yellow solid (38 mg for 0.09 mmol scale, 88% yield). m.p.: 180-185 °C. R_f-value: 0.4 (5% EtOAc/hexane). ^{1}H NMR (CDCl$_3$, 400 MHz): δ 7.27-7.12 (m, 10H), 6.99 (d, J = 8.4 Hz, 1H), 6.87-6.75 (m, 11H), 3.33 (t, J = 8.4 Hz, 2H), 3.02 (t, J = 8.8 Hz, 2H). ^{13}C{^{1}H} NMR (CDCl$_3$, 100 MHz): δ 148.5, 141.9, 141.0, 140.9 (2C), 140.7, 140.6, 139.2, 138.8, 138.3, 136.0, 133.2, 131.7, 131.5, 131.0, 127.7 (2C), 127.2, 126.9, 126.8, 126.7, 126.5, 125.5, 125.1, 124.0, 119.0, 118.4, 48.2, 30.2. IR (KBr, cm^{-1}): 3053, 2986, 1420, 1264. HRMS (ESI) m/z: [M+H]$^+$ Calcd for C$_{36}$H$_{28}$N: 474.2216; Found: 474.2184.

1,2,3,4-tetraphenyl-9H-carbazole (9):
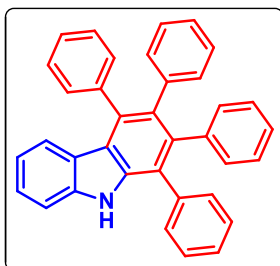

Physical State: yellow solid (39 mg for 0.10 mmol scale, 82% yield). m.p.: 232–234 °C. R_f-value: 0.3 (20% EtOAc/hexane). ^{1}H NMR (CDCl$_3$, 400 MHz): δ 8.08 (s, 1H), 7.33–7.28 (m, 11H), 6.90-6.84 (m, 13H). ^{13}C{^{1}H} NMR (CDCl$_3$, 176 MHz): δ 140.6, 140.4, 140.3, 138.5, 138.0, 137.7, 135.8, 133.6, 132.4, 132.0, 130.8, 130.6, 128.8, 128.2, 127.2, 127.0, 127.0, 126.8, 125.9, 125.7, 125.4, 123.9, 123.6, 122.8, 121.0, 119.5, 110.6. IR (KBr, cm^{-1}): 3445, 3053, 1436, 1274. HRMS (ESI) m/z: [M+Na]$^+$ Calcd for C$_{36}$H$_{25}$NNa: 494.1879; Found: 494.1835.

NMR spectra of 6,7,8,9-tetraphenyl-1-(pyridin-2-yl)-2,3-dihydro-1H-benzo[g]indole (3ba):

^{1}H NMR of 3ba (400 MHz, CDCl$_3$)

^{13}C{^{1}H} NMR of 3ba (100 MHz, CDCl$_3$)
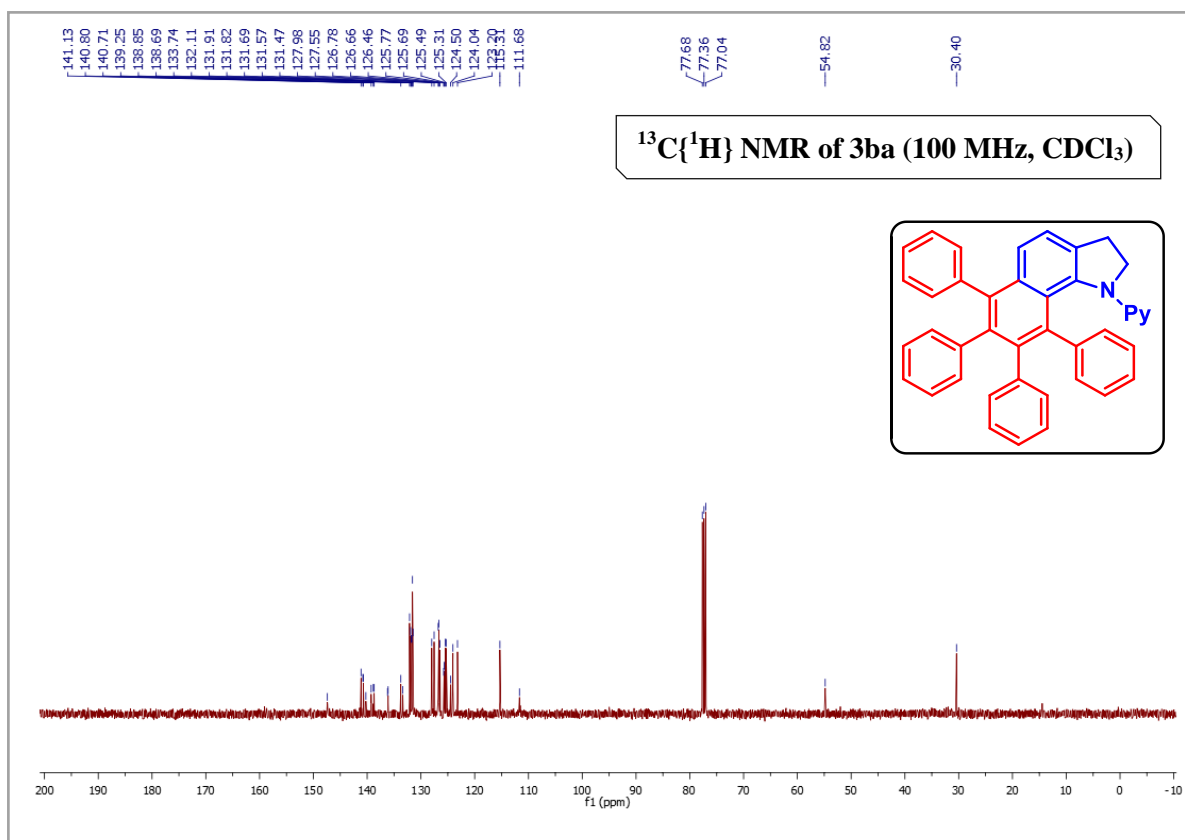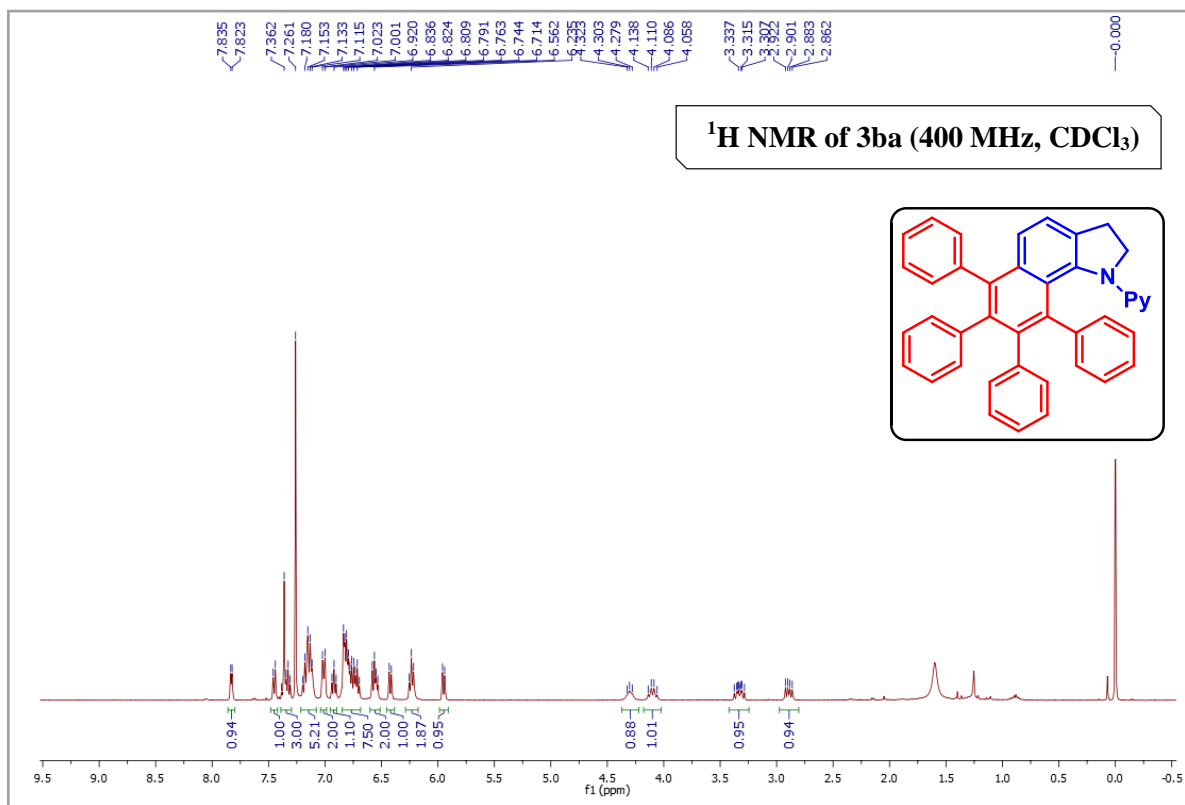
NMR spectra of 6,7,8,9-tetraethyl-1-(pyridin-2-yl)-2,3-dihydro-1H-benzo[g] indole (3bb):

^{1}H NMR of 3bb (400 MHz, CDCl$_3$)

^{13}C{^{1}H} NMR of 3bb (100 MHz, CDCl$_3$)
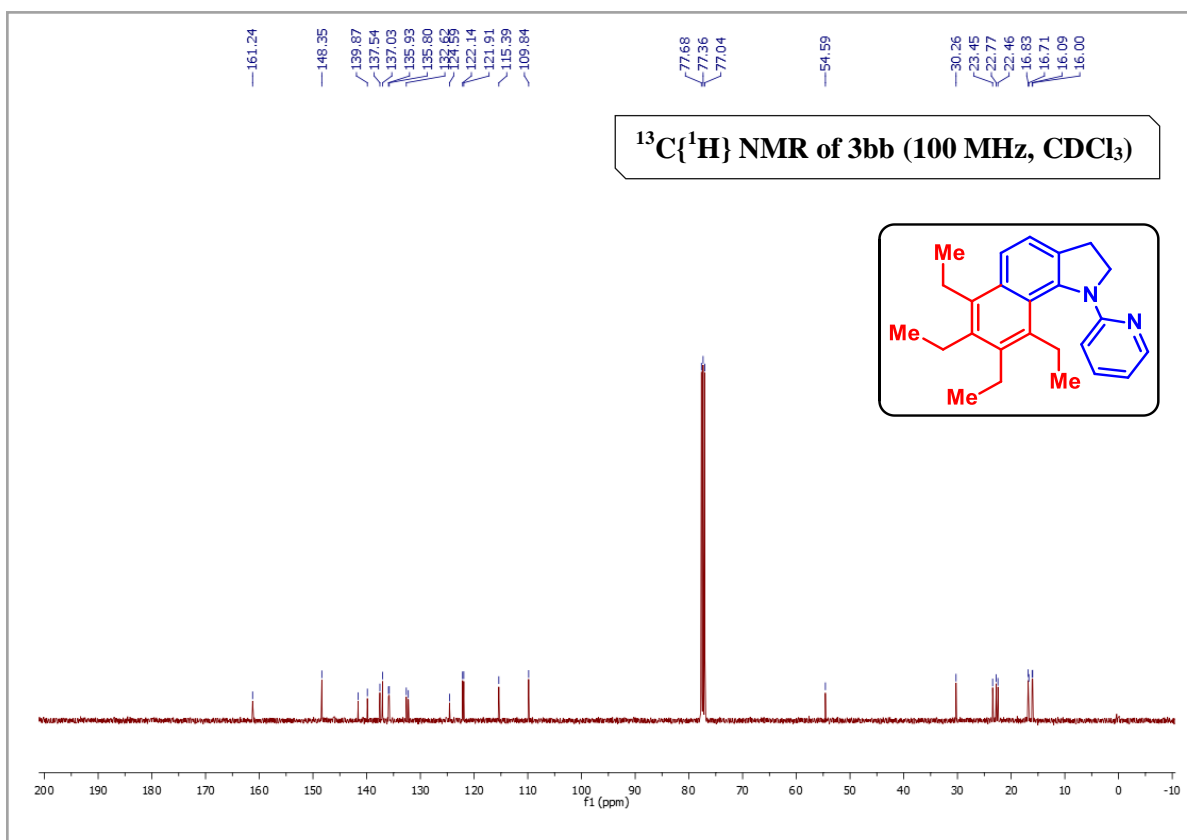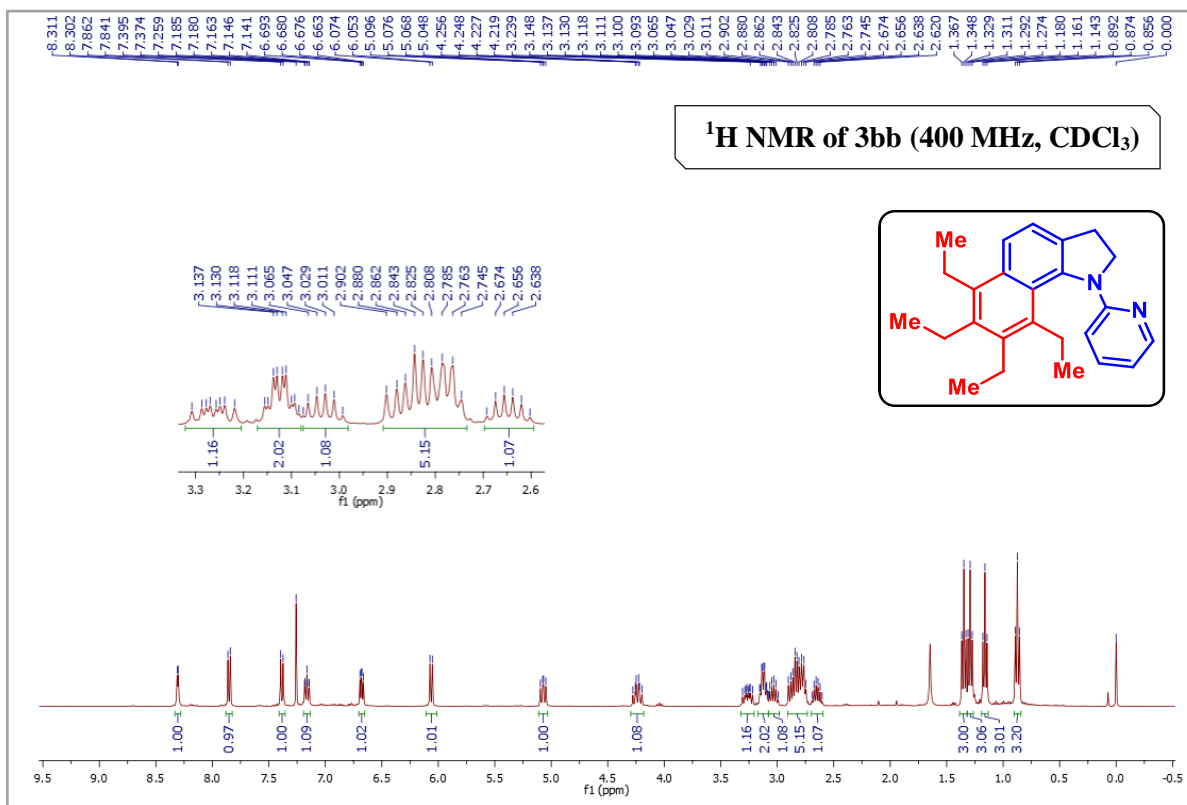
NMR spectra of 1,2,3,4-tetraphenyl-9-(pyridin-2-yl)-9H-carbazole (5ba):

^{1}H NMR of 5ba (400 MHz, CDCl$_3$)

^{13}C{^{1}H} NMR of 5ba (100 MHz, CDCl$_3$)

NMR spectra of 6,7,8,9-Tetraphenyl-1H-benzo[g]indole (7):

^{1}H NMR of 7 (400 MHz, CDCl$_3$)

^{13}C{^{1}H} NMR of 7 (176 MHz, CDCl$_3$)

Crystal Structure of 5ra

5ra   CCDC **2041963**

ORTEP diagram of **5ra** with 50% ellipsoid probability
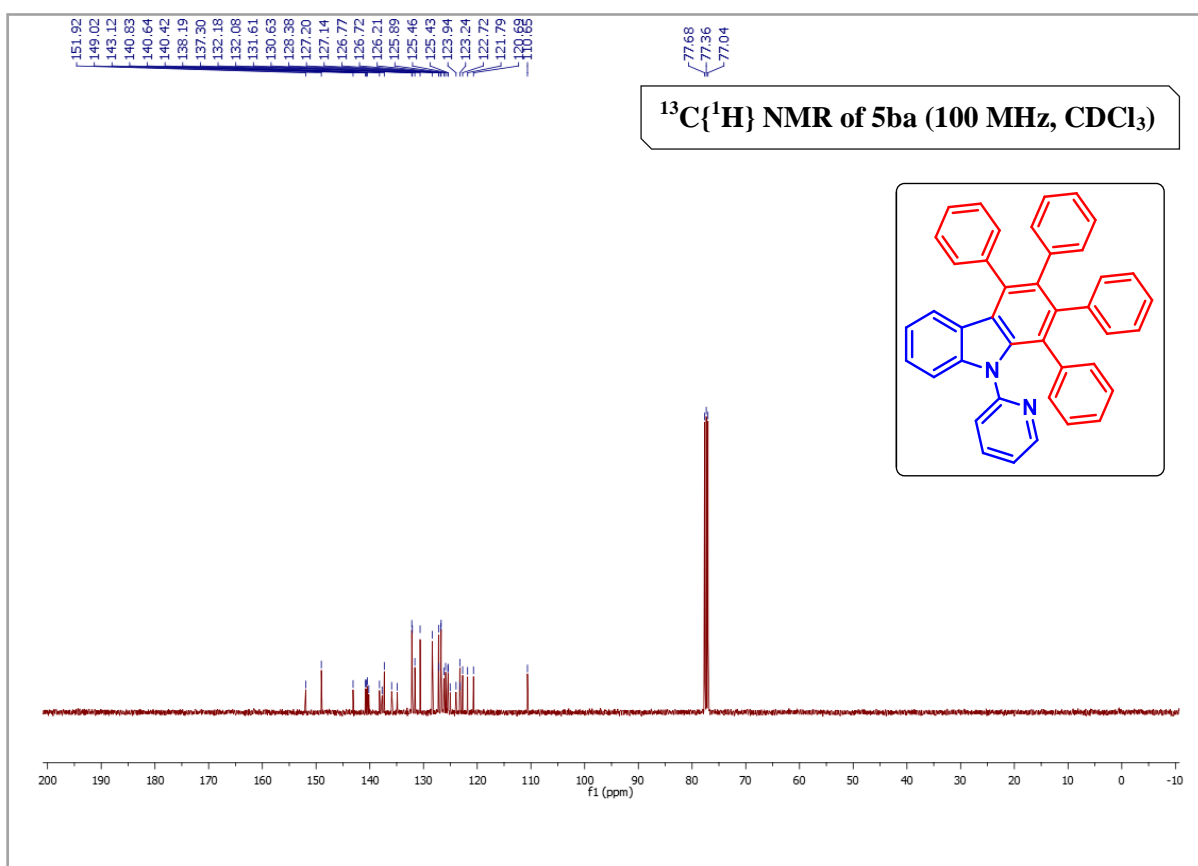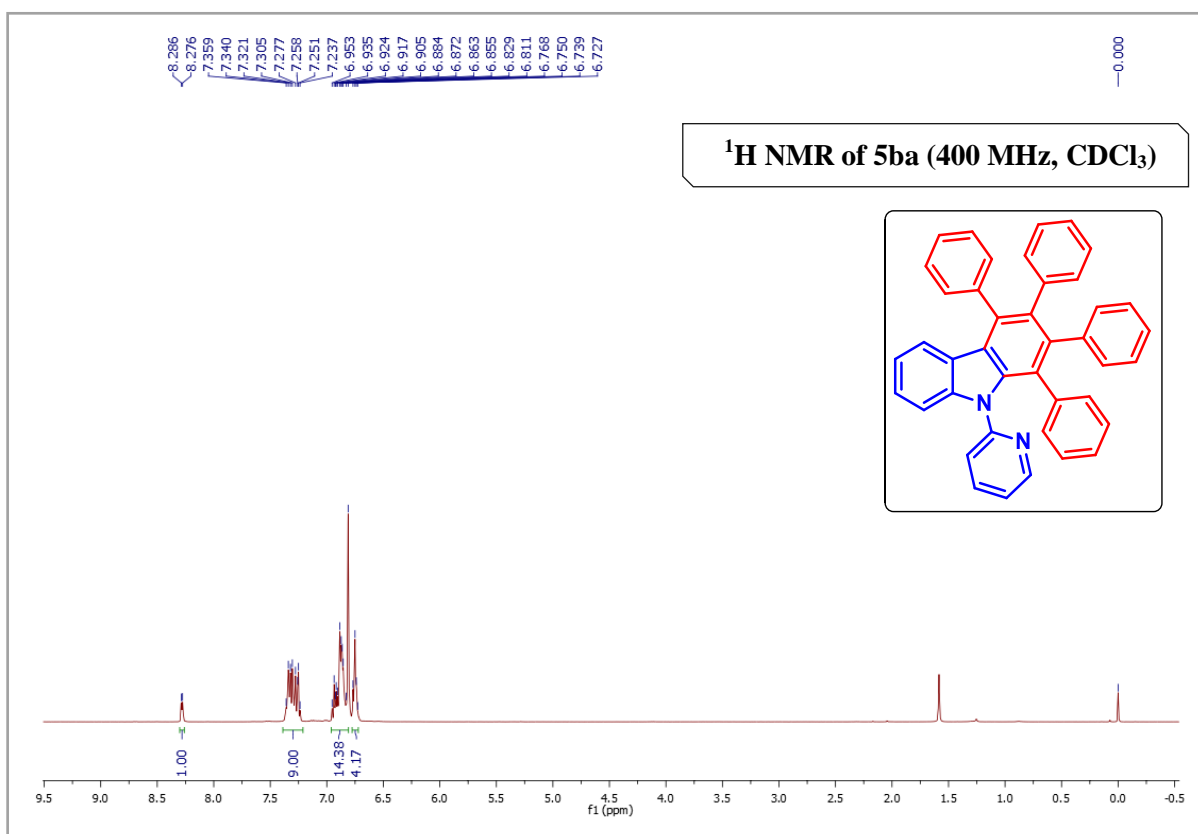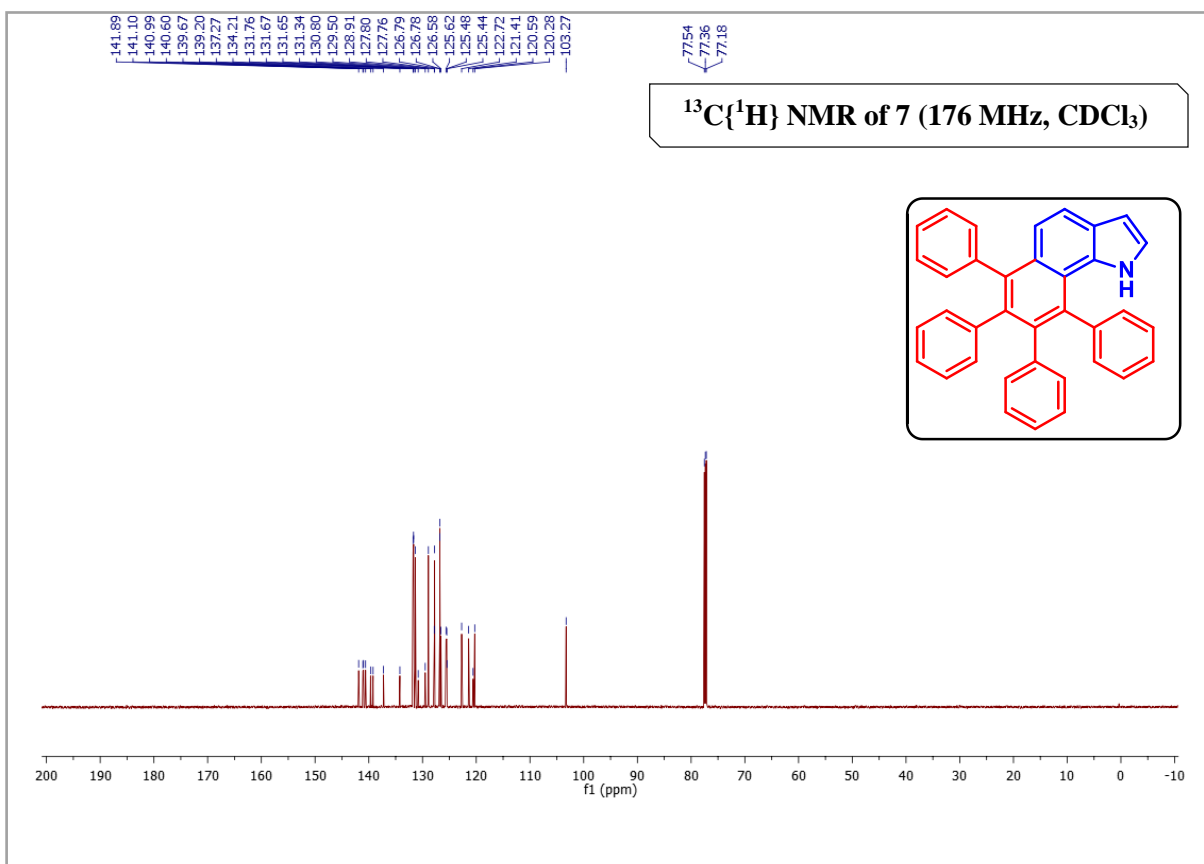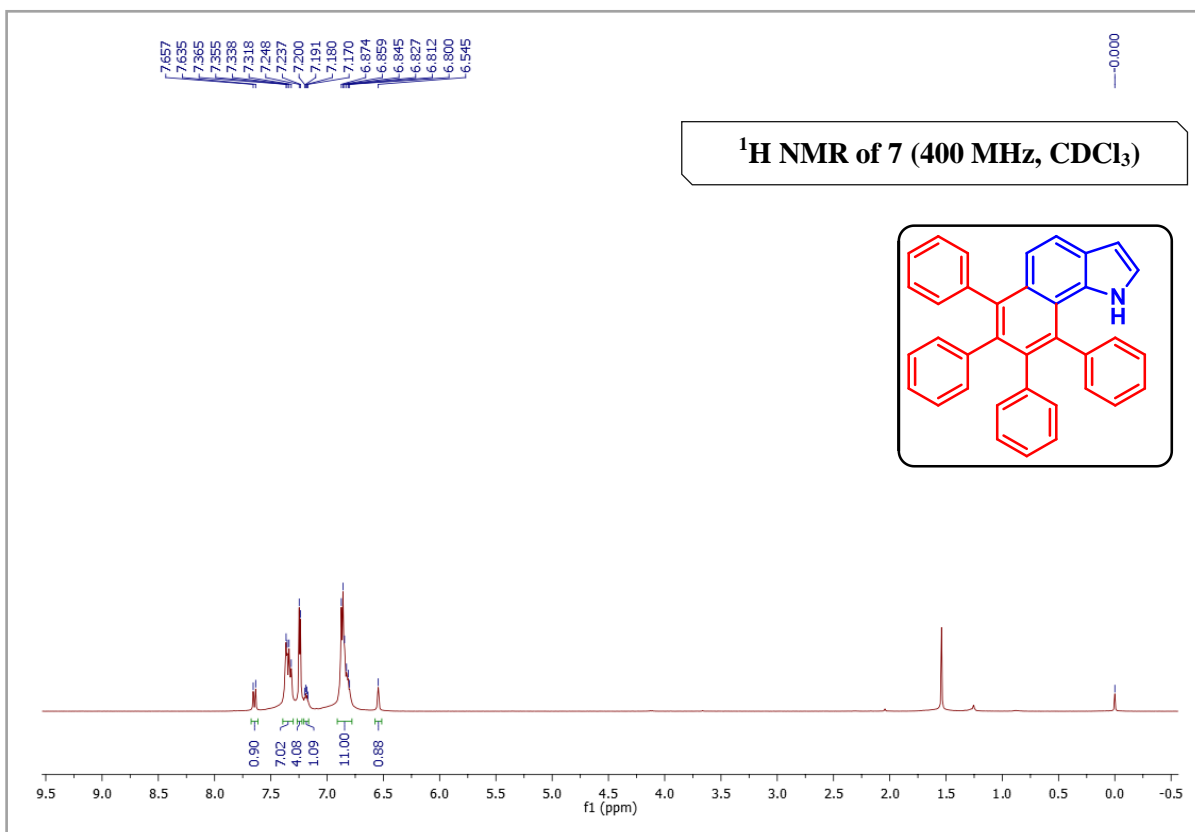
4.6 REFERENCES

1. (a) Jampilek, J. Heterocycles in Medicinal Chemistry. *Molecules* **2019**, *24*, 3839. (b) Kerru, N.; Gummidi, L.; Maddila, S.; Gangu, K. K.; Jonnalagadda, S. B. A Review on Recent Advances in Nitrogen-Containing Molecules and Their Biological Applications. *Molecules* **2020**, *25*, 1909.

2. Yan, Q.; Huang, H.; Zhang, H.; Li, M.-H.; Yang, D.; Song, M.-P.; Niu, J.-L. Synthesis of 7-Amido Indolines by Cp*Co(III)-Catalyzed C−H Bond Amidation *J. Org. Chem.* **2020**, *85*, 11190−11199.

3. Wen, J.; Shi, Z. From C4 to C7: Innovative Strategies for Site-Selective Functionalization of Indole C−H Bonds. *Acc. Chem. Res.* **2021**, *54*, 1723−1736.

4. Xiao, E. K.; Wu, X. T.; Ma, F.; Feng, X.; Chen, P.; Jiang, Y. J. Fe(OTf)$_3$- and gamma-Cyclodextrin-Catalyzed Hydroamination of Alkenes with Carbazoles. *Org. Lett.* **2021**, *23*, 449−453.

5. Ledwon, P. Recent Advances of Donor-Acceptor Type Carbazole-Based Molecules for Light Emitting Applications. *Org. Electron.* **2019**, *75*, 105422.

6. Shah, T. A.; De, P. B.; Pradhan, S.; Punniyamurthy, T. Transition-Metal-Catalyzed Site Selective C7-Functionalization of Indoles: Advancement and Future Prospects. *Chem. Commun.* **2019**, *55*, 572−587.

7. Harry, N. A.; Saranya, S.; Ujwaldev, S. M.; Anilkumar, G. Recent advances and prospects in nickel-catalyzed C−H activation. *Catal. Sci. Technol.* **2019**, *9*, 1726−1743.

8. Jagtap, R. A.; Punji, B. C−H Functionalization of Indoles by 3d Transition-Metal Catalysis. *Asian J. Org. Chem.* **2020**, *9*, 326−342.

9. (a) Gandeepan, P.; Koeller, J.; Ackermann, L. Expedient C–H Chalcogenation of Indolines and Indoles by Positional-Selective Copper Catalysis. *ACS Catal.* **2017**, *7*, 1030–1034. (b) Ahmad, A.; Dutta, H. S.; Khan, B.; Kant, R.; Koley, D. Cu(I)-Catalyzed SiteSelective Acyloxylation of Indoline Using O as the Sole Oxidant. *Adv. Synth. Catal.* **2018**, *360*, 1644–1649.

10. (a) De, P. B.; Pradhan, S.; Banerjee, S.; Punniyamurthy, T. Expedient Cobalt(II)-Catalyzed Site-Selective C7-Arylation of Indolines with Arylboronic Acids. *Chem. Commun.* **2018**, *54*, 2494–2497. (b) Jagtap, R. A.; Samal, P. P.; Vinod, C. P.; Krishnamurty, S.; Punji, B. Iron-Catalyzed C(sp^2)−H Alkylation of Indolines and Benzo[h]quinoline with Unactivated Alkyl Chlorides through Chelation Assistance. *ACS Catal.* **2020**, *10*, 7312−7321.

11. (a) Banjare, S. K.; Chebolu, R.; Ravikumar, P. C. Cobalt Catalyzed Hydroarylation of Michael Acceptors with Indolines Directed by a Weakly Coordinating Functional Group. *Org. Lett.* **2019**, *21*, 4049−4053. (b) Banjare, S.-K.; Biswal, P.; Ravikumar, P. C. Cobalt-Catalyzed One-Step Access to Pyroquilon and C-7 Alkenylation of Indoline with Activated Alkenes Using Weakly Coordinating Functional Groups. *J. Org. Chem.* **2020**, *85*, 5330−5341.

12. (a) Ding, Z.; Yoshikai, N. Mild and Efficient C2-Alkenylation of Indoles with Alkynes Catalyzed by a Cobalt Complex. *Angew. Chem., Int. Ed.* **2012**, *51*, 4698−4701. (b) Shi, L.; Zhong, X.; She, H.; Lei, Z.; Li, F. Manganese catalyzed C–H functionalization of indoles with alkynes to synthesize bis/trisubstituted indolylalkenes and carbazoles: the acid is the key to control selectivity. *Chem. Commun.* **2015**, *51*, 7136−7139.

13. (a) Misal Castro, L. C.; Obata, A.; Aihara, Y.; Chatani, N. Chelation-Assisted Nickel-Catalyzed Oxidative Annulation via Double C−H Activation/Alkyne

Insertion Reaction. *Chem. Eur. J.* **2016**, *22*, 1362−1367. (b) Wu, J.- Q.; Yang, Z.; Zhang, S.-S.; Jiang, C.-Y.; Li, Q.; Huang, Z.-S.; Wang, H. From indoles to carbazoles: tandem Cp*Rh(III)-catalyzed C−H activation/Brønsted acid-catalyzed cyclization reactions. *ACS Catal.* **2015**, *5*, 6453−6457. (c) Wang, L.; Xiong, D.; Jie, L.; Yu, C.; Cui, X. Rhodium-catalyzed oxidative homologation of *N*-pyrimidyl indolines with alkynes via dual C−H activation: Facile synthesis of benzo[g]indolines. *Chin. Chem. Lett.* **2018**, *29*, 907−910.

14. (a) Chinchilla, R.; Najera, C. Chemicals from alkynes with palladium catalysts. *Chem. Rev.* **2014**, *114*, 1783−1826. (b) Dinda, E.; Bhunia, S. K.; Jana, R. Palladium-Catalyzed Cascade Reactions for Annulative π-Extension of Indoles to Carbazoles through C–H Bond Activation. *Curr. Org. Chem.* **2020**, *24*, 2612−2633. (c) Kumar, K. S.; Meesa, S. R.; Naikawadi, P. K. PalladiumCatalyzed [2 + 2 + 2] Annulation via Transformations of Multiple C−H Bonds: One-Pot Synthesis of Diverse Indolo[3,2-a]carbazoles. *Org. Lett.* **2018**, *20*, 6079−6083.

15. (a) Liu, Y.-H.; Liu, Y.-J.; Yan, S.-Y.; Shi, B.-F. Ni(II)-Catalyzed Dehydrative Alkynylation of Unactivated (hetero)aryl C−H Bonds Using Oxygen: A User-Friendly Approach. *Chem. Commun.* **2015**, *51*, 11650−11653. (b) Shah, T. A.; De, P. B.; Pradhan, S.; Banerjee, S.; Punniyamurthy, T. Cp*Co(III)-Catalyzed Regioselective C2 Amidation of Indoles Using Acyl Azides, *J. Org. Chem.*, **2019**, *84*, 16278–16285. (c) Yang, X.-F.; Hu, X.- H.; Feng, C.; Loh, T.-P. Rhodium(iii)-catalyzed C7-position C–H alkenylation and alkynylation of indolines. *Chem. Commun.* **2015**, *51*, 2532−2535. (d) Park, J.; Mishra, N. K.; Sharma, S.; Han, S.; Shin, Y.; Jeong, T.; Oh, J. S.; Kwak, J. H.; Jung, Y. H.; Kim, I. S. Mild Rh(III)-Catalyzed C7-Allylation of Indolines with Allylic Carbonates. *J. Org. Chem.* **2015**, *80*, 1818−1827.

16. Ahmad, A.; Dutta, H. S.; Khan, B.; Kant, R.; Koley, D. Cu(I)-Catalyzed Site Selective Acyloxylation of Indoline Using O₂ as the Sole Oxidant. *Adv. Synth. Catal.* **2018**, *360*, 1644−1649.

17. Lee, S. H.; Jeong, T.; Kim, K.; Kwon, N. Y.; Pandey, A. K.; Kim, H. S.; Ku, J.-M.; Mishra, N. K.; Kim, I. S. Ruthenium (II)-Catalyzed Site-Selective Hydroxymethylation of Indolines with Paraformaldehyde. *J. Org. Chem.* **2019**, *84*, 2307−2315.

18. (a) Zhao, T.; Pu, X.; Han, W.; Gao, G. Nickel-Catalyzed 3,3-Dialkynylation of 2-Aryl Acrylamides: Direct Access to gem-Diethynylethenes via Double Vinylic C–H Bond Activation. *Org. Lett.* **2021**, *23*, 1199–1203. (b) Liu, Y.-H.; Xia, Y.-N.; Shi, B.-F. Ni-Catalyzed Chelation-Assisted Direct Functionalization of Inert C–H Bonds. *Chin. J. Chem.* **2020**, *38*, 635−662. (c) Guo, J.-R.; Gong, J.-F.; Song, M.-P. Nickel(ii)-catalyzed C(sp²)–H sulfuration/annulation with elemental sulfur: selective access to benzoisothiazolones. *Org. Biomol. Chem.* **2019**, *17*, 5029−5037. (d) Misal Castro, L. C.; Obata, A.; Aihara, Y.; Chatani, N. Chelation-Assisted Nickel-Catalyzed Oxidative Annulation via Double C−H Activation/Alkyne Insertion Reaction. *Chem. Eur. J.* **2016**, *22*, 1362−1367.

19. (a) *Molecular Fluorescence: Principle and Applications*; Valeur, B., Ed.; Wiley: Weinheim, Germany, **2005**. (b) Mei, J.; Leung, N. L.; Kwok, R. T.; Lam, J. W.; Tang, B. Z. Aggregation-Induced Emission: Together We Shine, United We Soar! *Chem. Rev.* **2015**, *115*, 11718−11940.

20. Prusty, N.; Kinthada, L. K.; Meena, R.; Chebolu, R.; Ravikumar, P. C. Bismuth(III)-catalyzed regioselective alkylation of tetrahydroquinolines and

indolines towards the synthesis of bioactive core-biaryl oxindoles and CYP19 inhibitors. *Org. Biomol. Chem.*, **2021**, *19*, 891−905.

21. Gottlieb, H. E.; Kotlyar, V.; Nudelman, A. NMR chemical shifts of common laboratory solvents as trace impurities. *J. Org. Chem.* **1997**, *62*, 7512-7515.

22. Gribble, G. W.; Hoffman, J. H. Reactions of sodium borohydride in acidic media. vi. reduction of indoles with cyanoborohydride in acetic acid. *Synthesis*, **1977**, 859−860.

23. (a) Premi, C.; Dixit, A.; Jain, N. Palladium-Catalyzed Regioselective Decarboxylative Alkylation of Arenes and Heteroarenes with Aliphatic Carboxylic Acids. *Org. Lett*. **2015**, *17*, 2598−2601. (b) Lee, S. H.; Jeong, T.; Kim, K.; Kwon, N. Y.; Pandey, A. K.; Kim, H. S.; Ku, J.-M.; Mishra, N. K.; Kim, I. S. Ruthenium (II)-Catalyzed Site-Selective Hydroxymethylation of Indolines with Paraformaldehyde. *J. Org. Chem.* **2019**, *84*, 2307−2315. (c) Whyte, A.; Torelli, A.; Mirabi, B.; Prieto, L.; Rodriguez, J. F.; Lautens, M. Cobalt-Catalyzed Enantioselective Hydroarylation of 1, 6-Enynes. *J. Am. Chem. Soc*. **2020**, *142*, 9510−9517. (d) Zhao, X.; She, Y.; Fang, K.; Li, G. *CuCl-catalyzed Ullmann-type C–N cross-coupling reaction of carbazoles and 2-bromopyridine derivatives. J. Org. Chem*. **2017**, *82*, 1024−1033.

24. Mio, M. J.; Kopel, L. C.; Braun, J. B.; Gadzikwa, T. L.; Hull, K. L.; Brisbois, R. G.; Markworth, C. J.; Grieco, P. A. One-pot synthesis of symmetrical and unsymmetrical bisarylethynes by a modification of the Sonogashira coupling reaction. *Org. Lett.* **2002**, *4*, 3199−3202.
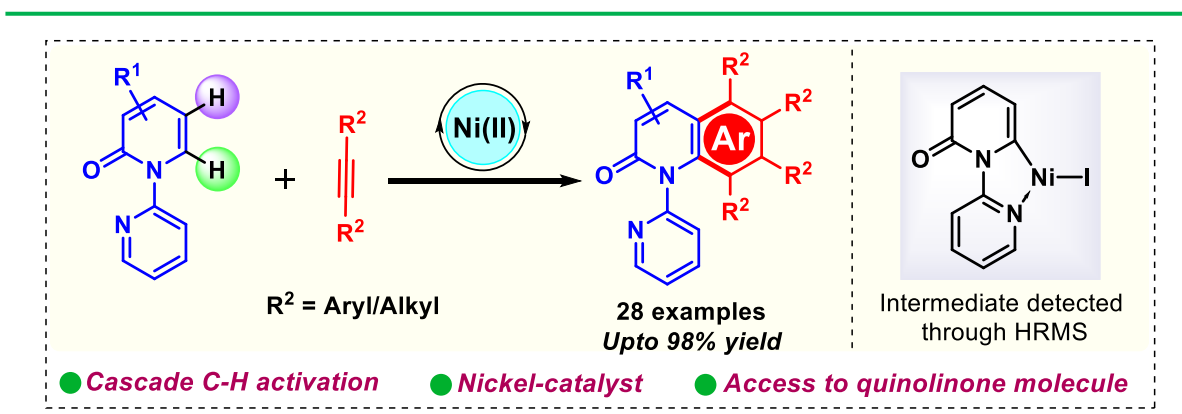
Chapter 5

Switching the Reactivity of the Nickel-Catalyzed reaction of 2-Pyridones with Alkynes: Easy Access to Polyaryl/Polyalkyl Quinolinones

Chapter 5

Switching the Reactivity of the Nickel Catalyzed reaction of 2-Pyridones with Alkynes: Easy Access to Polyaryl/Polyalkyl Quinolinones
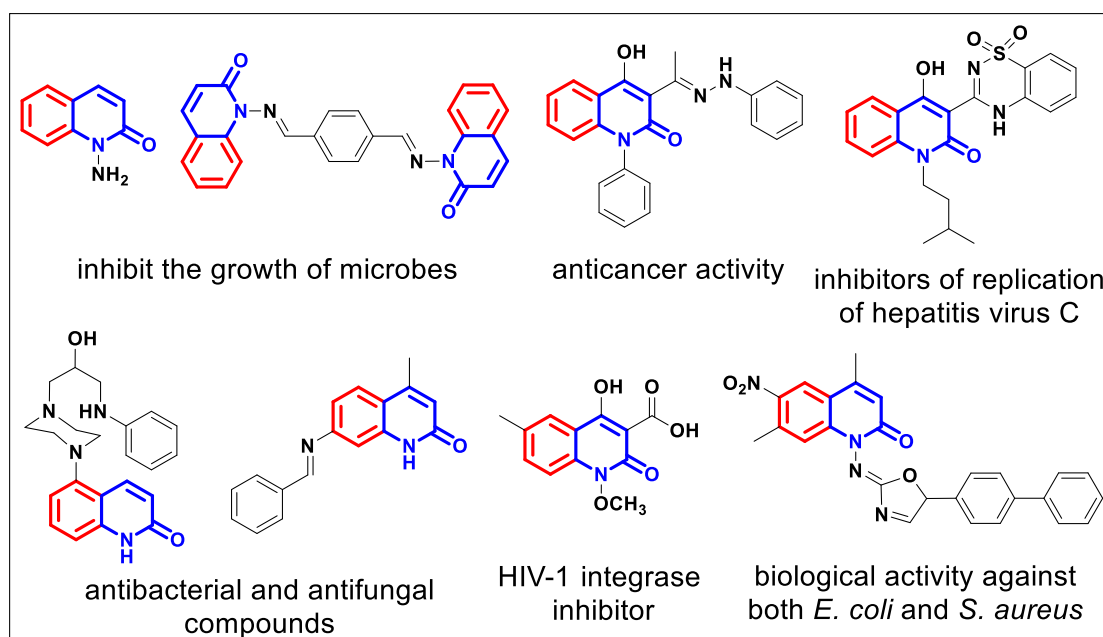
5.1 ABSTRACT: A Ni-catalyzed C6- followed by C5 cascade C-H activation/[2+2+2] annulation of 2-pyridone with alkynes has been achieved. A change in the reaction pathway was achieved by tuning the reaction condition and incorporation of the directing group. A wide variety of substrates and alkynes are amenable to this transformation. The key to success for this transformation is the use of sodium iodide as an additive. More importantly, we detected the five-membered metallacycle intermediate through HRMS wherein iodide is ligated to the metal.

5.2 INTRODUCTION

2-Pyridone is a key structural unit present in many natural products and bioactive molecules[1] and acts as a valuable building block for the synthesis of many bioactive N-heterocycles (Figure 5.1),[2] which can be used to treat a range of ailments, including Alzheimer's disease,[3a] HIV, type 2 diabetes.[3b] Therefore, functionalization of the 2-pyridone has gained immense attention among synthetic chemists. Direct C-H bond functionalization

of the 2-pyridone with transition metal catalysts has recently emerged as a viable and versatile synthetic approach for generating molecules in a highly atom economical manner.[3c] Rapid progress has been made with regard to site-selective C–H functionalization of 2-pyridones at the C3/C5/C6 sites.[4]

Figure 5.1: Selected bioactive 2-pyridone molecules and their applications.

inhibit the growth of microbes

anticancer activity

inhibitors of replication of hepatitis virus C

antibacterial and antifungal compounds

HIV-1 integrase inhibitor

biological activity against both *E. coli* and *S. aureus*

Miura and coworkers reported that the use of easily attachable and detachable 2-pyridyl directing groups to the nitrogen of 2-pyridone might efficiently enhance selective C(6)-H activation.[5] Alkynes, which are readily available building blocks in organic synthesis, offer chemists with a fertile testing ground for the development of complex organic compounds.[6] In these contexts, various research groups have investigated the C6-functionalization of 2-pyridone with alkynes, but the majority of reports are with 2nd-row transition metals.[7] C-C bond formation at the C6 position of pyridone employing alkyne as a reaction partner with 1st-row transition metals has been reported in a limited number of instances.[8-14] As 1st-row transition metals are less expensive and earth-abundant than 2nd and 3rd-row transition metals,[15] use of these metals in catalytic synthetic methods is more economic and C6-sustainable. In this regard, the Ackermann and Li group have demonstrated Mn-catalyzed

functionalization of 2-pyridone with alkyne for the synthesis of indolone alkaloid derivatives[8] (Figure 5.2).

Figure 5.2: C-H functionalization of 2-pyridones using 1st-row transition metals.
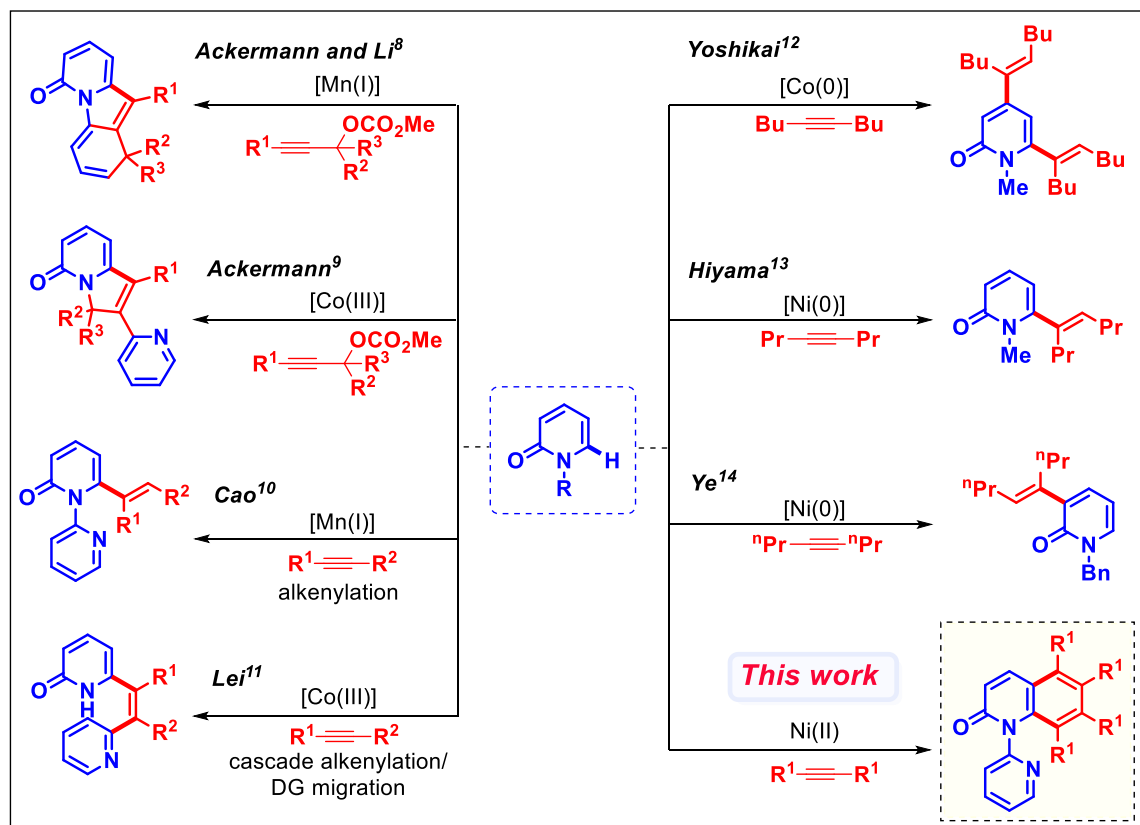
Later, Ackermann et al. demonstrated domino C–H activation/pyridine directing group migration/alkyne annulation catalyzed by Cobalt.[9] In 2021, the Cao group reported high regioselective C(6)-alkenylation of 2-pyridones with internal alkyne using Mn catalysts[10]. Simultaneously, by tuning the reaction condition, Lei's group observed directing group migrated product with Co catalyst.[11] As a result of this, we can conclude that the reaction condition has a significant impact on reactivity, which leaves plenty of opportunity for further exploration. So, in this context, Yoshikai group has reported that Co/Lewis acid catalytic system gives hydrocarbofunctionalization of alkynes with 2-pyridone where they found both C(4) as well as C(6)-alkenylated product[12] (Figure 5.2). Furthermore, the Hiyama group has reported a high-selectivity C(6)-alkenylated product by employing a

nickel catalyst.[13] Later, Ye group developed Ni-catalyzed C(3)−H alkenylation of 2-pyridone with alkynes, affording selectively C(3)-alkenylated product.[14] In any synthetic endeavor controlling selectivity is very essential, especially when there are numerous possibilities from the same starting material with the same metal as the catalyst. Therefore, regulating the reaction condition to preferentially obtain a specific product is a challenging task.

As per the literature reports varying the reaction conditions can switch the reaction pathways between alkenylation and annulation.[16] Generally, the reaction of pyridone with alkyne under the nickel catalyst leads to the formation of alkenylated product at C(3) and C(6)-position of 2-pyridone, which is dictated by (i) coordinating ability of directing group, (ii) the reaction condition.[17] However, there are no reports on the nickel catalyzed C6/C5-H annulation of 2-pyridone with alkyne in a 2+2+2 fashion. So, herein we have explored the first Ni-catalyzed chelation assisted C(6) followed by C(5)-functionalization of 2-pyridone giving the cascade annulated quinolinone product.

5.3 RESULTS AND DISCUSSION

We initiated the optimization studies by employing *N*-pyridyl pyridone **1a** as the model substrate and diphenylacetylene **2a** as the coupling partner (Table 5.1). After a brief survey of the reaction parameters, the desired product **3aa** was obtained in 89% yield using a combination of Ni(acac)$_2$ (10 mol %), PPh$_3$ (20 mol %), NaI (50 mol %) in CH$_3$CN (0.2 M) at 160 °C for 24h (entry 1). When other solvents such as toluene and dioxane were used, the results were all inferior (entries 2-3). Changing the ligand from PPh$_3$ to PPh$_2$Me, davephos resulted in the desired products with lower yields (entries 4-5). Though the combination of Ni(acac)$_2$ and NaI works well for this transformation, we presumed that the combination of NiI$_2$ and NaI might work better. However, surprisingly, when NiI$_2$ was used as a catalyst, it gave the product **3aa** in moderate yield (44%) (entry 6) which suggests

that the combination of Ni(acac)$_2$ and NaI plays a superior role. Such improvement in product yield after the addition of NaI has been observed earlier as well.[18] Further, changing the catalyst to Ni(OTf)$_2$ was found to be less effective (entry 7). Furthermore, screening with different additives such as NaIO$_4$, KI led to a drastic decrease in yields (entries 8-9).
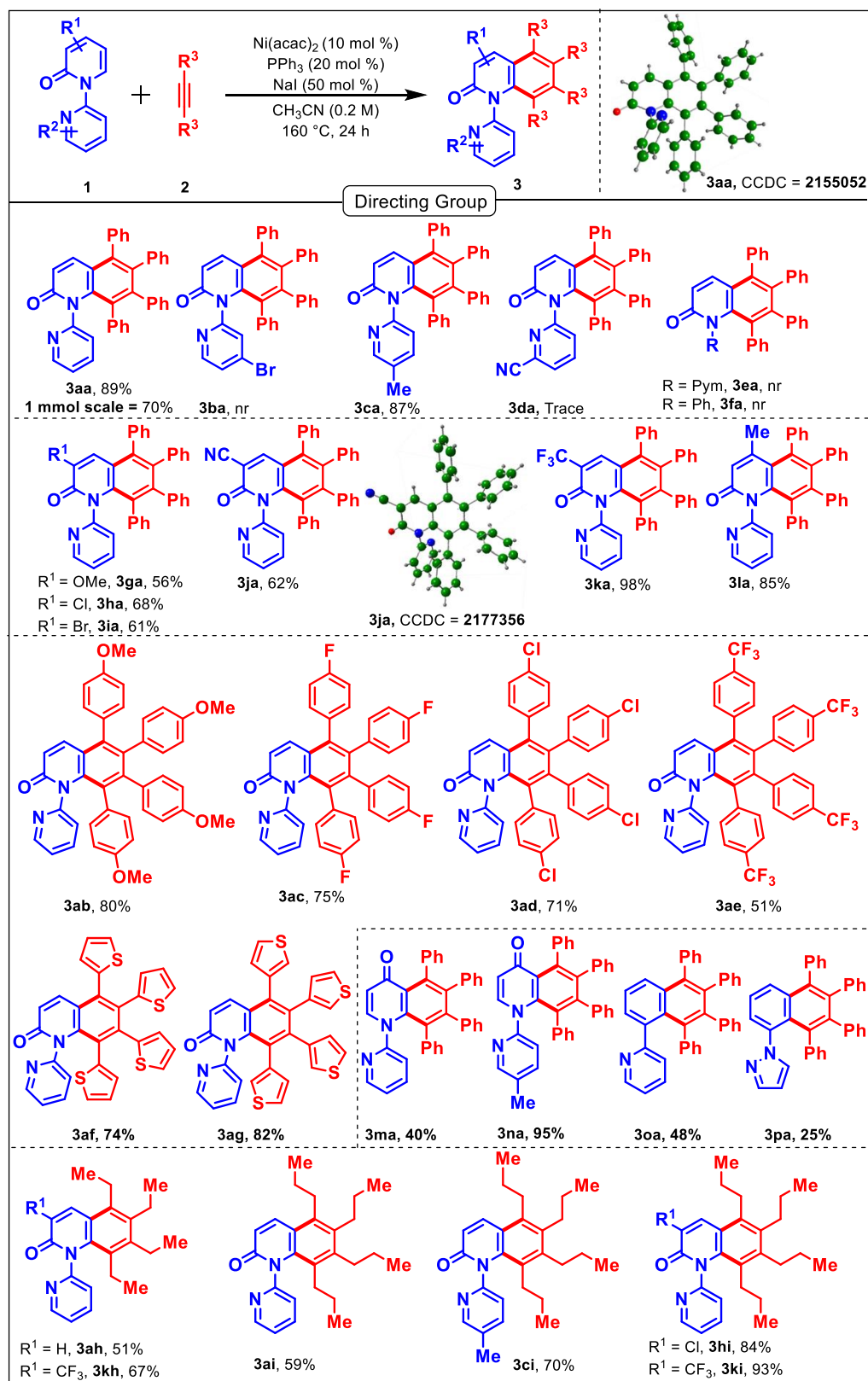
Table 5.1. Optimization of the reaction conditions[a]
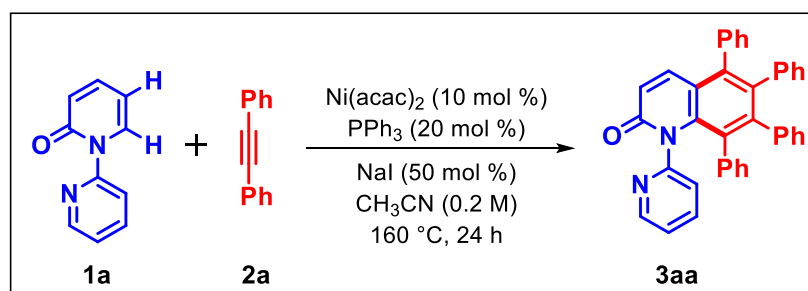
entry	solvent	catalyst	ligand	additive	yield of 3aa[b]
1	*No variation in reaction conditions*				**89**
2	Toluene	Ni(acac)$_2$	PPh$_3$	NaI	56
3	1,4-dioxane	Ni(acac)$_2$	PPh$_3$	NaI	67
4	CH$_3$CN	Ni(acac)$_2$	PPh$_2$Me	NaI	40
5	CH$_3$CN	Ni(acac)$_2$	Davephos	NaI	66
6	CH$_3$CN	NiI$_2$	PPh$_3$	NaI	44
7	CH$_3$CN	Ni(OTf)$_2$	PPh$_3$	NaI	7
8	CH$_3$CN	Ni(acac)$_2$	PPh$_3$	NaIO$_4$	48
9	CH$_3$CN	Ni(acac)$_2$	PPh$_3$	KI	10
10[c]	CH$_3$CN	Ni(acac)$_2$	PPh$_3$	NaI	69
11[d]	CH$_3$CN	Ni(acac)$_2$	PPh$_3$	NaI	61
12	CH$_3$CN	-	PPh$_3$	NaI	nr
13	CH$_3$CN	Ni(acac)$_2$	-	NaI	16
14	CH$_3$CN	Ni(acac)$_2$	PPh$_3$	-	nr

[a]Reaction conditions: **1a** (0.10 mmol), **2a** (4 equiv), catalyst (10 mol %), ligand (20 mol %), additive (50 mol %), solvents (0.5 mL, 0.2 M w.r.t. **1a**), 160 °C, 24 h. [b]Isolated yields. [c]temp = 140 °C. [d]Ni(acac)$_2$ = 5 mol %, PPh$_3$ = 10 mol %

It has been observed that lowering the temperature and catalyst or ligand loading decreases the yield of the product (entries 10-11). Control experiments indicate that Ni(acac)$_2$ was
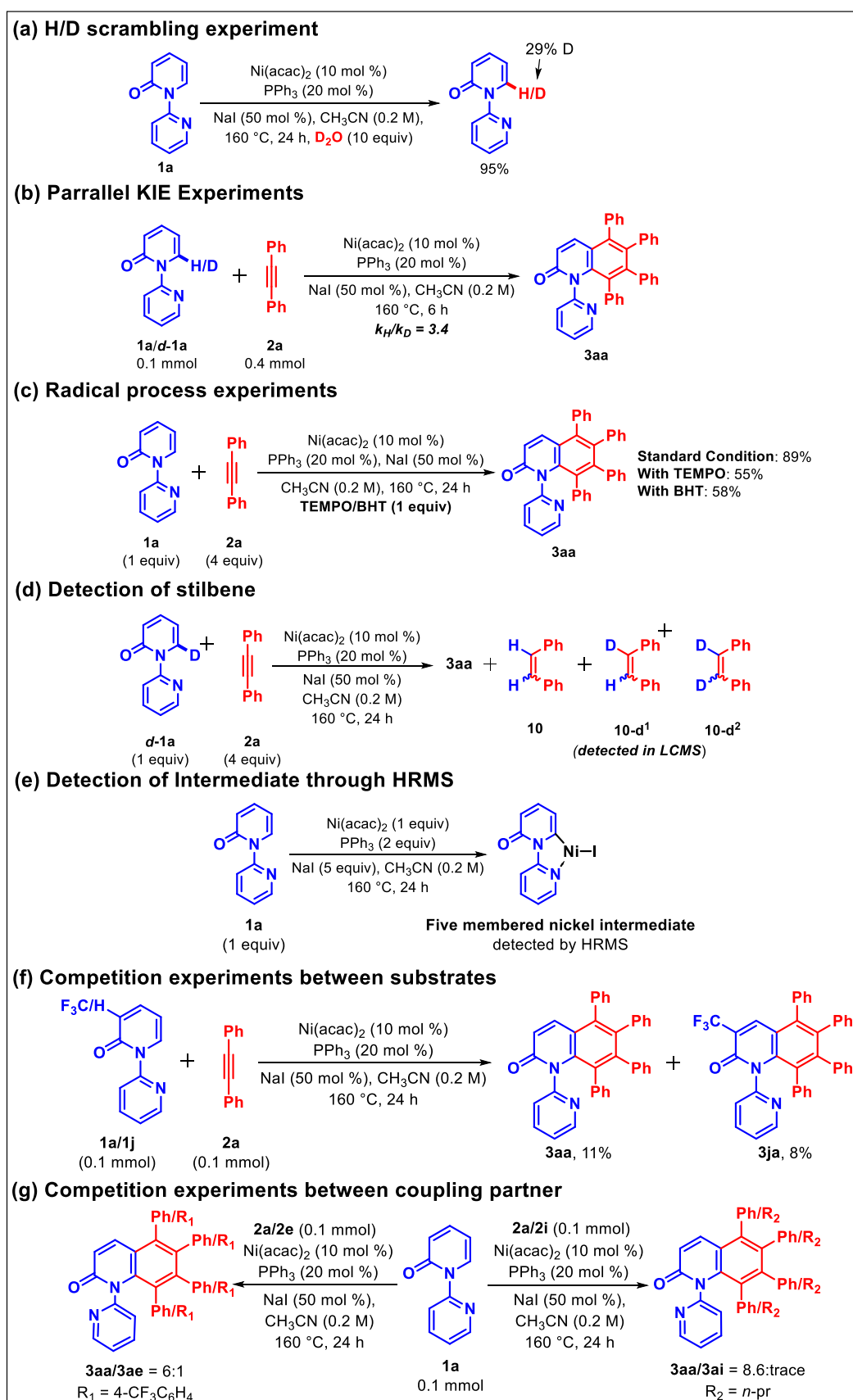
essential for the cascade annulation and also PPh$_3$ ligand is enhancing the reaction rate (entries 12-13). Moreover, it was found that the reaction is not proceeding without NaI, demonstrating the critical role of NaI in the reaction (entry 14).

With the optimized reaction condition in hand, we have examined various substrate scopes of 2*H*-[1,2'-bipyridin]-2-one **1** with alkyne **2**. While screening directing groups, only 5-Me pyridyl directing group gave the product **3ca** (87%) (Scheme 5.1). Whereas, other directing groups are found to be inefficient. Delightfully, this protocol works with a wide range of structurally and electronically different molecules. With C(3)-substitution in the substrate (-OMe/Cl/Br), the products **3ga-3ia** are found in good yield (Scheme 5.1). In addition, the electron-withdrawing group (-CN, -CF$_3$) at C(3)-position of 2-pyridone reacted smoothly to afford the annulated product **3ja** and **3ka** in good to excellent yield. The structure of **3ja** was unambiguously confirmed through single-crystal X-ray analysis. The substitution at C(4)-position of the substrate gave the product **3la** in 85% yield. After screening various substituted pyridone, further, the generality of aromatic internal alkynes was explored, which gave good to excellent yields of the products **3ab-3ag**. The developed protocol was applied on an electronically similar substrate, wherein it was found that the 4-pyridone substrate gave the product **3ma** with a moderate yield of 40%. But with 5'-methyl-bipyridinone substrate, the product **3na** was obtained with a 95% yield. The phenyl pyridine substrate gave the product **3oa** with moderate yield whereas phenyl pyrazole gave the product **3pa** in 25% yield. Further, we extended the scope of this methodology with aliphatic alkynes, it furnished the desired products **3ah-3ai** in good yields. Notably, C(3)-CF$_3$ substituted pyridone reacted with 3-hexyne and 4-octyne resulting in good to excellent yields of desired products **3kh**, **3ki** respectively. Substrate bearing a (–Me) group at the C-5 position of the directing group afforded the alkenylated product **3ci** in 70% yield. In addition, C(3)-Cl substituted pyridone reacted smoothly with 4-octyne giving 84% of the

Scheme 5.1: Substrate scope for the synthesis of 3[a,b]

3aa, CCDC = 2155052

3aa, 89%
1 mmol scale = 70%

3ba, nr

3ca, 87%

3da, Trace

R = Pym, 3ea, nr
R = Ph, 3fa, nr

R[1] = OMe, 3ga, 56%
R[1] = Cl, 3ha, 68%
R[1] = Br, 3ia, 61%

3ja, 62%

3ja, CCDC = 2177356

3ka, 98%

3la, 85%

3ab, 80%

3ac, 75%

3ad, 71%

3ae, 51%

3af, 74%

3ag, 82%

3ma, 40%

3na, 95%

3oa, 48%

3pa, 25%

R[1] = H, 3ah, 51%
R[1] = CF$_3$, 3kh, 67%

3ai, 59%

3ci, 70%

R[1] = Cl, 3hi, 84%
R[1] = CF$_3$, 3ki, 93%

[a]Reaction conditions: **1a** (0.2 mmol), **2a** (0.8 mmol), Ni(acac)$_2$ (10 mol %), PPh$_3$ (20 mol%), NaI (50 mol %), CH$_3$CN (1 mL, 0.2 M w.r.t. **1a**), 160 °C, 24 h. [b]Isolated yields.

Scheme 5.2: Mechanistic Studies

(a) H/D scrambling experiment

(b) Parrallel KIE Experiments

(c) Radical process experiments

Standard Condition: 89%
With TEMPO: 55%
With BHT: 58%

(d) Detection of stilbene

(e) Detection of Intermediate through HRMS

Five membered nickel intermediate
detected by HRMS

(f) Competition experiments between substrates

(g) Competition experiments between coupling partner

annulated product **3hi**. Overall, our methodology was found to be compatible with a broad range of substrates.

To understand the mechanism of this reaction, initially the H/D scrambling experiment has been done. In absence of a coupling partner, 29% deuteration at C(6) position was observed (Scheme 5.2a). It indicates that the reaction is reversible. From the high KIE value, it is concluded that the C-H activation step may be the rate-determining step (Scheme 5.2b). Further, when the reaction was performed in presence of a radical scavenger (TEMPO/BHT), a good yield of the product was observed, indicating that the reaction is going through ionic pathways (Scheme 5.2c). It was found that stilbene was produced during the reaction. For further confirmation, C(6)-deuterated pyridone **1a** along with diphenylacetylene **2a** has been exposed under the standard reaction condition, where the formation of deuterated stilbene was detected by LCMS (Scheme 5.2d). This result implies that the diphenylacetylene is acting as a coupling partner as well as an internal oxidant to carry forward the reaction. The reaction was also carried out in the presence of a stoichiometric amount of nickel catalyst, and the formation of a five-membered nickelacycle was confirmed by HRMS (Scheme 5.2e). Electron donating substrates has been found to dominate over electron-withdrawing substrates in an intermolecular competition study (Scheme 5.2f). From the intermolecular competition study of the coupling partners, it has been found that electron-donating aryl alkyne dominates over electron-withdrawing aryl alkyne whereas aryl alkyne dominates over aliphatic alkyne (Scheme 5.2g).

The directing group removal experiment was carried out in the presence of MeOTf and NaBH4 yielded the product **4** in 59% yield (Scheme 5.3a). The **3aa** have been subjected for further functionalization which give the product **5** in trace amount, detected in HRMS (Scheme 5.3b).

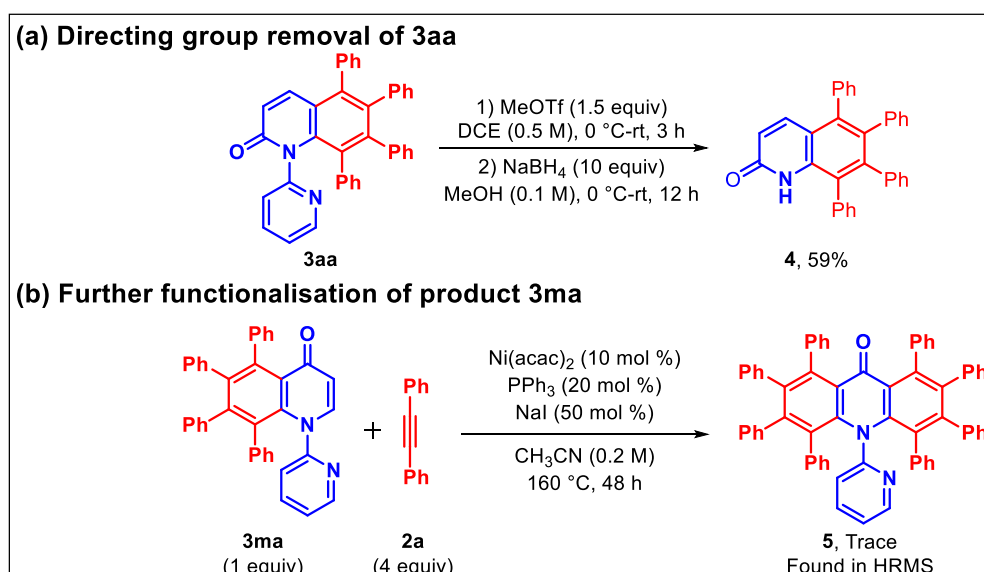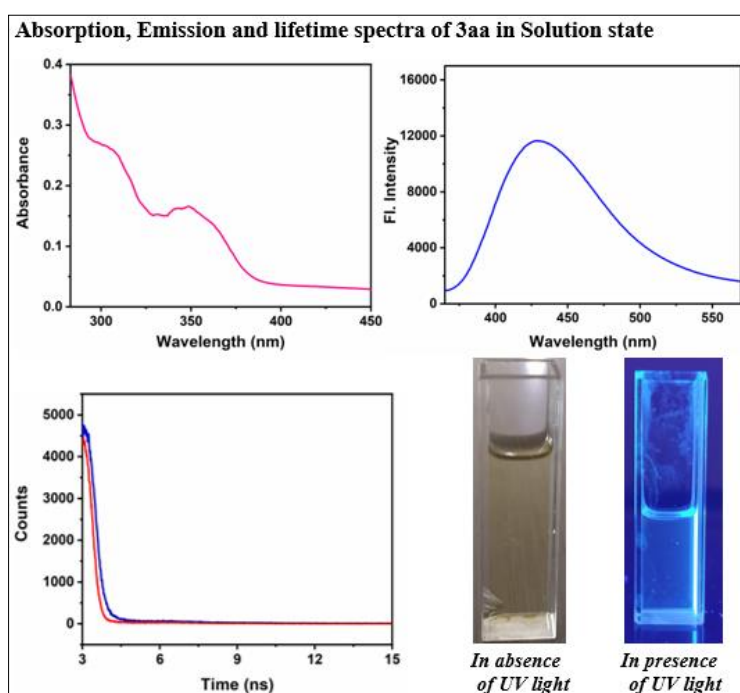**Scheme 5.3: DG removal and further functionalization of product**

(a) Directing group removal of 3aa

1) MeOTf (1.5 equiv)
DCE (0.5 M), 0 °C-rt, 3 h

2) NaBH$_4$ (10 equiv)
MeOH (0.1 M), 0 °C-rt, 12 h

3aa

4, 59%

(b) Further functionalisation of product 3ma

Ni(acac)$_2$ (10 mol %)
PPh$_3$ (20 mol %)
NaI (50 mol %)

CH$_3$CN (0.2 M)
160 °C, 48 h

3ma
(1 equiv)

2a
(4 equiv)

5, Trace
Found in HRMS

Figure 5.3: Optical Property of the product 3aa:

Additionally, photophysical studies of 3aa was investigated to demonstrate their potential application as an optical material. The products were studied in solution state (dichloromethane) at room temperature. The absorption and emission spectra of these species were shown in Figure 5.3. The fluorescence spectra of 3aa show emission maxima

at 430 nm. It is found that the product 3aa shows lifetime (1 ns) in excited state. Generally, all these π-conjugated systems exhibited interesting optical properties.

Scheme 5.4: Proposed Catalytic cycle

Based on the above mechanistic studies and literature,[19] a plausible catalytic cycle for the synthesis of **3** is depicted in scheme 5.4. Initially, the Ni(II)-catalyst undergoes ligand exchange to generate the pre-catalyst (PPh$_3$)$_2$Ni(acac)I. Then pyridone substrate **1** coordinates with (PPh$_3$)$_2$Ni(acac)I to give intermediate **A** through a concerted metallation–

deprotonation (CMD) pathway. As acac$^-$ is a stronger ligand than I$^-$, there is a possible ligand exchange of active catalyst **A** with acac ligand replacing I. Therefore, addition of NaI is helpful in maintaining a critical concentration of the active catalyst **A** to enable the catalytic cycle. Then, alkyne **2** coordinates with intermediate **A** and gives intermediate **B**. Migratory insertion of alkyne forms the intermediate **C**. Then, the second C-H bond activation leads to the formation of five-membered cyclic intermediate **D**. Further, alkyne insertion gives the intermediate **E** which undergoes reductive eliminations and delivers the desired product **3** along with the formation of $L_2Ni(0)$ intermediate **F**. Then, the oxidative addition of $L_2Ni(0)$ **F** species into the C-H bond of substrate **1** gives intermediate **G**. Reduction of the alkyne (stilbene detected in LCMS) regenerates active catalyst **A** for the next catalytic cycle.

5.4 CONCLUSION

In summary, we have successfully developed a Ni-catalyzed [2+2+2] annulation reaction of pyridone with an alkyne, and a distinct class of quinolones has been obtained. 5-membered nickelacycle has been confirmed by HRMS, which confirms the catalytic pathway. A wide variety of substrates and alkynes are well tolerated and form the annulated product up to 98% yield. Here, no external oxidant is required. Alkyne is playing a dual role both as a coupling partner and internal oxidant. The use of sodium iodide as an additive plays a crucial role to synthesize the quinolone moiety. Further photophysical studies of the tetrasubstituted quinolinone molecule has been studied which demonstrated their potential utility in material chemistry.[20]

5.5 EXPERIMENTAL SECTION:[21]

Reactions were performed using oven dried borosil seal-tube glass vial with Teflon-coated magnetic stirring bars under N_2 atmosphere. Column chromatography was done by using 100-200 and 230-400 mesh size silica gel of Acme synthetic chemicals Company. A

gradient elution was performed by using distilled petroleum ether and ethyl acetate. TLC plates were detected under UV light at 254 nm. ^{1}H NMR, ^{13}C NMR & ^{19}F NMR were recorded on Bruker AV 400 and 700 MHz spectrometers using CDCl$_3$ as the deuterated solvent.[22] Chemical shifts (δ) are reported in ppm relative to the residual solvents (CHCl$_3$) signal (δ = 7.26 for ^{1}H NMR and δ = 77.36 for ^{13}C NMR). Data for ^{1}H NMR spectra are reported as follows: chemical shift (multiplicity, coupling constants, number of hydrogen). Abbreviations are as follows: s (singlet), d (doublet), t (triplet), q (quartet), quint (quintet), m (multiplet), dd (double doublet), br (broad signal), J (coupling constants) in Hz (hertz). High-Resolution Mass Spectrometry (HRMS) data was recorded using Bruker micro TOF Q-II mass spectrometer using methanol as solvent. IR spectra were recorded on a FTIR system and values are reported in frequency of absorption (cm^{-1}). Melting point was performed using Stuart^{TM} melting point apparatus SMP10. X-ray analysis was conducted using Rigaku Smartlab X-ray diffractometer, Steady state absorption and emission spectra are recorded using a Jasco V-730 spectrophotometer and Shimadzu RF-6000 fluorescence spectrophotometer (Shimadzu Corporation), respectively. For emission spectra, samples were excited at 430 nm at SCS, NISER. For the measurement of time-resolved fluorescence, a time-correlated single-photon counting (TCSPC) spectrometer (Edinburgh, OB920) was used. Reagents and starting materials were purchased from Sigma Aldrich, Alfa Aesar, TCI, Avra, Spectrochem and other commercially available sources and used without further purification unless otherwise noted.

5.5.1 General procedure for the preparation of *N*-protected pyridones 1:

N-protected pyridone substrates **1** were prepared according to the reported procedures[23] and all are known compounds and its spectral data were in good agreement with the corresponding literature values. To an oven dried sealed tube charged with a stirring bar, 2-hydroxypyridine (1 equiv), CuI (5 mol %) and toluene (0.75 M) were added sequentially

under nitrogen atmosphere. Then K_3PO_4 (2 equiv) was added to reaction mixture inside the glove-box. To the solution, 2-halo pyridine (2 equiv), DMEDA (10 mol %) were added in N_2 atmosphere and close the sealed tube. The reaction tube kept on a pre-heated aluminum block at 120 °C for 15-20 h. After completion of the reaction (as monitored by TLC analysis), the reaction mixture was quenched with ethylene diamine solution (2 mL). The organic material was extracted with DCM (100 mL $\times$ 3), washed with brine, dried over anhydrous Na_2SO_4 and concentrated using a rotary evaporator to give crude reaction mixture. The crude mixture was purified by column chromatography using EtOAc/hexane mixture on silica-gel to furnish the pure product **1**.

5.5.2 General procedure for preparation of internal alkynes 2:

Alkynes **2** were prepared according to the reported procedures[24] and all are known compounds and its spectral data were in good agreement with the corresponding literature values. To an oven dried sealed tube charged with a stirring bar, dry benzene (0.1 M), aryl iodide (4 equiv), trimethyl silylacetylene (1 equiv), $PdCl_2(PPh_3)_2$ (5 mol %), CuI (80 mol %), DBU (6 equiv) and distilled water (40 mol %) were added sequentially under nitrogen atmosphere. The solution was stirred at rt for 20-30 minute and then kept it in a pre-heated aluminum block at 60 °C for 15-20 h. After completion of the reaction (as monitored by TLC analysis), the reaction mixture was quenched with 10% HCl (10 mL). Then the crude mixture was extracted with EtOAc and washed with saturated NaCl. After drying over anhydrous Na_2SO_4, the crude mixture was purified by column chromatography using EtOAc/hexane mixture on silica-gel to furnish the pure product **2**.

5.5.3 General reaction procedure for C(6)-H & C(5)-H activation of *2H*-[1,2'-bipyridin]-2-one with diphenyl acetylene as coupling partner 3:

To an oven dried sealed tube charged with a stirring bar under N_2 atmosphere, the *2H*-[1,2'-bipyridin]-2-one **1** (0.1 mmol, 1equiv), alkyne **2** (0.4 mmol, 4 equiv), $Ni(acac)_2$ (10 mol %),

PPh$_3$ (20 mol %), NaI (50 mol %) were added and sealed. The sealed tube was high-vacuumed and refilled with N$_2$. Then CH$_3$CN solvent (0.5 mL, 0.2 M w.r.t. **1a**) was added to the reaction mixture. Then the reaction mixture was vigorously stirred at 160 °C on preheated aluminum block for 24 h. After 24 h (upon completion of reaction as monitored by TLC analysis), the reaction mixture was cooled to room temperature and diluted with EtOAc and passed through a short celite pad. The solvent was evaporated under reduced pressure and the residue was purified by column chromatography using 35% EtOAc/hexane mixture on silica gel to give the pure product **3**.

5.5.4 Directing group removal of 3aa:[25]

To an oven dried sealed tube charged with a stirring bar under N$_2$ atmosphere, the compound **3aa** (32 mg, 0.06 mmol, 1 equiv) was added followed by addition of DCE (0.5 M, 0.12 mL) solvent. The reaction mixture was cooled to 0 °C and then MeOTf (14.8 mg, 0.09 mmol, 1.5 equiv) was added to the reaction mixture over 1 min under cold condition. Then the reaction mixture was stirred for 3 h at rt. After 3 h, MeOH (0.1 M, 0.6 mL), NaBH$_4$ (22.7 mg, 0.6 mmol, 10 equiv) were added to the reaction mixture at 0 °C, which was further stirred for 12 h at rt. The resulting mixture was quenched with saturated aqueous NH$_4$Cl (2 mL) solution and concentrated in vacuum. The aqueous layer was extracted with EtOAc (5 mL) and the organic layer was dried on anhydrous MgSO$_4$ and concentrated in vacuum. The residue was purified by column chromatography using EtOAc/hexane mixture on silica gel to give the pure product **4** (16 mg, 59% yield).

5.5.5 Detection of nickel-intermediate:
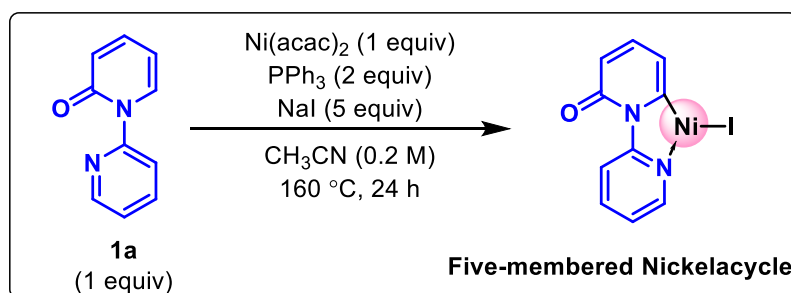
Intermediate HRMS: HRMS (ESI) m/z: M+H]$^+$ Calcd for C$_{10}$H$_8$IN$_2$NiO: 356.9029, Found: 356.9027.
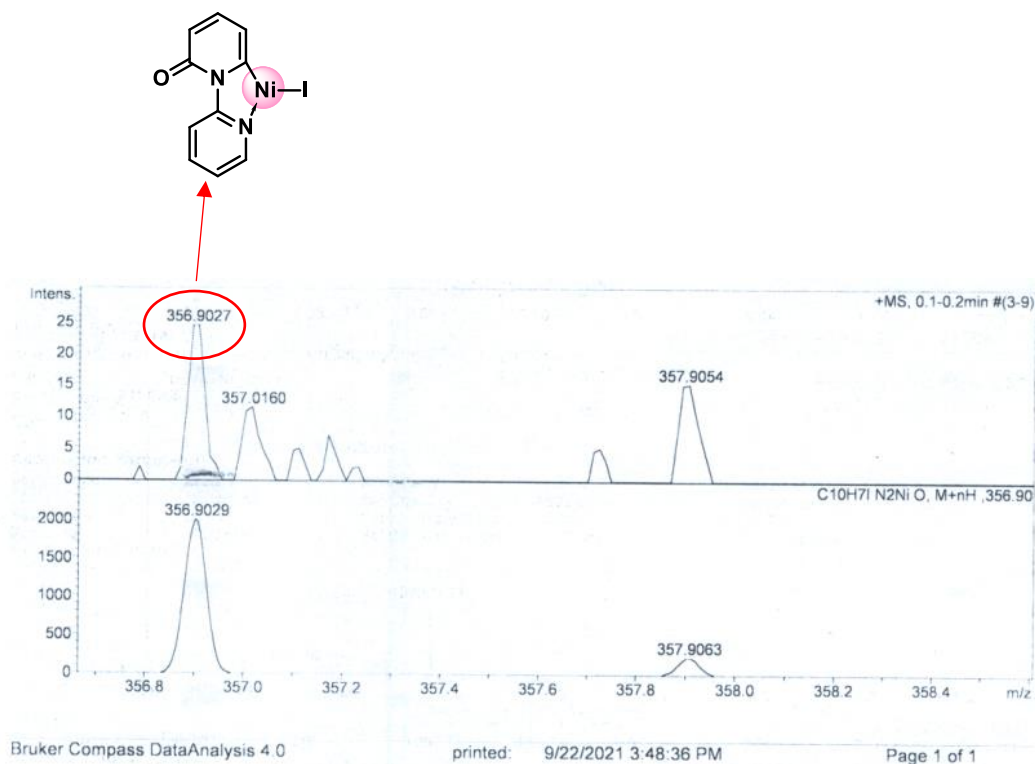
To an oven dried sealed tube charged with a stirring bar under N$_2$ atmosphere, the *2H*-[1,2'-bipyridin]-2-one **1a** (0.1 mmol), Ni(acac)$_2$ (0.1 mmol, 1 equiv), PPh$_3$ (0.2 mmol, 2 equiv), NaI (0.5 mmol, 5 equiv) were added and sealed. The sealed tube was high-vacuumed and refilled with N$_2$. Then CH$_3$CN solvent (0.2 M) was added to the reaction mixture. Then the reaction mixture was vigorously stirred at 160 °C on preheated aluminum block for 24 h. After 24 h, the reaction mixture was cooled to room temperature. A little aliquot was taken from the reaction mixture and diluted with MeOH and filtered. The crude was filtered and submitted for HRMS in methanol, from which formation of five membered nickel cycle was confirmed.

5.5.6 Detection of Stilbene:
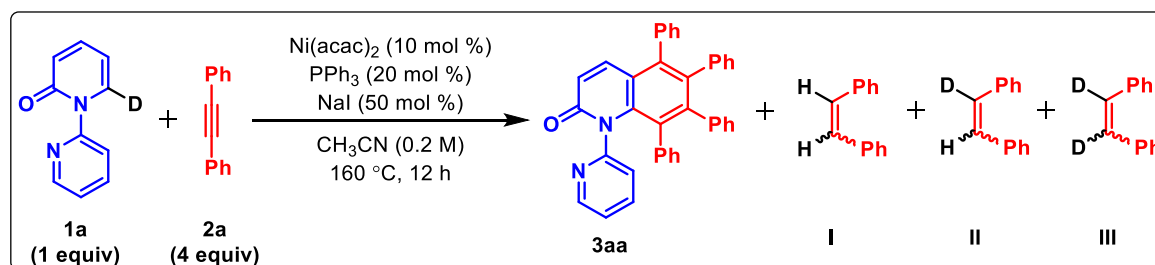
(a) LCMS (ESI) m/z of **I**: $[M+H]^+$ Calcd for $C_{14}H_{12}$: 181.1; Found: 181.1.

(b) LCMS (ESI) m/z of **II**: $[M+H]^+$ Calcd for $C_{14}H_{11}D$: 182.1; Found: 182.1.

(c) LCMS (ESI) m/z of **III**: $[M+H]^+$ Calcd for $C_{14}H_{10}D_2$: 183.1; Found: 183.1.
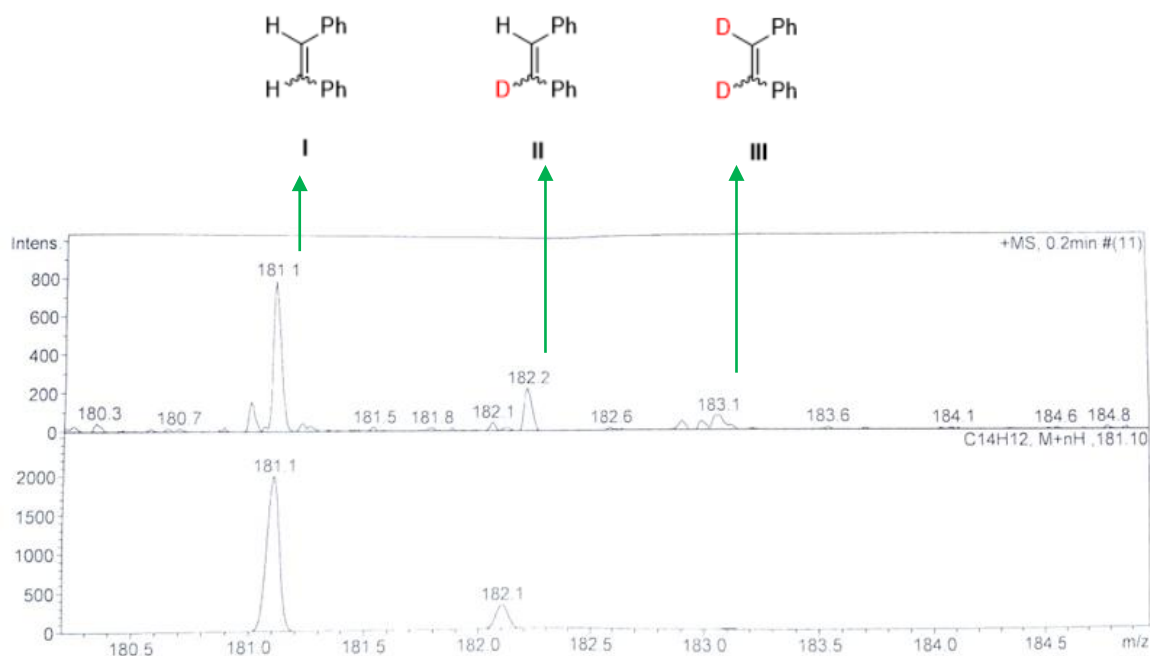
To an oven dried sealed tube charged with a stirring bar under N_2 atmosphere, the deuterated pyridone *d*-**1a** (0.1 mmol), diphenylacetylene **2a** (4 equiv), Ni(acac)$_2$ (10 mol %), PPh$_3$ (20 mol %), NaI (50 mol %) were added and sealed. The sealed tube was high-vacuumed and refilled with N_2. Then CH$_3$CN solvent (0.2 M) was added to the reaction mixture. Then the reaction mixture was vigorously stirred at 160 °C on preheated aluminum block for 12 h. After 12 h, the reaction mixture was cooled to room temperature and diluted with EtOAc and passed through a short celite pad. The solvent was evaporated under

reduced pressure and the residue was submitted for LCMS in methanol from which formation of deuterated stilbenes (**10, 10-d^1, 10-d^2**) was detected along with the formation of product **3aa**.

5.5.7 Experimental characterization data for starting materials:[23,24]

2H-[1,2'-bipyridin]-2-one (1a):[23]
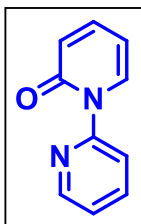
Physical State: white solid (155 mg for 1.0 mmol scale, 90% yield). R_f-value: 0.3 (50% EtOAc/hexane). ^{1}H NMR (CDCl$_3$, 400 MHz): δ 8.55–8.54 (m, 1H), 8.01 (d, J = 8.4 Hz, 1H), 7.94 (dd, J = 7.2, 1.6 Hz, 1H), 7.84–7.80 (m, 1H), 7.38–7.34 (m, 1H), 7.31–7.28 (m, 1H), 6.61 (d, J = 9.2 Hz, 1H), 6.28–6.24 (m, 1H). ^{13}C{^{1}H} NMR (CDCl$_3$, 100 MHz): δ 162.6, 152.2, 149.3, 140.5, 138.1, 136.4, 123.5, 122.5, 121.8, 106.6.

4'-bromo-2H-[1,2'-bipyridin]-2-one (1b):[23]
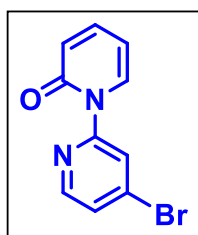
Physical State: white solid (126 mg for 1.0 mmol scale, 50% yield). R_f-value: 0.7 (50% EtOAc/hexane). ^{1}H NMR (CDCl$_3$, 700 MHz): δ 8.39–8.37 (m, 1H), 8.23–8.22 (m, 1H), 7.88–7.86 (m, 1H), 7.49–7.47 (m, 1H), 7.41–7.37 (m, 1H), 6.65–6.63 (m, 1H), 6.31–6.28 (m, 1H). ^{13}C{^{1}H} NMR (CDCl$_3$, 176 MHz): δ 162.4, 152.8, 149.5, 140.7, 135.9, 134.1, 126.9, 125.1, 122.6, 106.9.

5'-methyl-2H-[1,2'-bipyridin]-2-one (1c):[23]
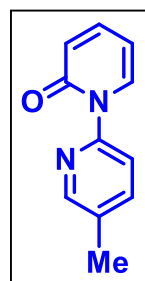
Physical State: pale yellow solid (162 mg for 1.0 mmol scale, 87% yield). R_f-value: 0.5 (50% EtOAc/hexane). ^{1}H NMR (CDCl$_3$, 700 MHz): δ 8.38 (d, J = 1.4 Hz, 1H), 7.82 (dd, J = 7.0, 1.4 Hz, 1H), 7.81 (d, J = 7.7 Hz, 1H), 7.64 (dd, J = 8.4, 2.1 Hz, 1H), 7.40–7.37 (m, 1H), 6.64 (d, J = 9.1 Hz, 1H), 6.29–6.27 (m, 1H), 2.39 (s, 3H). ^{13}C{^{1}H} NMR (CDCl$_3$, 176 MHz): δ 162.6, 150.1, 149.4, 140.4, 138.7, 136.6, 133.4, 122.4, 121.1, 106.5, 18.35.

2-oxo-2*H*-[1,2'-bipyridine]-6'-carbonitrile (1d):[23]
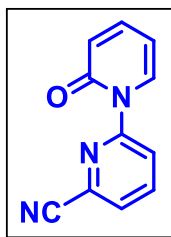
Physical State: white solid (140 mg for 1.0 mmol scale, 71% yield). R_f-value: 0.2 (50% EtOAc/hexane). ^{1}H NMR (CDCl$_3$, 400 MHz): δ 8.36–8.34 (m, 1H), 8.00–7.95 (m, 2H), 7.72–7.70 (m, 1H), 7.45–7.40 (m, 1H), 6.67–6.66 (m, 1H), 6.37–6.33 (m, 1H). ^{13}C{^{1}H} NMR (CDCl$_3$, 176 MHz): δ 162.4, 153.0, 141.1, 139.1, 135.5, 132.8, 127.9, 125.5, 122.7, 116.7, 107.3.

1-(pyrimidin-2-yl)pyridin-2(1*H*)-one (1e):[23]
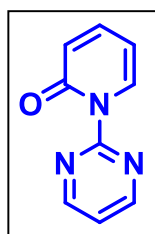
Physical State: brown solid (78 mg for 1.0 mmol scale, 45% yield). R_f-value: 0.5 (50% EtOAc/hexane). ^{1}H NMR (CDCl$_3$, 700 MHz): δ 8.62 (d, J = 4.9 Hz, 2H), 8.39 (dd, J = 4.9, 1.4 Hz, 1H), 7.85–7.82 (m, 1H), 7.22–7.21 (m, 1H), 7.14 (d, J = 7.7 Hz, 1H), 7.11 (t, J = 4.9 Hz, 1H). ^{13}C{^{1}H} NMR (CDCl$_3$, 176 MHz): δ 164.9, 160.8, 160.1, 148.8, 140.2, 121.6, 117.4, 115.5.

1-phenylpyridin-2(1*H*)-one (1f):[23]
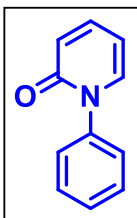
Physical State: white solid (128 mg for 1.0 mmol scale, 75% yield). R_f-value: 0.3 (50% EtOAc/hexane). ^{1}H NMR (CDCl$_3$, 700 MHz): δ 7.49 (t, J = 7.7 Hz, 2H), 7.43–7.38 (m, 4H), 7.34–7.33 (m, 1H), 6.66 (d, J = 9.8 Hz, 1H), 6.25–6.23 (m, 1H). ^{13}C{^{1}H} NMR (CDCl$_3$, 176 MHz): δ 162.8, 141.3, 140.2, 138.3, 129.7, 128.8, 126.9, 122.3, 106.2.

3-methoxy-2*H*-[1,2'-bipyridin]-2-one (1g):[23]
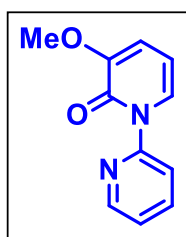
Physical State: brown liquid (101 mg for 1.0 mmol scale, 50% yield). R_f-value: 0.5 (50% EtOAc/hexane). ^{1}H NMR (CDCl$_3$, 400 MHz): δ 8.56–8.55 (m, 1H), 7.95 (d, J = 8.0 Hz, 1H), 7.83 (td, J = 7.6, 1.6 Hz, 1H), 7.51 (dd, J = 7.2, 1.6 Hz, 1H), 7.32–7.29 (m, 1H), 6.67 (dd, J = 7.2, 1.2 Hz, 1H), 6.23 (t, J = 7.2 Hz, 1H), 3.86 (s, 3H). ^{13}C{^{1}H} NMR

(CDCl$_3$, 176 MHz): δ 158.1, 152.1, 150.7, 149.0, 138.1, 127.2, 123.4, 121.8, 112.6, 105.3, 56.3.

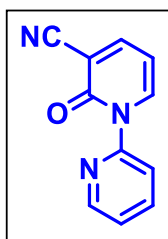### 3-chloro-2*H*-[1,2'-bipyridin]-2-one (1h):[23]
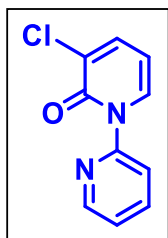
Physical State: brown solid (182 mg for 1.0 mmol scale, 88% yield). R$_f$-value: 0.5 (50% EtOAc/hexane). ^{1}H NMR (CDCl$_3$, 700 MHz): δ 8.57–8.56 (m, 1H), 7.97 (d, J = 8.4 Hz, 1H), 7.88–7.85 (m, 2H), 7.62–7.60 (m, 1H), 7.36–7.34 (m, 1H), 6.28 (t, J = 7.0 Hz, 1H). ^{13}C{^{1}H} NMR (CDCl$_3$, 176 MHz): δ 158.8, 151.9, 149.2, 138.5, 138.2, 135.1, 127.6, 123.9, 121.7, 105.8.

3-bromo-2*H*-[1,2'-bipyridin]-2-one (1i):[23]
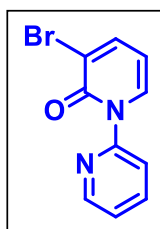
Physical State: brown solid (201 mg for 1.0 mmol scale, 80% yield). R$_f$-value: 0.4 (50% EtOAc/hexane). ^{1}H NMR (CDCl$_3$, 700 MHz): δ 8.56–8.54 (m, 1H), 7.97–7.91 (m, 2H), 7.87–7.80 (m, 2H), 7.36–7.33 (m, 1H), 6.23–6.20 (m, 1H). ^{13}C{^{1}H} NMR (CDCl$_3$, 176 MHz): δ 158.8, 152.0, 149.2, 142.5 (2C), 138.2, 136.1, 123.9, 121.7, 106.6.

### 2-oxo-2*H*-[1,2'-bipyridine]-3-carbonitrile (1j):[23]

Physical State: brown solid (132 mg for 1.0 mmol scale, 67% yield). R$_f$-value: 0.3 (40% EtOAc/hexane). ^{1}H NMR (CDCl$_3$, 700 MHz): δ 8.58 (dd, J = 4.9, 1.4 Hz, 1H), 8.24 (dd, J = 7.0, 2.1 Hz, 1H), 8.00 (d, J = 8.4 Hz, 1H), 7.91–7.88 (m, 2H), 7.41–7.39 (m, 1H), 6.42 (t, J = 7.0 Hz, 1H). ^{13}C{^{1}H} NMR (CDCl$_3$, 176 MHz): δ 159.5, 150.7, 149.4, 148.3, 141.7, 138.5, 124.4, 121.4, 115.6, 107.5, 106.0.

### 3-(trifluoromethyl)-2*H*-[1,2'-bipyridin]-2-one (1k):[23]
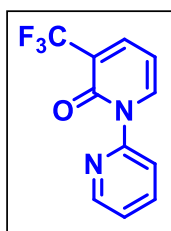
Physical State: white solid (185 mg for 1.0 mmol scale, 77% yield). R$_f$-value: 0.6 (50% EtOAc/hexane). ^{1}H NMR (CDCl$_3$, 400 MHz): δ 8.59–8.57 (m, 1H), 8.14 (dd, J = 7.2, 1.6 Hz, 1H), 8.02–8.00 (m, 1H), 7.88–7.82 (m, 2H), 7.38–7.35 (m, 1H), 6.38 (t, J = 7.2 Hz, 1H). ^{13}C{^{1}H} NMR (CDCl$_3$, 176 MHz): δ 158.4, 151.1, 149.4, 140.5, 140.0 (q, J_{C-F} = 5.3 Hz), 138.2, 124.1, 122.9 (q, J_{C-F} = 271.0 Hz), 122.1 (q, J_{C-F} = 31.7 Hz), 121.8, 104.7.

4-methyl-2*H*-[1,2'-bipyridin]-2-one (1l):[23]
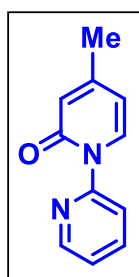
Physical State: white solid (128 mg for 1.0 mmol scale, 69% yield). R$_f$-value: 0.2 (30% EtOAc/hexane). ^{1}H NMR (CDCl$_3$, 700 MHz): δ 8.55 (d, J = 4.9 Hz, 1H), 7.95 (d, J = 8.4 Hz, 1H), 7.83–7.79 (m, 2H), 7.30–7.28 (m, 1H), 6.44 (s, 1H), 6.15 (d, J = 7.7 Hz, 1H), 2.23 (s, 3H). ^{13}C{^{1}H} NMR (CDCl$_3$, 176 MHz): δ 162.5, 152.3, 152.2, 149.1, 138.0, 135.2, 123.3, 121.8, 120.4, 190.4, 21.6.

4*H*-[1,2'-bipyridin]-4-one (1m):[23]
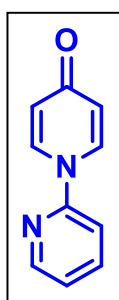
Physical State: white solid (100 mg for 1.0 mmol scale, 58% yield). R$_f$-value: 0.2 (5% Methanol/DCM). ^{1}H NMR (CDCl$_3$, 400 MHz): δ 8.55–8.54 (m, 1H), 8.23–8.19 (m, 2H), 7.93–7.89 (m, 1H), 7.40 (d, J = 8.4 Hz, 1H), 7.35–7.32 (m, 1H), 6.53–6.50 (m, 2H). ^{13}C{^{1}H} NMR (CDCl$_3$, 100 MHz): δ 180.3, 152.4, 149.5, 139.9, 136.3, 122.8, 119.2, 113.2.

5'-methyl-4*H*-[1,2'-bipyridin]-4-one (1n):
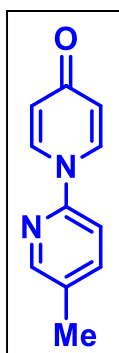
Physical State: brown solid (112 mg for 1.0 mmol scale, 60% yield). m.p.: 147-149 °C. R_f -value: 0.3 (5% Methanol/DCM). ^{1}H NMR (CDCl$_3$, 700 MHz): δ 8.34 (s, 1H), 8.15 (d, J = 7.7 Hz, 2H), 7.70 (d, J = 8.4 Hz, 1H), 7.28–7.27 (m, 1H), 6.51 (d, J = 7.7 Hz, 2H), 2.41 (s, 3H). ^{13}C{^{1}H} NMR (CDCl$_3$, 176 MHz): δ 180.1, 150.3, 149.4, 140.3, 136.5, 132.8, 118.9, 112.8, 18.0. IR (KBr, cm^{-1}): 3421, 2924, 1637, 1555, 1484, 1284, 1191. HRMS (ESI) m/z: [M+H]$^+$ Calcd for C$_{11}$H$_{11}$N$_2$O 187.0871; Found 187.0857.

1,2-bis(4-methoxyphenyl)ethyne (2b):[24]
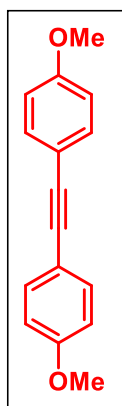
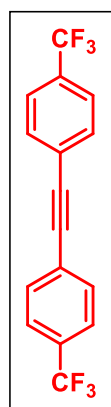Physical State: white solid (162 mg for 1.0 mmol scale, 68% yield). R_f-value: 0.2 (5% E/hexane). ^{1}H NMR (CDCl$_3$, 700 MHz): δ 7.44 (d, J = 8.4 Hz, 4H), 6.85 (d, J = 9.1 Hz, 4H), 3.80 (s, 6H). ^{13}C{^{1}H} NMR (CDCl$_3$, 176 MHz): δ 159.7, 133.2, 116.0, 114.3, 88.3, 55.6.

1,2-bis(4-fluorophenyl)ethyne (2c):[24]
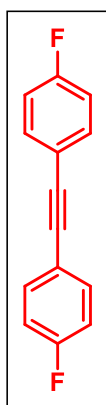
Physical State: white solid (161 mg for 1.0 mmol scale, 75% yield). R_f-value: 0.9 (100% Hexane). ^{1}H NMR (CDCl$_3$, 700 MHz): δ 7.50–7.48 (m, 4H), 7.05–7.03 (m, 4H). ^{13}C{^{1}H} NMR (CDCl$_3$, 176 MHz): δ 162.9 (d, $J_{C\text{-}F}$ = 249.9 Hz), 133.8 (d, $J_{C\text{-}F}$ = 7.0 Hz), 119.5 (d, $J_{C\text{-}F}$ = 1.8 Hz), 116.0 (d, $J_{C\text{-}F}$ = 22.9 Hz), 88.3.

1,2-bis(4-chlorophenyl)ethyne (2d):[24]
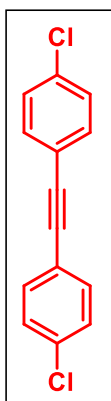
Physical State: white solid (178 mg for 1.0 mmol scale, 72% yield). R_f-value: 0.8 (100% Hexane). ^{1}H NMR (CDCl$_3$, 700 MHz): δ 7.45–7.44 (m, 4H), 7.33–7.32 (m, 4H). ^{13}C{^{1}H} NMR (CDCl$_3$, 176 MHz): δ 134.9, 133.1, 129.1, 121.8, 89.5.

1,2-bis(4-(trifluoromethyl)phenyl)ethyne (2e):[24]

Physical State: white solid (201 mg for 1.0 mmol scale, 64% yield). R_f-value: 0.8 (100% Hexane). ^{1}H NMR (CDCl$_3$, 700 MHz): δ 7.66–7.62 (m, 8H). ^{13}C{^{1}H} NMR (CDCl$_3$, 176 MHz): δ 132.3, 130.8 (q, J_{C-F} = 33.4 Hz), 126.7, 125.7 (q, J_{C-F} = 3.5 Hz), 124.2 (q, J_{C-F} = 271.0 Hz), 90.5.

5.5.8 Experimental characterization data for annulated products:

5,6,7,8-tetraphenyl-1-(pyridin-2-yl)quinolin-2(1*H*)-one (3aa):
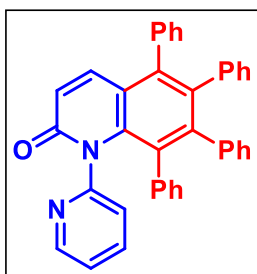
Physical State: white solid (47 mg for 0.10 mmol scale, 89% yield). m.p.: 264-269 °C. R_f -value: 0.5 (50% EtOAc/hexane). ^{1}H NMR (CDCl$_3$, 400 MHz): δ 8.27 (dd, J = 2.8, 0.8 Hz, 1H), 7.62 (d, J = 5.6 Hz, 1H), 7.35 (d, J = 4.4 Hz, 1H), 7.31 (t, J = 4.4 Hz, 1H), 7.20–7.17 (m, 2H), 7.15 (t, J = 4.0 Hz, 1H), 7.02 (brs, 2H), 6.99 (t, J = 4.0 Hz, 1H), 6.88–6.86 (m, 2H), 6.81–6.72 (m, 8H), 6.67–6.64 (m, 2H), 6.59 (d, J = 5.6 Hz, 1H), 6.43 (t, J = 4.4 Hz, 1H), 6.39 (d, J = 4.4 Hz, 1H), 6.03 (d, J = 4.4 Hz, 1H). ^{13}C{^{1}H} NMR

(CDCl$_3$, 100 MHz): δ 164.1, 153.8, 148.5, 145.2, 140.1, 139.8 (2C), 139.6, 139.4, 139.3, 138.4, 137.4, 136.5, 132.3, 131.7, 131.4, 131.2, 131.1, 131.0, 130.9, 130.6, 128.1, 128.0, 127.7, 127.3, 127.0, 126.9, 126.8, 126.7, 126.6, 125.9, 125.8 (2C), 122.4, 121.5, 121.1. **IR** (KBr, cm^{-1}): 3052, 1661, 1608, 1467, 1280, 1116. **HRMS (ESI) m/z:** [M+H]$^+$ Calcd for C$_{38}$H$_{27}$N$_2$O 527.2123; Found 527.2126.

1-(5-methylpyridin-2-yl)-5,6,7,8-tetraphenylquinolin-2(1*H*)-one (3ca):
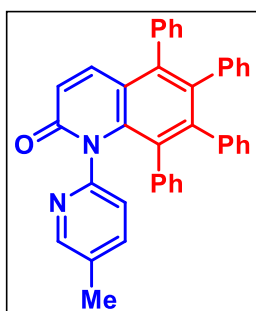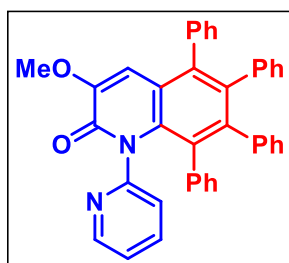

Physical State: yellow solid (47 mg for 0.10 mmol scale, 87% yield). m.p.: 271-274 °C. R$_f$-value: 0.4 (50% EtOAc/hexane). ^{1}H NMR (CDCl$_3$, 400 MHz): δ 8.07 (brs, 1H), 7.62 (d, *J* = 10.0 Hz, 1H), 7.35–7.29 (m, 2H), 7.21–7.13 (m, 2H), 7.03–6.92 (m, 4H), 6.88–6.84 (m, 1H), 6.81–6.71 (m, 7H), 6.68–6.64 (m, 3H), 6.61 (d, *J* = 9.6 Hz, 1H), 6.46–6.39 (m, 2H), 6.03 (d, *J* = 7.6 Hz, 1H), 2.16 (s, 3H). ^{13}C{^{1}H} NMR (CDCl$_3$, 176 MHz): δ 164.2, 151.3, 148.6, 145.3, 140.0, 139.8, 139.7, 139.5, 139.4, 138.4, 137.3, 137.1, 132.2, 132.1, 131.7, 131.5, 131.2, 131.1, 131.0, 130.7, 130.6, 128.1, 128.0, 127.3, 127.1, 127.0, 126.9, 126.7, 126.6, 125.8, 125.7 (2C), 121.5, 121.0, 18.2. IR (KBr, cm^{-1}): 3057, 1651, 1550, 1407, 1277, 1157. HRMS (ESI) m/z: [M+H]$^+$ Calcd for C$_{39}$H$_{29}$N$_2$O 541.2280; Found 541.2277.

**3-methoxy-5,6,7,8-tetraphenyl-1-(pyridin-2-yl)quinolin-2(1*H*)-one (3ga)**:

Physical State: yellow solid (31 mg for 0.10 mmol scale, 56% yield). m.p.: 277-279 °C. R$_f$-value: 0.1 (50% EtOAc/hexane). ^{1}H NMR (CDCl$_3$, 400 MHz): δ 8.26 (dd, *J* = 4.8, 0.4 Hz, 1H), 7.38–7.29 (m, 2H), 7.21–7.15 (m, 3H), 7.05–6.96 (m, 3H), 6.89–6.86 (m, 2H), 6.82–6.71 (m, 9H), 6.66–6.64 (m, 2H), 6.41 (dd, *J* = 15.6, 7.6 Hz, 2H), 6.03 (d, *J* = 7.2 Hz, 1H), 3.67 (s, 3H). ^{13}C{^{1}H} NMR (CDCl$_3$, 176 MHz): δ 160.0, 153.7, 148.4, 148.1, 142.2, 140.2, 139.9, 139.5, 139.0, 138.2, 137.6, 136.5, 134.9, 132.3, 131.9, 131.5, 131.1,

131.0, 130.9, 130.6, 128.2, 128.1, 128.0, 127.7, 127.2, 127.0, 126.9, 126.8, 126.7, 126.5, 125.8, 125.7, 125.6, 122.5, 121.1, 111.2, 56.1. IR (KBr, cm^{-1}): 3055, 1671, 1625, 1410, 1229. HRMS (ESI) m/z: [M+Na]$^+$ Calcd for $C_{39}H_{28}N_2O_2Na$ 579.2043; Found 579.2020.

3-chloro-5,6,7,8-tetraphenyl-1-(pyridin-2-yl)quinolin-2(1*H*)-one (3ha):
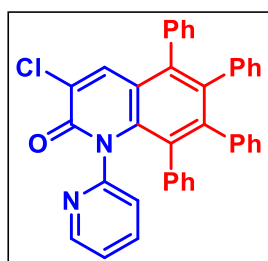
Physical State: yellow solid (38 mg for 0.10 mmol scale, 68% yield). m.p.: 295-297 °C. R$_f$-value: 0.7 (50% EtOAc/hexane). ^{1}H NMR (CDCl$_3$, 400 MHz): δ 8.26 (d, *J* = 4.8 Hz, 1H), 7.81 (s, 1H), 7.35 (d, *J* = 2.8 Hz, 2H), 7.22–7.15 (m, 3H), 7.02–7.01 (m, 3H),

6.91–6.86 (m, 2H), 6.82–6.73 (m, 8H), 6.66 (dd, *J* = 16.4, 8.0 Hz, 2H), 6.45–6.38 (m, 2H), 6.01 (d, *J* = 7.6 Hz, 1H). ^{13}C{^{1}H} NMR (CDCl$_3$, 176 MHz): δ 160.1, 153.6, 148.4, 145.4, 139.6,139.4, 139.3, 138.9, 138.3, 138.0, 137.9, 137.4, 136.7, 132.2, 131.6, 131.4, 131.1, 131.1, 131.1, 130.9, 130.5, 128.3, 128.2, 127.9, 127.8, 127.6, 127.1, 127.0, 126.8, 126.6, 126.1, 126.0, 125.9, 122.7, 120.6. IR (KBr, cm^{-1}): 2921, 1672, 1550, 1024, 736. HRMS (ESI) m/z: [M+H]$^+$ Calcd for $C_{38}H_{26}ClN_2O$ 561.1734; Found 561.1733.

**3-bromo-5,6,7,8-tetraphenyl-1-(pyridin-2-yl)quinolin-2(1*H*)-one (3ia):**
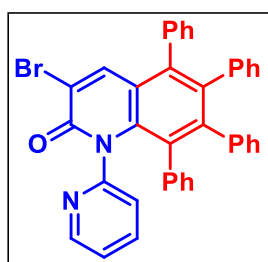
Physical State: yellow solid (37 mg for 0.10 mmol scale, 61% yield). m.p.: 284-287 °C. R$_f$-value: 0.4 (30% EtOAc/hexane). ^{1}H NMR (CDCl$_3$, 400 MHz): δ 8.28 (s, 1H), 8.25–8.24 (m, 1H), 7.34 (d, *J* = 3.6 Hz, 2H), 7.24–7.15 (m, 3H), 7.02–7.00 (m, 3H), 6.90–

6.85 (m, 2H), 6.82–6.72 (m, 8H), 6.68–6.62 (m, 2H), 6.44–6.38 (m, 2H), 6.01 (d, *J* = 7.6 Hz, 1H). ^{13}C{^{1}H} NMR (CDCl$_3$, 100 MHz): δ 160.6, 153.9, 149.0, 148.4, 148.3, 145.7, 141.5, 139.5, 139.4, 138.9 (2C), 137.8 (2C), 136.6 (2C), 132.2, 131.7, 131.4, 131.1 (2C), 130.9, 130.5, 128.2, 127.9, 127.8, 127.6, 127.1, 127.0 (2C), 126.8, 126.6, 126.1, 126.0,

125.9, 122.7, 122.6, 122.3, 94.4. IR (KBr, cm^{-1}): 3055, 1660, 1651, 1441, 1265, 1018. HRMS (ESI) m/z: [M+H]$^+$ Calcd for C$_{38}$H$_{26}$BrN$_2$O 605.1229; Found 605.1211.

2-oxo-5,6,7,8-tetraphenyl-1-(pyridin-2-yl)-1,2-dihydroquinoline-3-carbonitrile (3ja):
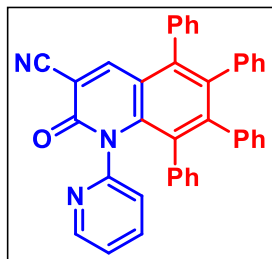
Physical State: yellow solid (34 mg for 0.10 mmol scale, 62% yield). m.p.: 291-295 °C. R$_f$-value: 0.7 (50% EtOAc/hexane). ^{1}H NMR (CDCl$_3$, 700 MHz): δ 8.27 (dd, J = 4.9, 1.4 Hz, 1H), 8.14 (s, 1H), 7.37 (t, J = 7.7 Hz, 1H), 7.34–7.32 (m, 1H), 7.27–7.25 (m, 1H), 7.22 (td, J = 7.7, 2.1 Hz, 1H), 7.20–7.18 (m, 1H), 7.04–7.02 (m, 2H), 6.99 (d, J = 7.7 Hz, 1H), 6.93 (dd, J = 7.7, 4.9 Hz, 1H), 6.89 (t, J = 7.7 Hz, 1H), 6.84–6.76 (m, 7H), 6.72 (d, J = 7.7 Hz, 1H), 6.70–6.68 (m, 1H), 6.63 (d, J = 7.7 Hz, 1H), 6.44 (t, J = 7.7 Hz, 1H), 6.38 (d, J = 7.7 Hz, 1H), 5.99 (d, J = 7.7 Hz, 1H). ^{13}C{^{1}H} NMR (CDCl$_3$, 176 MHz): δ 160.3, 152.6, 148.9, 148.7, 148.6, 141.4, 140.6, 138.8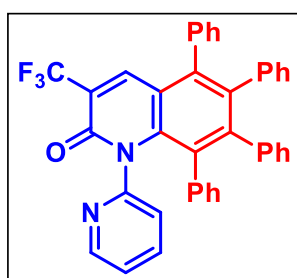 (2C), 138.6, 138.2, 136.9 (2C), 132.1, 131.6, 131.2, 131.1, 130.9, 130.7, 130.2, 128.5, 128.4, 128.2, 127.9, 127.8, 127.3, 127.2, 127.1, 127.0, 126.8, 126.4, 126.3, 126.2, 123.1, 119.8, 115.4, 106.8. IR (KBr, cm^{-1}): 3054, 2304, 1663, 1603, 1434, 1266. HRMS (ESI) m/z: [M+H]$^+$ Calcd for C$_{39}$H$_{26}$N$_3$O 552.2076; Found 552.2059.

5,6,7,8-tetraphenyl-1-(pyridin-2-yl)-3(trifluoromethyl)quinolin-2(1H)-one (3ka):

Physical State: yellow solid (58 mg for 0.10 mmol scale, 98% yield). m.p.: 297-299 °C. R$_f$-value: 0.2 (50% EtOAc/hexane). ^{1}H NMR (CDCl$_3$, 400 MHz): δ 8.27 (dd, J = 4.8, 1.6 Hz, 1H), 8.05 (s, 1H), 7.35–7.34 (m, 2H), 7.23–7.15 (m, 3H), 7.03–7.00 (m, 3H), 6.92–6.87 (m, 2H), 6.84–6.63 (m, 10H), 6.45–6.38 (m, 2H), 6.02 (d, J = 7.6 Hz, 1H). ^{13}C{^{1}H} NMR (CDCl$_3$, 100 MHz): δ 159.8, 152.9, 148.6, 147.7, 141.5, 140.5, 140.0 (q, J_{C-F} = 5.0 Hz), 139.2, 139.1, 138.6, 138.3, 137.3, 136.6, 132.2, 131.6, 131.3 (2C), 131.2, 131.0,

130.9, 130.8, 130.3, 128.3 (2C), 128.1, 127.9, 127.8, 127.2, 127.1, 127.0, 126.9, 126.7, 126.2, 126.1 (2C), 122.8, 122.5 (q, J_{C-F} = 270.6 Hz), 120.9 (q, J_{C-F} = 31.1 Hz), 119.0. ^{19}F NMR (CDCl$_3$, 376 MHz): δ -65.6. IR (KBr, cm^{-1}): 3056, 1681, 1555, 1141, 721. HRMS (ESI) m/z: [M+H]$^+$ Calcd for C$_{39}$H$_{26}$F$_3$N$_2$O 595.1992; Found 595.1970.

### 4-methyl-5,6,7,8-tetraphenyl-1-(pyridin-2-yl)quinolin-2(1*H*)-one (3la):
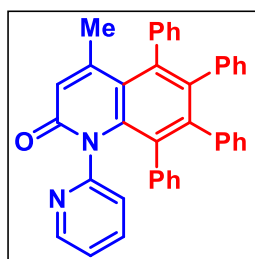
Physical State: white solid (46 mg for 0.10 mmol scale, 85% yield). m.p.: 238-245 °C. R$_f$ -value: 0.4 (50% EtOAc/hexane). ^{1}H NMR (CDCl$_3$, 400 MHz): δ 8.26 (d, *J* = 4.4 Hz, 1H), 7.37 (d, *J* = 6.8 Hz, 1H), 7.23–7.21 (m, 1H), 7.17–7.11 (m, 2H), 7.04–7.00 (m, 4H), 6.88–6.84 (m, 1H), 6.82–6.68 (m, 10H), 6.60 (d, *J* = 6.0 Hz, 1H), 6.51 (s, 1H), 6.40–6.35 (m, 2H), 5.89 (d, *J* = 7.2 Hz, 1H), 1.74 (s, 3H). ^{13}C{^{1}H} NMR (CDCl$_3$, 176 MHz): δ 163.1, 154.0, 150.6, 148.2, 144.1, 141.5, 140.5, 140.0, 139.9, 139.7, 139.3, 138.4, 136.3, 132.2, 131.8, 131.5, 131.2, 130.8, 130.5, 128.0, 127.7, 127.6, 127.4, 127.2, 127.0, 126.8, 126.7, 126.6, 125.8, 125.6, 125.5, 123.7, 122.4, 122.0, 25.2. IR (KBr, cm^{-1}): 3055, 1667, 1601, 1396, 1284. HRMS (ESI) m/z: [M+H]$^+$ Calcd for C$_{39}$H$_{29}$N$_2$O 541.2280; Found 541.2268.

### 5,6,7,8-tetrakis(4-methoxyphenyl)-1-(pyridin-2-yl)quinolin-2(1*H*)-one (3ab):
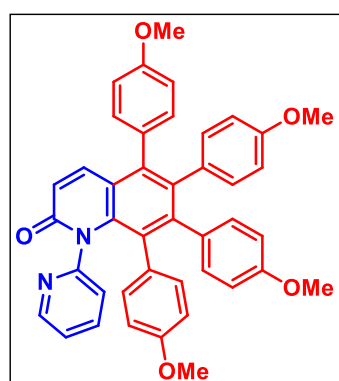
Physical State: brown solid (52 mg for 0.10 mmol scale, 80% yield). m.p.: 168-172 °C. R$_f$ -value: 0.15 (50% EtOAc/hexane). ^{1}H NMR (CDCl$_3$, 400 MHz): δ 8.25 (d, *J* = 4.0 Hz, 1H), 7.62 (d, *J* = 10.0 Hz, 1H), 7.29–7.23 (m, 2H), 6.90–6.84 (m, 4H), 6.82 (d, *J* = 8.0 Hz, 1H), 6.70–6.66 (m, 2H), 6.61–6.52 (m, 4H), 6.43 (d, *J* = 8.4 Hz, 1H), 6.37–6.34 (m, 2H), 6.31–6.24 (m, 2H), 5.99 (dd, *J* = 8.4, 2.4 Hz, 1H), 5.92 (dd, *J* = 8.4, 1.6 Hz, 1H), 3.78 (s, 3H), 3.65 (s, 3H), 3.60 (s, 3H), 3.56 (s, 3H). ^{13}C{^{1}H} NMR (CDCl$_3$, 100 MHz): δ 164.2, 158.8, 157.8, 157.4, 154.2, 148.5, 145.6, 140.2, 139.9, 139.7, 137.7, 136.3, 133.6,

133.5, 132.8, 132.7, 132.5, 132.5, 132.5, 132.4, 132.3, 132.2, 132.2, 131.9, 131.7, 131.7, 131.0, 130.9, 128.9, 128.8, 127.9, 122.3, 121.4, 121.2, 113.9, 113.4, 112.7, 112.4, 55.5, 55.5, 55.2. IR (KBr, cm^{-1}): 2933, 1664, 1608, 1514, 1245. HRMS (ESI) m/z: [M+H]$^+$ Calcd for $C_{42}H_{35}N_2O_5$ 647.2546; Found 647.2530.

5,6,7,8-tetrakis(4-fluorophenyl)-1-(pyridin-2-yl)quinolin-2(1H)-one (3ac):
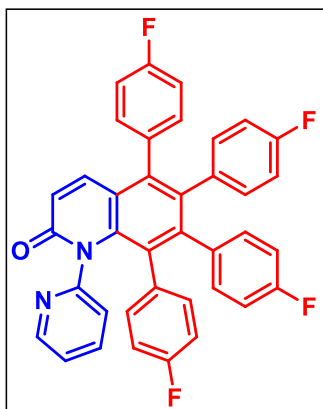
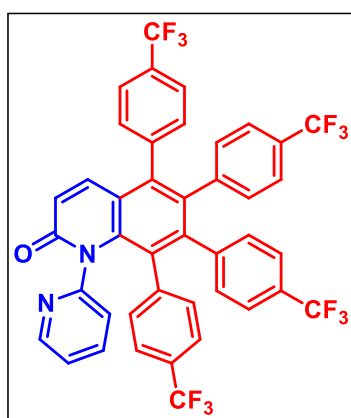Physical State: white solid (45 mg for 0.10 mmol scale, 75% yield). m.p.: 228-231 °C. R$_f$-value: 0.5 (50% EtOAc/hexane) ^{1}H NMR (CDCl$_3$, 700 MHz): δ 8.28 (dd, J = 4.9, 1.4 Hz, 1H), 7.57 (d, J = 9.8 Hz, 1H), 7.33 (td, J = 7.7, 2.1 Hz, 1H), 7.29–7.27 (m, 1H), 7.05–7.03 (m, 1H), 6.97–6.95 (m, 3H), 6.90–6.88 (m, 1H), 6.85 (d, J = 7.7 Hz, 1H), 6.75–6.71 (m, 2H), 6.67–6.65 (m, 1H), 6.62 (d, J = 9.8 Hz, 2H), 6.58–6.52 (m, 3H), 6.46–6.43 (m, 1H), 6.33 (t, J = 5.6 Hz, 1H), 6.20–6.18 (m, 1H), 6.01–6.00 (m, 1H). ^{13}C{^{1}H} NMR (CDCl$_3$, 176 MHz): δ 163.8, 162.2 (d, J_{C-F} = 248.2 Hz), 161.2 (d, J_{C-F} = 248.2 Hz), 161.1 (d, J_{C-F} = 244.6 Hz), 161.1 (d, J_{C-F} = 244.6 Hz), 153.7, 148.7, 144.4, 139.8, 139.6, 139.3, 136.8, 135.4 (d, J_{C-F} = 3.5 Hz), 135.2 (d, J_{C-F} = 3.5 Hz), 134.9 (d, J_{C-F} = 3.5 Hz), 133.9 (d, J_{C-F} = 3.5 Hz), 133.8 (d, J_{C-F} = 8.8 Hz), 133.0 (d, J_{C-F} = 7.0 Hz), 137.7 (d, J_{C-F} = 8.8 Hz), 132.6 (d, J_{C-F} = 8.8 Hz), 132.5 (d, J_{C-F} = 8.8 Hz), 132.2 (d, J_{C-F} = 7.0 Hz), 131.9 (d, J_{C-F} = 7.0 Hz), 130.3, 127.9, 122.8, 122.1, 121.4, 115.5, 115.4, 115.3, 115.0 (d, J_{C-F} = 21.1 Hz), 114.5, 114.4, 114.3, 114.2, 114.1 (2C). ^{19}F NMR (CDCl$_3$, 376 MHz): δ -114.2, -115.5, -115.8, -115.9. IR (KBr, cm^{-1}): 3040, 1651, 1513, 1416, 1222, 738. HRMS (ESI) m/z: [M+Na]$^+$ Calcd for $C_{38}H_{22}F_4N_2ONa$ 621.1560; Found 621.1583.

5,6,7,8-tetrakis(4-chlorophenyl)-1-(pyridin-2-yl)quinolin-2(1*H*)-one (3ad):
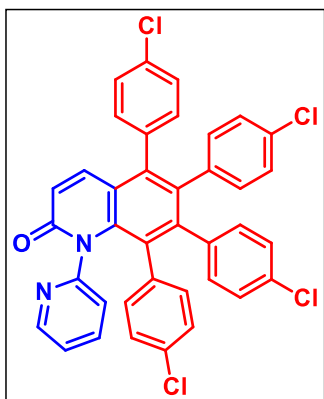
Physical State: light yellow solid (47 mg for 0.10 mmol scale, 71% yield). m.p.: 225-228 °C. R_f -value: 0.6 (50% EtOAc/hexane). ^{1}H NMR (CDCl$_3$, 700 MHz): δ 8.27 (d, J = 4.2 Hz, 1H), 7.53 (d, J = 9.8 Hz, 1H), 7.33 (t, J = 7.0 Hz, 2H), 7.24 (d, J = 1.8 Hz, 1H), 7.18 (d, J = 7.7 Hz, 1H), 7.02 (d, J = 7.7 Hz, 1H), 6.99 (dd, J = 7.0, 4.9 Hz, 1H), 6.94–6.91 (m, 3H),

6.85–6.83 (m, 3H), 6.75 (d, J = 7.7 Hz, 1H), 6.70 (d, J = 7.7 Hz, 1H), 6.64–6.62 (m, 2H),

6.54 (d, J = 7.7 Hz, 1H), 6.47 (d, J = 7.7 Hz, 1H), 6.32 (d, J = 7.7 Hz, 1H), 5.94 (d, J = 8.4

Hz, 1H). ^{13}C{^{1}H} NMR (CDCl$_3$, 176 MHz): δ 163.7, 153.6, 148.6, 143.7, 139.8, 139.3,

139.1, 137.6, 137.4, 137.1, 136.8, 136.2, 136.1, 134.0, 133.3, 132.7, 132.6, 132.5 (2C),

132.4, 132.2 (2C), 132.0, 131.7, 130.1, 128.8, 128.7, 128.2, 128.0, 127.9, 127.8, 127.6,

127.5, 127.4, 122.8, 122.4, 121.4. IR (KBr, cm^{-1}): 3052, 1666, 1568, 1264, 1089, 739.

HRMS (ESI) m/z: [M+H]$^+$ Calcd for C$_{38}$H$_{23}$Cl$_4$N$_2$O 663.0564; Found 663.0536.

1-(pyridin-2-yl)-5,6,7,8-tetrakis(4-(trifluoromethyl)phenyl)quinolin-2(1*H*)-one (3ae):

Physical State: light yellow solid (41 mg for 0.10 mmol scale, 51% yield). m.p.: 180-185 °C. R_f -value: 0.4 (30% EtOAc/hexane). ^{1}H NMR (CDCl$_3$, 400 MHz): δ 8.29–8.27 (m, 1H), 7.64 (d, J = 8.0 Hz, 1H), 7.52–7.47 (m, 3H), 7.31 (d, J = 7.6 Hz, 1H), 7.25–7.09 (m, 6H), 7.00 (d, J = 7.6 Hz, 1H), 6.98–6.94 (m, 1H), 6.92 (d, J = 7.6 Hz, 1H), 6.86 (d, J = 7.2 Hz, 1H), 6.82 (d, J = 8.0 Hz, 1H), 6.75 (br, 2H), 6.68

(d, J = 10.0 Hz, 1H), 6.52 (d, J = 7.6 Hz, 1H), 6.16 (d, J = 7.6 Hz, 1H). ^{13}C{^{1}H} NMR

(CDCl$_3$, 176 MHz): δ 163.4, 153.3, 148.8, 143.1, 142.3, 142.3, 142.1, 141.2, 139.9, 139.1,

138.9, 137.0, 135.6, 132.5, 131.8, 131.4, 131.2, 131.1, 130.7, 130.4 (q, J_{C-F} = 32.7), 130.0,

129.1 (q, $J_{C\text{-}F}$ = 32.4 MHz), 129.0, 128.9 (q, $J_{C\text{-}F}$ = 32.2 MHz), 128.1, 125.5, 124.8, 124.7, 124.6, 124.4, 124.2, 124.2, 124.1 (q, $J_{C\text{-}F}$ = 270.7 MHz), 124.0 (q, $J_{C\text{-}F}$ = 270.9 MHz), 123.9 (q, $J_{C\text{-}F}$ = 270.6 MHz), 123.1, 123.1, 121.4 ^{19}F NMR (CDCl$_3$, 376 MHz): δ -62.8, -62.9, -63.0, -63.0. IR (KBr, cm^{-1}): 3056, 1666, 1466, 1324, 1164, 844, 789. HRMS (ESI) m/z: [M+Na]$^+$ Calcd for C$_{42}$H$_{22}$F$_{12}$N$_2$ONa 821.1433; Found 821.1421.

1-(pyridin-2-yl)-5,6,7,8-tetra(thiophen-2-yl)quinolin-2(1*H*)-one (3af):
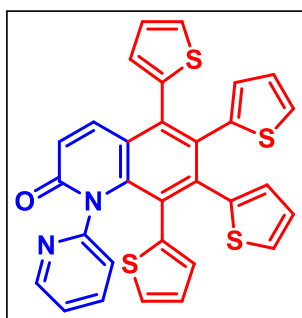
Physical State: yellow liquid (41 mg for 0.10 mmol scale, 74% yield). R$_f$-value: 0.6 (50% EtOAc/hexane). ^{1}H NMR (CDCl$_3$, 700 MHz): δ 8.31 (d, *J* = 3.5 Hz, 1H), 7.78 (d, *J* = 9.8 Hz, 1H), 7.38 (s, 1H), 7.34 (d, *J* = 5.6 Hz, 1H), 7.03–6.97 (m, 7H), 6.67 (d, *J* = 9.8 Hz, 1H), 6.64 (t, *J* = 4.2 Hz, 1H), 6.56 (s, 1H), 6.52 (d, *J* = 3.5 Hz, 1H), 6.40 (s, 1H), 6.28 (s, 1H), 5.65 (s, 1H). ^{13}C{^{1}H} NMR (CDCl$_3$, 100 MHz): δ 163.6, 153.8, 148.7, 141.8, 141.0, 140.1, 139.8, 139.4, 138.3, 136.8, 135.1, 133.2, 130.5, 130.3, 129.7, 129.3, 127.6, 126.9, 126.5, 126.3, 126.0, 125.7, 125.1, 123.1, 122.8, 122.4. IR (KBr, cm^{-1}): 3098, 1667, 1431, 1391, 1037. HRMS (ESI) m/z: [M+H]$^+$ Calcd for C$_{30}$H$_{19}$N$_2$OS$_4$ 551.0375; Found 551.0379.

1-(pyridin-2-yl)-5,6,7,8-tetra(thiophen-3-yl)quinolin-2(1*H*)-one (3ag):
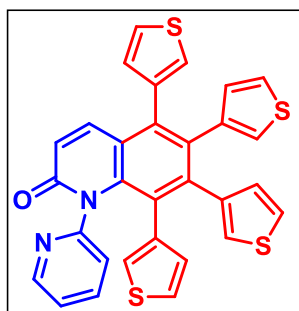
Physical State: yellow solid (45 mg for 0.10 mmol scale, 82% yield. m.p.: 280–282 °C. R$_f$-value: 0.2 (50% EtOAc/hexane). ^{1}H NMR (CDCl$_3$, 400 MHz): δ 8.74 (s, 1H), 7.93 (t, *J* = 7.2 Hz, 1H), 7.69–7.64 (m, 1H), 7.57–7.37 (m, 3H), 7.21 (dd, *J* = 4.8, 2.8 Hz, 1H), 7.16–7.10 (m, 3H), 6.99 (dd, *J* = 5.2, 3.2 Hz, 1H), 6.86–6.83 (m, 2H), 6.72–6.68 (m, 2H), 6.46 (d, *J* = 9.6 Hz, 2H), 6.32 (d, *J* = 5.2 Hz, 1H). ^{13}C{^{1}H} NMR (CDCl$_3$, 100 MHz): δ 163.2, 149.9, 142.7, 142.6, 142.4, 141.5, 141.0, 137.3, 136.7, 132.6, 132.5, 132.4, 132.2, 132.2, 130.4, 129.4, 129.2, 129.1, 128.9, 128.8, 127.5, 125.8,

125.7, 125.6, 124.9, 124.3, 123.6, 118.8, 117.6. IR (KBr, cm^{-1}): 3093, 1666, 1590, 1345, 1117. HRMS (ESI) m/z: [M+H]$^+$ Calcd for C$_{30}$H$_{19}$N$_2$OS$_4$ 551.0336; Found 551.0375.

5,6,7,8-tetraphenyl-1-(pyridin-2-yl)quinolin-4(1*H*)-one (3ma):
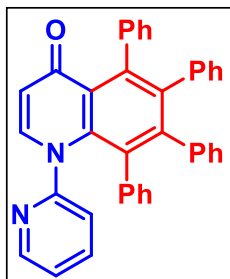
Physical State: colorless liquid (21 mg for 0.10 mmol scale, 40% yield). R$_f$-value: 0.65 (50% EtOAc/hexane). ^{1}H NMR (CDCl$_3$, 400 MHz): δ 8.18 (d, J = 3.6 Hz, 1H), 7.67 (dd, J = 12.0, 7.6 Hz, 1H), 7.58–7.53 (m, 1H), 7.49–7.45 (m, 1H), 7.34 (td, J = 8.0, 1.6 Hz, 1H), 7.14–7.04 (m, 5H), 6.90 (dd, J = 7.2, 4.8 Hz, 1H), 6.82–6.75 (m, 10H), 6.71–6.70 (m, 2H), 6.60 (d, J = 3.2 Hz, 2H), 6.19 (d, J = 8.0 Hz, 1H). ^{13}C{^{1}H} NMR (CDCl$_3$, 176 MHz): δ 179.3, 157.5, 149.2, 146.2, 143.9, 141.9, 141.5, 141.3, 139.9, 139.6, 139.5, 139.0, 138.8, 132.5, 132.4, 132.3, 132.3, 131.6, 130.8, 129.6, 128.9, 128.8, 127.4, 127.1, 126.8, 126.7, 126.3, 126.3, 125.9, 125.8, 125.7, 122.2, 121.3, 113.0. IR (KBr, cm^{-1}): 3054, 1632, 1586, 1440, 1264. HRMS (ESI) m/z: [M+H]$^+$ Calcd for C$_{38}$H$_{27}$N$_2$O 527.2118; Found 527.2133.

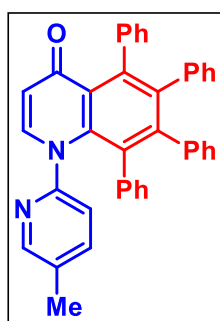### 1-(5-methylpyridin-2-yl)-5,6,7,8-tetraphenylquinolin-4(1*H*)-one (3na):

Physical State: yellow solid (51.5 mg for 0.10 mmol scale, 95% yield). m.p.: 195-200 °C. R$_f$-value: 0.1 (50% EtOAc/hexane). ^{1}H NMR (CDCl$_3$, 700 MHz): δ 7.98 (s, 1H), 7.67 (dd, J = 11.9, 7.7 Hz, 2H), 7.56–7.54 (m, 1H), 7.52 (d, J = 7.7 Hz, 1H), 7.47 (td, J = 7.7, 2.1 Hz, 2H), 7.12–7.11 (m, 3H), 7.07–7.06 (m, 2H), 6.81–6.77 (m, 4H), 6.75–6.74 (m, 3H), 6.70 (d, J = 7.0 Hz, 2H), 6.66 (d, J = 7.7 Hz, 1H), 6.59 (br, 2H), 6.18 (d, J = 7.7 Hz, 1H), 2.17 (s, 3H). ^{13}C{^{1}H} NMR (CDCl$_3$, 176 MHz): δ 179.4, 155.2, 149.1, 146.1, 144.0, 142.0, 141.4 (2C), 139.7, 139.6 (2C), 139.2, 139.1, 132.5, 132.4, 132.3 (3C), 132.1, 131.6, 130.8, 129.6, 128.9, 128.8, 127.1, 126.7 (2C), 126.1, 125.8, 125.7, 125.6, 121.0, 112.7,

18.1. IR (KBr, cm⁻¹): 3055, 1633, 1593, 1475, 1266, 1237. HRMS (ESI) m/z: [M+H]⁺ Calcd for $C_{39}H_{29}N_2O$ 541.2280; Found 541.2258.

2-(5,6,7,8-tetraphenylnaphthalen-1-yl)pyridine (3oa):
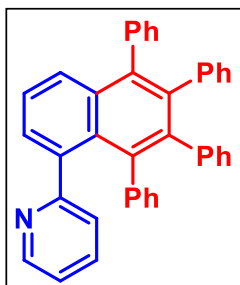

Physical State: yellow solid (24.5 mg for 0.10 mmol scale, 48% yield). m.p.: 127-130 °C. R_f-value: 0.2 (10% EtOAc/hexane). ¹H NMR (CDCl₃, 700 MHz): δ 8.24 (d, J = 4.2 Hz, 1H), 7.70 (t, J = 4.9 Hz, 1H), 7.41 (d, J = 4.9 Hz, 2H), 7.24–7.23 (m, 4H), 7.20 (td, J = 7.7, 1.4 Hz, 2H), 6.94 (d, J = 7.7 Hz, 1H), 6.85–6.79 (m, 5H), 6.77–6.75 (m, 8H), 6.66–6.64 (m, 1H), 6.61–6.60 (m, 2H). ¹³C{¹H} NMR (CDCl₃, 176 MHz): δ 162.1, 148.6, 141.5, 141.3 (2C), 141.0, 140.9, 140.3 (2C), 139.5 (2C),139.1, 139.0, 138.1, 138.0, 135.5, 135.4, 134.1, 133.3, 132.3, 131.9, 131.8, 131.6, 131.4, 131.1, 130.3, 128.5 (2C), 127.9, 127.8, 127.0, 126.9, 126.8, 126.6, 126.5, 125.7 (2C), 125.6 (2C), 125.3, 125.1, 120.6 (2C). IR (KBr, cm⁻¹): 3020, 1633, 1468, 1265. HRMS (ESI) m/z: [M+H]⁺ Calcd for $C_{39}H_{28}N$ 510.2216; Found 510.2194.

1-(5,6,7,8-tetraphenylnaphthalen-1-yl)-1*H*-pyrazole (3pa):
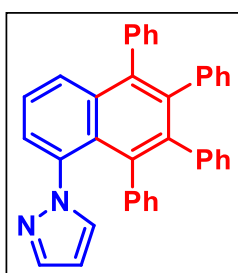
Physical State: yellow liquid (12.5 mg for 0.10 mmol scale, 25% yield). R_f-value: 0.3 (10% EtOAc/hexane). ¹H NMR (CDCl₃, 700 MHz): δ 7.75 (dd, J = 7.0, 2.1 Hz, 1H), 7.43–7.40 (m, 2H), 7.25–7.18 (m, 6H), 7.15 (d, J = 2.8 Hz, 1H), 6.84–6.80 (m, 5H), 6.79–6.75 (m, 8H), 6.62 (brs, 2H), 5.72–5.71 (m, 1H). ¹³C{¹H} NMR (CDCl₃, 100 MHz): δ 142.5, 140.6, 140.5, 140.3, 140.1, 139.9, 139.8, 139.0, 138.3, 136.5, 134.6, 132.7, 131.6, 131.5, 131.3, 129.3, 128.0, 127.9 (2C), 127.0, 126.9, 126.6, 125.7, 125.4 (2C), 125.1, 106.3. IR (KBr, cm⁻¹): 3055, 1601, 1441, 1265, 1072. HRMS (ESI) m/z: [M+H]⁺ Calcd for $C_{37}H_{27}N_2$ 499.2174; Found 499.2178.

5,6,7,8-tetraethyl-1-(pyridin-2-yl)quinolin-2(1*H*)-one (3ah):
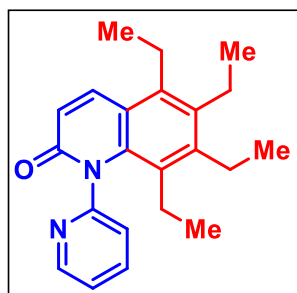
Physical State: colorless liquid (17 mg for 0.10 mmol scale, 51% yield). R_f-value: 0.35 (50% EtOAc/hexane). ^{1}H NMR (CDCl$_3$, 400 MHz): δ 8.50 (dd, J = 4.8, 1.2 Hz, 1H), 8.00 (d, J = 10.0 Hz, 1H), 7.87 (td, J = 8.0, 2.0 Hz, 1H), 7.75 (d, J = 8.0 Hz, 1H), 7.30 (dd, J = 7.2, 4.8 Hz, 1H), 6.60 (d, J = 10.0 Hz, 1H), 2.94 (q, J = 7.6 Hz, 2H), 2.75–7.65 (m, 4H), 1.29–1.19 (m, 8H), 1.11 (t, J = 7.6 Hz, 3H), 0.69 (t, J = 7.6 Hz, 3H). ^{13}C{^{1}H} NMR (CDCl$_3$, 176 MHz): δ 164.1, 154.9, 149.4, 145.2, 138.9, 138.5, 137.5, 137.4, 136.4, 129.7, 125.7, 123.1, 120.0, 119.9, 23.6, 22.9, 22.1, 21.8, 16.4, 16.0, 15.9, 15.2. IR (KBr, cm^{-1}): 2966, 2929, 1664, 1560, 1298. HRMS (ESI) m/z: [M+H]$^+$ Calcd for C$_{22}$H$_{27}$N$_2$O 335.2118; Found 335.2105.

5,6,7,8-tetraethyl-1-(pyridin-2-yl)-3-(trifluoromethyl)quinolin-2(1*H*)-one (3kh):
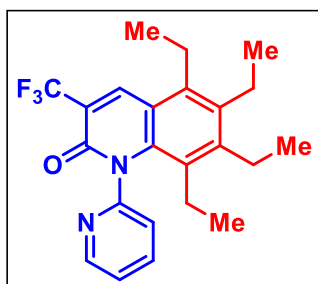
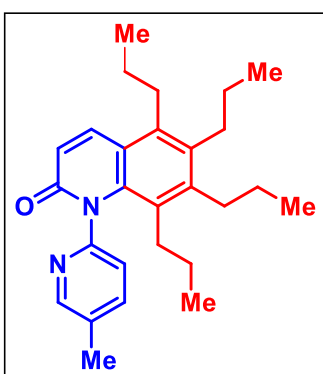Physical State: colorless liquid (27 mg for 0.10 mmol scale, 67% yield). R_f-value: 0.5 (50% EtOAc/hexane). ^{1}H NMR (CDCl$_3$, 400 MHz): δ 8.49 (dd, J = 4.8, 1.6 Hz, 1H), 8.43 (s, 1H), 7.90 (td, J = 7.6, 1.6 Hz, 1H), 7.82 (d, J = 8.0 Hz, 1H), 7.34–7.31 (m, 1H), 2.98 (q, J = 6.4 Hz, 2H), 2.77–2.68 (m, 4H), 1.32–1.19 (m, 8H), 1.12 (t, J = 7.6 Hz, 3H), 0.69 (t, J = 7.6 Hz, 3H). ^{13}C{^{1}H} NMR (CDCl$_3$, 100 MHz): δ 159.8, 153.9, 149.5, 148.3, 140.0, 139.2, 138.3 (q, $J_{C\text{-}F}$ = 5.0 Hz), 137.7, 137.3, 130.0, 125.9, 123.5, 123.0 (q, $J_{C\text{-}F}$ = 270.0 Hz), 119.1 (q, $J_{C\text{-}F}$ = 31.0 Hz), 117.8, 23.8, 22.9, 22.1, 21.7, 16.7, 15.9, 15.7, 15.1. ^{19}F NMR (CDCl$_3$, 376 MHz): δ -65.3.

IR (KBr, cm^{-1}): 2969, 2935, 1677, 1563, 1138, 1034. HRMS (ESI) m/z: [M+H]$^+$ Calcd for C$_{23}$H$_{26}$F$_3$N$_2$O 403.1997; Found 403.1992.

5,6,7,8-tetrapropyl-1-(pyridin-2-yl)quinolin-2(1*H*)-one (3ai):
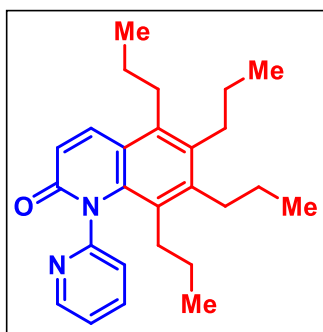
Physical State: yellow liquid (23 mg for 0.10 mmol scale, 59% yield). R_f-value: 0.55 (50% EtOAc/hexane). ^{1}H NMR (CDCl$_3$, 700 MHz): δ 8.50–8.49 (m, 1H), 7.96 (d, J = 9.8 Hz, 1H), 7.88 (td, J = 7.7, 2.1 Hz, 1H), 7.71 (d, J = 7.7 Hz, 1H), 7.30 (dd, J = 7.0, 4.2 Hz, 1H), 6.59 (d, J = 9.8 Hz, 1H), 2.84–2.81 (m, 2H), 2.60–2.54 (m, 4H), 1.64–1.52 (m, 7H), 1.50–1.40 (m, 2H), 1.11–1.06 (m, 7H), 0.99 (t, J = 7.0 Hz, 3H), 0.58 (t, J = 7.0 Hz, 3H). ^{13}C{^{1}H} NMR (CDCl$_3$, 176 MHz): δ 163.9, 154.7, 149.4, 144.1, 138.8, 138.6, 137.6, 136.2, 135.5, 128.5, 125.5, 123.0, 120.0, 119.9, 33.3, 32.7, 31.6, 31.0, 25.6, 25.0 (2C), 23.9, 15.3, 15.1, 14.1. IR (KBr, cm^{-1}): 2957, 2928, 1666, 1464, 1160. HRMS (ESI) m/z: [M+H]$^+$ Calcd for C$_{26}$H$_{35}$N$_2$O 391.2744; Found 391.2753.

### 1-(5-methylpyridin-2-yl)-5,6,7,8-tetrapropylquinolin-2(1*H*)-one (3ci):

Physical State: colorless liquid (28.5 mg for 0.10 mmol scale, 70% yield). R_f -value: 0.6 (50% EtOAc/hexane). ^{1}H NMR (CDCl$_3$, 700 MHz): δ 8.31 (s, 1H), 7.95 (d, J = 9.8 Hz, 1H), 7.68 (d, J = 7.7 Hz, 1H), 7.57 (d, J = 7.7 Hz, 1H), 6.59 (d, J = 9.8 Hz, 1H), 2.83–2.81 (m, 2H), 2.60–2.54 (m, 4H), 2.40 (s, 3H), 1.64–1.52 (m, 6H), 1.45–1.41 (m, 2H), 1.11–1.06 (m, 8H), 0.99 (t, J = 7.0 Hz, 3H), 0.58 (t, J = 6.3 Hz, 3H). ^{13}C{^{1}H} NMR (CDCl$_3$, 176 MHz): δ 164.1, 152.3, 149.5, 144.1, 138.9, 138.5, 138.2, 136.2, 135.3, 132.9, 128.4, 124.8, 119.9 (2C), 33.3, 32.7, 31.6, 31.0, 25.6, 25.0 (2C), 23.9, 18.5, 15.3, 15.2, 15.1, 14.1. IR (KBr, cm^{-1}): 2957, 2928, 1666, 1477, 1160. HRMS (ESI) m/z: [M+H]$^+$ Calcd for C$_{27}$H$_{37}$N$_2$O 405.2906; Found 405.2903.

3-chloro-5,6,7,8-tetrapropyl-1-(pyridin-2-yl)quinolin-2(1*H*)-one (3hi):
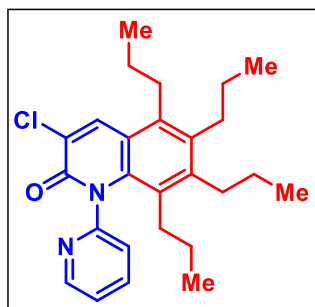
Physical State: colorless liquid (35.5 mg for 0.10 mmol scale, 84% yield). R$_f$ -value: 0.4 (20% EtOAc/hexane). ^{1}H NMR (CDCl$_3$, 400 MHz): δ 8.48 (d, J = 3.6 Hz, 1H), 8.14 (s, 1H), 7.90 (td, J = 8.0, 2.0 Hz, 1H), 7.76 (d, J = 8.0 Hz, 1H), 7.33 (dd, J = 7.2, 4.8 Hz, 1H), 2.83–2.79 (m, 2H), 2.61–2.53 (m, 4H), 1.67–1.49 (m, 6H), 1.48–1.38 (m, 2H), 1.14–1.06 (m, 8H), 0.99 (t, J = 7.6 Hz, 3H), 0.57 (t, J = 7.2 Hz, 3H). ^{13}C{^{1}H} NMR (CDCl$_3$, 176 MHz): δ 159.9, 154.4, 149.3, 144.4, 137.7 (2C), 136.2, 136.1, 135.7, 128.6, 125.5, 124.7, 123.4, 119.5, 33.3, 32.8, 31.6, 30.9, 25.6, 25.0, 24.9, 23.8, 15.3, 15.1, 14.0. IR (KBr, cm^{-1}): 2958, 2869, 1668, 1586, 1464, 1225, 785. HRMS (ESI) m/z: [M+H]$^+$ Calcd for C$_{26}$H$_{34}$ClN$_2$O 425.2360; Found 425.2352.

5,6,7,8-tetrapropyl-1-(pyridin-2-yl)-3-(trifluoromethyl)quinolin-2(1*H*)-one (3ki):
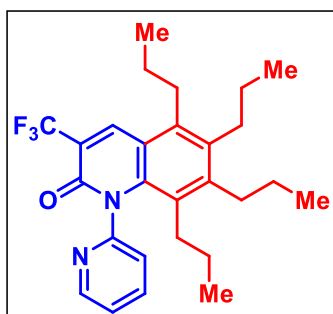
Physical State: colorless liquid (42.5 mg for 0.10 mmol scale, 93% yield). R$_f$ -value: 0.5 (50% EtOAc/hexane). ^{1}H NMR (CDCl$_3$, 400 MHz): δ 8.49 (d, J = 4.4 Hz, 1H), 8.39 (s, 1H), 7.90 (td, J = 7.6, 1.6 Hz, 1H), 7.77 (d, J = 8.0 Hz, 1H), 7.34 (dd, J = 7.2, 4.8 Hz, 1H), 2.89–2.85 (m, 2H), 2.63–2.56 (m, 4H), 1.68–1.39 (m, 8H), 1.14–1.06 (m, 8H), 1.00 (t, J = 7.2 Hz, 3H), 0.58 (t, J = 7.2 Hz, 3H). ^{13}C{^{1}H} NMR (CDCl$_3$, 100 MHz): δ 159.6, 153.8, 149.5, 147.2, 140.0, 138.4 (q, $J_{C\text{-}F}$ = 4.6 Hz), 138.0, 137.7, 136.4, 128.8, 125.7, 123.5, 123.0 (q, $J_{C\text{-}F}$ = 271.6 Hz), 119.0 (q, $J_{C\text{-}F}$ = 30.8 Hz), 117.8, 33.4, 32.7, 31.4, 30.9, 25.9, 24.9, 24.9, 23.8, 15.3, 15.1, 15.0, 14.0. ^{19}F NMR (CDCl$_3$, 376 MHz): δ -65.4. IR (KBr, cm^{-1}): 2960, 2930, 1680, 1421, 1141, 1051. HRMS (ESI) m/z: [M+H]$^+$ Calcd for C$_{27}$H$_{34}$F$_3$N$_2$O 459.2623; Found 459.2620.

5,6,7,8-tetraphenylquinolin-2(1*H*)-one (4):
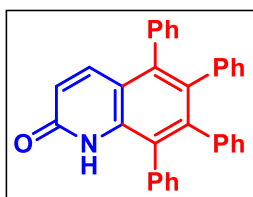
Physical State: yellow solid (26.5 mg for 0.10 mmol scale, 59% yield). m.p.: 217-221 °C. R_f-value: 0.4 (50% EtOAc/hexane). ^{1}H NMR (CDCl$_3$, 400 MHz): δ 8.57 (s, 1H), 7.62 (d, J = 9.6 Hz, 1H), 7.32–7.28 (m, 3H), 7.25–7.20 (m, 3H), 7.18–7.16 (m, 2H), 7.14–7.12 (m, 2H), 6.88–6.85 (m, 6H), 6.79–6.76 (m, 4H), 6.54 (dd, J = 9.6, 1.2 Hz, 1H). ^{13}C{^{1}H} NMR (CDCl$_3$, 100 MHz): δ 162.5, 143.9, 140.1, 139.9, 139.5, 139.4, 138.1, 136.4, 135.8, 134.8, 131.7, 131.2, 131.1, 131.0, 129.4, 128.5, 128.1, 127.6, 127.4, 127.2, 127.1, 126.3, 126.0, 121.7, 118.4. IR (KBr, cm^{-1}): 3438, 3046, 1660, 1441. HRMS (ESI) m/z: [M+H]$^+$ Calcd for C$_{33}$H$_{24}$NO 450.1852; Found 450.1842.

NMR spectra of 5'-methyl-4H-[1,2'-bipyridin]-4-one (1n):

^{1}H NMR of 1n (700 MHz, CDCl$_3$)

^{13}C{^{1}H} NMR of 1n (176 MHz, CDCl$_3$)

NMR spectra of 5,6,7,8-tetraphenyl-1-(pyridin-2-yl)quinolin-2(1*H*)-one (3aa):

¹H NMR of 3aa (400 MHz, CDCl₃)

¹³C{¹H} NMR of 3aa (100 MHz, CDCl₃)
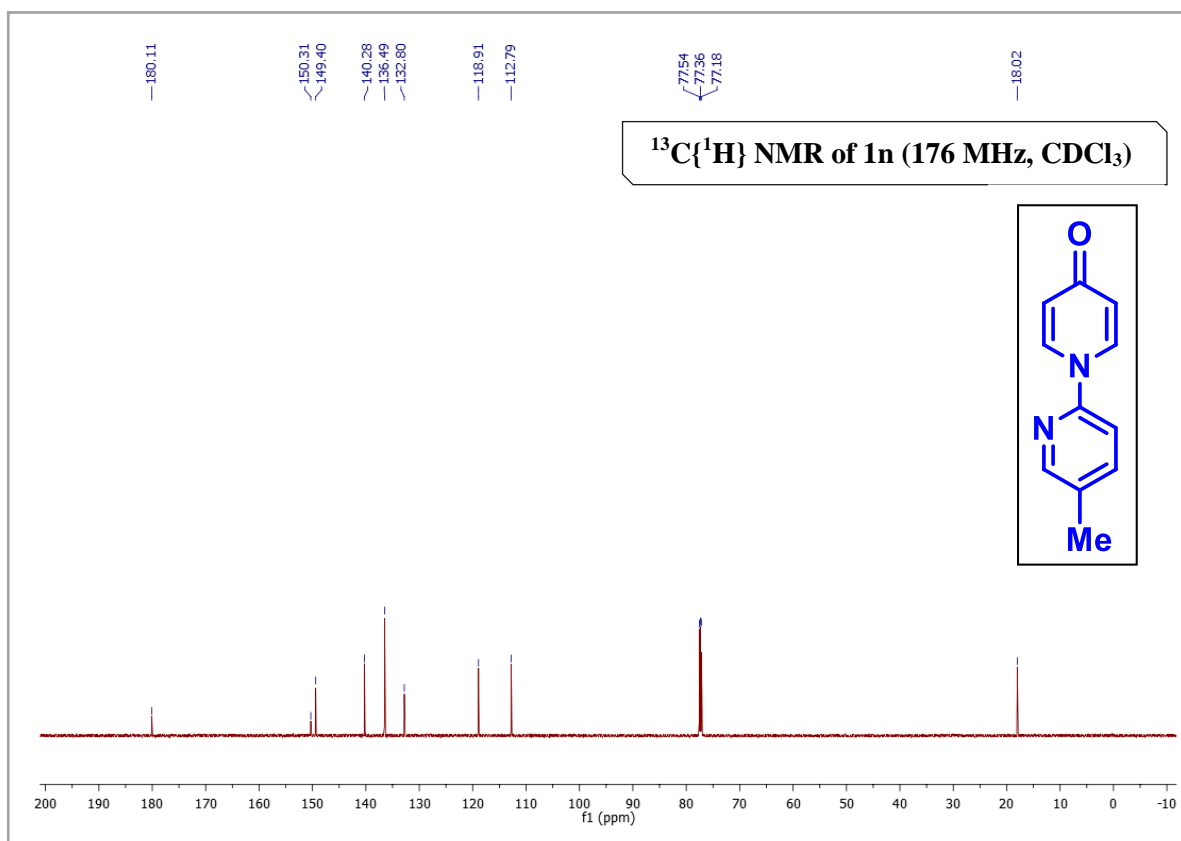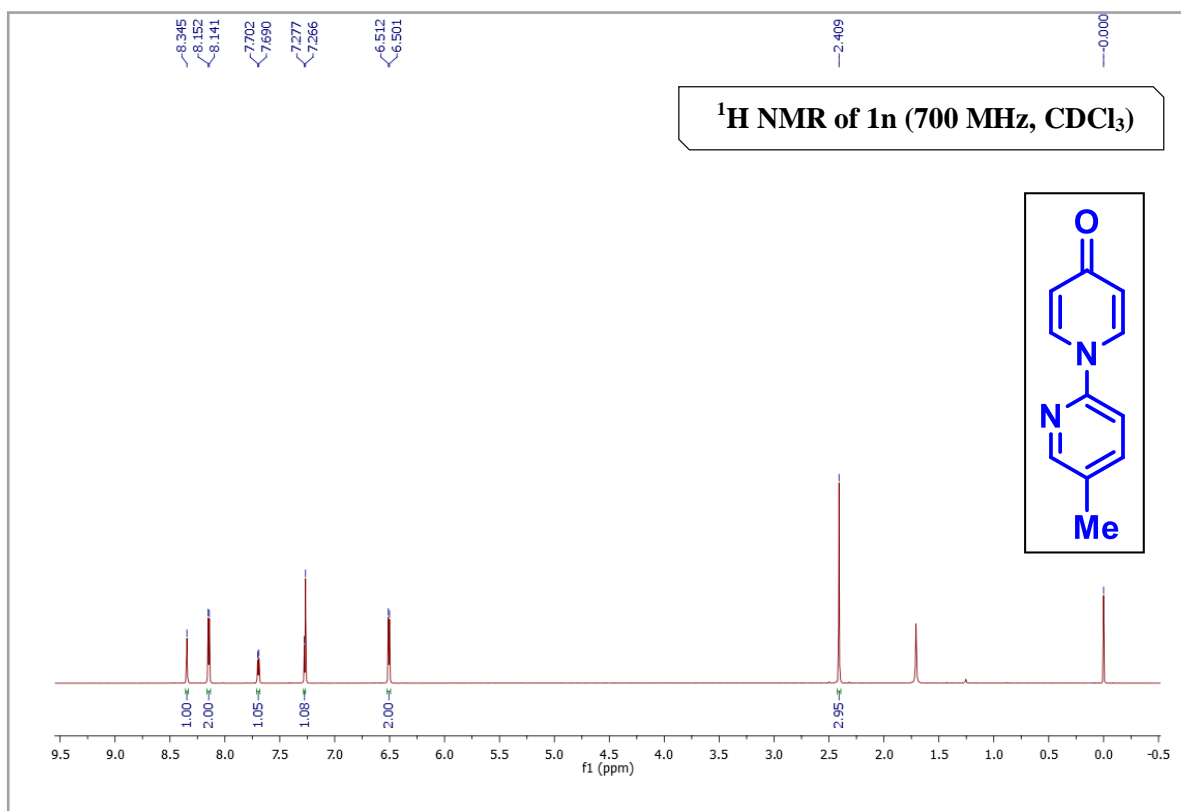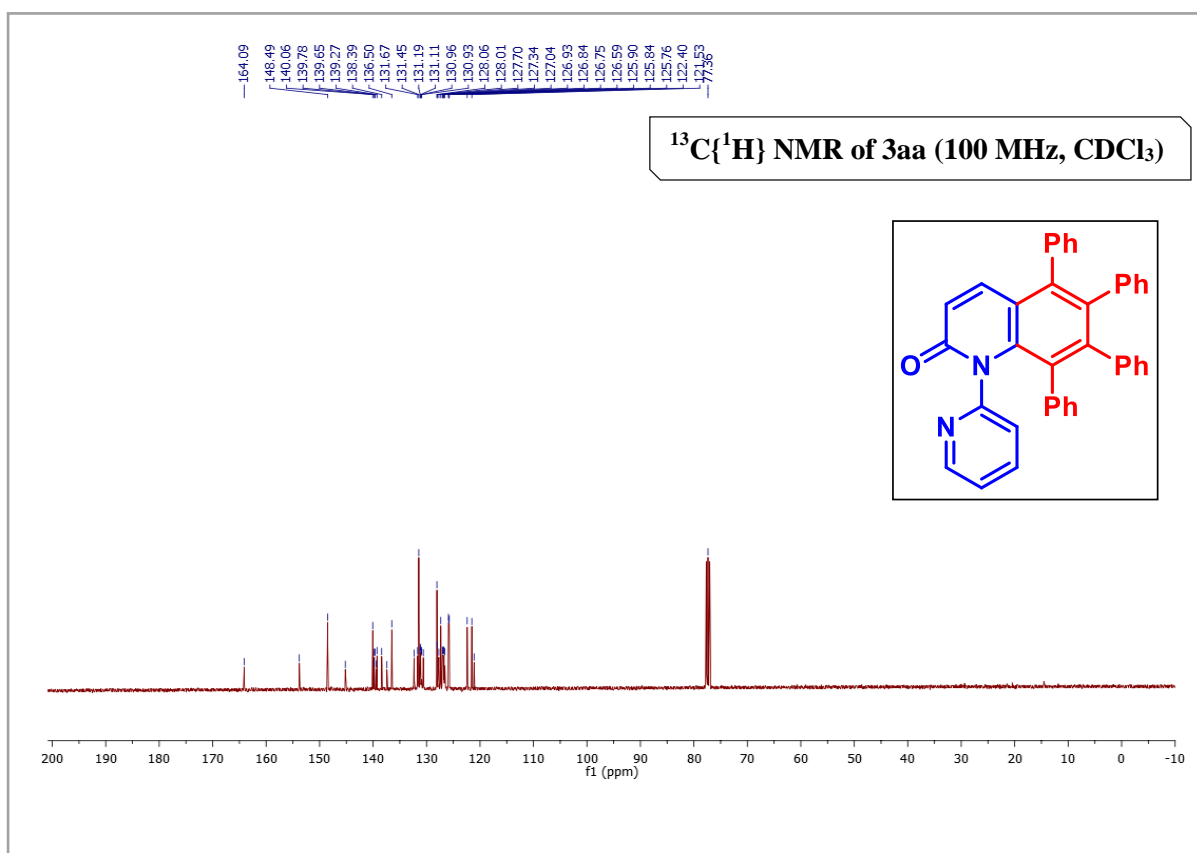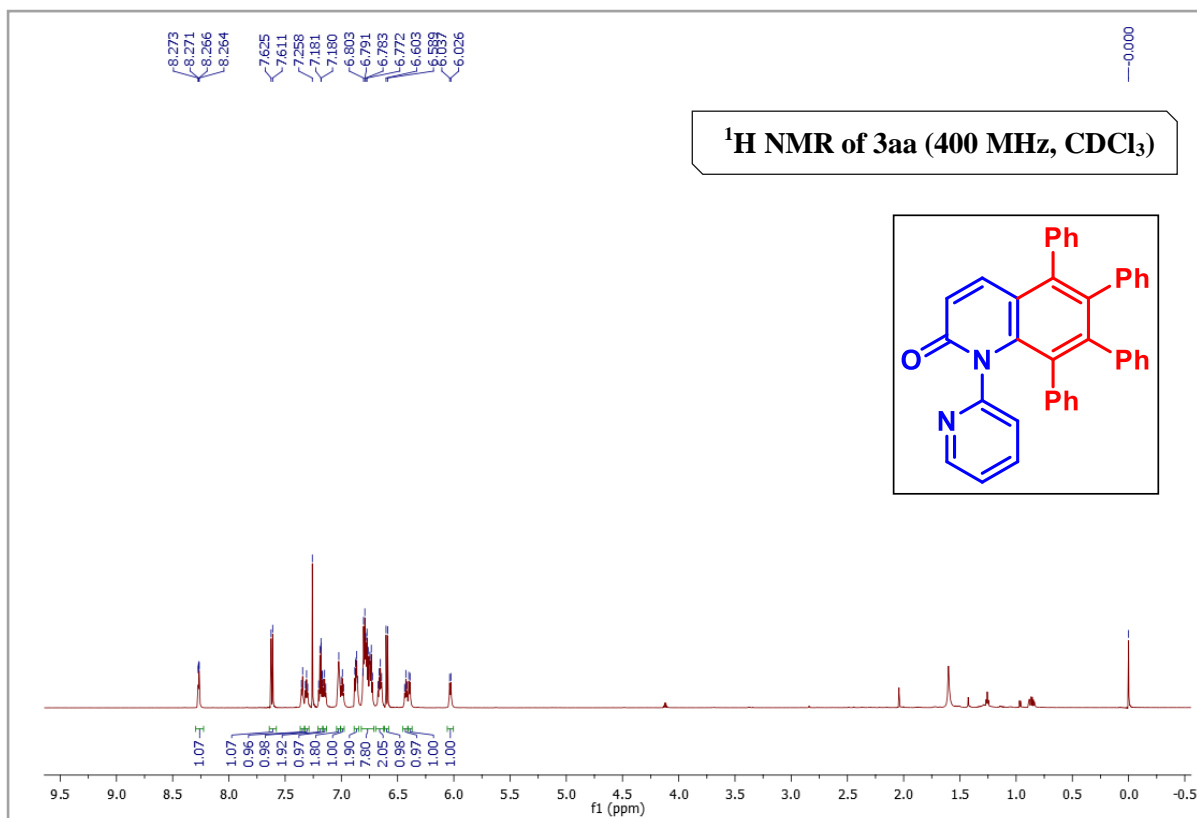
NMR spectra of 1-(pyridin-2-yl)-5,6,7,8-tetra(thiophen-2-yl)quinolin-2(1*H*)-one (3af):

^{1}H NMR of 3af (700 MHz, CDCl$_3$)

^{13}C{^{1}H} NMR of 3af (100 MHz, CDCl$_3$)
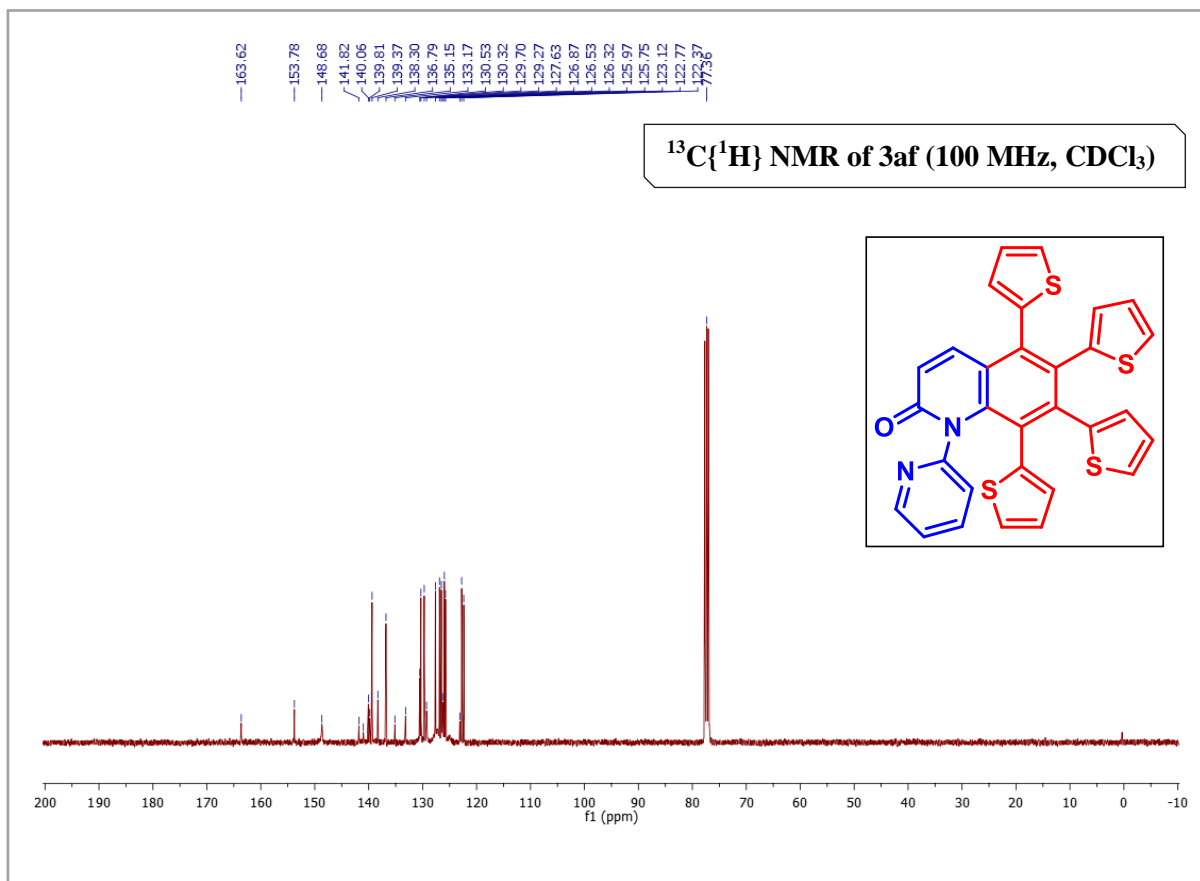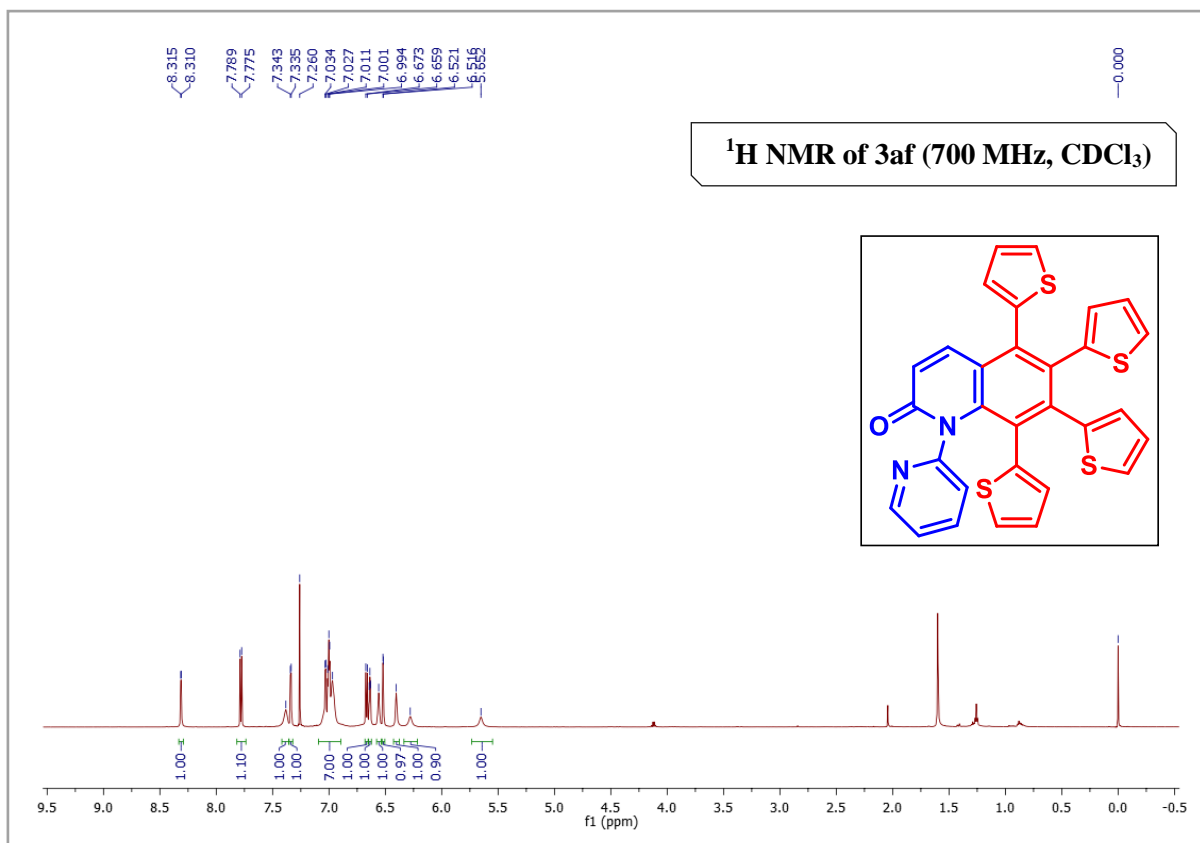
NMR spectra of 5,6,7,8-tetraethyl-1-(pyridin-2-yl)quinolin-2(1*H*)-one (3ah):

^{1}H NMR of 3ah (400 MHz, CDCl$_3$)

^{13}C{^{1}H} NMR of 3ah (176 MHz, CDCl$_3$)

NMR spectra of 5,6,7,8-tetraphenylquinolin-2(1*H*)-one (4):

^{1}H NMR of 4 (400 MHz, CDCl$_3$)

^{13}C{^{1}H} NMR of 4 (100 MHz, CDCl$_3$)

Crystal structure of 3aa

3aa
CCDC **2155052**
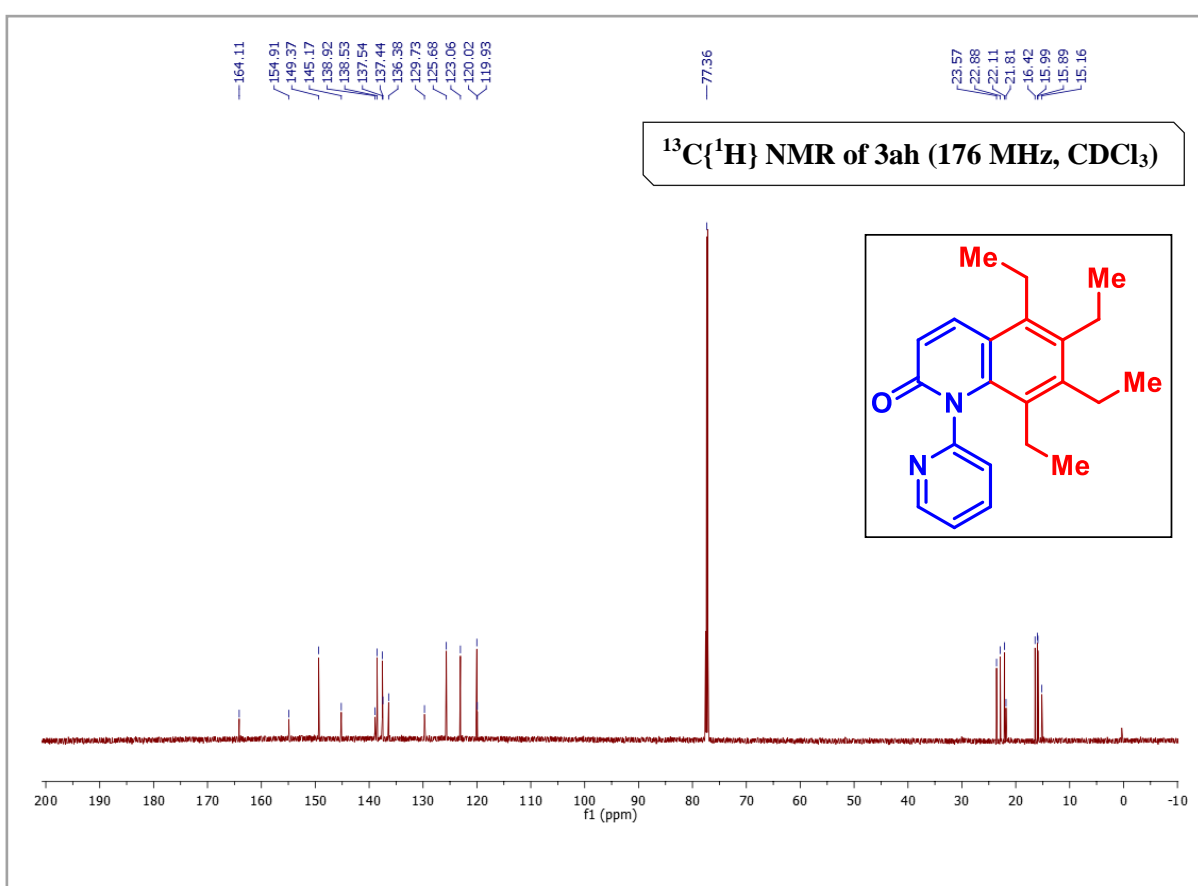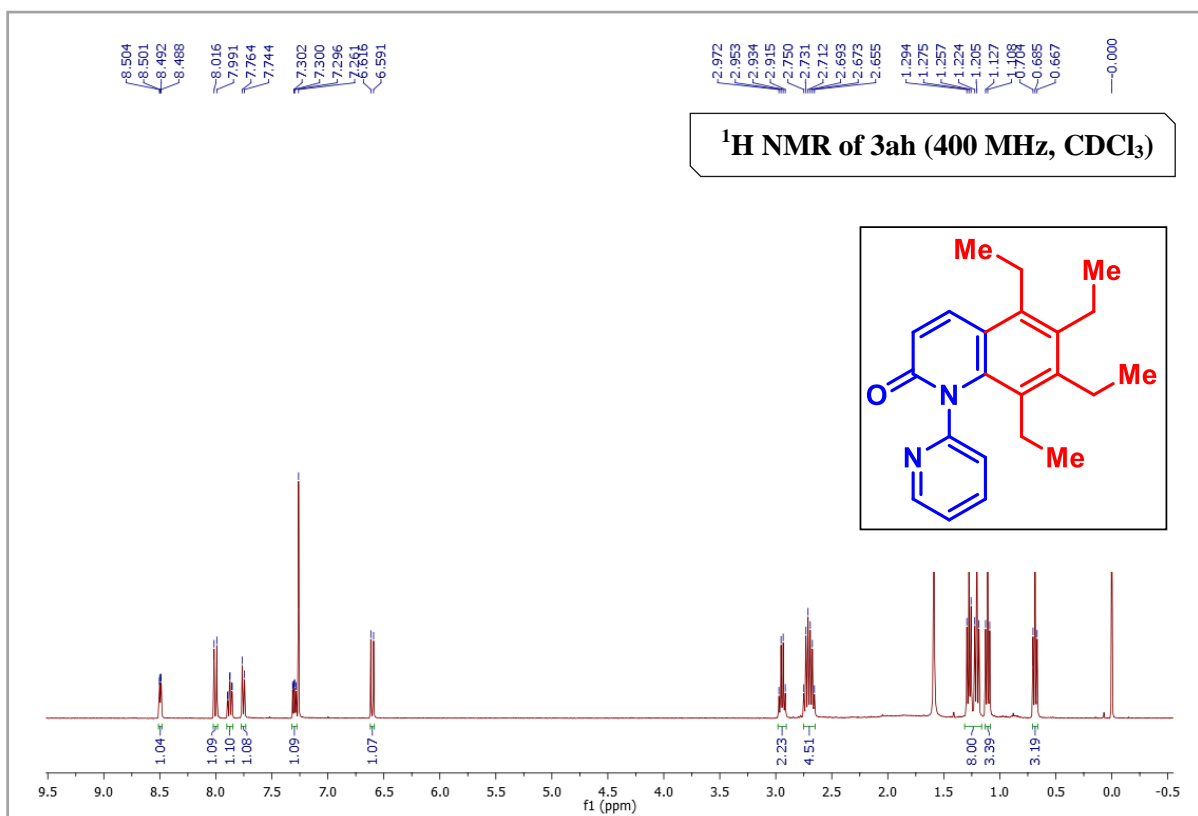
ORTEP diagram of **3aa** with 50% ellipsoid probability
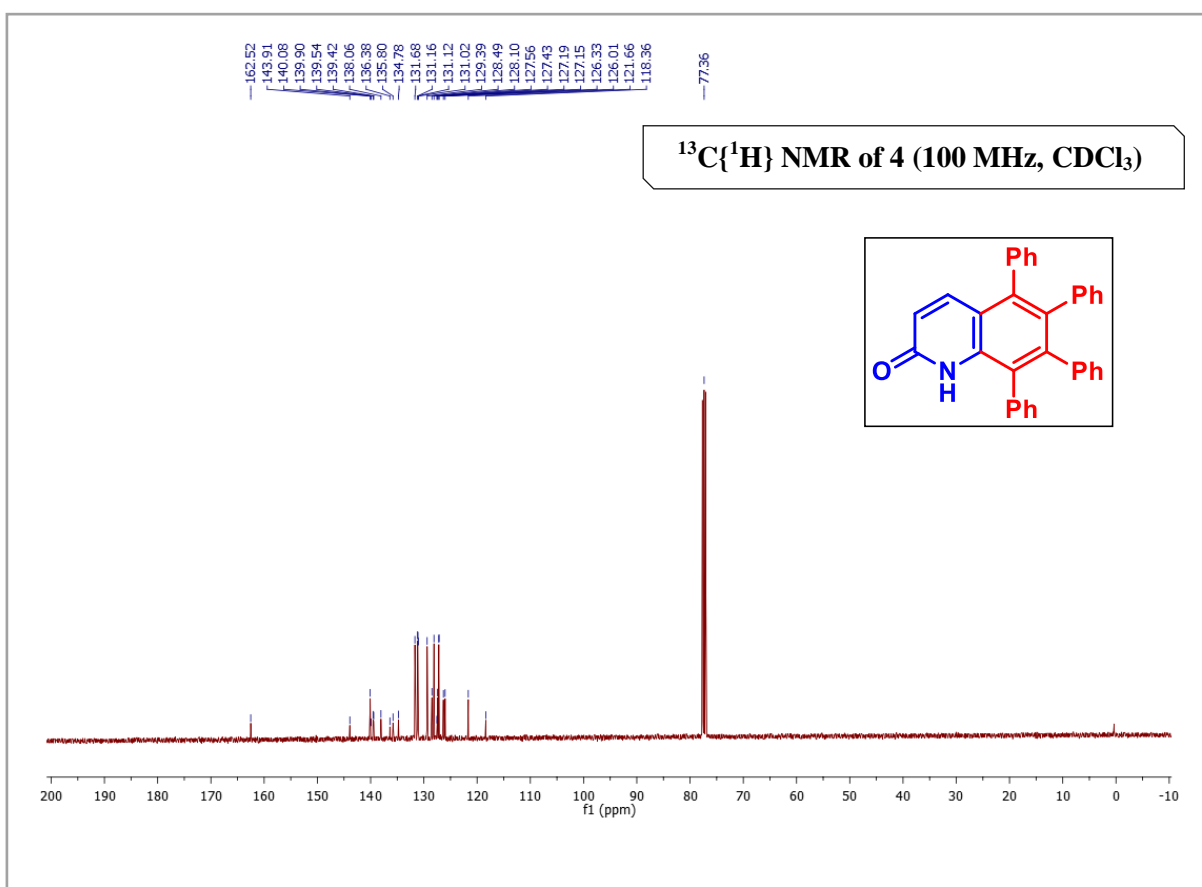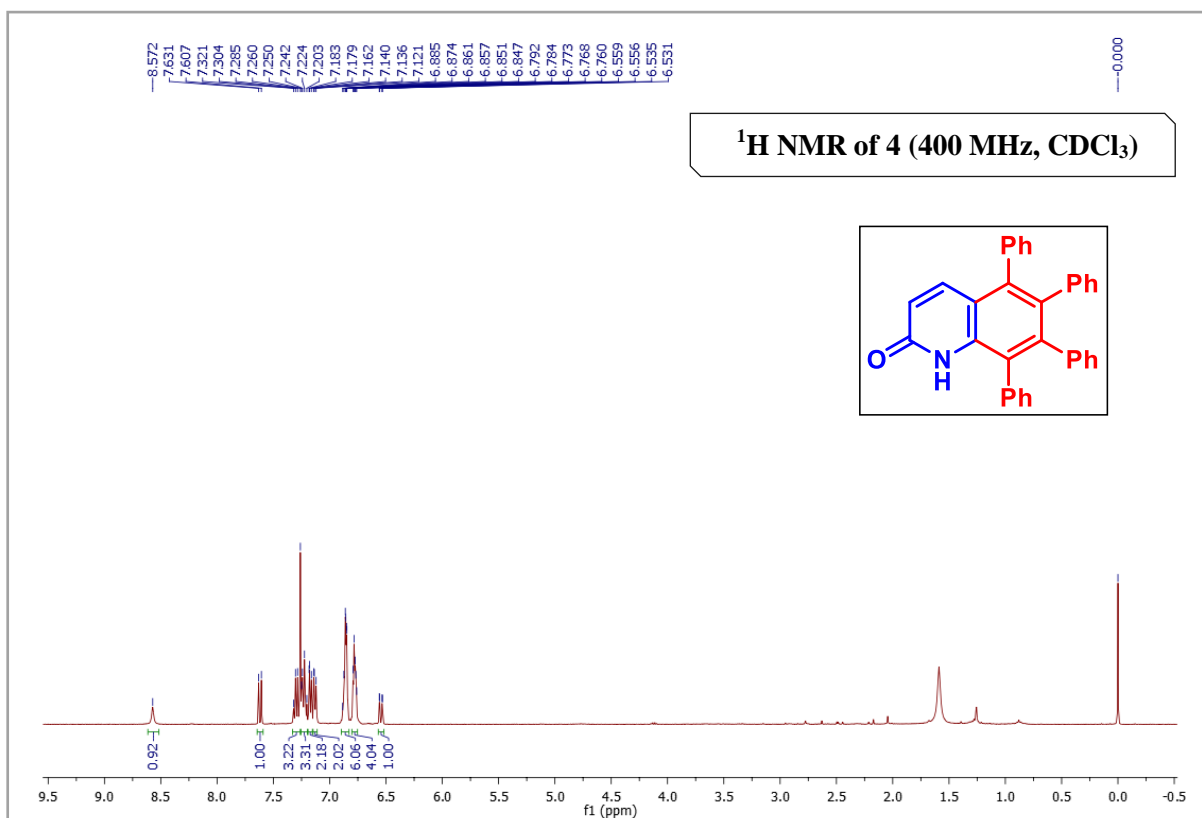
Crystal Structure of 3ja

3ja   CCDC 2177356
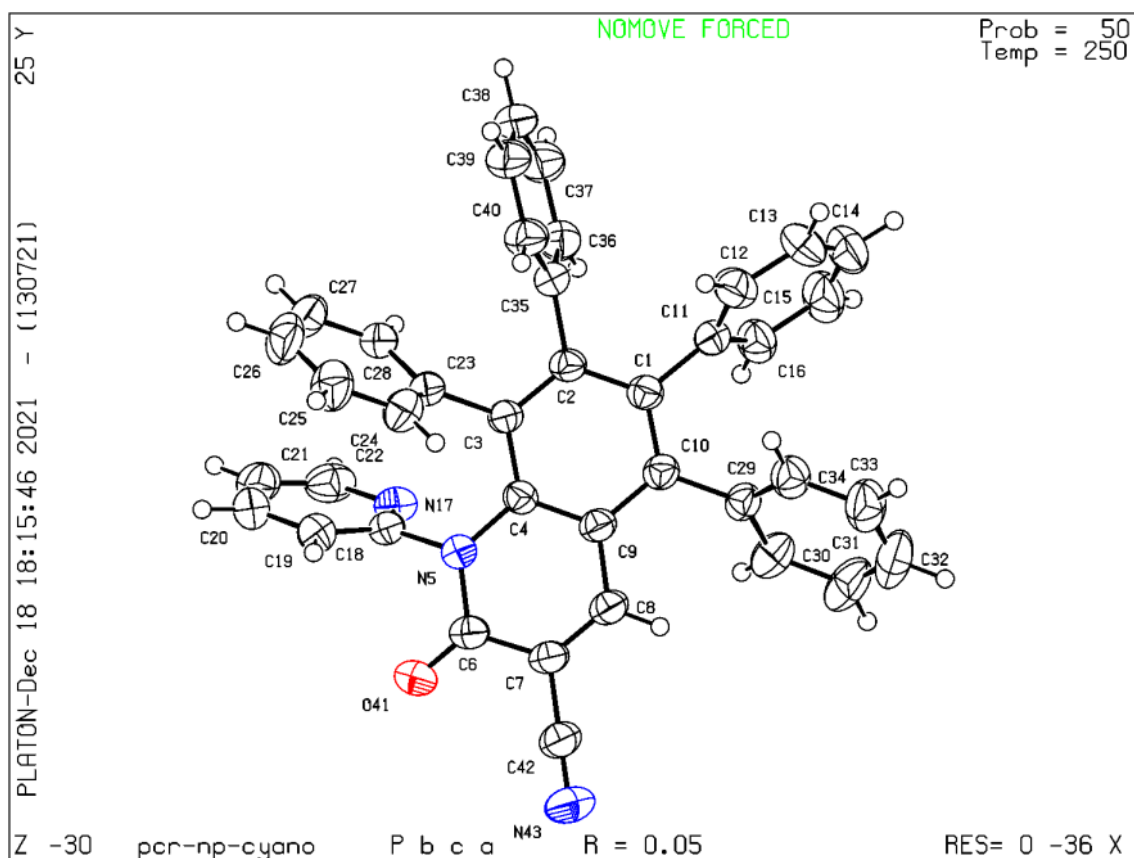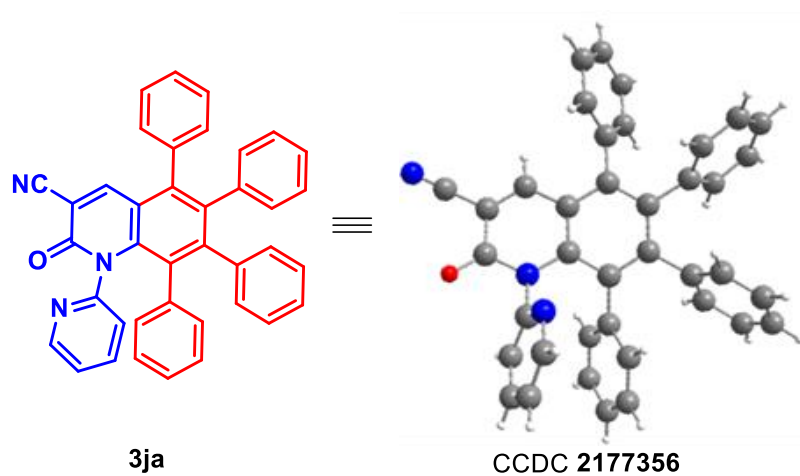
ORTEP diagram of **3ja** with 50% ellipsoid probability

5.6 REFERENCES

1. (a) Amer, M. M. K.; Aziz M. A.; Shehab, W. S.; Abdellattif, M. H.; Mouneir, S. M. Recent advances in chemistry and pharmacological aspects of 2-pyridone scaffolds. *J Saudichemical Soc.* **2021**, *25*, 101259. (b) Zhang, Y.; Pike, A. Pyridones in drug discovery: Recent advances. *Bioorg. Med. Chem. Lett.* **2021**, *38*, 127849.

2. Aly, A. A.; Ramadan, M.; Abuo-Rahma, G. E.-D. A.; Elshaier, Y. A. M. M.; Elbastawesy, M. A. I.; Brown, A. B.; Bräse, S. Chapter Three - Quinolones as prospective drugs: Their syntheses and biological applications. *In Adv. Heterocycl. Chem.; Academic Press.* **2021**, *135*, 147-196.

3. (a) Kuduk, S. D.; Chang, R. K.; Di Marco, C. N.; Ray, W. J.; Ma, L.; Wittmann, M.; Seager, M. A.; Koeplinger, K. A.; Thompson, C. D.; Hartman, G. D.; Bilodeau, M. T. Quinolizidinone Carboxylic Acids as CNS Penetrant, Selective M1 Allosteric Muscarinic Receptor Modulators. *ACS Med. Chem. Lett.* **2010**, *1*, 263-267. (b) Xu, Y.-S.; Zeng, C.-C.; Jiao, Z.-G.; Hu, L.-M.; Zhong, R.-G. Design, Synthesis and Anti-HIV Integrase Evaluation of 4-Oxo-4*H*-quinolizine-3-carboxylic Acid Derivatives *Molecules* **2009**, *14*, 868-883. (c) Hirano, K.; Miura, M. A Lesson for Site-selective C−H Functionalization on 2-Pyridones: Radical, Organometallic, Directing group and Steric Controls. *Chem. Sci.* **2018**, *9*, 22−32.

4. Hirano, K.; Miura, M. A lesson for site-selective C–H functionalization on 2-pyridones: radical, organometallic, directing group and steric controls. *Chem. Sci.* **2018**, *9*, 22–32.

5. R. Odani, K. Hirano, T. Satoh, M. Miura, Copper-Mediated C6-Selective Dehydrogenative Heteroarylation of 2-Pyridones with 1,3-Azoles. *Angew. Chem. Int. Ed.* **2014**, *53*, 10784–10788.

6. Diederich, F.; Stang, P. J.; Tykwinski, R. R. Acetylene Chemistry: Chemistry, Biology, and Material Science. Eds.; Wiley-VCH:Weinheim, Germany, **2005**.

7. (a) Li, T.; Wang, Z.; Xu, K.; Liu, W.; Zhang, X.; Mao, W.; Guo, Y.; Ge, X.; Pan, F. Rhodium-Catalyzed/Copper-Mediated Tandem C (sp^2)-H Alkynylation and Annulation: Synthesis of 11-Acylated Imidazo [1, 2-a: 3, 4-a′] dipyridin-5-ium-4-olates from 2 H-[1, 2′-Bipyridin]-2-ones and Propargyl Alcohols. *Org. Lett.* **2016**, *18*, 1064−1067. (b) Xu, X.; Luo, C.; Zhao, H.; Pan, Y.; Zhang, X.; Li, J.; Xu, L.; Lei, M.; Walsh, P. J. Rhodium(III)-Catalyzed C−H Bond Functionalization of 2-Pyridones with Alkynes: Switchable Alkenylation, Alkenylation/Directing Group Migration and Rollover Annulation. *Chem. Eur. J.* **2021**, *27*, 8811–8821. (c) Biswas, A.; Giri, D.; Das, D.; De, A.; Patra, S. K.; Samanta, R. A Mild Rhodium Catalyzed Direct Synthesis of Quinolones from Pyridones: Application in the Detection of Nitroaromatics. *J. Org. Chem.* **2017**, *82*, 10989−10996.

8. (a) Zhu, C.; Kuniyil, R.; Ackermann, L. Manganese(I)-Catalyzed C-H Activation/Diels-Alder/retro-Diels-Alder Domino Alkyne Annulation featuring Transformable Pyridines. *Angew. Chem., Int. Ed.* **2019**, *58*, 5338−5342. (b) Zheng, G.; Sun, J.; Xu, Y.; Zhai, S.; Li, X. Mn-Catalyzed Dehydrocyanative Transannulation of Heteroarenes and Propargyl Carbonates through C−H Activation: Beyond the Permanent Directing Effects of Pyridines/Pyrimidines. *Angew. Chem., Int. Ed.* **2019**, *58*, 5090-5094.

9. Zhu, C.; Kuniyil, R.; Jei, B. B.; Ackermann, L. Domino C−H Activation/Directing Group Migration/ Alkyne Annulation: Unique Selectivity by d^6-Cobalt(III) Catalysts. *ACS Catal.* **2020**, *10*, 4444−4450.

10. Wan, S.; Luo, Z.; Xu, X.; Yu, H.; Li, J.; Pan, Y.; Zhang, X.; Xu, L.; Cao, R. Manganese(I)-Catalyzed Site-Selective C6-Alkenylation of 2-Pyridones Using Alkynes via C−H Activation. *Adv. Synth. Catal.* **2021,** *363,* 2586–2593.

11. Xu, X.; Zhang, L.; Zhao, H.; Pan, Y.; Li, J.; Luo, Z.; Han, J.; Xu, L.; Lei, M. Cobalt(III)-Catalyzed Regioselective C6 Olefination of 2-Pyridones Using Alkynes: Olefination/Directing Group Migration and Olefination. *Org. Lett.* **2021**, *23*, 4624−4629.

12. Wang, C-S.; Monaco, S. D.; Thai, A. N.; Rahman, MdS.; Pang, B. P.; Wang, C.; Yoshikai, N. Cobalt/Lewis Acid Catalysis for Hydrocarbofunctionalization of Alkynes via Cooperative C−H Activation. *J. Am. Chem. Soc.* **2020**, *142*, 12878−12889.

13. Nakao, Y.; Idei, H.; Kanyiva, K. S.; Hiyama, T. Direct alkenylation and alkylation of pyridone derivatives by Ni/AlMe$_3$ catalysis. *J. Am. Chem. Soc.* **2009**, *131*, 15996−15997.

14. Yin, G.; Li, Y.; Wang, R. H.; Li, J. F.; Xu, X. T.; Luan, Y. X.; Ye, M. Ligand-Controlled Ni(0)-Al(III) Bimetal-Catalyzed C$_3$-H Alkenylation of 2-Pyridones by Reversing Conventional Selectivity. *ACS Catal.* **2021**, *11*, 4606−4612.

15. Harry, N. A.; Saranya, S.; Ujwaldev, S. M.; Anilkumar, G. Recent advances and prospects in nickel-catalyzed C-H activation. *Catal. Sci. Technol.* **2019**, *9*, 1726-1743.

16. Yadav, S. K.; Ramesh, B.; Jeganmohan, M. Cobalt(III)-Catalyzed Chemo- and Regioselective [4 + 2]-Annulation of Aromatic Sulfoxonium Ylides with 1,3-Diynes. *J. Org. Chem.* **2022**, 87, 4134–4153.

17. Mohanty, S. R.; Prusty, N.; Gupta, L.; Biswal, P.; Ravikumar, P. C. Cobalt(III)-catalyzed C-6 alkenylation of 2-pyridones by using terminal alkyne with high regioselectivity. *J. Org. Chem.* **2021**, *86*, 9444−9454.

18. Prusty, N.; Banjare, S. K.; Mohanty, S. R.; Nanda, T.; Yadav, K.; Ravikumar, P. C. Synthesis and Photophysical Study of Heteropolycyclic and Carbazole Motif: Nickel-Catalyzed Chelate-Assisted Cascade C–H Activations/Annulations. *Org. Lett.* **2021**, *23*, 9041–9046.

19. (a) Liu, Y.-H.; Xia, Y.-N.; Shi, B.-F. Ni-Catalyzed Chelation-Assisted Direct Functionalization of Inert C–H Bonds. *Chin. J. Chem.* **2020**, *38*, 635−662. (b) Misal Castro, L. C.; Obata, A.; Aihara, Y.; Chatani, N. Chelation-Assisted Nickel-Catalyzed Oxidative Annulation via Double C-H Activation/Alkyne Insertion Reaction. *Chem. Eur. J.* **2016**, *22*, 1362−1367. (c) Tenn, W. J.; Young, K. J. H.; Bhalla, G.; Oxgaard, J.; Goddard, W. A.; III; Periana, R. P. CH Activation with an O-Donor Iridium-Methoxo Complex. *J. Am. Chem. Soc.* **2005**, *127*, 14172−14173. (d) Campeau, L.-C.; Parisien, M.; Jean, A.; Fagnou, K. Catalytic Direct Arylation with Aryl Chlorides, Bromides, and Iodides: Intramolecular Studies Leading to New Intermolecular Reactions. *J. Am. Chem. Soc.* **2006**, *128*, 581−590. (e) García-Cuadrado, D.; Braga, A. A.; Maseras, F.; Echavarren, A. M. Proton abstraction mechanism for the palladium-catalyzed intramolecular arylation. *J. Am. Chem. Soc.* **2006**, *128*, 1066−1067. (f) Lapointe, D.; Fagnou, K. Overview of the Mechanistic Work on the Concerted Metallation−Deprotonation Pathway. *Chem. Lett.* **2010**, *39* (11), 1118−1126.

20. (a) Molecular Fluorescence: Principle and Applications; Valeur, B., Ed.; Wiley: Weinheim, Germany, **2005**. (b) Mei, J.; Leung, N. L.; Kwok, R. T.; Lam, J. W.; Tang, B. Z. Aggregation-Induced Emission: Together We Shine, United We Soar! *Chem. Rev.* **2015**, *115*, 11718−11940.

21. Prusty, N.; Kinthada, L. K.; Meena, R.; Chebolu, R.; Ravikumar, P. C. Bismuth(III)-catalyzed regioselective alkylation of tetrahydroquinolines and indolines towards the synthesis of bioactive corebiaryl oxindoles and CYP19 inhibitors. *Org. Biomol. Chem.* **2021**, *19*, 891-905.

22. Gottlieb, H. E.; Kotlyar, V.; Nudelman, A. NMR chemical shifts of common laboratory solvents as trace impurities. *J. Org. Chem.* **1997**, *62*, 7512-7515.

23. (a) Mohanty, S. R.; Prusty, N.; Gupta, L.; Biswal, P.; Ravikumar, P. C. Cobalt(III)-Catalyzed C-6 Alkenylation of 2-Pyridones by Using Terminal Alkyne with High Regioselectivity. *J. Org. Chem.* **2021**, *86*, 14, 9444–9454. (b) Huang, G.; Shan, Y.; Yu, J.-T.; Pan, C. Rh(III)-Catalyzed C6-Selective Oxidative C−H/C−H Crosscoupling of 2-Pyridones with Thiophenes. *Chem. -Eur. J.* **2021**, *27*, 12294-12299.

24. Mio, M. J.; Kopel, L. C.; Braun, J. B.; Gadzikwa, T. L.; Hull, K. L.; Brisbois, R. G.; Markworth, C. J.; Grieco, P. A. One-pot synthesis of symmetrical and unsymmetrical bisarylethynes by a modification of the Sonogashira coupling reaction. *Org. Lett.* **2002**, *4*, 3199−3202.

25. Biswas, A.; Giri, D.; Das, D.; De, A.; Patra, S. K.; Samanta, R. A Mild Rhodium Catalyzed Direct Synthesis of Quinolones from Pyridones: Application in the Detection of Nitroaromatics. *J. Org. Chem.* **2017**, *82*, 10989−10996.

Chapter 6

Introduction to C–N bond Activation

Chapter 6

Introduction to C–N bond Activation
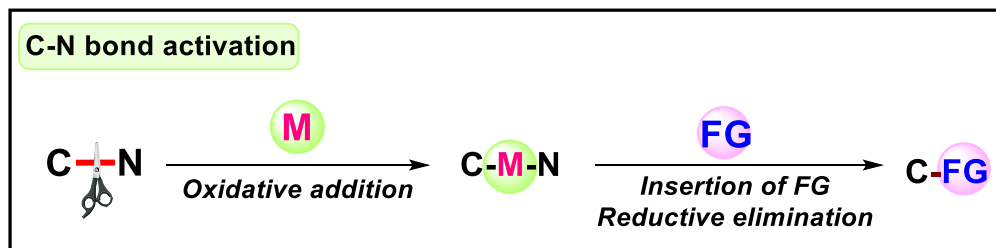
6.1 ABSTRACT

The C−N bond is one of the most common chemical bonds present in many organic molecules. The activation and transformation of C−N bonds by using transition-metal catalysis has emerged as a powerful tool for the formation of C−C, C−N, C−X (X = O, S) bond. As compared to catalytic C−H bond activation reactions, transition-metal catalyzed C−N bond activation is considerably underexplored. It has been identified as an emerging area of organic transformations. Transition metal mediated C–N bond activation reactions have been found to be a key step in several catalytic coupling methods. The reactive C−M−N intermediate formed from the C–N bond activation reacts with suitable coupling partners to form new C−C bonds

6.2 INTRODUCTION

One of the most common chemical bonds found in many organic molecules is the C−N bond. So, the reaction involving formation as well as transformation of the C−N bond is of high importance in organic chemistry, biochemistry, and organometallic chemistry.[1] Considering the example of the two-way process where synthesizing proteins from α-amino acids by employing C−N bond formation method and formation of α-amino acids back from the proteins by employing C−N activation method in the presence of enzyme are

crucial for human life.[2] The functionalisation/activation of other inert bonds like C−H,[3] C−C,[4] and C−O[5] bonds in presence of transition metal catalyst are well explored and gained a huge attention from synthetic community over the years. As comparison to those, the transition metal catalyzed functionalisation/activation of C−N bond is quite less explored. Because of the high bond dissociation energy[6] of the C−N bond and the unusual stability of unactivated nitrogen carrying compounds, these compounds are less reactive. Hence it is very challenging to functionalize the inert C−N bond which create an opportunity for the researcher to explore these areas and finding a several unexpected transformations.

Generally, there are two types of nitrogen carrying compounds available[7] (i) compounds with unactivated C−N bonds, e.g., hydrazines, amides, amines, etc., and (ii) compounds having activated C−N bonds, e.g diazonium salts, ammonium salts, and strained N-heterocycles (Figure 6.1).

Figure 6.1: Types of nitrogen carrying compounds
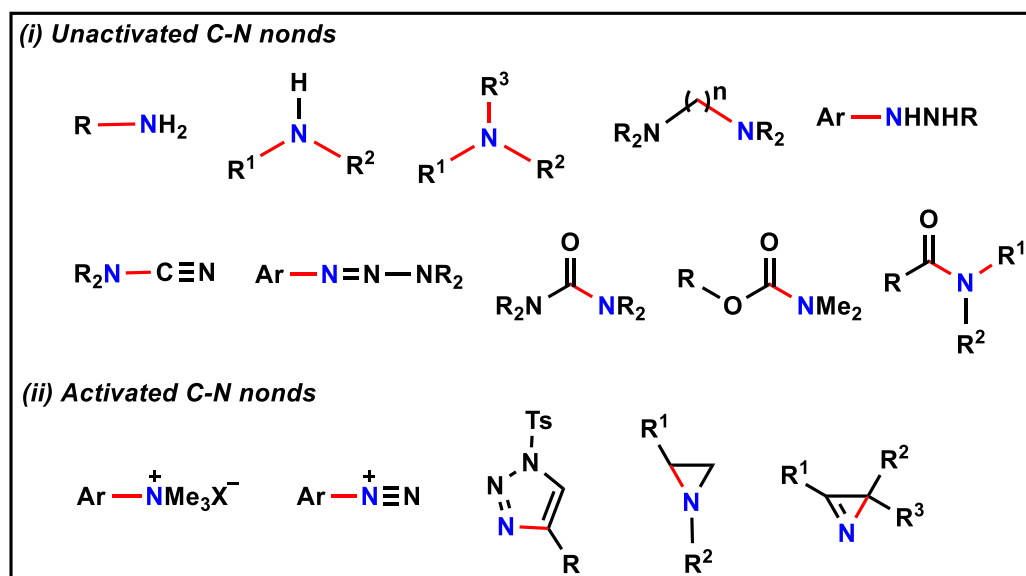
The selectivity in C−N bond cleavage process has been observed when the nitrogen carrying molecules (secondary amines, tertiary amines, ammonium salts, amides etc.) have more than one C−N bond. It is found that less hindered C−N bond cleaved earlier than the

more hindered C−N bond and the selectivity in reaction depend on the structure of the substrate as well as the reaction conditions.[7]

6.3 DIFFERENT MODES INVOLVED IN C−N ACTIVATION:

There are different modes involved in the transition metal catalyzed C−N bond cleavage process.[7,8] These are (a) oxidative addition (b) C−H bond cleavage triggered C−N activation *via* iminium species, (c) de-alkylation of ammonium species, (d) *β*-amino elimination, (e) insertion/de-insertion (Figure 6.2).

Figure 6.2: Various pathways involved in C−N activation
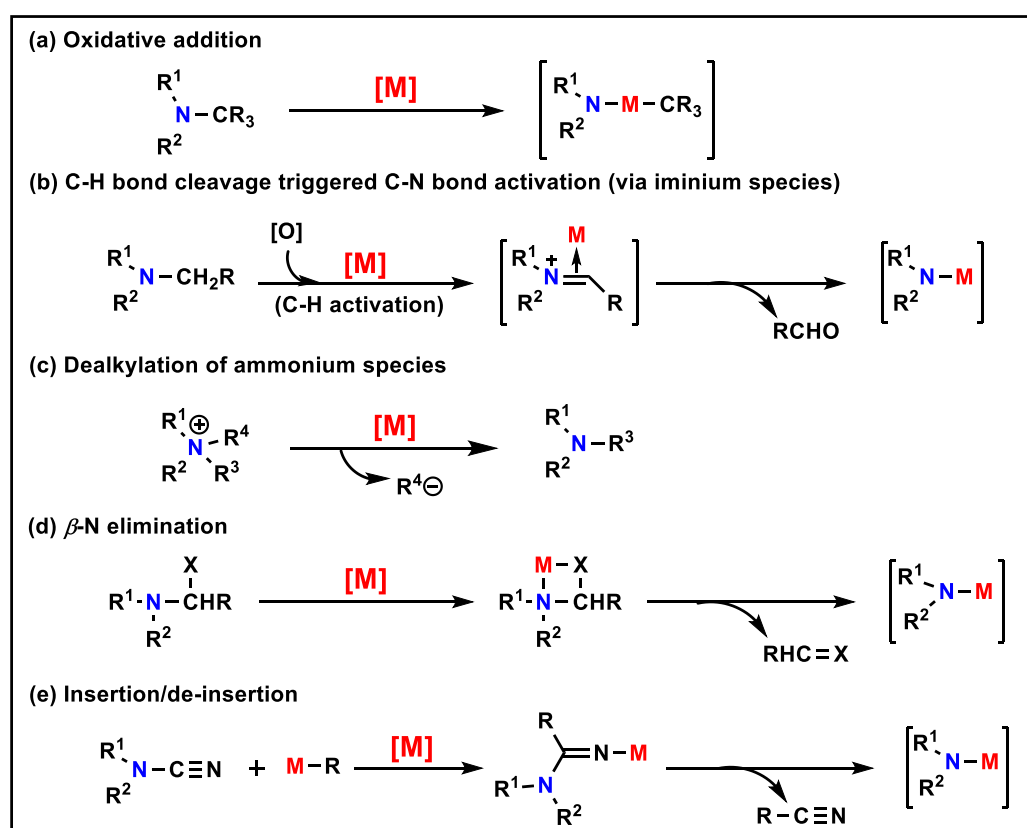
The overall process of C−N functionalization can be properly explained from a general catalytic cycle (Figure 6.3).[8]

Figure 6.3: General catalytic cycle for metal catalyzed C−N functionalization
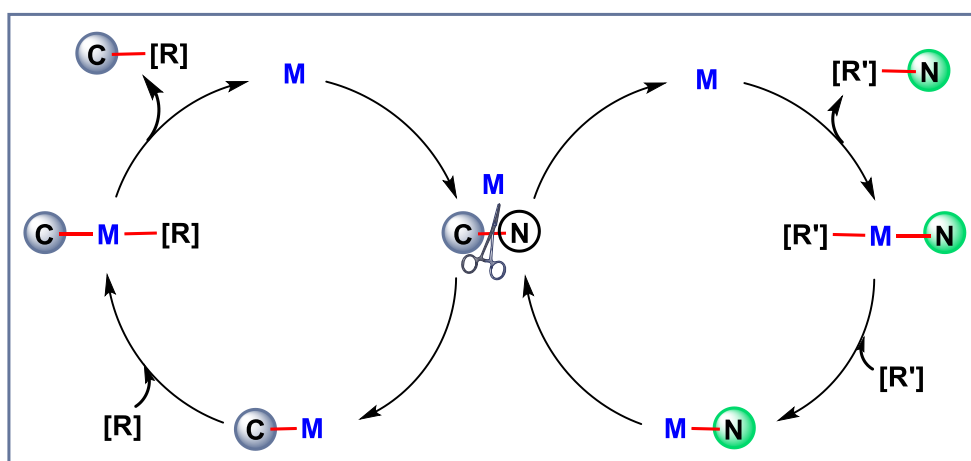
Stage 1: The active transition metal catalyst interact with **C−N** bond forming **C−M−N** intermediate which produces both **C−M** and **M−N** species.

Stage 2: Then the C-M as well as M-N species in the presence of coupling partner react with other coupling partner affording **C−M−[R]** and **[R']−M−N** intermediate.

Stage 3: Both **C−M−[R]** and **[R']−M−N** intermediate react with other coupling partners affording new **C−C** and **N−C** bonds with regeneration of catalyst.

6.4 REPORTS ON C−N ACTIVATION

C−N bond activation with noble metals like palladium and others are quite explored.[9] According to literature survey specially palladium metal has gained a huge attention in this area affording new transformation. But these metals are of high price and low natural abudance.[10] Hence, utilising first-row 3d transition metals like Nickel and other would be cost-effective and environmentally friendly as these metals have high natural abundance, and of low cost.[11] And, considering nickel as the catalyst for such transformation, it is isoelectronic to Palladium and it shows unique reactivity because of its variable oxidation state.

Scheme 6.1 Reports of C−N functionalization in Nickel catalyst
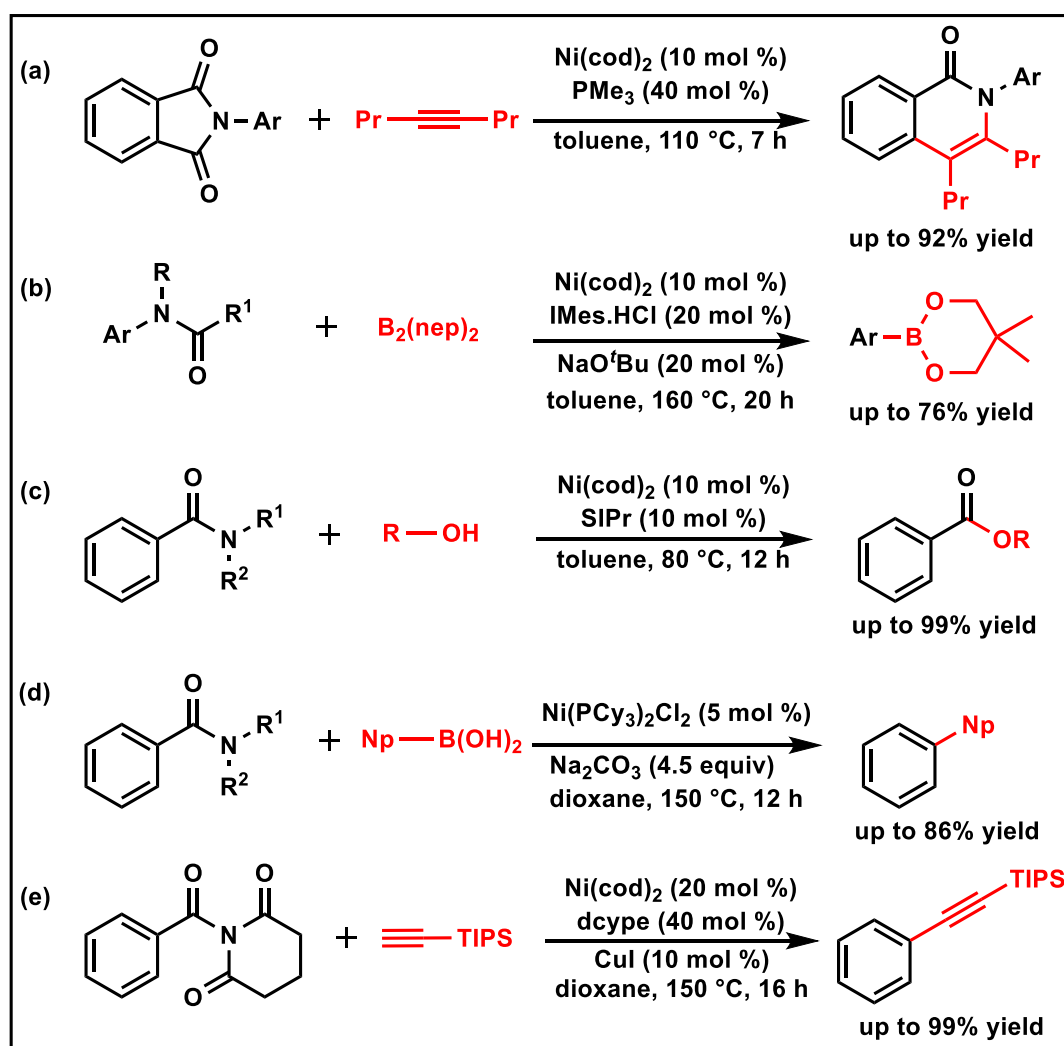
In this context, Kurahashi group reported carboamination with alkyne using nickel catalyst in 2008. They employed *N*-phenylphthalimide in combination with 4-octyne to synthesize the isoquinolone product (Scheme 6.1a).[12] Chatani reported a work in 2014 describing the synthesis of a borylation product utilising diboron reagent and *N*-aryl amide substrate, with a high yield of the borylated product (Scheme 6.1b).[13] Later, in 2015, the Garg group reported esterification of the C−N bond of the benzamide substrate using various alcohols and they found good to excellent yield of ester product (Scheme 6.1c).[14] In 2016, Szostak group demonstrated synthesis of biarylated product employing C−N activation method.

They observed a good yield of the biarylated product using a wide spectrum of amide and boronic acid substrates (Scheme 6.1d).[15] Then Rueping group in 2017 reported a nickel-catalyzed deamidative cross-coupling reaction of amides by using terminal alkynes as the coupling partner (Scheme 6.1e).[16] With the help of this newly developed method, the amides can be directly converted into alkynes and afford the $C(sp^2)−C(sp)$ bonds in a simple and moderate way. All these transformations (carboamination, borylation, arylation, esterification, transmidation, alkenylation etc.) have also been explored by other groups by employing transition metal catalyzed C−N activation methods.[17]

6.5 CONCLUSION

In this chapter, we have discussed the importance and functionalization of C−N bond in the organic transformation. There are two types of C−N bond present in the molecule (i) unactivated C−N bond, (ii) activated C−N bond. The transition metal catalyzed C−N bond activation involves various pathways and has been used as an efficient method to construct C−C and C−Hetero bonds. This area unfolds new transformation and enable to synthesize complex molecules of importance to pharmaceutical industries. In this area, where noble metals like palladium have drawn more attention, first-row metals like nickel are now gaining hold. Hence this area need to be explored further. Considering all this, we are trying to explore the reactivity of Nickel catalyst in the C−N activation/functionalisation area.

6.6 REFERENCES

1. (a) Hartwig, J. F. Carbon−Heteroatom Bond-Forming Reductive Eliminations of Amines, Ethers, and Sulfides. *Acc. Chem. Res.* **1998**, *31*, 852−860. (b) Ley, S. V.; Thomas, A. W. Modern Synthetic Methods for Copper-Mediated C(aryl)−O, C(aryl)−N, and C(aryl)−S Bond Formation. *Angew. Chem., Int. Ed.* **2003**, *42*, 5400−5449. (c) Schlummer, B.; Scholz, U. Palladium-Catalyzed C−N and C−O Coupling − A Practical Guide from an Industrial Vantage Point. *Adv. Synth. Catal.* **2004**, *346*, 1599−1626. (d) Beccalli, E. M.; Broggini, G.; Martinelli, M.; Sottocornola, S. C−C, C−O, C−N Bond Formation on sp^2 Carbon by Pd(II)-Catalyzed Reactions Involving Oxidant Agents. *Chem. Rev.* **2007**, *107*, 5318−5365. (e) Song, G.; Wang, F.; Li, X. C−C, C−O and C−N Bond Formation *via* Rhodium(III)-Catalyzed Oxidative C−H Activation. *Chem. Soc. Rev.* **2012**, *41*, 3651−3678. (f) Wang, T.; Jiao, N. Direct Approaches to Nitriles via Highly Efficient Nitrogenation Strategy through C−H or C−C Bond Cleavage. *Acc. Chem. Res.* **2014**, *47*, 1137−1145. (g) Yang, Q.; Wang, Q.; Yu, Z. Substitution of Alcohols by *N*-Nucleophiles *via* Transition-Metal-Catalyzed Dehydrogenation. *Chem. Soc. Rev.* **2015**, *44*, 2305−2329. (h) Krüger, K.; Tillack, A.; Beller, M. Recent Innovative Strategies for the Synthesis of Amines: From C−N Bond Formation to C−N Bond Activation. *ChemSusChem* **2009**, *2*, 715−717.

2. Lawrence, S. A. Amines: *Synthesis, Properties and Applications*; Cambridge University Press: Cambridge, U.K., **2004**.

3. (a) Kakiuchi, F.; Chatani, N. Catalytic Methods for C−H Bond Functionalization: Application in Organic Synthesis. *Adv. Synth. Catal.* **2003**, *345*, 1077−1101. (b) Davies, H. M. L.; Beckwith, R. E. J. Catalytic Enantioselective C−H Activation by Means of Metal-Carbenoid-Induced C−H Insertion. *Chem. Rev.* **2003**, *103*, 2861−2903. (c) Alberico, D.; Scott, M. E.; Lautens, M. Aryl-Aryl Bond Formation by Transition-Metal-Catalyzed Direct Arylation. *Chem. Rev.* **2007**, *107*, 174−238. (d) Chen, X.; Engle, K. M.; Wang, D.-H.; Yu, J.-Q. Palladium(II)-Catalyzed C−H Activation/C−C Cross-Coupling Reactions: Versatility and Practicality. *Angew. Chem., Int. Ed.* **2009**, *48*, 5094−5115. (e) Mkhalid, I. A. I.; Barnard, J. H.; Marder, T. B.; Murphy, J. M.; Hartwig, J. F. C−H Activation for the Construction of C−B Bonds. *Chem. Rev.* **2010**, *110*, 890−931. (f) Wencel-Delord, J.; Dröge, T.; Liu, F.;

Glorius, F. Towards Mild Metal-Catalyzed C−H bond Activation. *Chem. Soc. Rev.* **2011**, *40*, 4740−4761. (g) Baudoin, O. Transition-Metal-Catalyzed Arylation of Unactivated C(sp³)−H bonds. *Chem. Soc. Rev.* **2011**, *40*, 4902−4911. (h) Newhouse, T.; Baran, P. S. If C−H Bonds Could Talk: Selective C−H Bond Oxidation. *Angew. Chem., Int. Ed.* **2011**, *50*, 3362−3374. (i) Yang, L.; Huang, H. Transition-Metal-Catalyzed Direct Addition of Unactivated C−H Bonds to Polar Unsaturated Bonds. *Chem. Rev.* **2015**, *115*, 3468−3517. (j) Cheng, C.; Hartwig, J. F. Catalytic Silylation of Unactivated C−H Bonds. *Chem. Rev.* **2015**, *115*, 8946−8975.

4. (a) Schröder, D.; Schwarz, H. C−H and C−C Bond Activation by Bare Transition-Metal Oxide Cations in the Gas Phase. *Angew. Chem., Int. Ed. Engl.* **1995**, *34*, 1973−1995. (b) Rybtchinski, B.; Milstein, D. Metal Insertion into C−C Bonds in Solution. *Angew. Chem., Int. Ed.* **1999**, *38*, 870−883. (c) Matsumura, S.; Maeda, Y.; Nishimura, T.; Uemura, S. Palladium-Catalyzed Asymmetric Arylation, Vinylation, and Allenylation of *tert*-Cyclobutanols *via* Enantioselective C−C Bond Cleavage. *J. Am. Chem. Soc.* **2003**, *125*, 8862−8869. (d) Jun, C.-H. Transition-Metal-Catalyzed Carbon−Carbon Bond Activation. *Chem. Soc. Rev.* **2004**, *33*, 610−618. (e) Park, Y. J.; Park, J.-W.; Jun, C.-H. Metal-Organic Cooperative Catalysis in C−H and C−C Bond Activation and Its Concurrent Recovery. *Acc. Chem. Res.* **2008**, *41*, 222−234.

5. (a) Yamamoto, A. Carbon−Oxygen Bond Activation by Transition Metal Complexes. *Adv. Organomet. Chem.* **1992**, *34*, 111−147. (b) Li, B.-J.; Yu, D.-G.; Sun, C.-L.; Shi, Z.-J. Activation of "Inert" Alkenyl/Aryl C−O Bond and Its Application in Cross-Coupling Reactions. *Chem. - Eur. J.* **2011**, *17*, 1728−1759. (c) Li, W.-N.; Wang, Z.-L. Kumada−Tamao−Corriu Cross Coupling Reaction of O-based Electrophiles with Grignard Reagents *via* C−O Bond Activation. *RSC Adv.* **2013**, *3*, 25565−25575. (d) Cornella, J.; Zarate, C.; Martin, R. Metal-Catalyzed Activation of Ethers *via* C−O Bond Cleavage: A New Strategy for Molecular Diversity. *Chem. Soc. Rev.* **2014**, *43*, 8081−8097.

6. Blanksby, S. J.; Ellison, G. B. Bond Dissociation Energies of Organic Molecules. *Acc. Chem. Res.* **2003**, *36*, 255−263.

7. (a) Ouyang, K.; Hao, W.; Zhang, W.-X.; Xi, Z. Transition-Metal Catalyzed Cleavage of C−N Single Bonds. *Chem. Rev.* **2015**, *115*, 12045−12090. (b) Jensen, K. L.; Standley, E. A.; Jamison, T. F. Highly regioselective nickel-catalyzed cross-

coupling of N-tosylaziridines and alkylzinc reagents. *J. Am. Chem. Soc.* **2014**, 136, 11145– 11152.

8. Wang, Q.; Su, Y.; Li, L.; Huang, H. Transition-metal catalysed C−N bond activation. *Chem. Soc. Rev.* **2016**, *45*, 1257−1272.

9. (a) Lei, P.; Meng, G.; Szostak, M. General Method for the Suzuki-Miyaura Cross-Coupling of Amides Using Commercially Available, Air- and Moisture-Stable Palladium/NHC (NHC = *N*-Heterocyclic Carbene) Complexes. *ACS Catal.* **2017**, *7*, 1960–1965. (b) Wu, H.; Li, Y.; Cui, M.; Jian, J.; Zeng, Z. Suzuki Coupling of Amides *via* Palladium-Catalyzed C–N Cleavage of *N*-Acylsaccharins. *Adv. Synth. Catal.* **2016**, *358*, 3876–3880. (c) Meng, G.; Szostak, R.; Szostak, M. Suzuki–Miyaura Cross-Coupling of *N*-Acylpyrroles and Pyrazoles: Planar, Electronically Activated Amides in Catalytic N–C Cleavage. *Org. Lett.* **2017**, *19*, 3596–3599. (d) Cui, M.; Wu, H.; Jian, J.; Wang, H.; Liu, C.; Daniel, S.; Zeng, Z. Palladium-catalyzed Sonogashira coupling of amides: access to ynones *via* C–N bond cleavage. *Chem. Commun.* **2016**, *52*, 12076−12079. (e) Shi, S.; Szostak, M. Decarbonylative Cyanation of Amides by Palladium Catalysis. *Org. Lett.* **2017**, *19*, 3095–3098. (f) Meng, G.; Szostak, M. Site-Selective C–H/C–N Activation by Cooperative Catalysis: Primary Amides as Arylating Reagents in Directed C–H Arylation. *ACS Catal.* **2017**, *7*, 7251–7256. (g) Meng, G.; Szostak, M. Rhodium-Catalyzed C–H Bond Functionalization with Amides by Double C–H/C–N Bond Activation. *Org. Lett.* **2016**, *18*, 796– 799.

10. Dalton, T.; Faber, T.; Glorius, F. C−H Activation: Toward Sustainability and Applications. *ACS Cent. Sci.* **2021**, *7*, 245-261.

11. (a) Su, B.; Cao, Z.-C.; Shi, Z.-J. Exploration of Earth-Abundant Transition Metals (Fe, Co, and Ni) as Catalysts in Unreactive Chemical Bond Activations. *Acc. Chem. Res.* **2015**, *48*, 886–896. (b) Zhou, J.-Y.; Tian, R.; Zhu, Y.-M. Nickel-Catalyzed Selective Decarbonylation of *α*-Amino Acid Thioester: Aminomethylation of Mercaptans. *J. Org. Chem.* **2021**, *86*, 12148– 12157.

12. Kajita, Y.; Matsubara, S.; Kurahashi, T. Nickel-Catalyzed Decarbonylative Addition of Phthalimides to Alkynes. *J. Am. Chem. Soc.* **2008**, *130*, 6058– 6059.

13. Tobisu, M.; Nakamura, K.; Chatani, N. Nickel-Catalyzed Reductive and Borylative Cleavage of Aromatic Carbon–Nitrogen Bonds in *N*-Aryl Amides and Carbamates. *J. Am. Chem. Soc.* **2014**, *136*, 5587–5590.

14. Hie, L.; Fine Nathel, N. F.; Shah, T. K.; Baker, E. L.; Hong, X.; Yang, Y. F.; Liu, P.; Houk, K. N.; Garg, N. K. Conversion of amides to esters by the nickel-catalysed activation of amide C−N bonds. *Nature* **2015**, *524*, 79–83.

15. Shi, S.; Meng, G.; Szostak, M. Synthesis of biaryls through Nickel-catalyzed Suzuki-Miyaura coupling of amides by carbon nitrogen bond cleavage. *Angew. Chem.* **2016**, *55*, 6959−6963.

16. Srimontree, W.; Chatupheeraphat, A.; Liao, H.-H.; Rueping, M. Amide to Alkyne Interconversion *via* a Nickel/Copper-Catalyzed Deamidative Cross-Coupling of Aryl and Alkenyl Amides. *Org. Lett.* **2017**, *19*, 3091–3094.

17. (a) Shi, S.; Szostak, M. Nickel-catalyzed diaryl ketone synthesis by N–C cleavage: direct Negishi cross-coupling of primary amides by site-selective *N,N*-di-boc activation. *Org. Lett.* **2016**, *18*, 5872–5875. (b) Weires, N. A.; Baker, E. L.; Garg, N. K. Nickel-catalysed Suzuki−Miyaura coupling of amides. *Nat. Chem.* **2016**, *8*, 75–79. (c) Baker, E. L.; Yamano, M. M.; Zhou, Y.; Anthony, S. M.; Garg, N. K. A Two-Step Approach to Achieve Secondary Amide Transamidation Enabled by Nickel Catalysis. *Nat. Commun.* **2016**, *7*, 11554. (d) Dander, J. E.; Baker, E. L.; Garg, N. K. Nickel-Catalyzed Transamidation of Aliphatic Amide Derivatives. *Chem. Sci.* **2017**, *8*, 6433–6438. (e) Boit, T. B.; Weires, N. A.; Kim, J.; Garg, N. K. Nickel-catalyzed Suzuki–Miyaura coupling of aliphatic amides. *ACS Catal.* **2018**, *8*, 1003–1008. (f) Zhang, Z.-B.; Ji, C.-L.; Yang, C.; Chen, J.; Hong, X.; Xia, J.-B. Nickel-Catalyzed Kumada Coupling of Boc-Activated Aromatic Amines *via* Nondirected Selective Aryl C–N Bond Cleavage. *Org. Lett.* **2019**, *21*, 1226–1231. (g) Buchspies, J.; Rahman, M.; Szostak, M. Transamidation of Amides and Amidation of Esters by Selective N–C(O)/O–C(O) Cleavage Mediated by Air- and Moisture-Stable Half-Sandwich Nickel(II)–NHC Complexes. *Molecules* **2021**, *26*, 188.
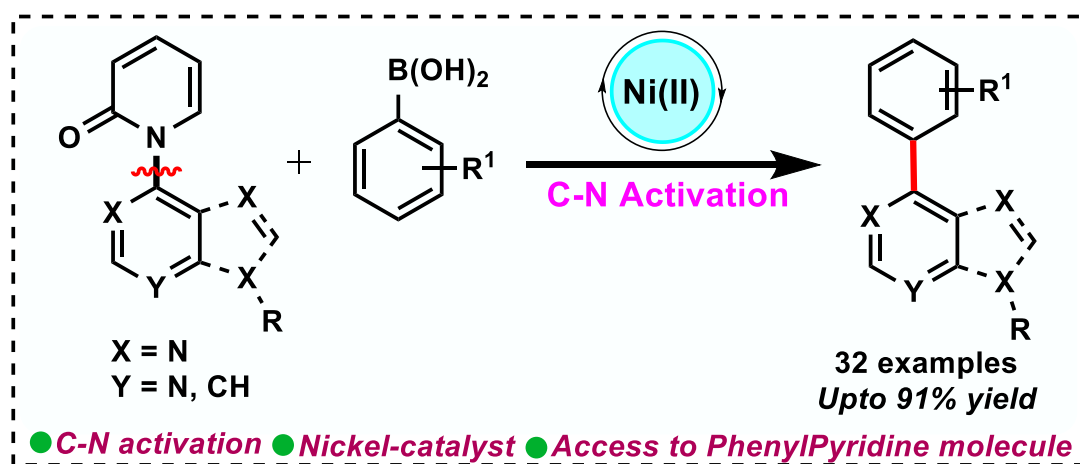
Chapter 7

Nickel Catalyzed Aryl–Aryl Bridging C–N Bond activation of

2-Pyridylpyridones and 6-Purinylpyridones

Chapter 7

Nickel Catalyzed Aryl–Aryl Bridging C–N Bond activation of

2-Pyridylpyridones and 6-Purinylpyridones

X = N
Y = N, CH

32 examples
Upto 91% yield

● *C-N activation* ● *Nickel-catalyst* ● *Access to PhenylPyridine molecule*

7.1 ABSTRACT: A Ni-catalyzed C−N bond activation of 2-pyridylpyridone and 1-(9*H*-purin-6-yl)pyridin-2(1*H*)-one and coupling with arylboronic acid has been achieved. A unique feature of this reaction is the strategic activation of hindered bridging C−N bond and replacement of pyridone unit with aryl groups using Nickel catalyzed Suzuki-Miyaura coupling. This provides exciting new tool to build C−C bonds in the place of pyridones. A wide variety of substrates and boronic acids are amenable to this transformation. More importantly, we have successfully synthesized a variety of C(6)-arylated purines *via* deaminative cross coupling which are very useful in developing unnatural nucelobases, nucleotides and nucleosides.
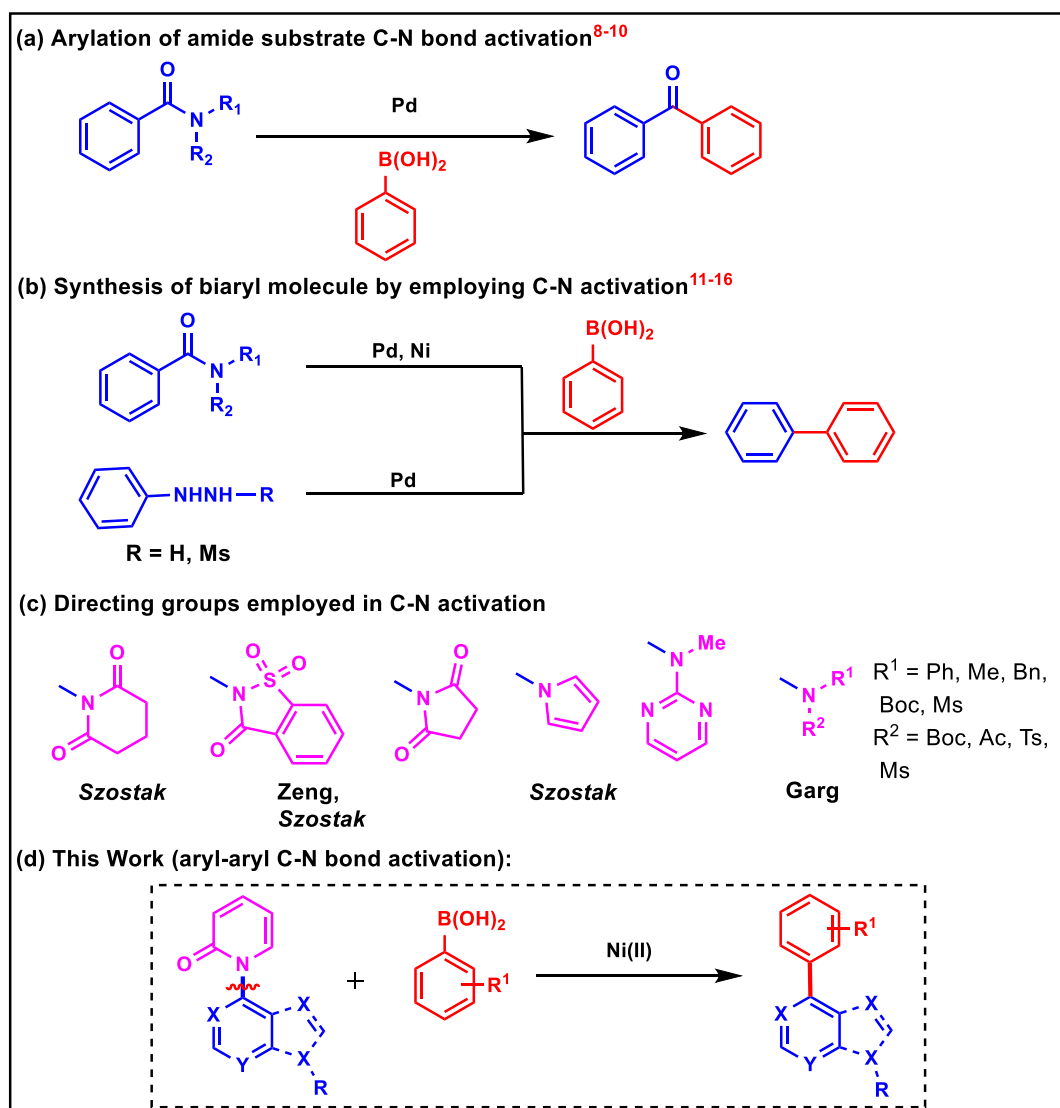
7.2 INTRODUCTION

Rapid advancements in methods development continue to expand the boundaries of chemical synthesis. C−H bond activation was once thought to be practically unachievable. But recent development in C−H bond activation has changed the scenario and it has become

one of the main stream organic chemistry reactions.[1] One of the current challenges in the field of organic synthesis is the activation and functionalization of C–N bonds which are considered to be one of the strongest and inert bonds.[2] Generally C−N bond containing molecules exists as amines or amides.[3] A wide variety of bioactive natural products, pharmaceuticals have nitrogen containing functional groups, such as cyano, amine, amide etc.,[4] hence, the ability to convert these groups to other groups/scaffolds enables drug diversification and modification. Therefore, the functionalization of inert C−N bond is important from synthetic and medicinal chemistry point of view.

In this regard, the functionalization of primary, secondary, and tertiary amines, diamines, amides and hydrazines have already been reported during the last decade *via* the transition metal catalyzed cleavage of C−N bond.[5] Various transition metal catalyzed cross-coupling reactions such as Kumada, Negishi and Suzuki coupling, have been used for C−N activation/functionalization reactions.[6] Due to the commercial availability of variety of organoboronate reagents, high functional group tolerance, and eco-friendly reaction conditions, Suzuki-Miyaura cross-coupling reactions involving C−N activation in particular has drawn significant attention among the research community.[7] In this context, pioneering research groups of Szostak, Zeng and Garg. have investigated the C−N functionalization with a variety of amide substrates by taking aryl boronic acid as the coupling partner which leads to benzoyl arylated product in each case (Figure 7.1a).[8-10] Szostak[11] and Zeng[12] group have also reported the synthesis of biaryl molecule by modifying the reaction condition on same substrate. Followed by this result, Peng[13] and Gao[14] group reported the synthesis of biaryl molecule by using arylhydrazine as substrate where aromatic C−N bond is functionalized (Figure 7.1b). But all these reports are with second-row transition metal catalysts. There are very limited reports of C−N bond functionalization employing aryl-boronic acid as a reaction partner with first-row transition

Figure 7.1: C−N activation of Pyridylpyridones using transition metal catalyst

(a) Arylation of amide substrate C-N bond activation[8-10]

(b) Synthesis of biaryl molecule by employing C-N activation[11-16]

R = H, Ms

(c) Directing groups employed in C-N activation

Szostak

Zeng, Szostak

Szostak

Garg

R^1 = Ph, Me, Bn, Boc, Ms
R^2 = Boc, Ac, Ts, Ms

(d) This Work (aryl-aryl C-N bond activation):

metals (Figure 7.1b).[15, 16] As first-row row transition metals are less expensive and earth abundant than 2nd and 3rd row transition metals,[17] use of these metals in catalytic synthetic methods is more economic and sustainable. In this regard, Szostak group have demonstrated Ni-catalyzed arylation of benzoylpiperidinedione molecule with aryl boronic acid for the synthesis of biaryl product.[15] Later, Johnson group reported arylation of isoindolinedione by employing Ni-catalyzed C−N bond cleavage.[16] It is to be noted that all the above discussed reports are with variety of substrates containing various C−N bond containing functional group (Figure 7.1c).

Inspired by this result we tried to explore C−N activation methodology with an unexplored substrate *N*-pyridylpyridone with arylboronic acid as the coupling partner. We hypothesized *N*-pyridylpyridone would undergo C−N bond activation and couple with boronic acid under Ni-catalyzed condition and in fact, this has been realized in this work. Herein, we report a novel and first example of nickel-catalyzed C−N bond activation of *N*-pyridylpyridone and 1-(9*H*-purin-6-yl)pyridin-2(1*H*)-one molecules where the hindered aromatic C−N bond got cleaved under catalytic reaction condition to give arylated product. Generally cleaving the hindered bond is quite difficult.[18] For the first time pyridone moiety has been used as the directing group in the C−N activation methodology (Figure 7.1d). A facile and alternative approach for the preparation of heteroaryl-aryl molecule was established with good functional group tolerance.

7.3 RESULTS AND DISCUSSION

We commenced our investigation with *N*-pyridylpyridone **1a** as the model substrate and *p*-tolyl boronic acid **2b** as the coupling partner and screened the reaction parameters (Table 7.1). While doing solvent screening, it was found that THF was giving good yield of the product **3ab** (entries 1-3). Changing the catalyst from $NiBr_2$ to other nickel catalyst such as $Ni(acac)_2$, $NiCl_2$, $Ni(PCy_3)_2Cl_2$, $Ni(OTf)_2$ resulted the desired product with improved yield of 87% in case of $Ni(OTf)_2$ (entries 4-7). Whereas, the ligand screening of reaction gave lower yield of the desired product (entries 8-10). Further, screening the reaction with additives other than K_3PO_4 such as KOAc, K_2CO_3 led to drastic decrease in yields (entries 11-12). Control experiments indicate that $Ni(OTf)_2$ was essential for the cross-coupling reaction and same with bipyridyl ligand as well as K_3PO_4 additive (entries 13-15). Moreover, it was found that the reaction is proceeding at a slower rate in low temperature (entry 16). When the reaction was allowed to run for longer time, the yield of the product decreased (entry 17). After a brief survey of the reaction parameters, the desired product

3ab was obtained in 87% yield using a combination of Ni(OTf)$_2$ (10 mol %), Bipyridyl (20 mol %), K$_3$PO$_4$ (2 equiv) in THF (0.2 M) at 110 °C for 12h (entry 1).
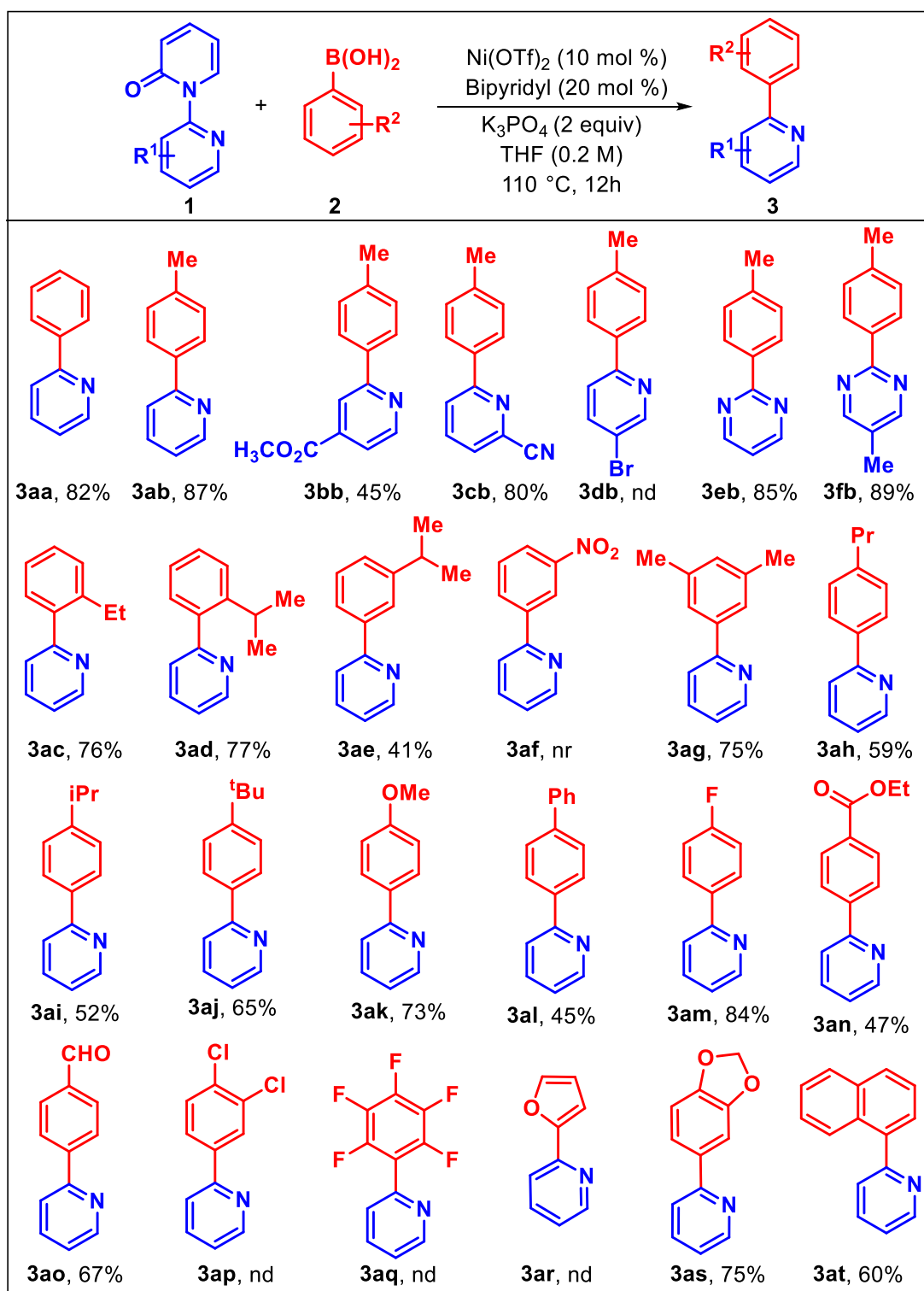
Table 7.1. Optimization of the reaction conditions[a]
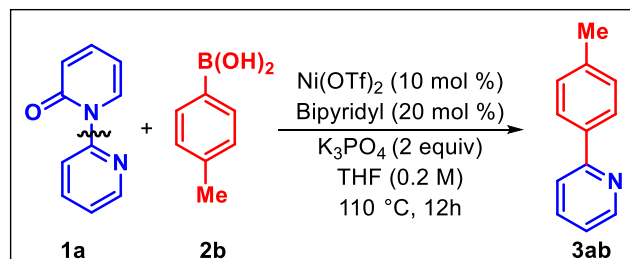
entry	solvent	catalyst	ligand	additive	3ab yield (%)[b]
1	DMA	NiBr$_2$	Bipyridyl	K$_3$PO$_4$	25
2	TFT	NiBr$_2$	Bipyridyl	K$_3$PO$_4$	29
3	THF	NiBr$_2$	Bipyridyl	K$_3$PO$_4$	44
4	THF	Ni(acac)$_2$	Bipyridyl	K$_3$PO$_4$	22
5	THF	NiCl$_2$	Bipyridyl	K$_3$PO$_4$	55
6	THF	Ni(PCy$_3$)$_2$Cl$_2$	Bipyridyl	K$_3$PO$_4$	80
7	**THF**	**Ni(OTf)$_2$**	**Bpyridyl**	**K$_3$PO$_4$**	**87**
8	THF	Ni(OTf)$_2$	PCy$_3$	K$_3$PO$_4$	26
9	THF	Ni(OTf)$_2$	Phenanthroline	K$_3$PO$_4$	24
10	THF	Ni(OTf)$_2$	Davephos	K$_3$PO$_4$	35
11	THF	Ni(OTf)$_2$	Bipyridyl	KOAc	nd
12	THF	Ni(OTf)$_2$	Bipyridyl	K$_2$CO$_3$	5
13	THF	-	Bipyridyl	K$_3$PO$_4$	nd
14	THF	Ni(OTf)$_2$	-	K$_3$PO$_4$	nd
15	THF	Ni(OTf)$_2$	Bipyridyl	-	nd
16[c]	THF	Ni(OTf)$_2$	Bipyridyl	K$_3$PO$_4$	70
17[d]	THF	Ni(OTf)$_2$	Bipyridyl	K$_3$PO$_4$	45

[a]Reaction conditions: **1a** (0.10 mmol), **2a** (3 equiv), catalyst (10 mol %), ligand (20 mol %), additive (2 equiv), solvents (0.2 M), 110 °C, 12 h. [b]Isolated yields. [c]temp = 100 °C. [d]time = 16 h. nd = not detected.

With the optimized reaction condition in hand, we have examined substrate scope of *N*-pyridyl pyridone **1** with boronic acids **2** (Scheme 7.1). Delightfully, this protocol works with a wide range of structurally and electronically different substrates and arylboronic acids (scheme 7.1). 2-Pyridylpyridone **1a** with phenyl boronic acid **2a** and *p*-tolyl boronic acid **2b** under optimized reaction condition gave the corresponding products **3aa** and **3ab**

Scheme 7.1: Substrate scope for the synthesis of 3[a,b]

3aa, 82%   **3ab**, 87%   **3bb**, 45%   **3cb**, 80%   **3db**, nd   **3eb**, 85%   **3fb**, 89%

3ac, 76%   **3ad**, 77%   **3ae**, 41%   **3af**, nr   **3ag**, 75%   **3ah**, 59%

3ai, 52%   **3aj**, 65%   **3ak**, 73%   **3al**, 45%   **3am**, 84%   **3an**, 47%

3ao, 67%   **3ap**, nd   **3aq**, nd   **3ar**, nd   **3as**, 75%   **3at**, 60%

[a]Reaction conditions: **1a** (0.1 mmol), **2a** (0.3 mmol), Ni(OTf)$_2$ (10 mol %), Bipyridyl (20 mol %), K$_3$PO$_4$ (2 equiv), THF (0.2 M), 110 °C, 12 h. [b]Isolated yields.

respectively in very good yields. Substitution on pyridine ring of the substrate **1** (-CO$_2$Me/ CN), smoothly gave the corresponding products **3bb** and **3cb** with moderate to very good yields. However, bromo (-Br) substituent, failed to give the desired product **3db**. When pyrimidinylpyridone and 5-methylpyrimidinylpyridone were employed as the substrates, the products **3eb** and **3fb** were found with a higher yield, indicating that the extra nitrogen present was not affecting the substrate's reactivity.

Later on, the generality of arylboronic acid were explored, and in most cases, we got good yields of the products. With substitution at the *ortho* (-Et/*i*Pr) position, the products **3ac, 3ad** were obtained in good yield (Scheme 1). While substitution of *i*Pr group at *m*-position of aryl boronic acid led to the product **3ae** with moderate yield. It has been observed that electron withdrawing NO$_2$ group substitution at *m*-position failed to give the desired product **3af**. Me-group at both the *m*-position of arylboronic acid gave the product **3ag** with high yield. Various *p*-substituted groups (-Pr/*i*Pr/^{t}Bu/OMe/Ph/F) on the arylboronic acid reacted smoothly to afford the arylated product **3ah-3am** in good to excellent yield. Functional group such as -CO$_2$Et, -CHO tolerate the reaction condition and gave the corresponding product **3an** and **3ao** with moderate yield. The halo group (-Cl/-F) substitution at multiple position leads to no product formation. The heteroatom containing boronic acid i.e., furan-2-ylboronic acid did not give the product **3ar** whereas benzodioxolylboronic acid gave the product **3as** with good yield. In addition to this, the polycyclic naphthalenylboronic acid also smoothly gave the product **3at** with good yield.

To know the scalability of this reaction, 1 mmol scale reaction has been performed and obtained 75% yield of the product **3ab** (Scheme 7.2a). Then to understand the mechanism (ionic/radical) of this reaction, a reaction was performed in presence of radical scavenger (TEMPO/BHT). Good yield of the product was observed, indicating that this reaction is not going through radical pathway (Scheme 7.2b).

## Scheme 7.2: Scale up reaction and Radical process experiment
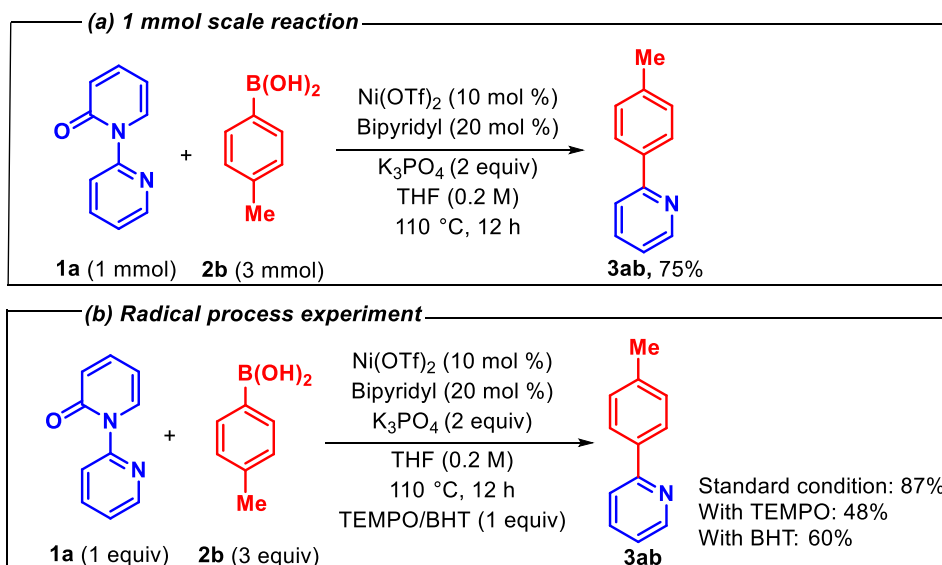
Scheme 7.3. Plausible Mechanism
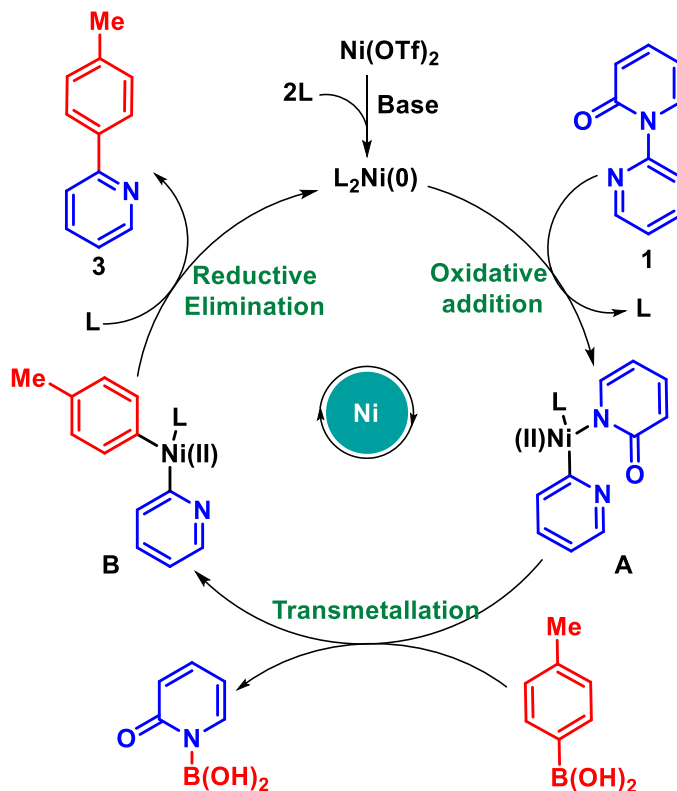
On the basis of above mechanistic studies and literature,[14,19] a plausible catalytic cycle for the synthesis of **3** is depicted in scheme 7.3. Initially, the Ni(II)-catalyst in the presence of base generate the active Ni(0)-catalyst. Then the substrate 2-pyridylpyridone **1** undergo

oxidative addition across the bridging C–N bond with active Ni(0)-catalyst to give intermediate **A**. Then, arylboronic acid **2** coordinates with intermediate **A** *via* transmetallation gives intermediate **B**. Intermediate **B** upon reductive elimination delivers the desired product **3** along with regeneration of active Ni(0)-catalyst for the next catalytic cycle.

Scheme 7.4. Application of the Methodology
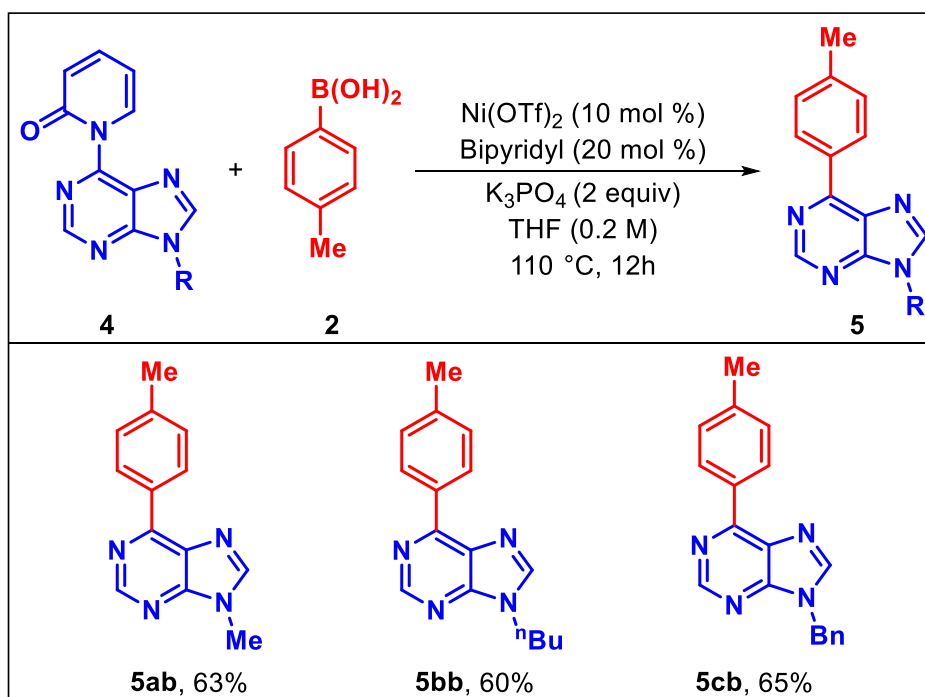
Further we extended the scope of this methodology to synthesize the biologically important arylated purine molecule which can be used as an unnatural nucleobase. Nucleobases are essential components of life and have been used in nanotechnology to construct metal coordination complexes with adaptive inclusion ability, fluorescence signal, enzyme-like activity, and other properties.[20] Hence, to synthesize arylated purine molecules, we have taken various *N*-protected 1-(9*H*-purin-6-yl)pyridin-2(1*H*)-one substrates **4**, which coupled with tolylboronic acid **2b,** furnishing the desired arylated products **5ab**-**5cb** in good yields (Scheme 7.4).

7.4 CONCLUSION:

We have successfully developed a Ni-catalyzed C–N activation of pyridylpyridone with arylboronic acid where hindered bridging C–N bond was cleaved affording arylated product. A distinct class of arylpyridines have been obtained. A wide variety of substrates and boronic acids are well tolerated and forming the arylated product up to 91% yield. The use of ligand plays a crucial role to synthesize the arylated moiety. Further synthetic application of this methodology has been studied by taking 1-(9*H*-purin-6-yl)pyridin-2(1*H*)-one substrate which gave the corresponding product in good yields under the optimized reaction condition. We expect that the developed methodology of aromatic C–N bond activation using Ni catalyst will become a starting point to functionalize many such hindered aryl-aryl C-N bonds in future.

7.5 EXPERIMENTAL SECTION:[21]

Reactions were performed using oven dried borosil seal-tube glass vial with Teflon-coated magnetic stirring bars under N_2 atmosphere. Column chromatography was done by using 100-200 and 230-400 mesh size silica gel of Acme synthetic chemicals Company. A gradient elution was performed by using distilled petroleum ether and ethyl acetate. TLC plates were detected under UV light at 254 nm. ^{1}H NMR, ^{13}C NMR & ^{19}F NMR were recorded on Bruker AV 400 and 700 MHz spectrometers using $CDCl_3$ as the deuterated solvent.[22] Chemical shifts (δ) are reported in ppm relative to the residual solvents ($CHCl_3$) signal ($\delta = 7.26$ for ^{1}H NMR and $\delta = 77.36$ for ^{13}C NMR). Data for ^{1}H NMR spectra are reported as follows: chemical shift (multiplicity, coupling constants, number of hydrogen). Abbreviations are as follows: s (singlet), d (doublet), t (triplet), q (quartet), quint (quintet), sext (sextet), sept (septet), m (multiplet), dd (double doublet), br (broad signal), *J* (coupling

constants) in Hz (hertz). High-Resolution Mass Spectrometry (HRMS) data was recorded using Bruker micro TOF Q-II mass spectrometer using methanol as solvent. IR spectra were recorded on a FTIR system and values are reported in frequency of absorption (cm^{-1}). Melting point was performed using Stuart^{TM} melting point apparatus SMP10. X-ray analysis was conducted using Rigaku Smartlab X-ray diffractometer. Reagents and starting materials were purchased from Sigma Aldrich, Alfa Aesar, TCI, Avra, Spectrochem and other commercially available sources and used without further purification unless otherwise noted.

7.5.1 General procedure for the preparation of substituted phenyl pyridine:
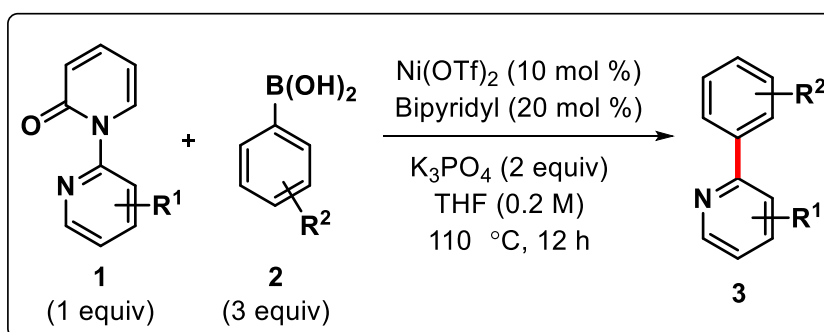
To an oven dried sealed tube charged with a stirring bar, *N*-pyridyl protected pyridone **1** (1 equiv), substituted phenyl boronic acid **2** (3 equiv) were added under nitrogen atmosphere. The sealed tube was applied for high vacuum and refilled with N$_2$. Ni(OTf)$_2$ (10 mol %), bipyridyl (20 mol %), K$_3$PO$_4$ (2 equiv) were added to the reaction mixture followed by addition of degassed THF solvent (0.2 M) inside the glove box. The reaction tube was stirred at 110 °C on a pre-heated aluminum block with constant stirring for 12 h. After completion of the reaction (as monitored by TLC), the reaction mixture was cooled to room temperature and quenched with ethyl acetate. The crude was purified by column chromatography using EtOAc/hexane mixture on silica gel to give the pure product **3**.

7.5.2 Experimental characterization data for arylated products:[23]

2-phenylpyridine (3aa):
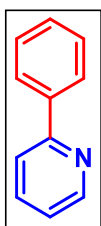
Physical State: colorless liquid (12.7 mg for 0.10 mmol scale, 82% yield). R_f-value: 0.7 (40% EtOAc/hexane). ^{1}H NMR (CDCl$_3$, 400 MHz): δ 8.69 (d, J = 4.4 Hz, 1H), 8.00–7.98 (m, 2H), 7.77–7.72 (m, 2H), 7.50–7.46 (m, 2H), 7.44–7.40 (m, 1H), 7.25–7.21 (m, 1H). ^{13}C{^{1}H} NMR (CDCl$_3$, 100 MHz): δ 157.6, 149.6, 139.2, 137.5, 129.5, 129.2, 127.3, 122.5, 121.1, 77.4.

2-(p-tolyl)pyridine (3ab):
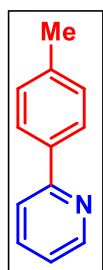
Physical State: colorless liquid (14.7 mg for 0.10 mmol scale, 87% yield). R_f-value: 0.8 (40% EtOAc/hexane). ^{1}H NMR (CDCl$_3$, 400 MHz): δ 8.68-8.67 (m, 1H), 7.89 (d, J = 8.0 Hz, 2H), 7.75–7.70 (m, 2H), 7.29–7.26 (m, 2H), 7.22-7.18 (m, 1H), 2.41 (s, 3H). ^{13}C{^{1}H} NMR (CDCl$_3$, 100 MHz): δ 157.8, 149.9, 139.3, 137.0, 136.9, 129.8, 127.1, 122.1, 120.6, 21.6.

methyl 2-(p-tolyl)isonicotinate (3bb):
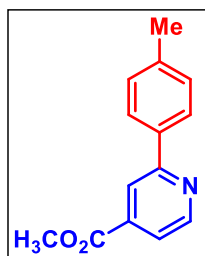
Physical State: colorless liquid (10.2 mg for 0.10 mmol scale, 45% yield). R_f-value: 0.8 (30% EtOAc/hexane). ^{1}H NMR (CDCl$_3$, 700 MHz): δ 8.81 (d, J = 4.9 Hz, 1H), 8.27 (s, 1H), 7.96 (d, J = 7.7 Hz, 2H), 7.74 (d, J = 4.9 Hz, 1H), 7.30 (d, J = 7.7 Hz, 2H), 3.99 (s, 3H), 2.42 (s, 3H). ^{13}C{^{1}H} NMR (CDCl$_3$, 176 MHz): δ 166.2, 158.8, 150.7, 140.0, 138.4, 136.1, 130.0, 127.2, 121.1, 119.8, 53.1, 21.6.

6-(p-tolyl)picolinonitrile (3cb):
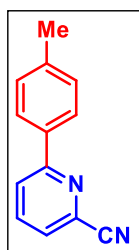
Physical State: white solid (15.6 mg for 0.10 mmol scale, 80% yield). R_f-value: 0.6 (30% EtOAc/hexane). ^{1}H NMR (CDCl$_3$, 700 MHz): δ 7.93 (t, J = 8.4 Hz, 3H), 7.85 (t, J = 7.7 Hz, 1H), 7.59 (d, J = 7.7 Hz, 1H), 7.31 (d, J = 7.7 Hz, 2H), 2.42 (s, 3H). ^{13}C{^{1}H} NMR (CDCl$_3$, 176 MHz): δ 159.3, 140.8, 137.9, 134.8, 134.1, 130.1, 127.3, 126.6, 123.5, 117.8, 21.7.

2-(p-tolyl)pyrimidine (3eb):
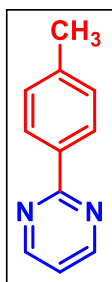
Physical State: white solid (14.5 mg for 0.10 mmol scale, 85% yield). R_f-value: 0.6 (20% EtOAc/hexane). ^{1}H NMR (CDCl$_3$, 400 MHz): δ 8.78 (d, J = 4.8 Hz, 2H), 8.37–8.32 (m, 2H), 7.30 (d, J = 8 Hz, 2H), 7.15 (t, J = 4.8 Hz, 1H), 2.42 (s, 3H). ^{13}C{^{1}H} NMR (CDCl$_3$, 176 MHz): δ 165.2, 157.5, 141.4, 135.2, 129.7, 128.4, 119.1, 21.8.

5-methyl-2-(p-tolyl)pyrimidine (3fb):
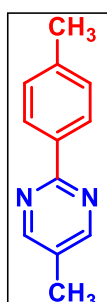
Physical State: white solid (16.4 mg for 0.10 mmol scale, 89% yield). R_f-value: 0.6 (20% EtOAc/hexane). ^{1}H NMR (CDCl$_3$, 400 MHz): δ 8.60 (s, 2H), 8.30–8.28 (m, 2H), 7.28 (d, J = 8.0 Hz, 2H), 2.41 (s, 3H), 2.32 (s, 3H). ^{13}C{^{1}H} NMR (CDCl$_3$, 176 MHz): δ 162.6, 157.3, 140.5, 134.9, 129.3, 127.9, 127.8, 21.4, 15.5.
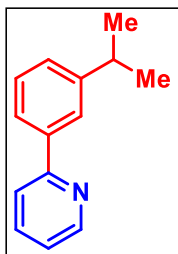
2-(2-ethylphenyl)pyridine (3ac):
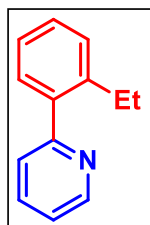
Physical State: colorless liquid (14 mg for 0.10 mmol scale, 76% yield). R_f-value: 0.8 (20% EtOAc/hexane). ^{1}H NMR (CDCl$_3$, 400 MHz): δ 8.70–8.68 (m, 1H), 7.76–7.72 (m, 1H), 7.40–7.37 (m, 1H), 7.35–7.31 (m, 3H), 7.28–7.23 (m, 2H), 2.72 (q, J = 7.6 Hz, 2H), 1.08 (t, J = 7.6 Hz, 3H). ^{13}C{^{1}H} NMR (CDCl$_3$, 176 MHz): δ 160.6, 149.5, 142.3, 140.5, 136.5, 130.0, 129.3, 128.8, 126.1, 124.4, 122.0, 26.4, 15.8.

2-(2-isopropylphenyl)pyridine (3ad):
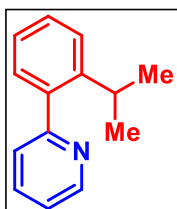
Physical State: colorless liquid (15.2 mg for 0.10 mmol scale, 77% yield). **R_f-value:** 0.7 (20% EtOAc/hexane). ^{1}H NMR (CDCl$_3$, 400 MHz): δ 8.70–8.68 (m, 1H), 7.73 (td, J_1 = 7.6 Hz, J_2 = 1.6 Hz, 1H), 7.43–7.34 (m, 3H), 7.30–7.22 (m, 3H), 3.16 (sept, J = 6.8 Hz, 1H), 1.18 (d, J = 7.2 Hz, 6H). ^{13}C{^{1}H} NMR (CDCl$_3$,

176 MHz): δ 160.7, 149.5, 146.8, 140.2, 136.3, 130.0, 128.9, 126.0, 125.8, 124.6, 121.9, 29.5, 24.4.
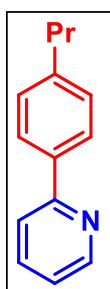
2-(3-isopropylphenyl)pyridine (3ae):

Physical State: colorless liquid (8.1 mg for 0.10 mmol scale, 41% yield). R$_f$-value: 0.7 (20% EtOAc/hexane). ^{1}H NMR (CDCl$_3$, 400 MHz): δ 8.71–8.69 (m, 1H), 7.88–7.87 (m, 1H), 7.78–7.72 (m, 3H), 7.40 (t, J = 7.6 Hz, 1H), 7.31–7.29 (m, 1H), 7.24–7.21 (m, 1H), 3.01 (sept, J = 6.8 Hz, 1H), 1.31 (d,

J = 6.8 Hz, 6H). ^{13}C{^{1}H} NMR (CDCl$_3$, 176 MHz): δ 158.2, 150.0, 149.8, 139.8, 137.0, 129.1, 127.4, 125.6, 124.8, 122.3, 121.1, 34.6, 24.4.

2-(3,5-dimethylphenyl)pyridine (3ag):
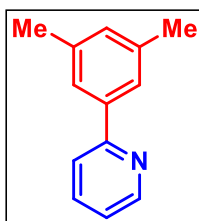
Physical State: Oily liquid (13.7 mg for 0.10 mmol scale, 75% yield). R$_f$-value: 0.6 (10% EtOAc/hexane). ^{1}H NMR (CDCl$_3$, 400 MHz): δ 8.68–8.67 (m, 1H), 7.73–7.69 (m, 2H), 7.59 (s, 2H), 7.22–7.19 (m, 1H), 7.06 (s, 1H), 2.39 (s, 6H). ^{13}C{^{1}H} NMR (CDCl$_3$, 176 MHz): δ 158.1, 149.9, 139.7,

138.6, 137.0, 131.0, 125.1, 122.3, 121.0, 21.7.

2-(4-propylphenyl)pyridine (3ah):

Physical State: colorless liquid (11.7 mg for 0.10 mmol scale, 59% yield). R$_f$-value: 0.8 (30% EtOAc/hexane). ^{1}H NMR (CDCl$_3$, 400 MHz): δ 8.68–8.67 (m, 1H), 7.91 (dt, J_1 = 8.4 Hz, J_2 = 2.0 Hz, 2H), 7.75–7.70 (m, 2H), 7.28 (d, J = 8.4 Hz, 2H), 7.22–7.18 (m, 1H), 2.64 (t, J = 7.6 Hz, 2H), 1.68 (sext, J = 7.6 Hz, 2H), 0.96 (t, J = 7.2 Hz, 3H). ^{13}C{^{1}H} NMR (CDCl$_3$, 176 MHz): δ 157.9, 149.9,

144.1, 137.2, 137.0, 129.2, 127.1, 122.1, 120.6, 38.1, 24.8, 14.1.

2-(4-isopropylphenyl)pyridine (3ai):
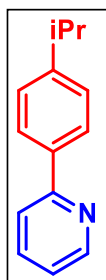
Physical State: colorless liquid (10.3 mg for 0.10 mmol scale, 52% yield). R_f-value: 0.5 (20% EtOAc/hexane). ^{1}H NMR (CDCl$_3$, 400 MHz): δ 8.67 (d, J = 4.8 Hz, 1H), 7.93–7.90 (m, 2H), 7.76–7.70 (m, 2H), 7.34 (d, J = 8.0 Hz, 2H), 7.22–7.18 (m, 1H), 2.97 (sept, J = 6.8 Hz, 1H), 1.29 (d, J = 6.8 Hz, 6H). ^{13}C{^{1}H} NMR (CDCl$_3$, 176 MHz): δ 157.9, 150.2, 149.9, 137.4, 137.0, 127.2 (2C), 122.1, 120.7, 34.3, 24.3.

2-(4-(tert-butyl)phenyl)pyridine (3aj):
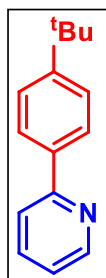
Physical State: colorless solid (13.8 mg for 0.10 mmol scale, 65% yield). R_f-value: 0.7 (20% EtOAc/hexane). ^{1}H NMR (CDCl$_3$, 400 MHz): δ 8.69–8.67 (m, 1H), 7.94–7.91 (m, 2H), 7.73–7.71 (m, 2H), 7.51–7.48 (m, 2H), 7.22–7.18 (m, 1H), 1.36 (s, 9H). ^{13}C{^{1}H} NMR (CDCl$_3$, 176 MHz): δ 157.8, 152.5, 149.9, 137.0, 136.9, 126.9, 126.0, 122.1, 120.7, 35.0, 31.6.

2-(4-methoxyphenyl)pyridine (3ak):
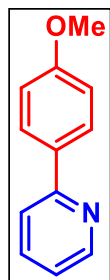
Physical State: white solid (13.6 mg for 0.10 mmol scale, 73% yield). R_f-value: 0.3 (5% EtOAc/hexane). ^{1}H NMR (CDCl$_3$, 400 MHz): δ 8.66–8.64 (m, 1H), 7.97–7.93 (m, 2H), 7.72–7.64 (m, 2H), 7.18–7.14 (m, 1H), 7.01–6.98 (m, 2H), 3.86 (s, 3H). ^{13}C{^{1}H} NMR (CDCl$_3$, 100 MHz): δ 161.0, 157.7, 150.1, 137.2, 132.6, 128.7, 122.0, 120.4, 114.7, 55.9.

2-([1,1'-biphenyl]-4-yl)pyridine (3al):
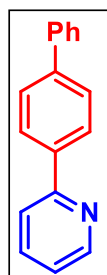
Physical State: white solid (10.4 mg for 0.10 mmol scale, 45% yield). R_f-value: 0.6 (20% EtOAc/hexane). ^{1}H NMR (CDCl$_3$, 700 MHz): δ 8.71 (d, J = 4.9 Hz, 1H), 8.08 (d, J = 7.7 Hz, 2H), 7.79–7.76 (m, 2H), 7.74–7.69 (m, 2H), 7.66 (d, J = 7.7 Hz, 2H), 7.47 (t, J = 7.0 Hz, 2H), 7.37 (t, J = 7.7 Hz, 1H), 7.25–7.24 (m, 1H).

^{13}C{^{1}H} NMR (CDCl$_3$, 176 MHz): δ 157.4, 150.1, 142.1, 140.9, 138.6, 137.1, 129.2, 127.9, 127.8, 127.6, 127.5, 122.5, 120.8.
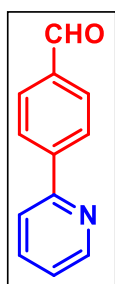
2-(4-fluorophenyl)pyridine (3am):
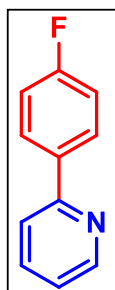
Physical State: Oily liquid (14.6 mg for 0.10 mmol scale, 84% yield). R$_f$-value: 0.8 (30% EtOAc/hexane). ^{1}H NMR (CDCl$_3$, 700 MHz): δ 8.67 (d, J = 4.2 Hz, 1H), 7.99-7.97 (m, 2H), 7.76–7.73 (m, 1H), 7.68 (d, J = 8.4 Hz, 1H), 7.24–7.22 (m, 1H), 7.17–7.14 (m, 2H). ^{13}C{^{1}H} NMR (CDCl$_3$, 176 MHz): δ 163.8 (d, $J_{C\text{-}F}$ = 246 Hz), 156.8, 150.0, 137.2, 135.9 (d, $J_{C\text{-}F}$ = 2.9 Hz), 129.0 (d, $J_{C\text{-}F}$ = 7.8 Hz), 122.3, 120.5, 116.0 (d, $J_{C\text{-}F}$ = 21 Hz). ^{19}F NMR (CDCl$_3$, 376 MHz): δ -113.2.

ethyl 4-(pyridin-2-yl)benzoate (3an):
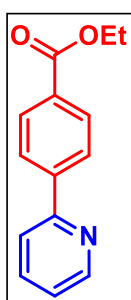
Physical State: colorless solid (10.7 mg for 0.10 mmol scale, 47% yield). R$_f$-value: 0.2 (5% EtOAc/hexane). ^{1}H NMR (CDCl$_3$, 400 MHz): δ 8.73 (dt, J_1 = 4.8 Hz, J_2 = 1.2 Hz 1H), 8.16–8.14 (m, 2H), 8.02–8.06 (m, 2H), 7.80–7.78 (m, 2H), 7.30–7.27 (m, 1H), 4.41 (q, J = 7.2 Hz, 2H), 1.4 (t, J =7.2 Hz, 3H). ^{13}C{^{1}H} NMR (CDCl$_3$, 176 MHz): δ 166.8, 156.6, 150.2, 143.8, 137.3, 131.0, 130.4, 127.1, 123.2, 121.4, 61.4, 14.7.

4-(pyridin-2-yl)benzaldehyde (3ao):

Physical State: Colorless solid (12.3 mg for 0.10 mmol scale) 67% yield. R$_f$-value: 0.6 (30% EtOAc/hexane). ^{1}H NMR (CDCl$_3$, 700 MHz): δ 10.09 (s, 1H), 8.75 (d, J = 4.9 Hz, 1H), 8.18 (d, J = 7.7 Hz, 2H), 7.99 (d, J = 8.4 Hz, 2H), 7.81–7.80 (m, 2H), 7.32–7.31 (m, 1H). ^{13}C{^{1}H} NMR (CDCl$_3$, 176 MHz): δ 192.3, 156.2, 150.3, 145.2, 137.4, 136.8, 130.5, 127.8, 123.5, 121.6.

2-(benzo[*d*][1,3]dioxol-5-yl)pyridine (3as):
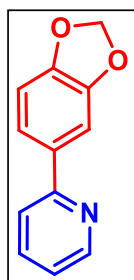
Physical State: Oily liquid (15 mg for 0.10 mmol scale, 75% yield). R_f-value: 0.8 (40% EtOAc/hexane). ^{1}H NMR (CDCl$_3$, 400 MHz): δ 8.63 (d, J = 4.8 Hz, 1H), 7.69 (t, J = 8.0 Hz, 1H), 7.63–7.61 (m, 1H), 7.52–7.48 (m, 2H), 7.18–7.15 (m, 1H), 6.89 (d, J = 8.0 Hz, 1H), 6.00 (brs, 2H). ^{13}C{^{1}H} NMR (CDCl$_3$, 100 MHz): δ 157.2, 149.8, 148.7, 148.5, 137.0, 134.2, 122.0, 121.2, 120.3, 108.7, 107.7, 101.6.

2-(naphthalen-1-yl)pyridine (3at):
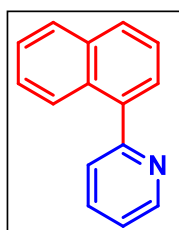
Physical State: Oily liquid (12.3 mg for 0.10 mmol scale) 60% yield. R_f-value: 0.3 (10% EtOAc/hexane). ^{1}H NMR (CDCl$_3$, 700 MHz): δ 8.79 (d, J = 4.9 Hz, 1H), 8.08 (d, J = 7.7 Hz, 1H), 7.91 (d, J = 7.7 Hz, 2H), 7.82 (t, J = 7.7 Hz, 1H), 7.60–7.58 (m, 2H), 7.55 (t, J = 7.7 Hz, 1H), 7.51–7.46 (m, 2H), 7.34–7.32 (m, 1H). ^{13}C{^{1}H} NMR (CDCl$_3$, 176 MHz): δ 159.6, 149.8, 138.8, 136.7, 134.3, 131.5, 129.2, 128.7, 127.8, 126.8, 126.2, 125.9, 125.6, 125.4, 122.4.

9-methyl-6-(p-tolyl)-9H-purine (5ab):
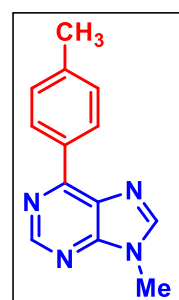
Physical State: white solid (14.2 mg for 0.10 mmol scale, 62% yield). R_f-value: 0.3 (40% EtOAc/hexane). ^{1}H NMR (CDCl$_3$, 400 MHz): δ 9.01 (s, 1H), 8.70 (d, J = 8.0 Hz, 2H), 8.08 (s, 1H), 7.37 (d, J = 8.0 Hz, 2H), 3.93 (s, 3H), 2.45 (s, 3H). ^{13}C{^{1}H} NMR (CDCl$_3$, 100 MHz): δ 155.2, 153.0, 152.8, 144.9, 141.8, 133.2, 131.1, 130.1, 129.8, 30.1, 21.9.

9-butyl-6-(p-tolyl)-9H-purine (5bb):
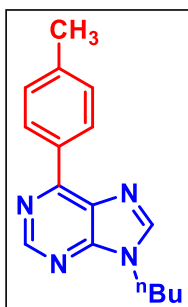
Physical State: white solid (16 mg for 0.10 mmol scale, 60% yield). R_f-value: 0.5 (30% EtOAc/hexane). ^{1}H NMR (CDCl$_3$, 400 MHz): δ 9.00 (s, 1H), 8.70 (d, J = 8.0 Hz, 2H), 8.10 (s, 1H), 7.37 (d, J = 8.0 Hz, 2H), 4.31 (t, J = 7.2 Hz, 2H), 2.45 (s, 3H), 1.94 (pent, J = 7.2 Hz, 2H), 1.40 (sext, J = 7.6 Hz, 2H), 0.98 (t, J = 7.6 Hz, 3H). ^{13}C{^{1}H} NMR (CDCl$_3$, 100 MHz):

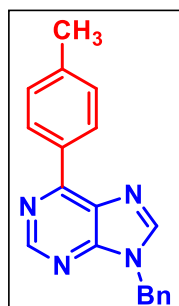δ 155.2, 152.7, 152.6, 144.3, 141.7, 133.3, 131.2, 130.0, 129.8, 44.0, 33.3, 21.9, 20.3, 13.8.

9-benzyl-6-(p-tolyl)-9H-purine (5cb):

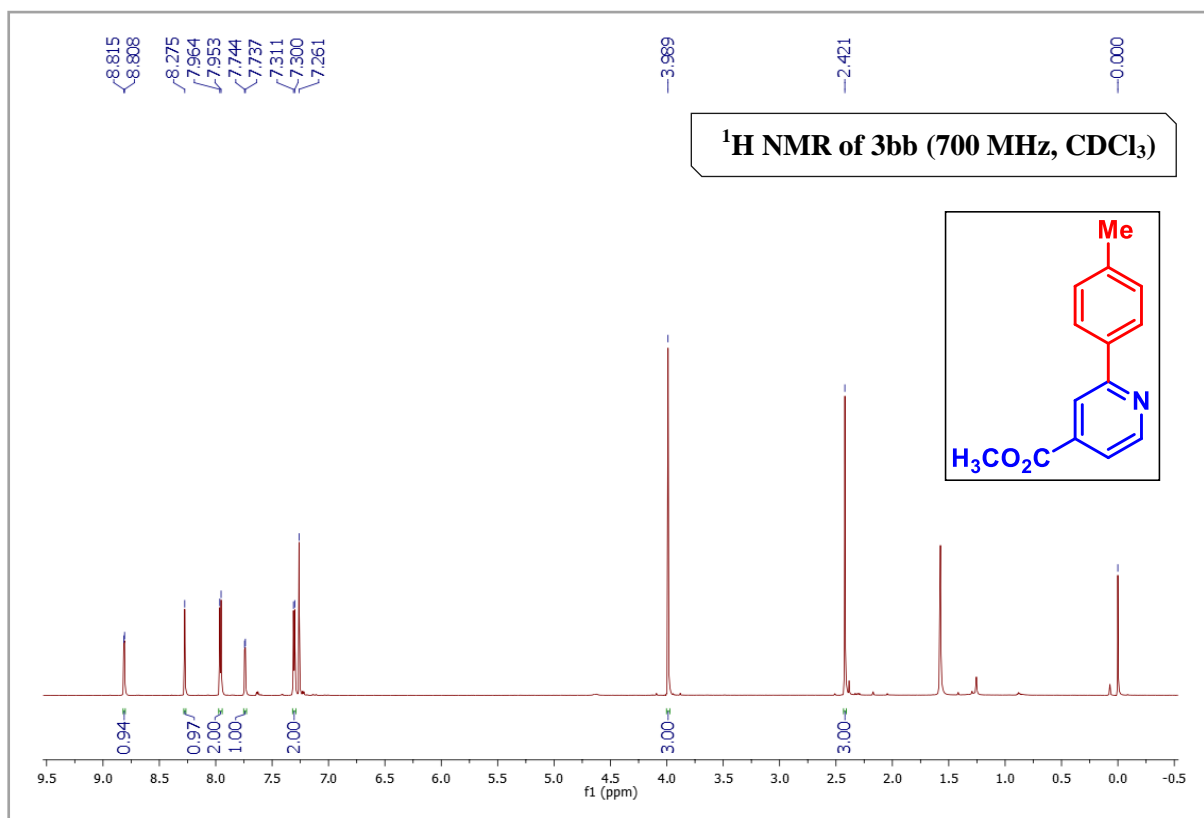Physical State: white solid (19.5 mg for 0.10 mmol scale, 65% yield). R_f-value: 0.5 (30% EtOAc/hexane). ^{1}H NMR (CDCl$_3$, 700 MHz): δ 9.03 (s, 1H), 8.70 (d, J = 8.4 Hz, 2H), 8.08 (s, 1H), 7.38–7.32 (m, 7H), 5.48 (s, 2H), 2.45 (s, 3H). ^{13}C{^{1}H} NMR (CDCl$_3$, 176 MHz): δ 155.4, 153.0, 152.8, 144.2, 141.8, 135.6, 133.2, 131.1, 130.1, 129.8, 129.5, 128.9, 128.2, 47.6, 22.0.

NMR spectra of methyl 2-(*p*-tolyl)isonicotinate (3bb):

^{1}H NMR of 3bb (700 MHz, CDCl$_3$)

^{13}C{^{1}H} NMR of 3bb (176 MHz, CDCl$_3$)
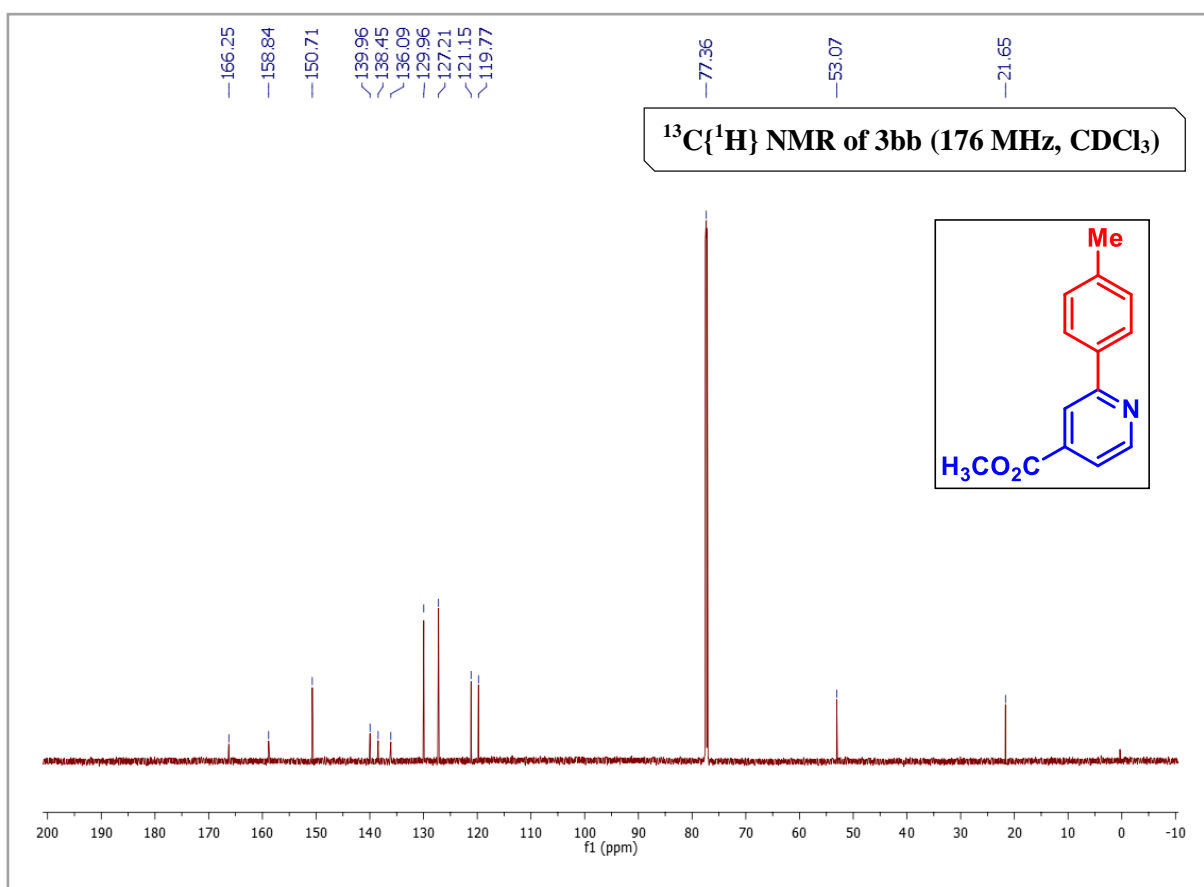
NMR spectra of 9-methyl-6-(*p*-tolyl)-9H-purine (5ab):

^{1}H NMR of 5ab (400 MHz, CDCl$_3$)

^{13}C{^{1}H} NMR of 5ab (100 MHz, CDCl$_3$)
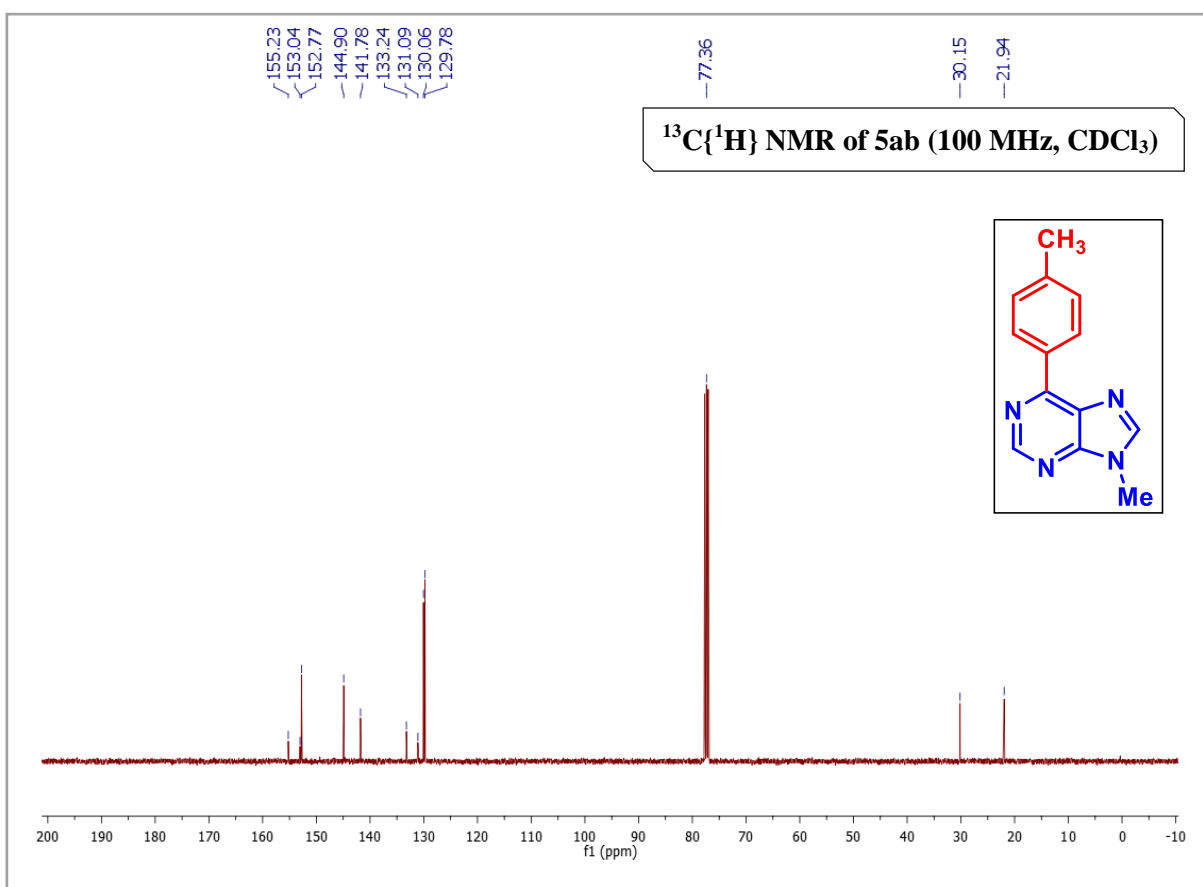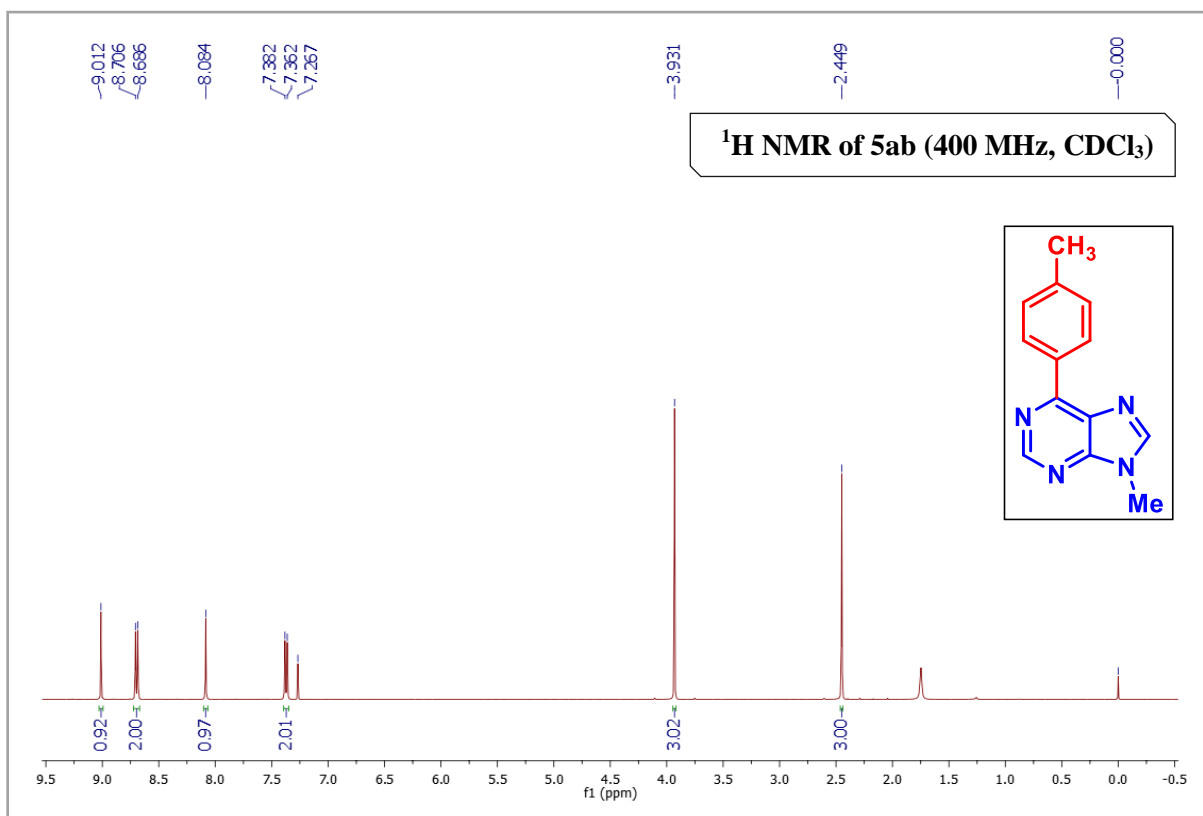
7.6 REFERENCES

1. Dalton, T.; Faber, T.; Glorius, F. C–H Activation: Toward Sustainability and Applications. *ACS Cent. Sci.* **2021**, *7*, 245−261.

2. Wang, Q.; Su, Y.; Li, L.; Huang, H. Transition-metal catalysed C−N bond activation. *Chem. Soc. Rev.* **2016**, 45, 1257−1272.

3. Fang B; Zhou C–H.; Rao X–C. Synthesis and biological activities of novel amine-derived bis-azoles as potential antibacterial and antifungal agents. *Eur J Med Chem* **2010**, *45*, 4388–4398.

4. Hili, R., Yudin, A. Making carbon-nitrogen bonds in biological and chemical synthesis. *Nat Chem Biol* **2006**, *2*, 284–287.

5. Xu, Z.-Y.; Yu, H.-Z.; Fu, Y. Mechanism of Nickel-Catalyzed Suzuki−Miyaura Coupling of Amides. *Chem. – Asian J.* **2017**, *12*, 1765−1772.

6. Boit, T. B.; Bulger, A. S.; Dander, J. E.; Garg, N. K. Activation of C−O and C−N Bonds Using Non-Precious-Metal Catalysis. *ACS Catal.* **2020**, *10*, 12109−12126.

7. Meng, G.; Szostak, M. Palladium-catalyzed Suzuki–Miyaura coupling of amides by carbon–nitrogen cleavage: general strategy for amide N−C bond activation. *Org. Biomol. Chem.* **2016**, *14*, 5690–5707.

8. (a) Lei, P.; Meng, G.; Szostak, M. General Method for the Suzuki-Miyaura Cross-Coupling of Amides Using Commercially Available, Air- and Moisture-Stable Palladium/NHC (NHC = *N*-Heterocyclic Carbene) Complexes. *ACS Catal.* **2017**, *7*, 1960−1965. (b) Liu, C.; Lalancette, R.; Szostak, R.; Szostak, M. Sterically Hindered Ketones *via* Palladium-Catalyzed Suzuki–Miyaura Cross-Coupling of Amides by N–C(O) Activation. *Org. Lett.* **2019**, *21*, 7976–7981. (c) Liu, C.; Meng, G.; Liu, Y.; Liu, R.; Lalancette, R.; Szostak, R.; Szostak, M. *N*-Acylsaccharins: Stable Electrophilic

Amide-Based Acyl Transfer Reagents in Pd-Catalyzed Suzuki–Miyaura Coupling *via* N–C Cleavage. *Org. Lett.* **2016**, *18*, 4194–4197. (d) Meng, G.; Szostak, R.; Szostak, M. Suzuki–Miyaura Cross-Coupling of *N*-Acylpyrroles and Pyrazoles: Planar, Electronically Activated Amides in Catalytic N–C Cleavage. *Org. Lett.* **2017**, *19*, 3596–3599. (e) Meng, G.; Lalancette, R.; Szostak, R.; Szostak, M. NMethylamino Pyrimidyl Amides (MAPA): Highly Reactive, Electronically-Activated Amides in Catalytic N−C(O) Cleavage. *Org. Lett.* **2017**, *19*, 4656−4659.

9. (a) Wu, H.; Li, Y.; Cui, M.; Jian, J.; Zeng, Z. Suzuki Coupling of Amides *via* Palladium-Catalyzed C−N Cleavage of *N*-Acylsaccharins. *Adv. Synth. Catal.* **2016**, *358*, 3876−3880. (b) Cui, M.; Chen, Z.; Liu, T.; Wang, H.; Zeng, Z. *N*-Acylsuccinimides: Efficient Acylative Coupling Reagents in Palladium-catalyzed Suzuki Coupling *via* C−N cleavage. *Tetrahedron Lett.* **2017**, *58*, 3819−3822.

10. Weires, N. A.; Baker, E. L.; Garg, N. K. Nickel-catalysed Suzuki–Miyaura coupling of amides. *Nat. Chem.* **2016**, *8*, 75-79.

11. Zhou, T.; Ji, C.-L.; Hong, X.; Szostak, M. Palladium-Catalyzed Decarbonylative Suzuki−Miyaura Cross-Coupling of Amides by Carbon−nitrogen Bond Activation. *Chem. Sci.* **2019**, *10*, 9865−9871.

12. Luo, Z.; Xiong, L.; Liu, T.; Zhang, Y.; Lu, S.; Chen, Y.; Guo, W.; Zhu, Y.; Zeng, Z. Palladium Catalyzed Decarbonylative Suzuki−Miyaura Coupling of Amides To Achieve Biaryls *via* C−N Bond Cleavage. *J. Org. Chem.* **2019**, *84*, 10559−10568.

13. Zhou, H.-P.; Liu, J.-B.; Yuan, J.-J.; Peng, Y.-Y. Palladium Catalyzed Suzuki Cross-Couplings of *N′*-Mesyl Arylhydrazines *via* C−N bond Cleavage. *RSC Adv.* **2014**, *4*, 25576−25579.

14. Peng, Z.; Hu, G.; Qiao, H.; Xu, P.; Gao, Y.; Zhao, Y. Palladium Catalyzed Suzuki Cross-Coupling of Arylhydrazines *via* C−N Bond Cleavage. *J. Org. Chem.* **2014**, *79*, 2733−2738.

15. Shi, S.; Meng, G.; Szostak, M. Synthesis of Biaryls through Nickel-Catalyzed Suzuki−Miyaura Coupling of Amides by Carbon−Nitrogen Bond Cleavage. *Angew. Chem., Int. Ed.* **2016**, *55*, 6959−6963.

16. Heyboer, E. M.; Johnson, R. L.; Kwiatkowski, M. R.; Pankratz, T. C.; Yoder, M. C.; DeGlopper, K. S.; Ahlgrim, G. C.; Dennis, J. M.; Johnson, J. B. *J. Org. Chem.* **2020**, *85*, 3757−3765.

17. Prusty, N.; Mohanty, S. R.; Banjare, S. K.; Nanda, T.; Ravikumar, P. C. Switching the Reactivity of the Nickel-Catalyzed Reaction of 2-Pyridones with Alkynes: Easy Access to Polyaryl/Polyalkyl Quinolinones. *Org. Lett.* **2022**, *24*, 6122-6127.

18. (a) Zhu, J.; Zhang, R.; Dong, G. Orthogonal cross-coupling through intermolecular metathesis of unstrained C(aryl)–C(aryl) single bonds. *Nat. Chem.* **2021**, *13*, 836–842. (b) Zhu, J.; Chen, P.-H.; Lu, G.; Liu, P.; Dong, G.-B. Ruthenium-Catalyzed Reductive Cleavage of Unstrained Aryl-Aryl Bonds: Reaction Development and Mechanistic Study. *J. Am. Chem. Soc.* **2019**, *141*, 18630–18640.

19. (a) Ji, C.-L.; Hong, X. Factors Controlling the Reactivity and Chemoselectivity of Resonance Destabilized Amides in Ni-Catalyzed Decarbonylative and Nondecarbonylative Suzuki-Miyaura Coupling. *J. Am. Chem. Soc.* **2017**, *139*, 15522–15529. (b) Guan, B.-T.; Wang, Y.; Li, B.-J.; Yu, D.-G.; Shi, Z.-J. Biaryl Construction *via* Ni-Catalyzed C−O Activation of Phenolic Carboxylates. *J. Am. Chem. Soc.* **2008**, *130*, 14468−14470. (c) Li, Z.; Zhang, S.-L.; Fu, Y.; Guo, Q.-X.; Liu, L. Mechanism of NiCatalyzed Selective C−O Bond Activation in Cross-Coupling of Aryl Esters. *J. Am. Chem. Soc.* **2009**, *131*, 8815−8823. (d) Quasdorf, K. W.; Tian, X.; Garg, N. K. Cross-

Coupling Reactions of Aryl Pivalates with Boronic Acids. *J. Am. Chem. Soc.* **2008**, *130*, 14422–14423.

20. (a) Pu, F.; Ren, J.; Qu, X. Nucleobases, nucleosides, and nucleotides: versatile biomolecules for generating functional nanomaterials. *Chem. Soc. Rev.* **2018**, *47*, 1285–1306. (b) Meher, S.; Sharma, N. K. Azulene tethered *N*-aryl nucleobases: synthesis, morphology and biochemical evaluations. *New Journal of Chemistry*, **2023**, *47*, 5593–5597.

21. Prusty, N.; Kinthada, L. K.; Meena, R.; Chebolu, R.; Ravikumar, P. C. Bismuth(III)-catalyzed regioselective alkylation of tetrahydroquinolines and indolines towards the synthesis of bioactive corebiaryl oxindoles and CYP19 inhibitors. *Org. Biomol. Chem.* **2021**, *19*, 891−905.

22. Gottlieb, H. E.; Kotlyar, V.; Nudelman, A. NMR chemical shifts of common laboratory solvents as trace impurities. *J. Org. Chem.* **1997**, *62*, 7512–7515.

23. (a) Li, M.; Hua, R. Gold(I)-catalyzed direct C-H arylation of pyrazine and pyridine with aryl bromides. *Tetrahedron Lett.* **2009**, *50*, 1478−1481. (b) Kobayashi, O.; Uraguchi, D.; Yamakawa, T. Cp2Ni-KOt-Bu-BEt3 (or PPh3) Catalyst System for Direct C-H Arylation of Benzene, Naphthalene, and Pyridine. *Org. Lett.* **2009**, *11*, 2679−2682. (c) Ackermann, L.; Potukuchi, H. K.; Kapdi, A. R.; Schulzke, C. Kumada-Corriu CrossCouplings with 2-Pyridyl Grignard Reagents. *Chem.-Eur. J.* **2010**, *16*, 3300−3303. (d) Molander, G. A.; Canturk, B.; Kennedy, L. E. Scope of the Suzuki-Miyaura CrossCoupling Reactions of Potassium Heteroaryltrifluoroborates. *J. Org. Chem.* **2009**, *74*, 973−980. (e) Xu, Y.; Zhou, X.; Zheng, G.; Li, X. Sulfoxonium Ylides as a Carbene Precursor in Rh(III)-Catalyzed C-H Acylmethylation of Arenes. *Org. Lett.* **2017**, *19*, 5256– 5259.
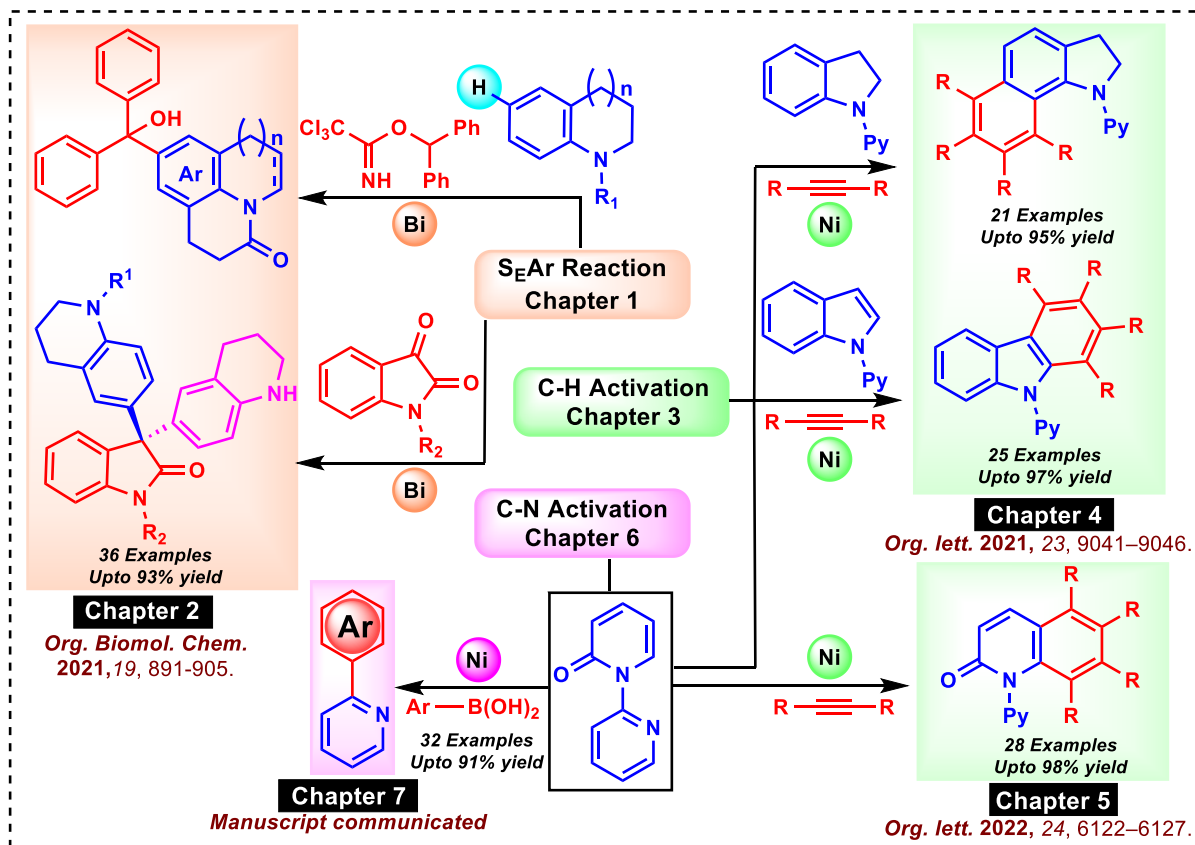
About The Author

Namrata Prusty completed her B.Sc. in chemistry from Utkal University in 2011 and her M.Sc. from Sambalpur University in 2013. She has completed her M.Phil. (organic chemistry) in 2014 from Sambalpur University, Sambalpur. She began working as a junior research fellow in January 2017 under the supervision of Prof. Ponneri C. Ravikumar at the National Institute of Science Education and Research (NISER) in Bhubaneswar. Then, she worked as a senior research scholar from January 2019 onwards. She has submitted her thesis on 23rd May, 2023. Her research is focused on "the synthesis and functionalization of N-heterocycles by C-H functionalization and C-N bond activation."